

STRUCTURAL GEOLOGY AND STRATIGRAPHY  
AT THE JUNCTION OF THE CURRAL ANTICLINE  
AND THE MOEDA SYNCLINE, QUADRILATERO FERRIFERO,  
MINAS GERAIS, BRAZIL

By  
FERNANDO R.M. PIRES

A DISSERTATION

Submitted in partial fulfillment of the requirements  
for the degree of  
DOCTOR OF PHILOSOPHY  
(Geology)

MICHIGAN TECHNOLOGICAL UNIVERSITY

1979

T  
551.809815  
P6675

ALVES

This dissertation, "Structural Geology And Stratigraphy At The Junction Of The Curral Anticline And The Moeda Syncline, Quadrilatero Ferrifero, Minas Gerais, Brazil", is hereby approved in partial fulfillment of the requirements for the degree of DOCTOR OF PHILOSOPHY in the field of Geology.

DEPARTMENT Geology & Geological Engineering

K. A. Kunkin  
Thesis Advisor

K. A. Kunkin  
Head of Department

Date July 13, 1978

61 69/71



AT THE JUNCTION OF THE CURRAL ANTICLINE  
AND THE MOEDA SYNCLINE, QUADRILATERO FERRIFERO,  
MINAS GERAIS, BRAZIL

TABLE OF CONTENTS

ABSTRACT . . . . .	i
ACKNOWLEDGMENTS . . . . .	iii
INTRODUCTION . . . . .	1
Location and Geography . . . . .	1
Previous Work . . . . .	3
Scope of Present Work . . . . .	3
Contribution by the Present Author . . . . .	4
REGIONAL GEOLOGY . . . . .	5
General Structure . . . . .	7
Western Contact . . . . .	8
Eastern Contact . . . . .	10
STRATIGRAPHY . . . . .	13
Introduction . . . . .	13
Basement Rocks . . . . .	13
Bonfim Gneiss . . . . .	13
Nova Lima Group . . . . .	14
Minas Series . . . . .	15
Caraca Group . . . . .	16
Moeda Formation . . . . .	17
Definition . . . . .	17
Thickness . . . . .	20
Basal and Upper Contacts . . . . .	21
Primary Bedding Features . . . . .	24
Stratigraphy and Lithology . . . . .	26
Details in the Serras da Moeda and Gaivotas . . . . .	33
Environment of Formation . . . . .	36
Batatal Formation . . . . .	38
General . . . . .	38
Stratigraphy . . . . .	38
Sericite Schist Unit . . . . .	38
Greenstone Unit . . . . .	41
Textural Characteristics of the Sericite Schist . . . . .	44
Petrology and Chemical Composition. . . . .	47
Sericite Schist . . . . .	47
Greenstones . . . . .	55
Correlations . . . . .	56
Itabira Group . . . . .	58
Caue Itabirite . . . . .	59
Distribution, Thickness . . . . .	59
Definitions and Types of Itabirites . . . . .	60
Textures and Compositions . . . . .	66

Itabirite in General . . . . .	66
Riebeckite Itabirite . . . . .	68
Gandarela Formation . . . . .	72
Definition, Regional Distribution and Thickness . . . . .	72
Greenstone and Amphibolite . . . . .	73
Distribution . . . . .	73
Field Description . . . . .	74
Microscopic Characteristics . . . . .	76
Petrology . . . . .	78
Dolomite . . . . .	80
Stratigraphic Position . . . . .	80
Field Description . . . . .	82
Piracicaba Group . . . . .	85
General . . . . .	85
Distribution and Thickness . . . . .	86
Lithology and Stratigraphy . . . . .	86
Primary Structures . . . . .	90
Environment of Deposition . . . . .	90
Sabara Formation . . . . .	93
COMPARISONS BETWEEN THE GEOLOGY OF THE QUADRILATERO FERRIFERO AND UPPER MICHIGAN . . . . .	94
STRUCTURAL GEOLOGY . . . . .	101
Domain Boundaries . . . . .	103
Structural Summary . . . . .	103
Domain I . . . . .	107
General . . . . .	107
Homogeneity and General Structure . . . . .	109
Curral Thrust Fault . . . . .	109
D <sub>1</sub> -Deformational Phase . . . . .	110
Mesosopic Analysis of S <sub>0</sub> -Surfaces . . . . .	110
Pattern of Z/S Symmetry in Folds . . . . .	116
Mesosopic Analysis of S <sub>1</sub> -Surfaces . . . . .	118
Mesosopic Analysis of L <sub>1</sub> -Lineations . . . . .	119
Microscopic Analysis of Rock Fabric . . . . .	120
Sigmoidal-Shaped Lenticles . . . . .	122
Pressure-Shadows Development . . . . .	124
Sigmoidal Recrystallized Fibrous Quartz Along S <sub>1</sub> -Surface . . . . .	125
Sigmoidal-Fibrous Quartz Formed Around Rotated Breccia Fragments . . . . .	126
D <sub>2</sub> -Deformational Phase . . . . .	127
General . . . . .	127
Folding and Lineations . . . . .	128
Geometric Analysis . . . . .	132
Domain II . . . . .	132
General . . . . .	132
Macroscopic Structures . . . . .	133
Curral-Gaivotas Recumbent Fold . . . . .	133
Mesosopic Analysis of S <sub>0</sub> -and S <sub>1</sub> -Surfaces . . . . .	137
Mesosopic Analysis of L <sub>1</sub> -Lineations . . . . .	142
Quartz Rods . . . . .	143
Elongation of Quartz Pebbles . . . . .	143
Deformation Along Lithologic Contacts . . . . .	143
Decollement Zone . . . . .	145



Schuppen Zone . . . . .	145
Moeda-Batatal Contact Zone . . . . .	146
Geometric Analysis of the Curral-Gaivotas	
Structures . . . . .	148
Tamandua Area . . . . .	152
Structures in the Tamandua Area . . . . .	152
Western Tamandua Belt . . . . .	154
Fabric Elements . . . . .	154
Mutuca Thrust Fault . . . . .	158
Eastern Tamandua Belt . . . . .	160
Macroscopic Structure . . . . .	160
Fabric Elements . . . . .	162
Distribution of Hematite Ore . . . . .	166
Moeda Syncline . . . . .	166
Domain III . . . . .	167
General . . . . .	167
W-Subdomain . . . . .	171
Mesosopic Analysis . . . . .	171
Microscopic Analysis . . . . .	174
Geometric Analysis . . . . .	174
Barreiro-Agua Quente Faults . . . . .	176
M-Subdomain . . . . .	177
Structural Complexity Below the Mutuca	
Thrust Fault . . . . .	177
Structural Situation Along the Mutuca	
Thrust Fault . . . . .	180
E-Subdomain . . . . .	184
Macroscopic Analysis . . . . .	184
Geometric Analysis . . . . .	186
Deformation Along the Mutuca Thrust Fault .	189
Domain IV . . . . .	192
General . . . . .	192
Caveiras Anticline . . . . .	193
Barreiro Structure . . . . .	193
Xavier Structure . . . . .	195
Limit Zone Between Domain III and Domain IV .	200
Concluding Remarks . . . . .	202
METAMORPHISM . . . . .	204
Itabirite . . . . .	205
Peraluminous Potassic Schists . . . . .	208
Greenstones . . . . .	210
References Cited . . . . .	213

## LIST OF ILLUSTRATIONS

Figures	
Fig. 1	Geologic Map of the Quadrilatero Ferrifero, M.G., Brazil, Showing Location of Map Area . . . . .
	3
Fig. 2	Geologic Setting of the Junction of the Curral and Moeda Structures . . . . .
	9

Fig. 3	Saboeiro Thrust Fault . . . . .	11
Fig. 4	Basal Contact of the Quartzose Moeda Formation With Nova Lima Greenschist. Casa de Pedra . . .	14
Fig. 5	Lithologic Sections Through the Moeda Formation . . . . .	19
Fig. 6	Cross-Section Through Serra das Gaivotas, Central Part . . . . .	22
Fig. 7	Cross-Section Through Serras das Gaivotas, Southern Part. . . . .	22
Fig. 8	Cross-Section Through Serra da Moeda, Near Retiro das Pedras . . . . .	22
Fig. 9	Conglomerate of the Lower Part of the Moeda Formation. Casa de Pedra . . . . .	23
Fig. 10	Cross-Bedding in Well-Laminated Quartzite, 1.5 Km South of Retiro das Pedras . . . . .	25
Fig. 11	Boulder Conglomerate Containing Boulders and Cobbles of An Earlier Conglomerate, Km 439, BR-040 . . . . .	31
Fig. 12	Fence Diagram Showing the Lithologic Variations in the Moeda Formation . . . . .	34
Fig. 13	Polymict Conglomerate Showing Elongated Pebbles of Quartz, Quartzite and Schist. Serra das Gaivotas . . . . .	35
Fig. 14	Polymict Conglomerate Showing Elongated Pebbles of Schist and Quartz. Serra das Gaivotas . . .	35
Fig. 15	Breccia in the Basal Part of the Batatal Formation. 1 Km South of Retiro das Pedras . .	40
Fig. 16	Sheared Laminated Feldspathic Mafic Rock of the Upper Part of the Batatal Formation. Mutuca Mine . . . . .	44
Fig. 17	Chemical Compositions of the Batatal and Piracicaba Potassic Peraluminous Schists Plotted As a Function of Log ( $\text{SiO}_2/\text{Al}_2\text{O}_3$ ) and Log ( $\text{Na}_2\text{O}+\text{CaO}/\text{K}_2\text{O}$ ) . . . . .	49
Fig. 18	Compositions of Batatal and Piracicaba Rocks In Relation to the Composition of Lutites Compared With Those of Igneous Rocks . . . . .	50
Fig. 19	Typical Relief Formed By the Itabiritic Terrain. Serras do Curral and Agua Quente . . . . .	59



Fig. 20	Distribution of the Itabirite Belts at the Junction Area . . . . .	61
Fig. 21	Laminated Itabirite . . . . .	62
Fig. 22	Itabirite Compositions As A Function of $\text{SiO}_2\text{-Al}_2\text{O}_3\text{-Fe}_2\text{O}_3$ . . . . .	63
Fig. 23	Weathered Amphibolite. Morro de Chapéu Road . .	75
Fig. 24	Possible Reaction Between A Partly Oxidized Magnetite and Chlorite . . . . .	77
Fig. 25	Cross-Section Through Serras do Saboeiro and Moeda . . . . .	81
Fig. 26	Stromatolites of the Collenia Type in the Gandarela Dolomite. Borges Quarry . . . . .	84
Fig. 27	White Quartzite With Thin Layers of Silver Sericite Schist. Cercadinho Formation. Barreiro Road . . . . .	87
Fig. 28	Black, Ferruginous Quartzite. Barreiro Road . .	88
Fig. 28b	Structural Map of the Junction Area . . . . .	102
Fig. 29	Block-Diagram Showing the Structure of the Study Area in Diagrammatic Form . . . . .	104
Fig. 30	Cross-Section Through Serras do Curral and Gaivotas . . . . .	108
Fig. 31	Mesoscopic Recumbent Fold Within Itabirite. Serra do Rola Moca . . . . .	109
Fig. 32	Slippage Along the $S_1$ -Surface in the Hinge Zone of a Mesoscopic Fold in Itabirite . . . . .	111
Fig. 32b	Cross-Section Through Serra do Curral-Barreiro, Showing the Curral Anticline . . . . .	113
Fig. 33	Isoclinal Similar Fold in Itabirite. Serra do Rola Moca . . . . .	114
Fig. 34	Mesoscopic Cascade Folds Within Itabirites Serra do Rola Moca . . . . .	115
Fig. 35	Tightly Folded Itabirite Showing S-Folds on the Upper Limb, and Fluxion in the Hinge Zone. Serra do Barreiro . . . . .	116

Mesoscopic Recumbent Similar Fold in Itabirite,  
Showing Reversed Fold in the Core. COMAG Tunnel,  
Gandarela Area. . . . . 141

Fig. 20	Distribution of the Itabirite Belts at the Junction Area . . . . .	61
Fig. 21	Laminated Itabirite . . . . .	62
Fig. 22	Itabirite Compositions As A Function of $\text{SiO}_2\text{-Al}_2\text{O}_3\text{-Fe}_2\text{O}_3$ . . . . .	63
Fig. 23	Weathered Amphibolite. Morro de Chapéu Road . .	75
Fig. 24	Possible Reaction Between A Partly Oxidized Magnetite and Chlorite . . . . .	77
Fig. 25	Cross-Section Through Serras do Saboeiro and Moeda . . . . .	81
Fig. 26	Stromatolites of the Collenia Type in the Gandarela Dolomite. Borges Quarry . . . . .	84
Fig. 27	White Quartzite With Thin Layers of Silver Sericite Schist. Cercadinho Formation. Barreiro Road . . . . .	87
Fig. 28	Black, Ferruginous Quartzite. Barreiro Road . .	88
Fig. 28b	Structural Map of the Junction Area . . . . .	102
Fig. 29	Block-Diagram Showing the Structure of the Study Area in Diagrammatic Form . . . . .	104
Fig. 30	Cross-Section Through Serras do Curral and Gaivotas . . . . .	108
Fig. 31	Mesosopic Recumbent Fold Within Itabirite. Serra do Rola Moca . . . . .	109
Fig. 32	Slippage Along the $S_1$ -Surface in the Hinge Zone of a Mesoscopic Fold in Itabirite . . . . .	111
Fig. 32b	Cross-Section Through Serra do Curral-Barreiro, Showing the Curral Anticline . . . . .	113
Fig. 33	Isoclinal Similar Fold in Itabirite. Serra do Rola Moca . . . . .	114
Fig. 34	Mesosopic Cascade Folds Within Itabirites Serra do Rola Moca . . . . .	115
Fig. 35	Tightly Folded Itabirite Showing S-Folds on the Upper Limb, and Fluxion in the Hinge Zone. Serra do Barreiro . . . . .	116

Fig. 35b	Mesosopic Recumbent Similar Fold in Itabirite, Showing Reversed Fold in the Core. COMAG Tunnel, Catarina Area. . . . .	117
----------	--	-----



Fig. 56	Contorted Slices of Competent Cherty Layers Within Itabirite Formed by Transposition of Bedding. COMAG Tunnel. Catarina Area . . . . .	142
Fig. 57	Bedding, Foliation and Lineation in the Curral-Gaivotas Structure . . . . .	144
Fig. 58	Breccia Showing Chert Fragments Within a Fine-Grained Matrix . . . . .	148
Fig. 59	S-Poles to Bedding. Gaivotas Syncline . . . . .	150
Fig. 60	S-Poles to Bedding. Upper Limb of the Catarina Anticline. Serra da Moeda . . . . .	151
Fig. 61	Geologic Map of the Tamandua Iron Ore Deposit. .	153
Fig. 62	Cross-Section Through the Moeda Syncline Showing the Tamandua Belts . . . . .	155
Fig. 63	S-Pole to Bedding. Serra do Tamandua, Western Belt . . . . .	156
Fig. 64	Kink-bands in Itabirite. Morro do Chapéu Road .	158
Fig. 65	Section of Gandarela-Caue Itabirite Formations, Morro do Chapéu Road, Western Tamandua Belt . .	159
Fig. 66	Cross-Section Through the Tamandua Ore Deposit Near Section 8800 . . . . .	161
Fig. 67	$L_1$ -and $L_2$ -Lineations and $B_1$ -and $B_2$ Fold Axes. Eastern Belt of Tamandua . . . . .	162
Fig. 68	Mesosopic Recumbent Cascade Folds With Sub-Horizontal Axial Planes. Eastern Tamandua . . .	163
Fig. 69	S-Pole to Bedding=Foliation. Eastern Tamandua .	165
Fig. 70	S-Pole to Bedding. Miguelao Dam . . . . .	168
Fig. 71	Map Showing the Distribution of the Subdomains in the Domain III . . . . .	170
Fig. 72	Moeda Quartzite With a Slice of Nova Lima Greenschist. Guarita . . . . .	173
Fig. 73	S-Pole to Foliation of Moeda and Nova Lima Rocks W-Subdomain . . . . .	175
Fig. 74	Deformational Picture of the Mutuca Overthrust .	178
Fig. 75	Recumbent Fold in the Axial Zone. M-Subdomain Mutuca Area . . . . .	179

Fig. 56	Contorted Slices of Competent Cherty Layers Within Itabirite Formed by Transposition of Bedding. COMAG Tunnel. Catarina Area . . . . .	142
Fig. 57	Bedding, Foliation and Lineation in the Curral-Gaivotas Structure . . . . .	144
Fig. 58	Breccia Showing Chert Fragments Within a Fine-Grained Matrix . . . . .	148
Fig. 59	S-Poles to Bedding. Gaivotas Syncline . . . . .	150
Fig. 60	S-Poles to Bedding. Upper Limb of the Catarina Anticline. Serra da Moeda . . . . .	151
Fig. 61	Geologic Map of the Tamandua Iron Ore Deposit. .	153
Fig. 62	Cross-Section Through the Moeda Syncline Showing the Tamandua Belts . . . . .	155
Fig. 63	S-Pole to Bedding. Serra do Tamandua, Western Belt . . . . .	156
Fig. 64	Kink-bands in Itabirite. Morro do Chapéu Road .	158
Fig. 65	Section of Gandarela-Caue Itabirite Formations, Morro do Chapéu Road, Western Tamandua Belt . .	159
Fig. 66	Cross-Section Through the Tamandua Ore Deposit Near Section 8800 . . . . .	161
Fig. 67	$L_1$ -and $L_2$ -Lineations and $B_1$ -and $B_2$ Fold Axes. Eastern Belt of Tamandua . . . . .	162
Fig. 68	Mesoscopic Recumbent Cascade Folds With Sub-Horizontal Axial Planes. Eastern Tamandua . . .	163
Fig. 69	S-Pole to Bedding=Foliation. Eastern Tamandua .	165
Fig. 70	S-Pole to Bedding. Miguelao Dam . . . . .	168
Fig. 71	Map Showing the Distribution of the Subdomains in the Domain III . . . . .	170
Fig. 72	Moeda Quartzite With a Slice of Nova Lima Greenschist. Guarita . . . . .	173
Fig. 73	S-Pole to Foliation of Moeda and Nova Lima Rocks W-Subdomain . . . . .	175
Fig. 74	Deformational Picture of the Mutuca Overthrust .	178
Fig. 75	Recumbent Fold in the Axial Zone. M-Subdomain Mutuca Area . . . . .	179



Fig. 76	Geologic Map of the Mutuca Mine . . . . .	181
Fig. 77	Mesoscopic Recumbent Folds in Itabirite Along the Mutuca Fault. Mutuca Mine. . . . .	183
Fig. 78	Rootless Intrafolial Folds, extension and Fold Hinge Disruption. Mutuca Mine. . . . .	184
Fig. 79	Sets of $L_2$ -Lineation Deform $L_1$ -Lineation on $S_0$ -Surface of Itabirite. Mutuca Mine . . . . .	185
Fig. 80	Lineation, Fold Axes, Quartz Rods, Kink Planes, Cleavage in Itabirites. Mutuca Mine. E-Subdomain . . . . .	187
Fig. 81	S-Pole to Foliation=Bedding in Itabirite. Mutuca Mine. E-Subdomain. . . . .	188
Fig. 82	Cross-Section Through Section 1050. Mutuca Mine . . . . .	190
Fig. 83	Cross-Section Through Section 100. Mutuca Mine . . . . .	190
Fig. 84	Recrystallization of Coarse-Grained Quartz Within Shear Zones. Serra da Mutuca. . . . .	191
Fig. 85	Hematite Filling Tear Fault Truncating Thrust Fault. Mutuca Mine. . . . .	191
Fig. 86	S-Pole to Bedding in Itabirite From the Caveiras Anticline. Domain IV. . . . .	194
Fig. 87	S-Poles to Bedding in Itabirite From Morro do Barreiro . . . . .	196
Fig. 88	Geologic Map of the Capao do Xavier Hematite Deposit . . . . .	197
Fig. 89	S-Pole to Foliation in Micaceous and Laminated Hematite From Capao do Xavier . . . . .	199
Fig. 90	Fold in Itabirite With the Axis Oriented Horizontally ( $L_2$ ). Capao do Xavier . . . . .	200
Fig. 91	Quartz-Filled Tension Gashes Exhibiting Relative Sense of Motion. North of Xavier. . . . .	201
Fig. 92	Contact Zone Between the Nova Lima Greenschist and Moeda Quartzite. North of Xavier . . . . .	202
Fig. 93	Metamorphic Grade of Itabirite by Quartz Grain- Size, As Used in Classification of Michigan Iron-Formation . . . . .	206

# MAPS

(in the pocket)

Map 1 Geologic Map of the Junction of the Moeda and Curral Structures, Quadrilatero Ferrifero, Minas Gerais, Brazil.

Map 2 Geologic Map of the Junction of the Moeda and Curral Structures, Quadrilatero Ferrifero, Minas Gerais, Brazil (overlay).



In the map area the rocks are divided into two large subdivisions: the Archaean Nova Lima greenstone and the Bonfim granitoid gneisses, and the overlying Proterozoic Minas metasedimentary and metavolcanic rocks, including abundant iron formation. These groups are separated by a major unconformity. These new studies in the Minas Series culminated with the following results: reassignment of the conglomerate-quartzite sequence of the Mutuca area to the Moeda Formation rather than to the Nova Lima Group; identification of a suite of greenstones and peraluminous potassic schists in the Batatal and Gandarela Formations and Piracicaba Group; recognition of the riebeckite in one of the itabirite sequences; and redefinition of the Gandarela Formation through the identification of stromatolites and greenstones.

The structure of the junction of the Curral and Moeda structures consists of two elements: on the north is the recumbent northeast-trending Curral anticline with its lower limb faulted against Archaean Nova Lima rocks, and the upper limb deformed into the Moeda syncline to the south. In the south, the westward overturned Moeda syncline trends north-south, with both of the limbs strongly deformed. The western limb is folded into recumbent folds indicating a northerly transport direction. The eastern limb has become rotated westward during thrusting until now it is overturned by Nova Lima greenstones. This overturned limb of the Moeda syncline is separated from the Curral anticline by the Barreiro-Agua Quente zone of tear faults. The features demonstrate

two major phases of deformation, the earlier  $D_1$  with a north-westward vergence and the later  $D_2$ -episode, with a westward vergence.

Extensive development of quartz and muscovite in the sediments and of chlorite and talc in the mafic and ultramafic greenstones, and the quartz grain-size in itabirite, in general, smaller than 0.1 mm are indicative of low-grade metamorphism in the area. The Quadrilatero Ferrifero and the Michigan iron ore district show similarities in the occurrence of peraluminous potassic schists indicated by the  $\log(\text{SiO}_2/\text{Al}_2\text{O}_3) - (\text{Na}_2\text{O} + \text{CaO}/\text{K}_2\text{O})$ -diagrams, the presence of greenstones, the strain-induced quartz grain-size variation in itabirites, and the basement controlling tectonics.



## EXPANDED ABSTRACT

In the study area the rocks are divided into two large subdivisions: the Archaean Nova Lima greenstones and Bonfim granitoid gneisses, and the overlying Proterozoic Minas meta-sedimentary and metavolcanic rocks including abundant itabirite or iron formation. These Series are separated by a major unconformity. The Nova Lima rocks, correlatable with the Barbacena Group, consist dominantly of mafic and ultramafic metavolcanic rocks with minor quartzitic chert, graphitic schist, itabirite and graywackes. The Minas Series is divided into three Groups, from bottom to top: Caraca, Itabira and Piracicaba.

The Caraca Group is subdivided into the basal Moeda Formation with abundant, poorly sorted conglomerate, quartzite, grit and quartz schist, and the Batatal Formation which consists of two units: a basal, boron-rich peraluminous potassic schist and an overlying greenstone unit composed of chlorite talc schist, serpentinite and amphibolites with sporadic dolomite lenses. The Itabira Group is subdivided into the lower Caue Itabirite composed of siliceous itabirite, magnetite itabirite and riebeckite itabirite, and the overlying Gandarela Formation composed of greenstone (magnetite chlorite talc schist) with dolomite lenses, frequently exhibiting stromatolitic structures and amphibolite. The Piracicaba Group consists of ferruginous and white quartzite, peraluminous potassic schist interlayered in thin beds and lenses, graphitic phyllite, dolomite lenses and magnetite chlorite schist, the later corresponding to layered metavolcanic rocks.

The present studies of the Minas Series culminated with the following results: reassignment of the conglomerate-quartzite sequence of the Mutuca area to the Moeda Formation rather than to the Nova Lima Group; identification of a suite of greenstones and peraluminous potassic, tourmaline-rich schists in the Batatal and Gandarela Formations and Piracicaba Group; recognition of the riebeckite in one of the itabirite sequences; and redefinition of the Gandarela Formation through the identification of stromatolites and greenstones. The potassic tourmaline-rich schists may have originated through the deposition of potassium-boron-rich brines in restricted basin, perhaps with some volcanic contributions.

The main objective of this thesis is the interpretation of the structure of the area where the overturned north-south trending Moeda syncline abuts the recumbent, northeast trending Curral anticline, in a nearly orthogonal pattern. This thesis represents the first study for this area of the deformational style and the sequence of deformational events. This junction area consists of two major structural elements: on the north is the northwest-overturned recumbent Curral anticline with its lower limb faulted against Archaean Nova Lima and Sabara rocks. To the south, structurally on the upper limb of this anticline, is the westward-overturned Moeda syncline. The geometry is allowed by a tear fault that separates the east limb of the syncline from the anticline. The linear Curral and Moeda structures reflect zones of discontinuity between the granitoid basement blocks to the north (Belo Horizonte Complex), to the west (Bonfim Complex), and the Nova Lima greenstones to the east.



The western or lower limb of the Moeda syncline contains recumbent folds with their fold axis plunging gently to the east, similar in geometry to the Curral anticline on the north, and representing northerly transport direction ( $D_1$ ). The eastern limb has become rotated westward during later thrusting ( $D_2$ ) until it is now overlain by Nova Lima greenstones. This overturned limb of the Moeda syncline is separated from the Curral anticline by the Barreiro-Agua Quente zone of tear faults. Detailed geometric analysis of the field data reveal that the deformation proceeded through the two main episodes  $D_1$  and  $D_2$ , perhaps almost synchronously.

Extensive development of quartz and muscovite in the sediments and of chlorite and talc in the mafic and ultramafic greenstones are indicative of low-grade metamorphism in the area. The study of the regional variation of quartz grain-size in itabirite (generally smaller than 0.1 mm) is indicative also of a low metamorphic grade, and local variation in grain-size can be related to differences in strain.

The Quadrilatero Ferriifero and the Michigan iron ore District show similarities in the general ages, petrographic character of the sedimentary rocks, the occurrence of iron formations and of peraluminous potassic schists indicated by the  $\log (SiO_2/Al_2O_3) - (Na_2O+CaO/K_2O)$  diagrams, the presence of greenstones, strain-induced quartz grain-size variation in itabirites, and basement-controlled tectonics.

## ACKNOWLEDGMENTS

Financial support for this thesis project has come from several sources. The academic year of 1974-75 was supported by an Organization of American States fellowship, and by the CBA-Companhia Brasileira de Amianto (SANO). The subsequent years (1975-77) were sponsored by a scholarship from the CAPES-Coordenacao Aperfeicoamento de Pessoal de Nivel Superior (proc. No. 177/75), Brazilian Government. The 1975 and 1976 winter-spring field work was made possible through the financial help of CAPES, MBR-Mineracoes Brasileiras Reunidas and CBA-SANO. During the winter and spring of 1978-1979 the thesis preparation was supported by a Graduate Research Assistantship from the Department of Geology and Geological Engineering of Michigan Technological University.

The financial assistance of CBA-SANO was possible mainly by Dr. Oscar Sjostedt, President of the company. The majority of the assistance and encouragement was provided by Dr. Jorma Kalliokoski, my advisor, who oriented the study, materially assisted in its beginning, and gave encouragement during the field and laboratory investigations. Many thanks are also to Drs. Albert P. Ruotsala, who helped the author in the identification of minerals in XRD-charts, to Brent Hamil for his interest and helpful comments, to Donald C. Noble and S. Douglas McDowell who clarified some points on metamorphism, to Nancy Scofield for instruction and supervision on quantitative analysis with the electron microprobe, to Stephan C. Nordeng for his help concerning



the stratigraphy and for his critical review of the thesis, to William I. Rose, Jr. for instruction and supervision on analysis with the AAS and discussion on petrology, all Michigan Technological University faculty members.

The author would like to express his gratitude to Dr. J. E. Gair of the U.S.G.S. for agreeing to assist as an outside examiner, and for his constructive comments.

During the field work, Dr. Oscar Tessari, geologist of MBR provided valuable material support as well as discussed with the author several points which benefited the study. Thanks are also extended to Drs. Claudio M. Mendes and Jose M. de Sousa of MBR for access to drill cores, drill information, chemical analysis and base map of Mutuca and Tamandua mines.

Many thanks to Prof. M. Lougheed who showed and explained the variation of structures and textures in thin section of iron formations of U.S. and Canada in his collection at Bowling Green; to Dr. S. S. Goldich who was a particularly helpful field-trip leader and took time to show important field relationships in the Gunflint iron formation in Canada and Minnesota.

The author is indebted to the fellow graduate students at Michigan Technological University for their helpful discussion and assistance throughout the research. The writer is grateful to Mr. Nilo Mello of MBR in helping during field work in the winter-spring of 1977, to Mr. Robert R. McCarthy for sample preparation, to Miss Julene Erickson for typing the first draft of the manuscript, to Mrs. Barbara Bohnstadt for typing the final copy, to Miss Margaret Hartshorn of Photo Services of MTU for photographic work.

The author would like to thank his wife Liege and family for their support, help and encouragement during the study.

## 1.1 GEOGRAPHY

The study area, about 135 sq. km in extent, is located in the southwestern corner of the Quadrilátero Ferrífero, in the southcentral part of the State of Minas Gerais, Brazil. The area includes the eastern part of the Serra da Curral, and the western part of the Itabirite Quadrangle. The Quadrilátero Ferrífero is an area of some 7000 sq. km.

It is famous for its iron deposits, but also contains deposits of gold, bauxite, manganese and imperialite.

The Quadrilátero Ferrífero is limited by four mountain ranges forming approximately a large quadrangle:

1. Serra da Curral, Moeda, Ouro Branco and Caraca respectively

to the north, west, south and east. These mountain ranges

form a part of the 1500 km-long Serra do Espinhaço which

crosses the states of Minas Gerais and Bahia.

Geologically the area is among the highest parts of

the country, and forms the watershed for the São Francisco

hydrographic system. The higher elevations ranging

from 1200 to 1500 m. form sharp ridges or gentle plateaus

mainly on Itabirites and quartzites, while the lower lands

are composed of schists, gneisses and phyllites. Weathering has been

extensive in the rocks, especially in the argillaceous and felsic

types; the Gandarela and Batatal sheared mafic feldspathic

rocks were kaolinized, and transformed into bauxite at the

surface. Itabirites were weathered and enriched to more than



## INTRODUCTION

### LOCATION AND GEOGRAPHY

The study area, about 155 sq. km in extent, is located at the northwestern corner of the Quadrilatero Ferrifero (Fig. 1), in the southcentral part of the State of Minas Gerais, Brazil. The area includes the eastern part of the Macacos and the western part of the Ibirite Quadrangles. The Quadrilatero Ferrifero is an area of some 7000 sq. km, especially famous for its iron deposits, but also containing important deposits of gold, bauxite, manganese and imperial topaz. The Quadrilatero Ferrifero is limited by four mountain ridges forming approximately a large quadrangle: Serras do Curral, Moeda, Ouro Branco and Caraca respectively on the north, west, south and east. These mountain ridges constitute part of the 1600 km-long Serra do Espinhaco which crosses the states of Minas Gerais and Bahia.

Morphologically the area is among the highest parts of the country, and forms the watershed for the San Francisco and Doce hydrographic systems. The higher elevations ranging from 1200 to 1600 m form sharp ridges or gentle plateaus dominantly on itabirites and quartzites, while the lower lands are on schists, gneisses and phyllites. Weathering has been deep in the rocks, especially in the argillaceous and feldspathic types: the Gandarela and Batatal sheared mafic feldspathic rocks were kaolinized, and transformed into bauxite at the surface. Itabirites were weathered and enriched to more than

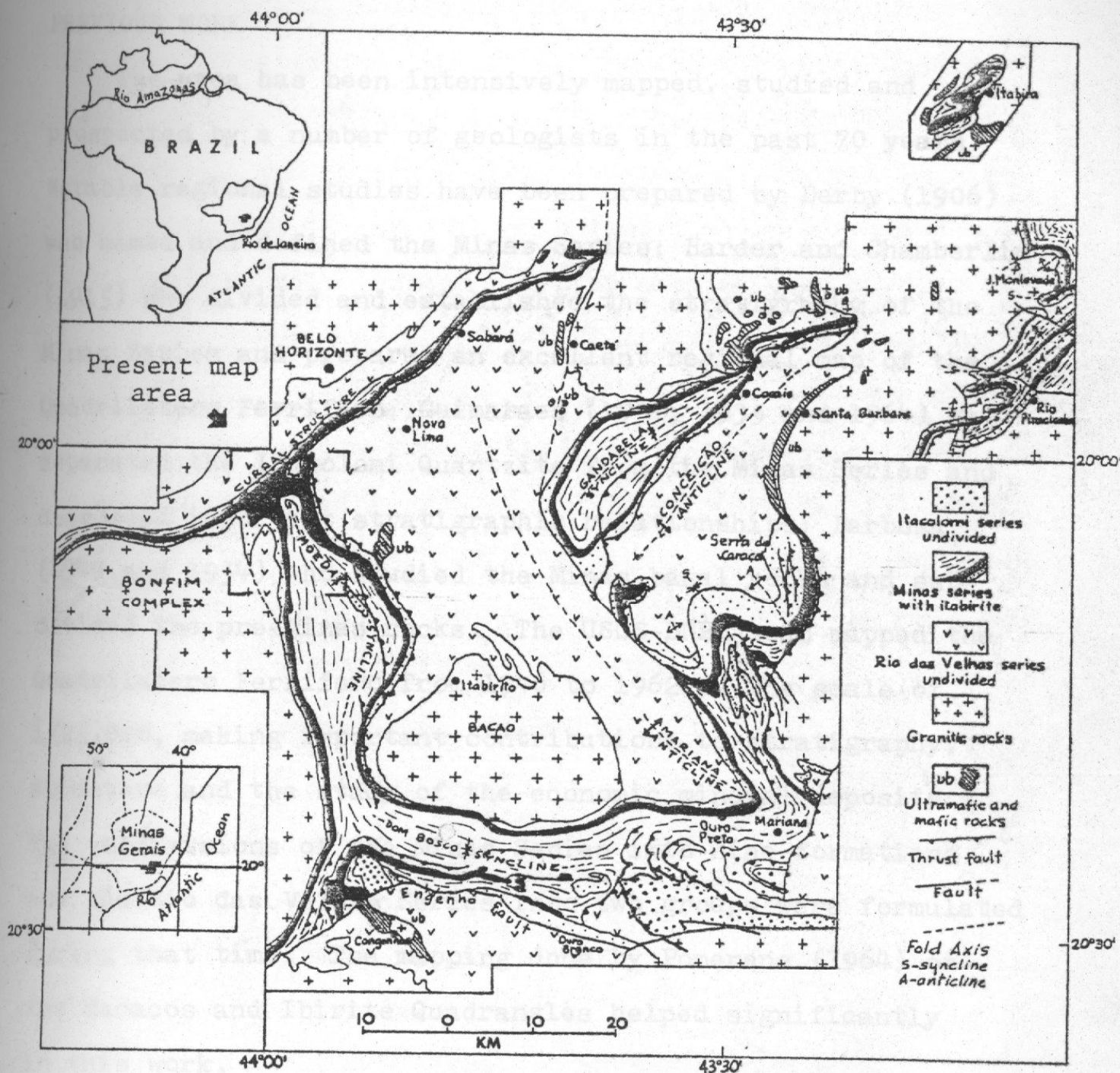


Fig.1-Geologic map of the Quadrilátero Ferrífero, Minas Gerais, Brazil. (Modified from Dorr, 1969). showing location of present map area.



200 m below the surface, but on the other hand they also form the highest parts of the relief.

#### PREVIOUS WORK

The area has been intensively mapped, studied and prospected by a number of geologists in the past 70 years. Notable regional studies have been prepared by Derby (1906) who named and defined the Minas Series; Harder and Chamberlin (1915) who divided and established the stratigraphy of the Minas Series and prepared an excellent regional map of the Quadrilatero Ferrifero; Guimaraes (1931, 1935 and 1964) who separated the Itacolomi Quartzite from the Minas Series and discussed important stratigraphic relationships; Barbosa (1949 and 1954) who studied the Minas basal rocks and subdivided the pre-Minas rocks. The USGS-DNPM team mapped the Quadrilatero Ferrifero from 1946 to 1962 on the scale of 1/25,000, making important contributions to stratigraphy, structure and the study of the economic mineral deposits. The subdivisions of the Minas Series into nine formations and the Rio das Velhas Series into two groups were formulated during that time. The mapping done by Pomerene (1964) on the Macacos and Ibirite Quadrangles helped significantly in this work.

#### SCOPE OF PRESENT STUDY

The author worked in this area for a total of 9 months during the years 1975, 1976, and 1977. The structural and lithologic field data were mapped at a scale of 1/25,000 for macroscopic analysis, and at 1/2,000 for the detailed studies

by plane table at Capao do Xavier, Tamandua and Mutuca iron ore deposits. Particular outcrops of critical areas were studied in detail, and structural cross sections were prepared in order to determine the overall structural relationships. Approximately 1400 structural fabric data points from both the regional and detailed studies were plotted on a Schmidt equal area net. Sixty-four thin sections and 36 polished sections from selected and oriented samples were studied to aid in the structural interpretation, and to obtain petrographic information. About 50 additional slides were studied by powder optical methods. About 22 X-ray diffraction mounts were prepared of fine-grained rocks and minerals. Fifteen rocks were analysed for major and minor elements by the AAs and XRF techniques, and eight riebeckites have been analysed by electron microanalysis methods (Maps 1 and 2).

#### CONTRIBUTIONS BY THE PRESENT AUTHOR

Mapping of critical areas on a scale of 1/25,000 gave the author the background data to make the following contributions to stratigraphy and structure.

1. Reassignment of quartzites and conglomerates previously assigned by Pomerene (1964) to the Nova Lima Group in the Guarita and Ribeirao da Mutuca areas to the Moeda Formation.
2. Identification of a suite of greenstones and amphibolites in the upper part of the Batatal Formation, and of boron- and potassium-rich aluminous schist in the lower part, and the establishment of a possible stratigraphy for the Formation.



3. First description and petrographic study of riebeckitic itabirite in the Quadrilatero Ferrifero.
4. Study of the grain-size variation in itabirites, and its correlation with structural position.
5. Comprehensive study and redefinition of the Gandarela Formation, including the positioning of dolomites within the Ribeirao do Mata Porcos, and the discovery of stromatolitic dolomites of the Collenia type within the greenstone sequence.
6. Recognition for the first time of regional polyphase deformation: a  $D_1$ -deformational episode which resulted in a succession of northward recumbent folds (Curral fold), followed by a  $D_2$ -deformational phase of westward thrusting (Moeda syncline). Instead of the structural relationship postulated by Pomerene (1964) and Dorr (1969) to exist between the Curral and Moeda structures, the writer is able to fit together many structural features previously unrecognized or not correlated, which provides a much more satisfactory geometric and temporal explanation for this structural complexity.

#### REGIONAL GEOLOGY

The metasedimentary and metavolcanic rocks of the Quadrilatero Ferrifero are divided into three series, from oldest to youngest: Rio das Velhas, Minas and Itacolomi (Table 1). Structurally the Quadrilatero Ferrifero consists of a rectangular, regional array of linear belts dominated by rocks of the Minas Series and bounded laterally by remobilized granitic-greenstone basement terrains (Fig. 1).

Table 1

Table of Formations  
(Modified from Dorr, 1969)

Absolute Ages (m.y.)	Group	Formation	Lithology
M I D D L E  1350  Minas Series   			



On the north the Quadrilatero Ferrifero is dominated by a northward overturned anticline. This is the northeast-trending, 150 km-long Curral structure. This anticline is abutted in the present map-area by the 50 km-long, north-south trending and westward overturned Moeda syncline, the main focus of the present work (Figs. 1 and 2).

The east limb of the Moeda syncline has a series of east-dipping thrust faults along almost its entire length, and the contact with the greenstone basement in many segments is structural rather than an unconformity.

The south end of the Moeda syncline splits in the Congonhas area, eastward into the Dom Bosco syncline, and westward into a complex system of east-dipping thrust faults (Guild, 1957). The Dom Bosco syncline is a very complex structure, between the Bacao Complex on the north, and the southern Congonhas-Lafaiete massif on the south. In the Ouro Preto area are numerous thrust sheets that have moved westward, truncating the Dom Bosco syncline (Barbosa, 1968). Thus, throughout the Quadrilatero Ferrifero there is evidence of both north-south compression and thrusting to the west. Obviously the large basement massifs were important elements in the evolution of these structures.

#### GENERAL STRUCTURE

The area encompasses the region in which the northeast-trending Curral anticline joins the north-northwest-trending Moeda syncline. The main structural feature associated with the Curral recumbent anticline is the frontal Curral thrust

fault. The syncline consists mostly of rocks of the Minas Series, and is overturned to the west (Dorr, et al., 1960), against the older Bonfim batholith by westward thrusting of the pre-Minas basement rocks (Nova Lima Group and Bacao Mantled Gneiss) (Fig. 2). The Bonfim Gneiss is strongly cataclastic along its contact with the Caraca Conglomerate. On the east, the contact with the pre-Minas greenstone basement is marked by thrust faults.

The main structure is thus a northeast-trending overturned anticline on the north whose south limb merges with a north-south syncline overturned to the west. The geometry is permitted because the eastern overturned limb of the syncline is separated from the south limb of the anticline by an east-west tear fault.

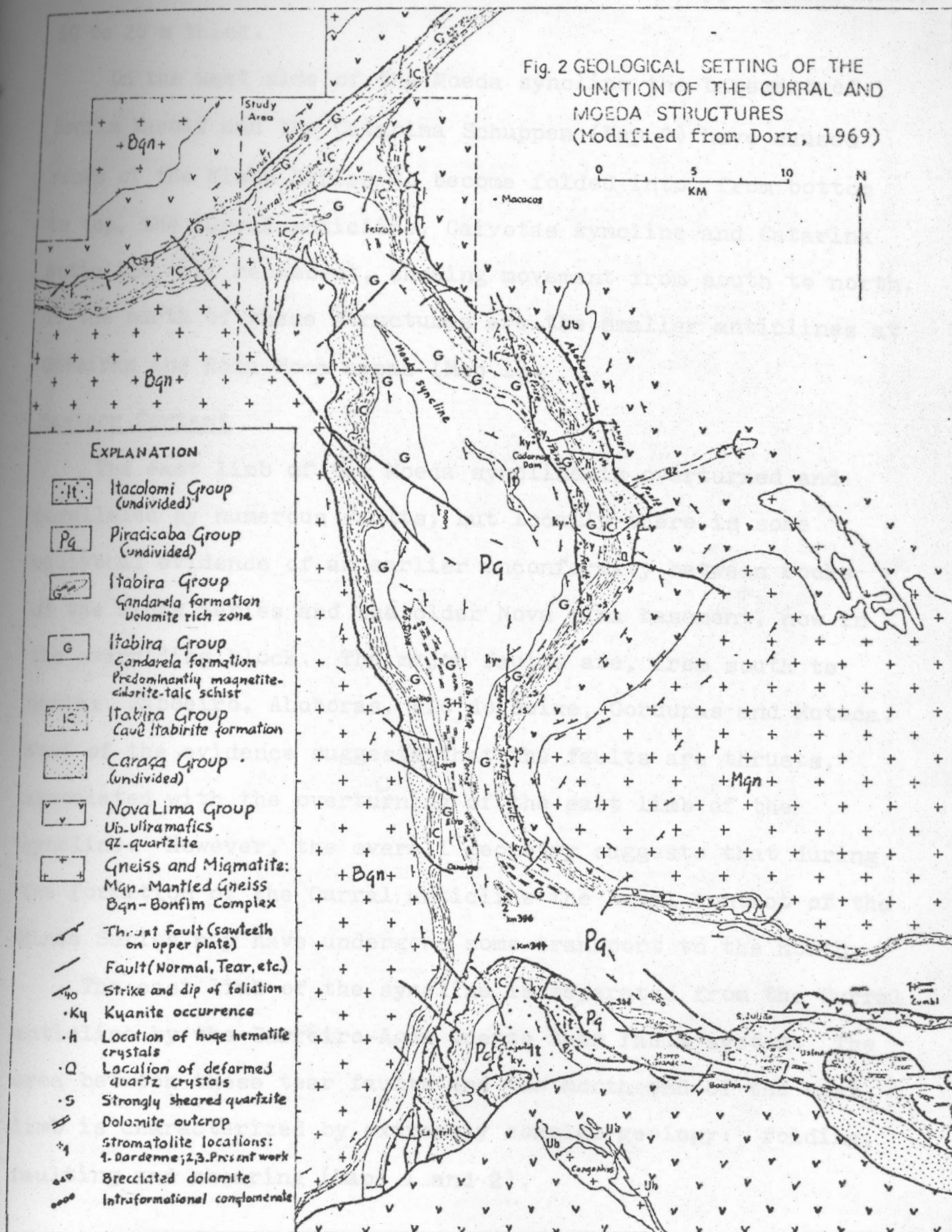
#### Western Contact

The remarkably straight contact for some 50 km, between rocks of the Bonfim Complex and the Moeda Syncline, and the parallelism between the foliation in the gneiss and the deformed bedding in the overlying Caraca Group is an indication of considerable movement along the contact, whether from north to south during the early stage of deformation, or east to west at the later stage (Fig. 2). Herz (1978) believes that shearing along this contact was responsible for the younger  $K^{40}/Ar^{40}$  ages within this zone.

Along the contact the Bonfim Gneiss shows extensive cataclasis and mylonitization. The mylonite zone ranges from 15 to 200 m thick, locally exhibiting elongate rods and flattened clots of former feldspar porphyroblasts, as well as extensive kaolinitization along it. Along this contact zone there are



Fig. 2 GEOLOGICAL SETTING OF THE  
JUNCTION OF THE CURRAL AND  
MOEDA STRUCTURES  
(Modified from Dorr, 1969)



several strongly laminated slices of Nova Lima-type greenschist, 10 to 20 m thick.

On the west side of the Moeda syncline the basement of Bonfim Massif and the Catarina Schuppen (Map 2) have caused rocks of the Minas Series to become folded into, from bottom to top, the Curral anticline, Gaivotas syncline and Catarina anticline, all recumbent, showing movement from south to north. To the north of these structures are the smaller anticlines at Caveiras and Rola Moca areas (Map 1).

#### Eastern Contact

The east limb of the Moeda syncline is overturned and paralleled by numerous faults, but locally there is some equivocal evidence of an earlier unconformity between rocks of the Minas Series and the older Nova Lima basement, now in the overriding block. The major faults are, from south to north: Saboeiro, Aboboras, Rio do Peixe, Gorduras and Mutuca. Most of the evidence suggests that the faults are thrusts, associated with the overturning of the east limb of the syncline. However, the overall geometry suggests that during the formation of the Curral anticline the basal contact of the Minas Series may have undergone some transport to the north.

The east limb of the syncline is separated from the Curral anticline by the Barreiro-Agua Quente tear fault system. The area between these tear faults and the north end of the east limb is characterized by extremely complex geology: folding, faulting and shearing (Maps 1 and 2).



The location of the Saboeiro thrust fault (Fig. 3) was probably controlled by the relative position of the Bacao mantled gneiss dome and the Nova Lima schist. An almandine-rich biotite schist exists where the thrust fault is in contact with Caraca quartzite, and kyanite disseminated in the Piracicaba phyllite has been recognized at both ends of this fault zone. Near the northern end of the Saboeiro thrust fault, at Ribeirao da Agua Quente is a perennial warm spring with temperatures around 25<sup>0</sup>C.

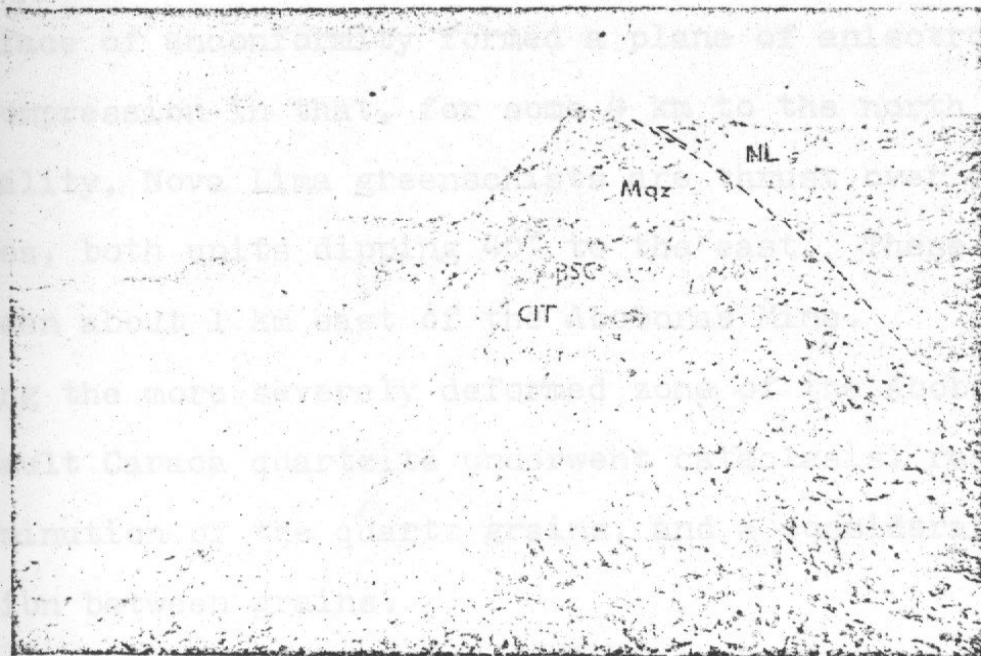


Fig. 3. Saboeiro thrust fault, showing the Nova Lima (NL) greenschist over Minas rocks; Mqz: Moeda quartzite; BSC: Batatal schist; CIT: Caue itabirite Serra do Saboeiro, eastern flank of the Moeda Syncline. The quartzite is about 60 m thick.

The Rio do Peixe thrust fault runs 2 to 3 km west of, and parallel to, the Aboboras thrust fault, passing near Pico do Itabirite ore deposit, the Codornas dam, Rio do Peixe Village,

Serra do Gama, along Corrego do Marimbe and near the Macacos village. At Serra do Gama the Rio do Peixe thrust fault produced in the Caraca rocks a very complex and poorly understood structure, probably due to a combination of thrusting and wrench fault movement. Where the fault zone intercepts the itabirite at Serra do Gama, rich powdery and compact hematite ore bodies have been formed.

In an area near the central part of the Aboboras thrust fault Rynearson and others (1954) reported an unconformity between the Minas Series and the Nova Lima Group. Apparently this surface of unconformity formed a plane of anisotropy during compression in that, for some 4 km to the north of this type locality, Nova Lima greenschists are thrust over Caraca quartzites, both units dipping  $40^{\circ}$  to the east. These details can be seen about 1 km east of the Aboboras Mine.

Along the more severely deformed zone of the Aboboras thrust fault Caraca quartzite underwent cataclasis, resulting in a comminution of the quartz grains, and a considerable loss of cohesion between grains.



## STRATIGRAPHY

### INTRODUCTION

In order to obtain better data on the structure of the area it was found necessary to remap the geology. The new data on the stratigraphy is discussed below (Table 1). Probably the most important discovery by the writer is that to the northwest of the Curral anticline the strata should not be assigned to the Sabara Formation but to the Nova Lima Group. This interpretation helped to clarify the structural relationships.

### BASEMENT ROCKS

For purposes of this study the Archaean basement rocks need not be described in detail. They consist of the Nova Lima Group of metavolcanic and metasedimentary rocks, possibly resting on granite and granitoid gneisses. Both rock types outcrop in basement highs, marginal to the narrow belts consisting of younger Precambrian rocks.

#### Bonfim Gneiss

Barbosa (1954) demonstrated the major subdivisions of the Brazilian Archaean to be the ancient Mantiqueira Series composed of migmatites and gneisses such as the Bonfim Gneissic Complex, and a younger overlying Barbacena Series (Table 1). Later Dorr and others (1957) defined the Rio das Velhas Series as comprising a lower Nova Lima Group, which they believed to be similar to the Barbacena rocks, and an upper Maquine Group. The latter does not occur in the study area and these writers described a discordance between the Rio das Velhas Series and the overlying

Minas Series. The migmatites and gneisses of the Bonfim Complex are generally medium to coarse in grain size, commonly strongly foliated, and locally contain mafic paleosomes. In the map area it is not possible to demonstrate that the Bonfim Gneiss is older than the Nova Lima rocks. What is apparent is that the gneiss was folded and reactivated with the Nova Lima rocks, many times.

The Bonfim granite-gneiss was formed apparently at about 2,300 m.y. ago, and successively reworked at about 1,930 m.y., 1,000 m.y., and 500 m.y. (Herz, 1970).

#### Nova Lima Group

Regionally the Nova Lima Group is composed of a large variety of greenstones, greenschists, serpentinites, talc schists, amphibolites, iron formation, graphitic schists, tourmalinites, cherty quartzites, manganese formation and minor sericite schists and graywackes. In the study area, Nova Lima rocks occur only in the northeastern, northwestern and southwestern corner and consist of weathered greenschists, cherty quartzites, sheared metavolcanics, and sericite schists. These rocks generally form the lowlands. At the eastern flank of the Moeda structure they occur in the block that overthrusts the Minas Series rocks.

Rb/Sr age dates for the Rio das Velhas rocks fall in the range of 2,790 and 2,400 m.y. (Herz, 1970). The Barbacena or Nova Lima rocks, in the Lafaiete District, 100 km south of the study area, were strongly deformed, intruded by synkinematic granodiorites, migmatized, and cut by at least two generations



of granite and pegmatites. No such younger intrusive rocks were noted in the present area.

Structurally these Archean rocks are important for two reasons: 1) the Moeda syncline occurs near the general boundary between gneisses on the west and greenstone on the east, and 2) the greenstones were much more ductile than the gneisses, thereby forming the overriding block.

#### MINAS SERIES

The Proterozoic rocks of the Quadrilatero Ferrifero, containing the itabirites, were first described and named by Derby (1906) as Minas Series which comprise part of a "schistose series of the Serra do Espinhaco". The Minas Series was subdivided into Caraca Quartzite, Batatal Schist, Itabira Iron Formation, Piracicaba Formation and Itacolomi Quartzite by Harder and Chamberlin (1915). The Itacolomi Quartzite was separated from the Minas Series and elevated to Series category by Guimaraes (1931). The remaining part of the Minas Series has become subdivided into nine formations: the Moeda Formation (Wallace, 1958) and the Batatal Formation (Maxwell, 1958) which comprise the Caraca Group; the Caue Itabirite and the Gandarela Formations (Dorr, 1958) which comprise the Itabira Group; and the Cercadinho, Tabooes and Barreiro Formations (Pomerene, 1958), Fecho do Funil Formation (Simmons, 1958), and Sabara Formation (Gair, 1958) which comprise the Piracicaba Group.

The present writer has adopted all of these stratigraphic subdivisions. It was not found necessary to subdivide the Piracicaba Group in this work (Table 1).

The deposition of the Minas Series seemingly occurred later than 1,930 m.y. according to Herz (1970).<sup>1</sup>

#### Caraca Group

In the Moeda syncline, the base of the structure is outlined by the clastic units of the Caraca Group, (Harder and Chamberlin, 1915, and Dorr and others, 1957) at the Serra do Caraca, about 50 km east of the study area. As originally described at the type locality on Serra do Caraca by Harder and Chamberlin (1915), these basal clastic rocks of the Minas Series were named the Caraca Quartzite (below) and Batatal Schist (above). Later, at Serra da Moeda the Caraca Quartzite, renamed the Moeda Formation (Maxwell, 1958), was subdivided into three members, and the Batatal Schist was renamed the Batatal Formation. Dorr (1969) redefined the Caraca Group, proposed to maintain its type locality at the Serra do Caraca, and postulated that the Moeda Formation occurs in two intergradational facies.

It appears possible to recognize the three members of the Moeda Formation only at Serra da Moeda, (Fig. 5, Sec. 7), because of lateral variations in lithology which also correspond to changes in thickness. Hence, members will be designated only at that one locality. In this thesis the Batatal Formation is redefined and several new lithologic types described within it.

It should be noted that the sedimentary rocks have undergone dynamothermal metamorphism to about greenschist facies.

---

<sup>1</sup>The similarity between the reactivation of the basement rocks and the age of the iron bearing sequence here and in Michigan is noteworthy (e.f. Sims, 1976).



Pebbles are commonly elongated, all strata are sheared or deformed to some degree parallel to bedding, and in thin sections the rocks exhibit similar evidence of deformation and alteration, grain growth, and grain deformation. Thus, it has not been possible to find many primary sedimentary features that would be useful in determining more precisely the nature and origin of the various sedimentary rocks.

## Moeda Formation

### Definition

The Moeda Formation exhibits a characteristic outcrop against the underlying, more subdued Nova Lima Schists (Fig. 4).



Fig. 4. Basal contact of the quartzose Moeda Formation (left) with Nova Lima greenschist, which shows a gentle relief. Casa de Pedra, western flank of Serra da Moeda.

Dorr (1969) redescribed the Moeda Formation as containing two intergrading facies: 1) "A more prominent coarse-grained facies composed of quartzite, grit, conglomerate, and phyllite, which averages in thickness more than 300 m, and the maximum apparent thickness greater than 1000 m; 2) a thinner, usually less than 700 m thick, fine-grained facies, which is peripheral to the coarser facies has been mapped in the eastern, western, southern, and northern extremities of the Quadrilatero Ferrifero region. Quartzite is more evenly grained and finer-grained, and in many localities is very phyllitic, and phyllite in separate beds and members has not been found."

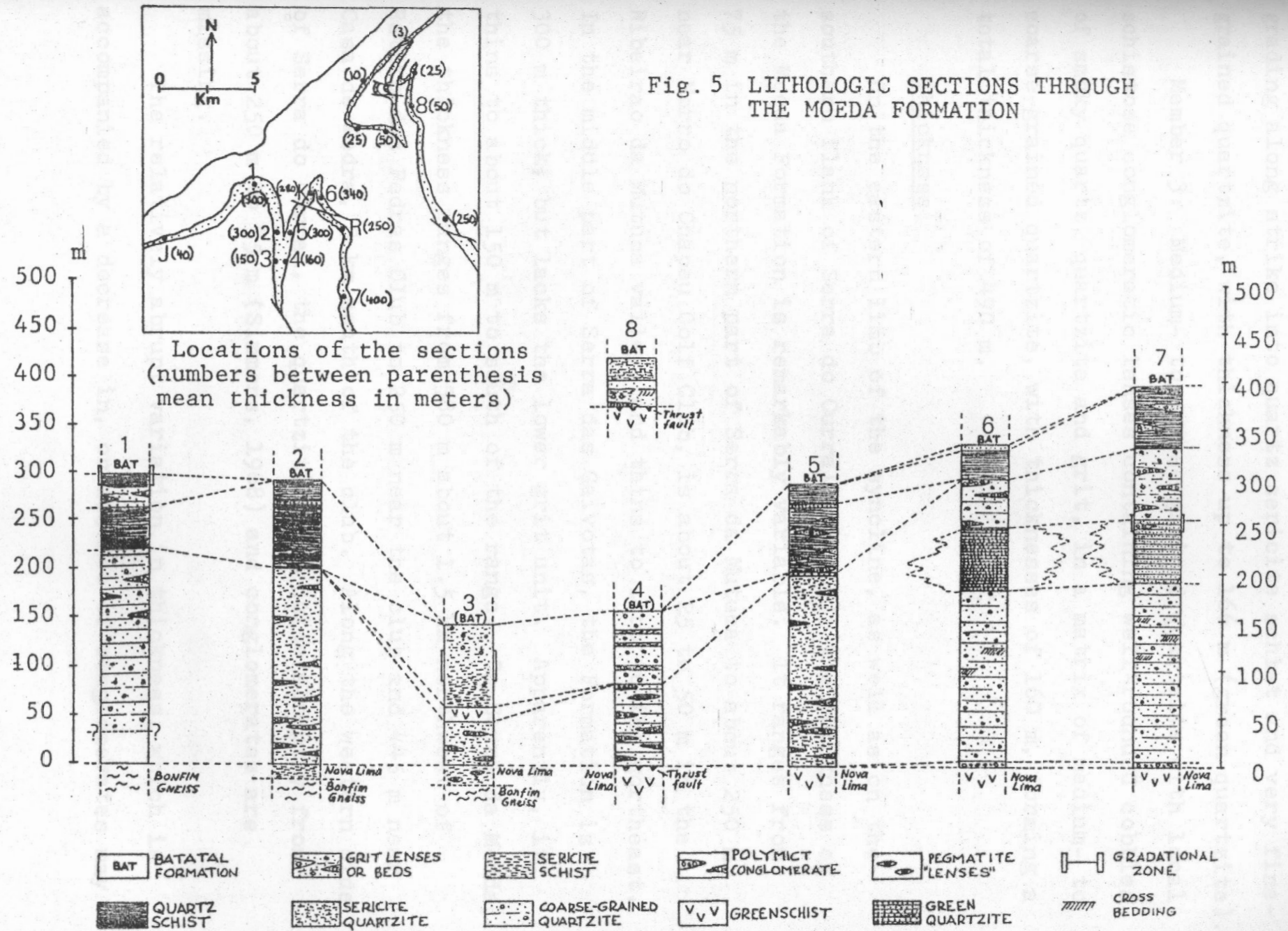
This writer has found that this model is not sufficiently precise for work on the local scale, and his more restricted observations appear below.

The Moeda Formation, composed predominantly of quartz-rich, clastic rocks, was divided into three members by Wallace (1958) on the west limb of the Moeda Syncline, in the Pico do Itabirite District. These members can be identified also in the present area, but only on the west limb of the Moeda syncline, (Fig. 5, Section 7):

Member 1 (lowermost): Medium- to coarse-grained quartzite, as much as 165 m thick, some beds being argillaceous and sericitic and some pure; a schistose basal polymict conglomerate, ranging in thickness from a few centimeters to more than 10 m, with the pebbles, cobbles and boulders consisting of smoky quartz, white vein quartz, quartzite, schist and phyllite, in a matrix of argillaceous quartzite. Conglomeratic quartzite and grit are present at the middle of the unit.



Fig. 5 LITHOLOGIC SECTIONS THROUGH THE MOEDA FORMATION



Member 2: Light-gray to light-brown siliceous phyllite, grading along strike into quartz sericite schist and very fine-grained quartzite, with thickness up to 166 m (green quartzite).

Member 3: Medium- to coarse-grained quartzite with local schistose conglomeratic lenses containing well-rounded cobbles of smoky quartz, quartzite and grit, in a matrix of medium- to coarse-grained quartzite, with thicknesses of 160 m, forming a total thickness of 490 m.

### Thickness

On the eastern limb of the syncline, as well as on the southern flank of Serra do Curral (Fig. 5), the thickness of the Moeda Formation is remarkably variable. It ranges from 75 m in the northern part of Serra da Mutuca to about 250 m near Morro do Chapéu Golf Club, is about 25 to 50 m in the Ribeirão da Mutuca valley, and thins to zero to the northeast. In the middle part of Serra das Gaivotas, the Formation is 300 m thick, but lacks the lower grit unit. Apparently, it thins to about 150 m to south of the range. On Serra da Moeda, the thickness ranges from 380 m about 1.5 km northwest of Retiro das Pedras Club to 250 m near the club and 445 m near Casa de Pedra, 3 km south of the club. Along the western side of Serra do Curral, the quartzite thins quite abruptly from about 250 m to 35 m (Simmons, 1968) and conglomerates are missing.

The relatively abrupt variation in thickness, which is accompanied by a decrease in, or absence of conglomerates may



reflect variations in the stream regime, such as irregularities near the floor, or the relative proximity to the source area. Both thickness and general grain size of the formation decrease westward and northeastward from the central part of the area, (Fig. 5) suggesting that these parts may represent the deeper and more distal portions of the depositional basin. However, one should also note that the area of extreme thinning coincides rather closely with the boundary of Domains I and III, and hence, that this thinning may be due to tectonism (Map 2).

#### Basal and Upper Contacts

The basal contact between the Moeda Formation and the basement rocks represents the remarkable separation of a suite of younger rocks of the Minas Series from the older rocks of the repeatedly reactivated granitic gneiss complex in the Archaean Rio das Velhas Series. Ryneerson and others (1954) described what they thought to be an angular and erosional unconformity between the north-south trending Moeda Formation and the east-west striking Nova Lima Group in the Itabirito Quadrangle, about 10 km southeast of the present area. The present writer has confirmed the geometry, but has found the contact to be an east-dipping thrust fault. In most places in the present area, this basal contact is such a fault.

Thus, in parts of the south flank of western Serra do Curral, Simmons (1968) described the unconformity between Nova Lima greenschist and the Moeda Formation as "the marked difference in structure on opposite sides of the contact." To the east of this area the writer has seen the contact to be gradational and tectonic between the basal Moeda quartzite,

Fig. 6 SERRA DAS GAIVOTAS - C  
(Central part)

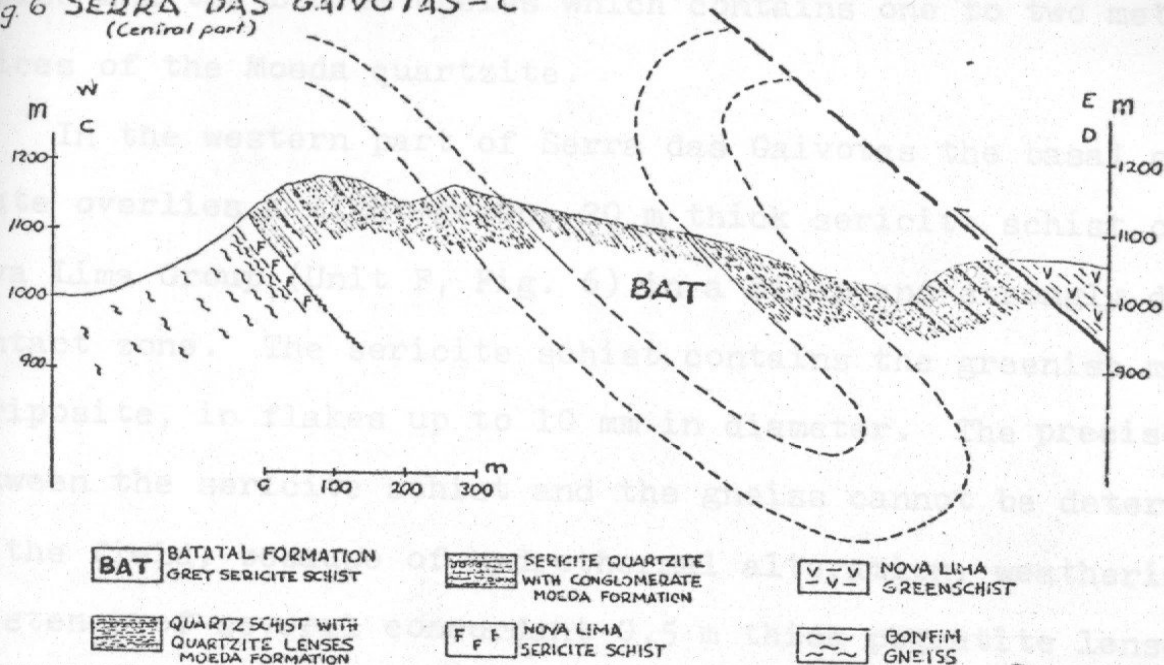


Fig. 7 SERRA DAS GAIVOTAS - S  
(Southern part)

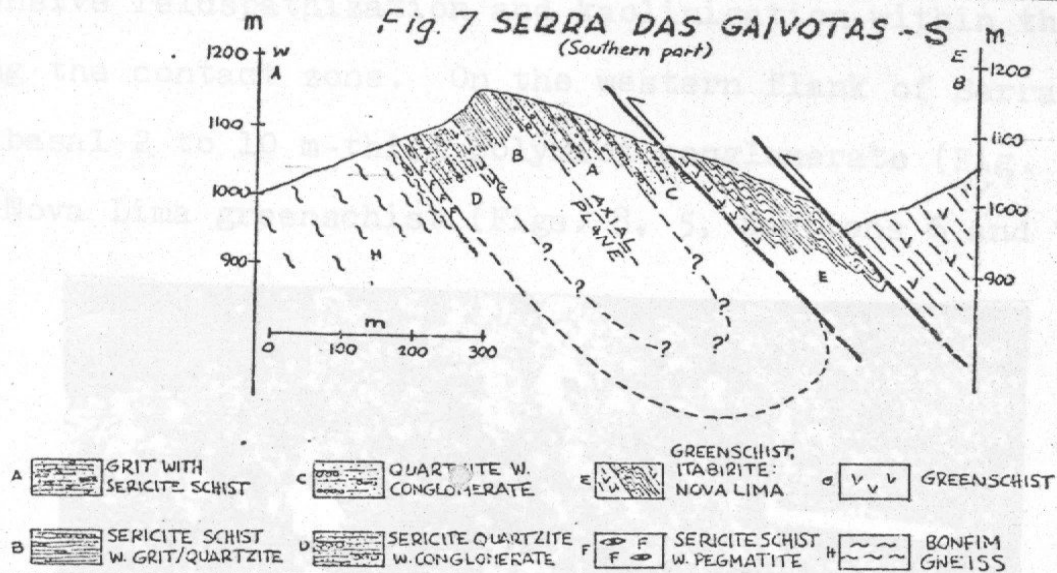
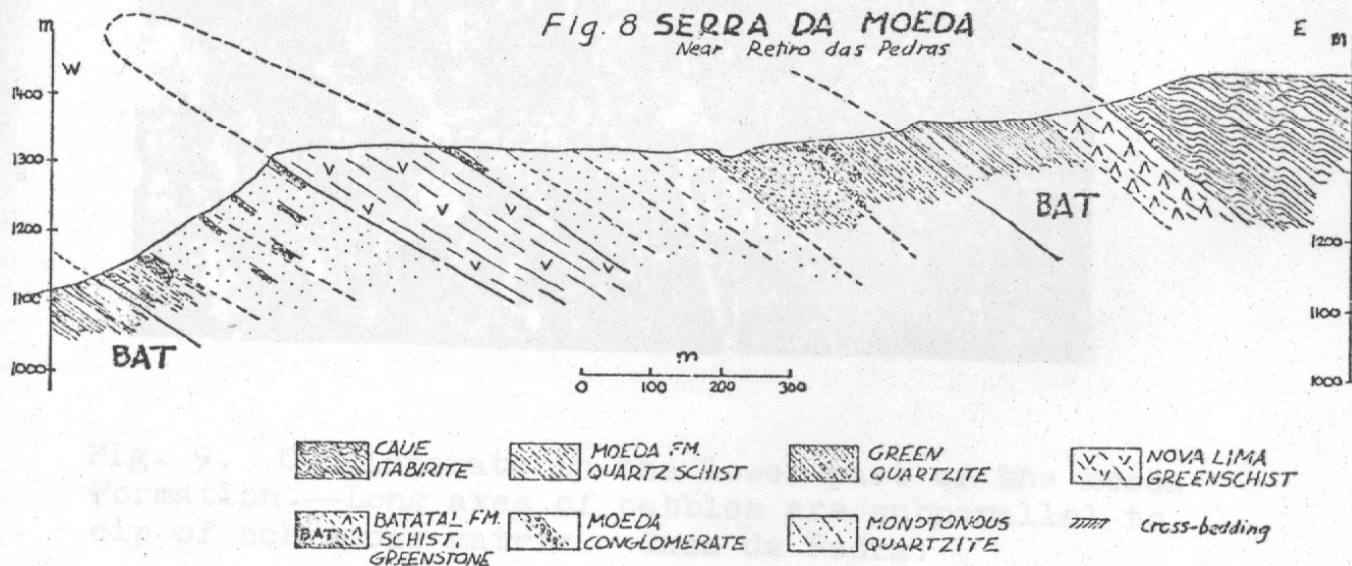


Fig. 8 SERRA DA MOEDA  
Near Retiro das Pedras





which contains abundant tectonically incorporated porphyroblastic gneiss and the Bonfim Gneiss which contains one to two meter slices of the Moeda quartzite.

In the western part of Serra das Gaivotas the basal conglomerate overlies a light-green, 20 m thick sericite schist of the Nova Lima Group (Unit F, Fig. 6) in a steep and strongly deformed contact zone. The sericite schist contains the greenish mica, mariposite, in flakes up to 10 mm in diameter. The precise contact between the sericite schist and the gneiss cannot be determined in the field, because of hydrothermal alteration, weathering, the existence of several concordant 0.5 m thick pegmatite lenses, and extensive feldspathization and kaolinization within the schist along the contact zone. On the western flank of Serra da Moeda, the basal 2 to 10 m-thick polymict conglomerate (Fig. 9) overlies the Nova Lima greenschist (Figs. 8, 5, Sections 6 and 7).

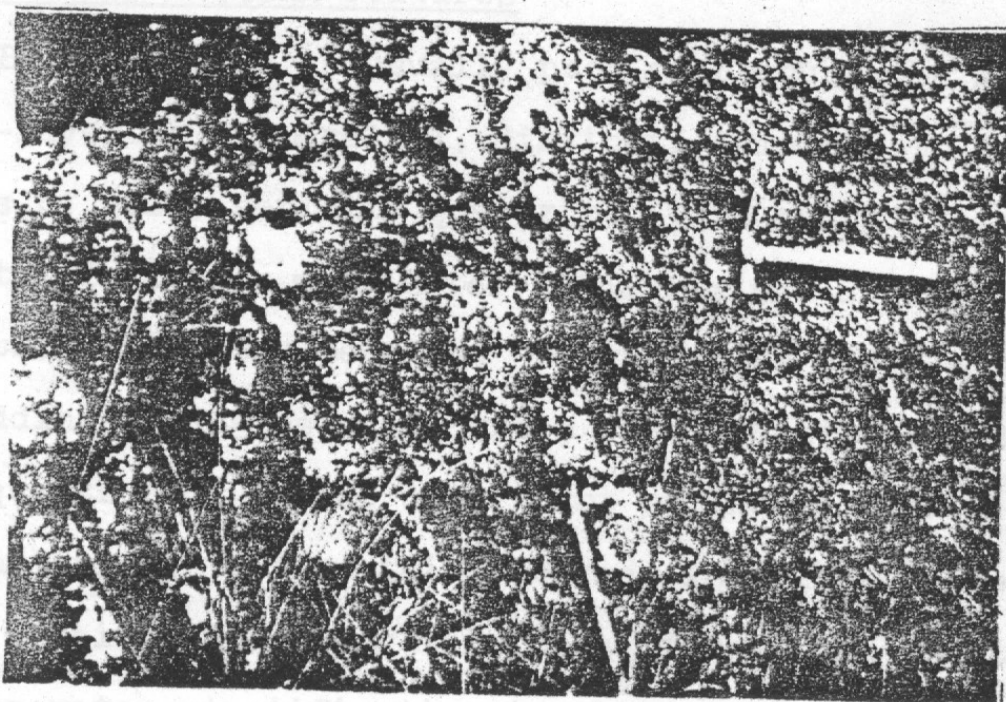


Fig. 9. Conglomerate in the lower part of the Moeda Formation.—Long axes of pebbles are subparallel to dip of schistose matrix. Casa da Pedra.

In Serra da Mutuca, near Mutuca mine, at the eastern limb of the structure, the 25 to 35 cm-thick basal conglomerate is overthrust by the Nova Lima greenschist along a well defined fault. To the west of the Ribeirao da Mutuca valley the contact is very steep, and near Capao do Xavier ore deposit one can trace the fault zone by means of stretched and blackened quartz pebbles in the residual soil.

The upper contact between the Batatal and Moeda Formations is usually concealed throughout the study area, but at the nose of the Gaivotas structure it is marked by a sharp, conformable surface (Fig. 6). To the north the contact is indefinite with the appearance of thin lenses of coarse-grained quartzite within the dark, fine-grained sericite schist of the Batatal Formation.

#### Primary Bedding Features

Bedding which is usually poor or obscure, is marked by the inter-layering of parallel, distinct, thin, 10 to 15 cm-thick layers of grit, sericite quartzite, pure quartzite and sericite schist. In places millimeter thick laminae of opaques (mainly martite) define the bedding. Near Casa de Pedra a semblance to bedding is suggested by grain size variations within almost pure quartz beds in the upper part of the section. Here several alternating, 3 to 5 cm-thick coarse- and fine-grained layers occur within a one-meter thickness of the pure quartzite. In conglomerates stratification is quite indistinct because where the pebbles are not deformed, they are so rounded that their shapes preclude determination of preferred orientation parallel to bedding planes, and where deformed, the elongation



can only be assumed to parallel bedding.

A strong foliation, approximately parallel to bedding, obscures the bedding almost everywhere. In other places close-spaced shear planes at a low angle to the bedding in the quartzite, can be misinterpreted for cross beds. Nevertheless, in a few localities, as at Serra da Moeda (Fig. 10), and locally on Serra da Mutuca, cross-bedding has been preserved.

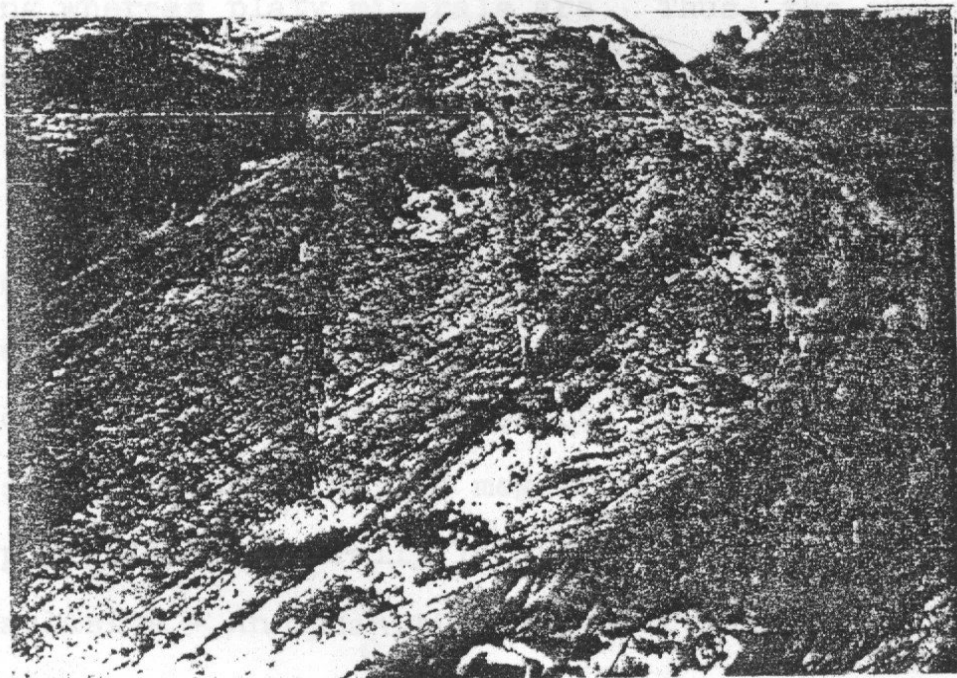


Fig. 10. Cross bedding in well laminated quartzite, about 1.5 km south of Retiro des Pedras Club. Pencil for scale.

Distinct, small- to medium-scale (McKee and Weir, 1953) cross-beds are conspicuous near Casa de Pedra, in sedimentary rocks consisting of darker laminae of muscovite with brownish yellow Fe oxide stains, quartz grains, and martite, and lighter laminae of almost pure quartz grains. The sets are up to 20 cm thick, but the exact geometry of the cross-beds is not known because of the poor exposures. The structure does resemble that described by Allen (1965), which he explained to be the

result of migration of small scale ripples under low-intensity currents.

### Stratigraphy and Lithology

The general lithologic characteristics of each rock type are listed in Table 2. The lithologies, varying from highly quartzose sandstones and conglomerates to argillaceous types, show corresponding effects of strain--quartz is not susceptible to gliding whereas platy minerals are. Thus, the quartzose sediments are converted to cataclasites and mylonites during folding; whereas, the less quartzose rocks show much weaker evidence for such cataclasis. Thus, to describe the more quartzose rocks the writer used the following textural terms, after the definition of Higgins (1971):

Mylonite - A coherent microscopic pressure-breccia with fluxion structure which may be megascopic or microscopic and with porphyroblasts generally larger than 0.2 mm.

Cataclasite - An aphanitic, structureless cohesive cataclastic rock in which most of the fragments are less than about 0.5 mm, and make up less than about 30% of the rock. Essentially like a mylonite but lacking fluxion structure.

Shearing stress - A stress causing or tending to cause two adjacent parts of a solid to slide past one another parallel to the plane of contact.

Blastomylonite - A coherent rock intermediate between medium- to fine-grained mylonite or ultramylonite. Its texture is the result of combined cataclastic and crystalloblastic process.



Table 2

## Mineralogical Composition of Rocks of the Konda Formation

Mineralogical Composition of Rocks of the Moeda Formation										
MATRIX						PEBBLE				
	Rock Texture	Grain Composition	Grain Size (mm)	Grain Shape	Composition (%)	Recrystallization	Size (cm)	Shape	Composition	Pebble/Matrix Proportion %
Polymict Conglomerate (Galvotas) (222A)	Mylonitic, with very small, armored relicts	Quartz - larger - smaller comminuted relict Muscovite Magnetite Zircon Pyrite	2.0-2.5 0.8-0.3 0.02-0.03 0.2 x 0.4 0.4 0.2 0.1 0.3	polygon  blades irregular rounded cubes	Matrix: 90% quartz grains (clean and smaller), 9% muscovite 1% other	Extensive recrystall. polygon. texture matrix and grain	1-3	Elongated Flattened	Vein quartz: 70 Greenschist: 20 Black chert: 10 Quartzite: 10	40/60
Polymict conglomerate (Galvotas) (236)	Mylonitic to blasto-mylonitic in bands  Clean quartz and muscovite in polygonized bands and fine-grained comminuted grains	Quartz - comminuted - recryst. - larger Muscovite - small - large Magnetite Zircon Pyrite	0.02-0.05 0.1-0.4 0.5-0.6 0.01-0.02 0.5-0.6 0.1 0.2-0.3 0.5	angular? polygon  blades  irregular rounded broken cubes	65% quartz 25% muscovite 5% pyrite 5% other	Varies from band to band: recrystall. and cataclasis	1-7	Flattened	Quartzite: } 70 Grit: } Black chert: } 5-10 Schist: } Vein quartz: 15-20	60/40
Polymict conglomerate (Guarita) (172)	Mylonitic to cataclastic  Sericite and quartz with black list of Fe-oxides around quartz grains	Quartz - large - smaller Composite grains: quartz and feldspar Muscovite Magnetite Zircon	0.2-0.5 1.5 0.2-0.4  0.3 0.1 0.1	round to subangular rounded  rounded  blades irregular rounded	60% quartz 30% sericite 10% other	Grain bound. deformat. slightly recrystal. matrix	1-12	Rounded Elongate Flattened	Vein quartz: 30 Quartzite: 60 Schist: } 10 Chert: }	60/40
Schist pebble (172)	Schistose	Sericite white lenticles dark lenticles	0.06-0.2 0.1-0.25	ovoidal ovoidal	80% sericite 20% quartz	_____	1-2	Flattened	Sericite schist	_____
Polymict conglomerate (Casa de Pedra) (180)	Mylonite to cataclastic	Quartz  Sericite Zircon Magnetite	1-3  0.2 0.1 0.1	rounded, angular, subangular broken minute blades rounded irregular	75% quartz 22% sericite 3% other	Grain bound. deformat.	2-20	Rounded and Elongated	Vein quartz: 75 Schist: 20 Grit: } 5 Quartzite: }	35/65
Polymict conglomerate (Mutuca) (269)	Cataclastic to mylonitic	Quartz  Muscovite Magnetite  Hematite Zircon Goethite Pyrite Tourmaline	0.1-0.8  0.1-0.3 0.1  0.2 0.15 0.05 0.1 0.2	Round to polygonal (mortar) bladed flattened octahedra irregular rounded spherulitic cubes elongate	quartz: 60% sericite: 39% other: 1%	Extensive recrystallization in matrix; grain edge deformation by pressure solution.	2-15	Rounded	Vein quartz Quartzite	_____

Table 2 (continued)							
	Rock Texture	Matrix Composition	Grain Composition	Grain Size (mm)	Grain Shape	Rock Composition	Recrystallization
Gray Quartz Schist (Upper part of the Formation) (179) (Cava de Pedras)	Massive to vague, thinly foliated; cataclastic	Sericite largely predominates over quartz. Fe-oxides in dark dust.	Quartz - avrg. - rare Muscovite  Epidote   Zircon  Magnetite	0.05-0.1 0.8-1.0 0.15-0.4  0.1-0.2   < 0.2  0.05-0.1	{angular elongate hexagonal tubular elongate prismatic, elongate, irregular, pseudo- hexagonal well- formed, euhedral irregular	60% matrix 40% grains	slightly around larger quartz grains only
Green Sericite Quartzite (185) (Retiro das Pedras)	Slightly banded, mylonitic to cataclastic	Yellowish green sericite	Quartz - avrg.  -min. max. - composite - cherty lens Muscovite Hematite - dark bands - rare - light band  Zircon	0.2-0.1  0.05-0.3 0.3-0.4 0.1-0.15 0.1-0.2 0.01-0.07 0.15 0.01-0.05 0.05-0.25	round to subangular, elongate  round  elongate  irregular euhedral pseudo-morph aft. magnetite broken	30-35% matrix yellowish green sericite 50-55% quartz 2-5% hematite (light bands)  10-15% hematite (dark bands)	Deformed grains: flattening and fracturing. Matrix recrystall.
Coarse-grained Quartzite (Monotonous Quartzite) (181) (Retiro das Pedras)	Slightly cataclastic	Stained sericite + fine-grained quartz	Quartz Muscovite Magnetite Hematite Zircon Goethite	0.5-2.5 0.1-0.6 0.1-0.4 0.1-0.4 0.1-0.2	round to subangular tabular, blades irregular, octahedra irregular rounded beads spherulitic	30% matrix  70% grains Scattered quartz pebbles 1 to 3 cm in diameter	Recrystall. at grain boundaries. Sericite and hematite grew.



Cataclastic to Mylonitic - A rock which corresponds to a protomylonite stage represents the early stages of mylonitization, with less recrystallization.

The Moeda Formation consists predominantly of poorly sorted, medium- to coarse-grained quartzite and grits, with conglomeratic lenses interdispersed both near the base and at the top of the formation. Near the top of the formation a quartz schist unit (Fig. 5) locally contains grit and quartzite layers and lenses. Along the western flank, at Serra da Moeda (Fig. 5, Sections Nos. 6 and 7; Fig. 8), it can be demonstrated that some clastic units are continuous laterally, but that the green quartzite does not extend to Serra das Gaivotas (Fig. 6). Whereas conglomerate lenses are relatively abundant at Serras da Moeda (Fig. 5) and Gaivotas (Figs. 6 and 7), on the eastern flank of the Moeda syncline, the section is thinner and quartzites predominate. This lateral impersistence of individual lithologies is a characteristic of the formation, making it impossible to recognize the members as defined by Wallace (1958) except at the Serra de Moeda (Fig. 5, Sections Nos. 6 and 7).

The basal conglomerate in the northeastern part of the area warrants special discussion. This conglomerate has been mapped and studied in great detail by the present writer, and his results clarify a previous puzzle. The area is characterized by structural complexity, an intricate stratigraphy and deep weathering. The geological puzzle concerns the discovery by Pomerene (1964) of quartzose conglomerates within the Nova Lima only in this small area in the western Quadrilatero Ferrifero.

In summary, Pomerene (1964) was able to define a lithologic succession in the northwest part of the Macacos Quadrangle as the "Conglomerate-Quartzite Sequence", but was unable to establish the stratigraphic position of this sequence with certainty. However, in that the material overlying the Sequence seemed to be typical of rocks of the Nova Lima Group, he placed this Sequence within the Nova Lima Group.

Several observations were made by the writer regarding the problematic rocks:

1. Conglomerates of the "Conglomerate-Quartzite Sequence" are continuous with outcrops of the typical Moeda conglomerate northeast of Capao do Xavier ore deposit, near km 438 and 439 of Highway BR 040 (see Geologic Map). This continuity was not recognized by Pomerene. Both the conglomerates described by Pomerene and those within the basal member of the Moeda Formation are similar compositionally. Furthermore, grits and coarse-grained quartzites, typical of the Moeda Formation, are intimately associated with the conglomerate (Table 2, Nos. 172, 269).

2. In the Nova Lima Group, which can be correlated with the Barbacena Group, such conglomerates and conglomerate-quartzite sequence have not been identified. The Nova Lima Group, as described by Dorr and others (1957), is composed mainly of metamorphosed mafic and ultramafic rocks, cherts, manganese formation, graphitic schists, iron-formation, as well as of rocks of the Barbacena Group (Barbosa, 1954, redefined by Ebert, 1963 and Pires, 1977). The absence of conglomerates in the Nova Lima Group is noteworthy.



3. Metamorphosed mafic and ultramafic rocks belonging to the upper part of the Batatal Formation overlie the Conglomerate-Quartzite Sequence. Contrary to Pomerene, the present writer has been able to distinguish between the Batatal mafic and ultramafic rocks and the similar lithologies in the Nova Lima Groups, as follows. The mafic and ultramafic rocks of the Batatal Formation are associated with the dark gray, potassic aluminous sericite schist, and the Nova Lima mafic and ultramafic rocks are associated with cherty quartzite and are thicker than the Batatal greenstones.

4. The writer has discovered boulders of an earlier conglomerate (Fig. 11) within the boulder conglomerate of the "Conglomerate-Quartzite Sequence".



Fig. 11. Boulder conglomerate containing boulders and cobbles of an ancient conglomerate. Km 439 of Highway BR 040.

These boulders and cobbles are composed of quartz to 2 cm in diameter in a well-bedded, coarse-grained quartose matrix, very similar to the grits and gritty quartzites found in the monotonous quartzitic sequence of the west limb of Serra da Moeda (Fig. 5, Section No. 7). The matrix of the conglomerate is composed of quartz, sericite and altered chloritic material, and present a well-defined foliation which parallels the foliation of the Nova Lima greenschist (described as red phyllite by Dorr, 1969) in a roadcut near Km 439 of Highway BR 040. This foliation is curved around the cobbles, but also penetrates into the cobbles and boulders. In zones of higher deformation, pebbles and cobbles are extremely flattened along the foliation, and the matrix is more chloritic. The similarities between the cobbles and boulders of this conglomerate and the grits and coarse-grained quartzite of the Moeda Formation suggests that the boulder conglomerate corresponds to an intraformational conglomerate in that formation.

As has been shown, in the Nova Lima Group such boulder conglomerate has not been found. Grits or coarse-grained quartzite also have not been found in this group.

5. The heavy mineral contents of the quartzite of the Moeda Formation at Serra da Mutuca, near the Mutuca Mine, and of the quartzite of the "Conglomerate-Quartzite Sequence" are indistinguishable in composition. Zircon, magnetite, black tourmaline, hematite, rutile, pyrite cubes and small amounts of epidote are present in both.



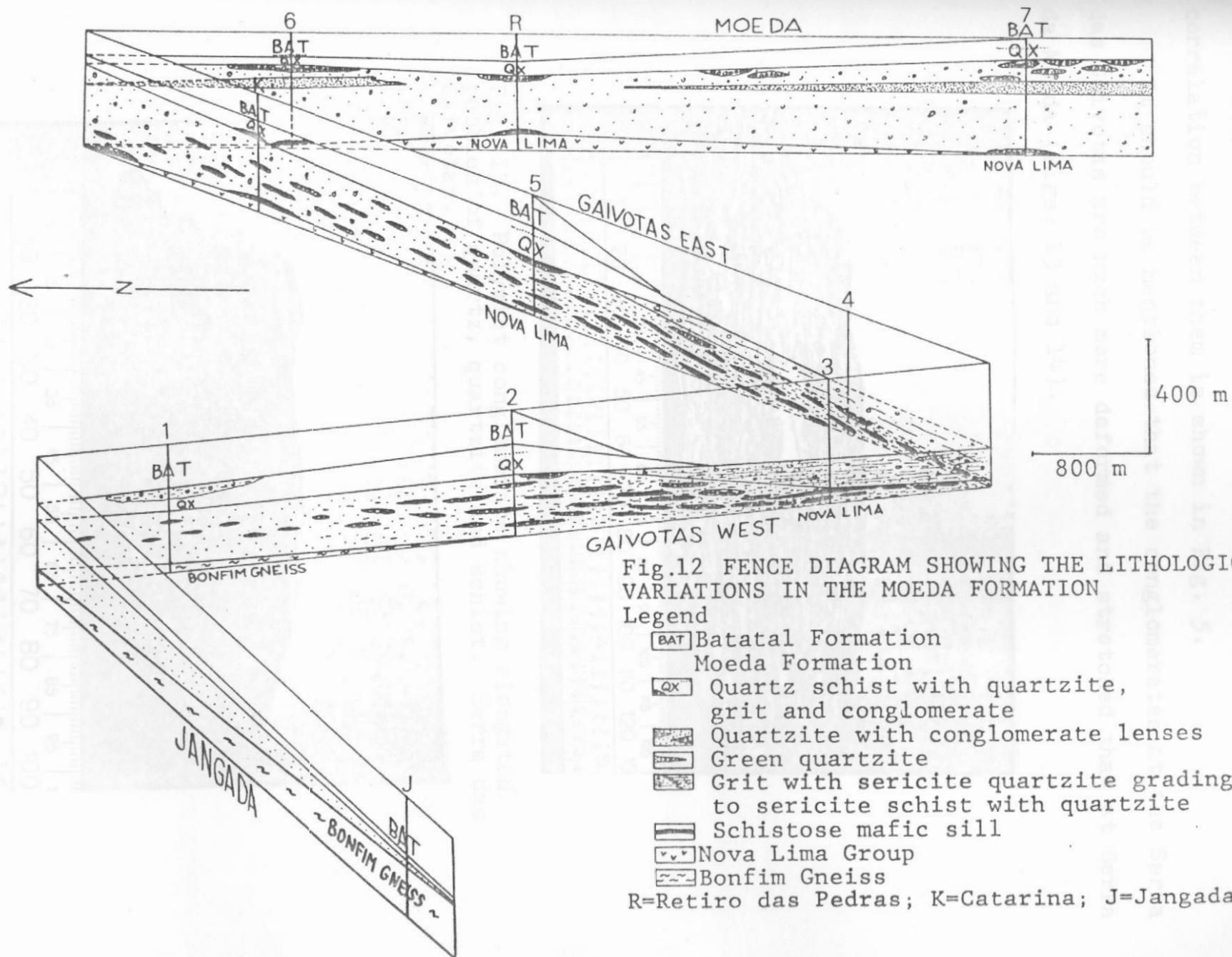
### Details in the Serras da Moeda and Gaivotas

Because of the excellent outcrop on the two adjoining ridges and the doubling of the Formation on Gaivotas, this area provides the best information on the lateral and vertical variations of lithologies, and hence on possible patterns of sedimentation. Several patterns are apparent from the fence-diagram (Fig. 12):

1. Basal conglomerates are local.
2. Conglomerates are more abundant at Serra das Gaivotas.
3. The conglomeratic quartzites grade laterally into grits.
4. The green quartzite is a local lithology only occurring at Serra da Moeda.
5. The upper conglomeratic unit can be distinguished only in the Serra da Moeda.
6. The pattern suggests that the lower conglomerates were introduced from a southerly direction, under high stream velocity.
7. The top most clastic unit, the quartz schist, thins to the east and to the west, and hence, may represent a transgressive blanket with a source to the north or south.

At Serras da Moeda and Gaivotas, the Moeda Formation is thicker, the exposures are better and more continuous, and the rocks are less deformed than anywhere else in the study area. The possibility of correlating the Moeda Formation in this area with the members defined by Wallace (1958) in a contiguous area to the south, and the facts outlined above, led the author to concentrate mostly on the study of the Moeda Formation in those regions.

The description of the lithologic types, presented in Table 2, follows approximately this stratigraphic succession, from bottom to top: conglomerates, monotonous coarse-grained quartzites, green quartzite, and quartz schist. The relative





stratigraphic position of each clastic unit and a tentative correlation between them is shown in Fig. 5.

It should be mentioned that the conglomerates at the Serra das Gaivotas are much more deformed and stretched than at Serra da Moeda (Figs. 13 and 14).

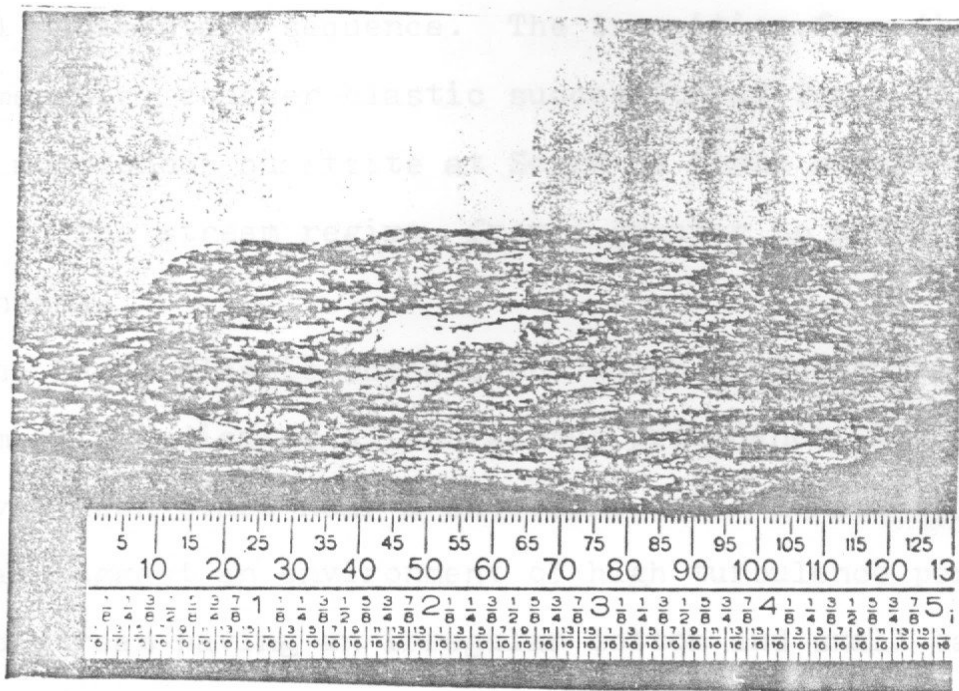


Fig. 13. Polymict conglomerate showing elongated pebbles of quartz, quartzite and schist. Serra das Gaivotas.

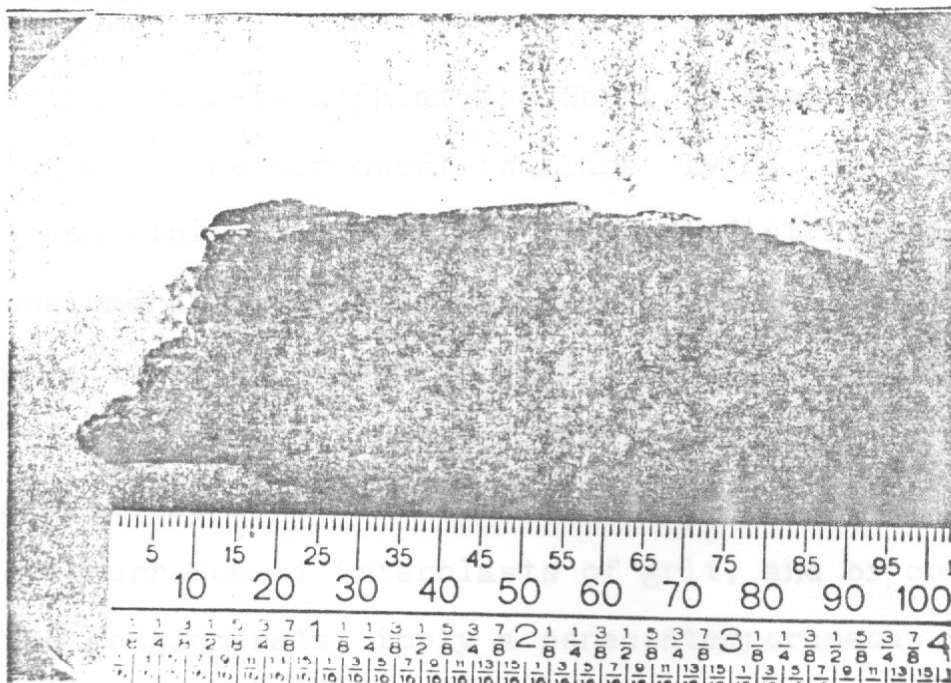


Fig. 14. Polymict conglomerate showing elongated pebbles of schist and quartz. Serra das Gaivotas.

### Environment of Deposition

The Moeda Formation is a coarse clastic unit characterized by the presence of conglomerate lenses in poorly-sorted, coarse-grained quartz sands. The size of the pebbles and thickness of individual beds decrease upward in the column, suggesting a fluvial sedimentary sequence. The transition from the more conglomeratic, coarser clastic succession at Serra das Gaivotas to the monotonous quartzite at Serra da Moeda suggests a major change in the stream regime, from a greater to a lesser energy environment.

The basal clastic succession, which includes the polymict conglomerate indicates a terrigenous provenance, but the deposition may have taken place near a shoreline. The lenses of coarser material suggest an environment of high turbulence perhaps in braided stream having an irregular bottom and small barriers and channels. The poorly sorted character of the sediments indicates they were deposited in an environment protected from surf and waves.

Fluvial cross-bedding at the Serra da Moeda indicates the source to be to the northwest (Wallace, 1958), or to the north-east or east (this report). The regional distribution of the basal conglomerate suggests a southerly source.

The relative abundance of quartz indicates a mature provenance, and the occasional occurrence of pyrite and graphite points to ephemeral euxinic conditions.

The occurrence of interclasts of grit, and of conglomerate within the conglomerate, imply a penecontemporaneous reworking and sedimentation, resulting in the formation of intraformational



conglomerates. These variations might be explained by abrupt and local changes in a high-energy depositional regime.

The quartz schist, generally cataclastic, at the top of the formation represents the end of a fining-upward cycle, denoting achievement of base level.

In summary, the fluvial environment of the Gaivotas-Moeda area is characterized by extensive lateral migration of streams. The wide variation in grain size and the presence of significant amounts of conglomerate imply deposition in a relatively high gradient, decreasing upward, when the quartz schist was formed.

The 15 m-thick laminated greenschist overlying the conglomerate at Gaivotas, and the greenschists which occur in the middle of the Moeda sedimentary section, south of the study area, indicate that sporadic igneous episodes took place during Moeda sedimentation.

## Batatal Formation

### General

The rock sequence occurring between the top of the Moeda Formation (quartz schist and fine-grained quartzite) and the base of the Itabira Group (itabirite) was described originally as Batatal Schist by Harder and Chamberlin (1915, p. 356-357), and as Batatal Formation by Maxwell (1958). The stratigraphic column (Table 3) shows the approximate relative position and degree of exposure of the various rock types. There are two major lithologies: a basal unit composed predominantly of dark gray sericite schist and an overlying unit consisting of a variety of mafic to ultramafic rocks, with some chert lenses and intraformational breccia zones.

### Stratigraphy

#### Sericite Schist Unit

The typical lithology within the formation, consisting perhaps of one-half to two-thirds of the formation, is a laminated dark grey sericite phyllite or schist, ranging in thickness from tens of meters to more than 250 m. The sericite schist persists over the whole map area and is restricted to the lower half of the formation.

Characteristically it underlies lowlands between small ridges of quartzite, forming elongate outcrops parallel to the foliation, and particularly good outcrops can be studied on the western flank of Serra da Moeda, the eastern flank of Serra das Gaivotas, and between km 438 and 440 on Highway BR 040. Where weathered, the schist acquires a light-gray to whitish



Table 3 POSSIBLE STRATIGRAPHY OF THE BATATAL  
FORMATION IN THE STUDY AREA

		Bad	Na	Good	Dr
CAUE ITABIRITE					
	Greenschist with amphibolite lenses				
	Chert lenses				
	Greenschist altered to a creamy phyllite				
	Talc chlorite schist with serpentinite lenticular bodies				
	Feldspathic mafic rock				
	Fine-grained mafic rock with micro-breccia and kaolinitic laminae				
	Yellowish magnetite itabirite				
	Massive mafic rock with micro-breccia				
	Feldspathic mafic rock				
	Greenschist (magnetite chlorite schist) with dolomitic lenses				
	Dark gray sericite schist with local finely disseminated graphite				
	Thin lenses of quartzite				
	Breccia zones				
MOEDA FORMATION					
	Quartz schist				

yellow color, and planes of schistosity or fissility become less conspicuous; where severely weathered, the rock exhibits reddish brown colors, and limonitic stains along foliation and fracture planes; where fractured, the rock produces plates of schist that cover the land surface.

At the base of the formation above a quartz schist, in the middle of the hill 1 km south of Retiro das Pedras Club, is a 50 cm-thick layer of brecciated material, consisting of 5 to 10 cm-long fragments of fine-grained yellowish rock, with minute magnetite octahedra, within a sericitic schist matrix. The fragments have been deformed with the matrix (Fig. 15).

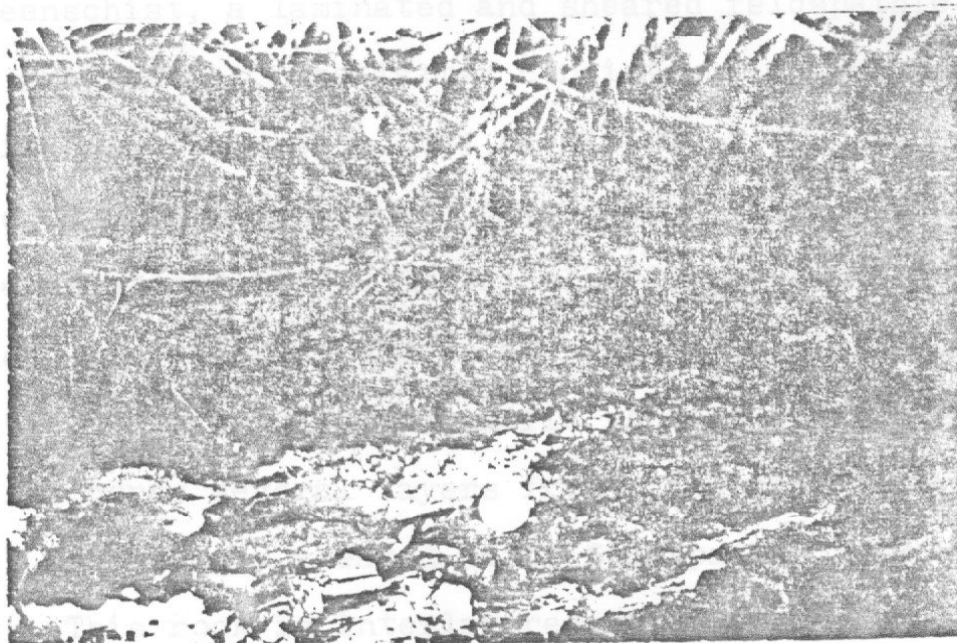


Fig. 15. Breccia in the basal part of the Batatal Formation, containing a contorted and elongated fragment of fine-grained magnetite itabirite within a sericite schist matrix; 1 km south of Retiro das Pedras Club. Coin is 2.5 cm in diameter.

Sporadic thin lenses, 2 to 3 m thick of coarse-grained quartzite are present in the lower part of the unit, mainly at Serra das Gaivotas. In the Lagoa Grande area, chert and fine-grained quartzite have been reported by Dorr (1969) as lenses in the sericite schist. Simmons (1968) mentioned the existence of dark gray to nearly black graphitic and carbonaceous phyllite containing organic material in the western Serra do Curral Quadrangle, some 35 km west of the study area.

### Greenstone Unit

In the upper half of the formation the author has identified a very persistent, 50 to 150 m thick marker horizon, consisting of greenschist, a laminated and sheared feldspathic mafic rock, and a greenstone. The latter consists of a fine-grained, greenish chloritic matrix with a dust of altered Fe-oxides, with partly weathered reddish spots and patches. Similar greenstones have been encountered in MBR drill holes in the eastern part of the Tamandua ore deposit. There are also some lithologies that resemble in texture an ultramafic rock or a massive serpentinite. In drill cores several layers from a few centimeters to 25 m thick, of strongly sheared mafic feldspathic rock have been found. This rock is interlayered with greenish layers, 2 to 5 cm thick, of chlorite and talc, and well-laminated yellowish itabirite (slaty itabirite) and siliceous itabirite with talc flakes in cherty mesobands.

In the upper part of the topmost unit of the Batatal Formation, at Mutuca and Zoroastro Mines, are three layers, 50 cm thick, of well-laminated and partly weathered rock (Fig. 16). These consist of alternating 1 cm thick layers of



kaolinitic and reddish brown argillaceous material, interbedded in a yellowish cream phyllite and ferruginous phyllite. A heavy residuum of magnetite, hematite, black tourmaline, zircon, apatite and elongate pseudomorphs of limonite after pyrite was recovered from a mass of the weathered kaolinitic banded material, by panning. The original nature of the material is obscure.

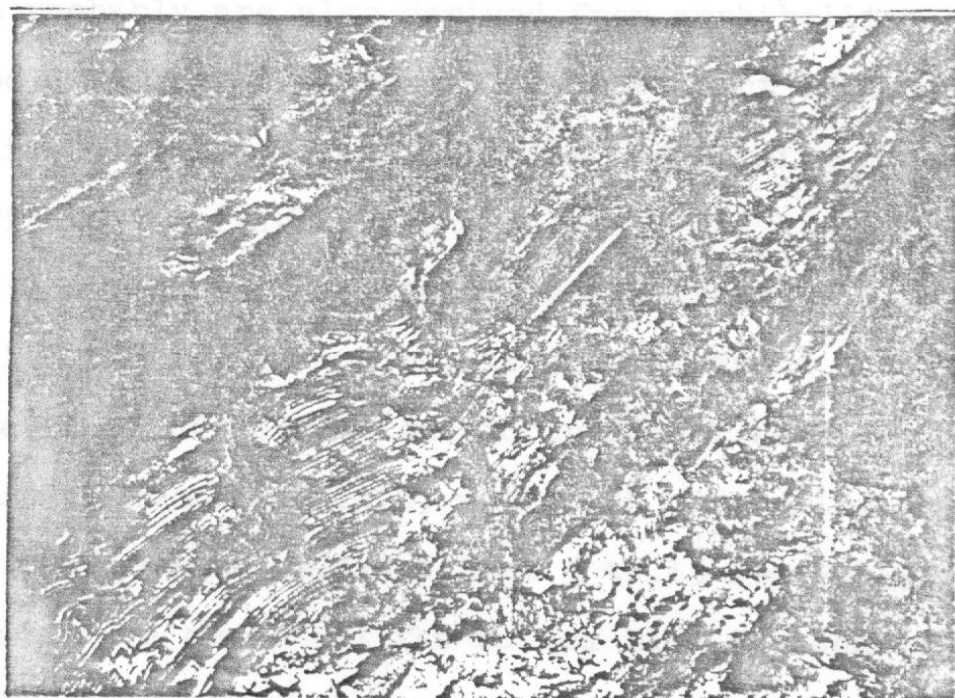


Fig. 16. Sheared laminated feldspathic basic rock of the upper part of the Batatal Formation at Mutuca Mine. Pencil for scale.

Well-foliated talc chorite schist interfingers with green-schist and sericite schist in outcrops in the western hills of Serra da Mutuca, close to Highway BR 040 between km 437 and 439. Near Guarita (see map) tight folding, slip-faulting and conjugate fracturing have produced an irregular repetition of greenschist, dark sericite schist, talc schist, and quartzite. More conspicuous greenschist occurs in the valley between Serras do Curral and Gaivotas, on the left margin of Corrego da Catarina and the

western flank of Serra da Mutuca. The greenschist weathers to a creamy and yellowish clay with brownish stains of Fe-oxides, but purplish, dark brown and red colors also have been observed. Probably the persistent exposures of laminated creamy phyllite cropping out on the western flank of Serra da Moeda, underlying Caue Itabirite is also a weathered greenschist, and kaolinitic clay deposits located in the northern part of the Tamandua ore deposits probably are also derived from amphibolites. Several small bodies of amphibolite lie in upper part of the unit, making direct contact with itabirite, or forming concordant lenses within the itabirite.

The contacts between itabirite and creamy phyllite, and between itabirite and amphibolite are marked by 1 to 2 m-thick supergene zones of concretions, composed of hard avocado-like rounded lumps in a limonitic, yellowish cream fine-grained matrix. These avocados range from 5 to 15 cm in length, and some have a free core. At the Mutuca Mine the contact between the Batatal and Itabirite Formations is characterized by an interlayering probably due to tectonic slicing of thin lenses of chlorite schist and amphibolite within the itabirite, and thin beds of itabirite within the chlorite schist. Dorr (1969) and Maxwell (1972) have observed the same features in the Itabira and Alegria districts.

This unit, representing volcanism, may be an important geological component in this setting that also produced an iron formation. Contrary to the opinion of James (1955), there may be some relationship between volcanism and the origin of iron formations.

### Textural Characteristics of the sericite schist

Under the microscope the dark gray sericite schist exhibits a very fine-grained matrix that is either uniform or consists of irregular darker and lighter laminae, micro-lenses, and clots generally parallel to bedding (Table 4). The lighter laminae are slightly coarser than the darker ones. In some hand specimens the layering is on a millimeter scale, with the lighter laminae containing about 1 percent Fe and a trace of Cr. The presence of iron is responsible for the greenish pleochroism of the mica (Deer and others, 1971, pp. 203).

Locally in some of the more deformed zones, the lighter and darker bands resemble those described by Read (1951) from mylonites derived from felsic rocks. He ascribes such banding to the segregation during strain of the minerals into lighter and darker colored laminae.

Tourmaline, in subidiomorphic grains occurs in the sericite schist, locally in anomalously high quantities, commonly parallel to the foliation. Tourmaline grains that bisect strained and flattened quartz lenticles may be post-tectonic, and those that are surrounded by pressure shadows filled by quartz may be pre-tectonic. Similar large concentrations of tourmaline in the Batatal sericite schist were described by Dorr and Barbosa (1963) in the Itabira District and by Fleischer and Routhier (1973) in the Passagem de Mariana gold deposit in Ouro Preto District, 80 km southeast of the present area. The significance of this high boron content will be discussed in the next section.



Table 4

## Mineralogical Composition of the Rocks of the Batatal Formation

	Rock Texture	Grain Composition	Grain Size (mm)	Grain Shape, Color	Est. Rock Composition	Recrystallization
Sericite Schist (225)	Foliated, light and dark foliae (0.3 to 2 mm thick). Cataclastic to mylonitic	<u>Light foliae</u> Muscovite:  Quartz: Tourmaline:  <u>Dark foliae</u> Sericite:  Quartz: Tourmaline:  <u>General</u> Apatite:  Magnetite: Hematite: Zircon: Rutile:	0.06 - 0.2  0.02 - 0.08 0.02 - 0.08  0.01 - 0.04  <0.01 0.02 - 0.04  0.02 0.01 - 0.03 0.01 - 0.02 0.02 - 0.04 <0.01	Greenish, tabular, elongate flakes Irregular Subidiomorphic, elongate, irregular, tabular, pseudo hexagonal amber color Stained flakes Irregular Irregular, elongate, fractured Hexagonal, elongate Irregular Irregular Irregular, rounded Irregular	Sericite: 75% Quartz: 20% Tourmaline: 2% Other: 2%	Muscovite recrystallized in the lighter laminae, and perhaps quartz and tourmaline
Sericite Schist (175)	Cataclastic, faint foliated. Grains with dimensional orientation parallel to foliation.	Muscovite: Large: Small:  Matrix Sericite:  Quartz: Large: Small: Feldspar:  Tourmaline:  Zircon:  Opagues:  Apatite:	0.5 - 1 0.05 - 0.15  <0.01  0.15 - 0.3 0.01 - 0.1 0.05 - 0.12  0.03 - 0.12  0.02 - 0.03  0.05 - 0.1  0.01 - 0.02	Light green deep green, elongate, tabular flakes Tiny flakes Angular, broken, irregular Cloudy, poikilitic, angular, irregular Yellowamber, angular, elongate, rounded, pseudo-hexagonal Elongate, rounded, irregular Irregular. Red: hematite Yellow: goethite Rounded, elongate	Matrix: 60% Sericite grains: 40% Quartz: 29% Composite: 8% (Feldspar + quartz + sericite) Feldspar: 5% (cloudy) Tourmaline: 1% Other: 1%	Muscovite recrystallized. Apparently quartz & feldspar did not recrystallize.  XRD: Kaolinite + quartz + muscovite

# Petrology and Chemical Composition

## Sericite Schist

Table 4  
(Continued)

Talc-chlorite Schist (272)	Strongly foliated, with lentilles; mylonitic?	Talc:  Talc-chlorite matrix:  Quartz:  Magnetite:	0.02 - 0.1 0.01 - 0.02 0.02 - 0.3 0.01 - 0.02	Greenish flakes Greenish, dusty matrix Fibrous, granular Irregular, altered to goethite	Matrix: 60% Lentilles: 40%	Lentilles range in size from 0.2 to 0.8 mm, containing quartz, talc and magnetite. Quartz replaces the other minerals.
Talc-chlorite Schist (165)	Strongly foliated, darker, thin streaks and talc-rich lentilles; mylonitic?	Talc:  Talc-chlorite matrix: Opaque:  Dark Chloritic streaks and chert films	0.1 - 0.2 <0.01 0.01 - 0.03 0.1 - 0.5	Green, white flakes Greenish, dusty matrix Irregular, platy Red: hematite Bluish interf. colors, elongate	Matrix: 70% Talc-rich lentilles: 15% Darker lentilles: 15%	Talc recrystallized inside lentilles; chlorite recrystallized inside dark streaks.

the diagrams of Garrels and Mackenzie (1971; Figs. 17 and 18) suggesting a possible compositional anomaly. The unusually high tourmaline content (Table 4) also suggests an abnormality.

Both the sericite schists from the Batatal Formation and Piracicaba Group contain carbon or graphite (Simmons, 1968) in discrete disseminated zones (Batatal), or within the graphitic phyllite (Barreiro Formation), indicating a sedimentary affiliation. The relatively low  $K_2O$  content (Table 5) places the rock in the compositional range of illitic sediments. Their high  $K_2O$  contents are quite similar to the Mesnard and Tyler slates of Michigan (Nanz, 1963; Fig. 17). However, some of the sericite schist compositions resemble those of pillowed felsic lavas

## Petrology and Chemical Composition

### Sericite Schist

The chemical composition of the dark gray sericite schist (Table 5) is noteworthy for its high  $K_2O$  content (7.0 to 8.3%), a high  $Al_2O_3$  content (19.1 to 21.5%), a low but consistent content of  $MgO$  and  $Fe_2O_3$ , and a locally very high content of boron, in tourmaline. It should be noted that similar  $K_2O$ - $Al_2O_3$  rich schists occur also in the Piracicaba Group.

The relatively low content of quartz (Table 4) and the high content of sericite and muscovite are reflected in the low silica and the high alumina abundances. However, the origin of the rock is obscure. Its  $K_2O$  content is much higher than the 3.5%  $K_2O$  average reported for shales (Pettijohn, 1975). Furthermore the rock composition does not fall within the range of rhyolites (Johannsen, 1937).

This aluminous potassic schist plots in distinct fields in the diagrams of Garrels and Mackenzie (1971; Figs. 17 and 18) suggesting a possible compositional anomaly. The unusually high tourmaline content (Table 4) also suggests an abnormality.

Both the sericite schists from the Batatal Formation and Piracicaba Group contain carbon or graphite (Simmons, 1968) in discrete disseminated zones (Batatal), or within the graphitic phyllite (Barreiro Formation), indicating a sedimentary affiliation. The relatively low  $Na_2O$  content (Table 5) places the rock in the compositional range of illitic sediments. Their high  $K_2O$  contents are quite similar to the Mesnard and Tyler slates of Michigan (Nanz, 1953; Fig. 17). However, some of the sericite schist compositions resemble those of pillowed felsic lavas



Table 5

Chemical Analysis of Rocks from the Batatal Formation  
(Weight Percent)

Rock Sample	MU-22	262	325	321	RO	JH	VV-1	VV-2	JO	AC
SiO <sub>2</sub>	60.18	63.34	60.54	62.19	61.6	62.4	73.66	78.44	77.82-68.10	58.10
TiO <sub>2</sub>	0.75	0.58	0.89	0.74	0.4	0.62	0.02	0.54	.47-TR	.65
Al <sub>2</sub> O <sub>3</sub>	20.67	19.14	21.09	21.50	24.5	19.2	11.57	15.52	16.74-11.27	15.40
Fe <sub>2</sub> O <sub>3</sub>	2.30	2.75	2.38	3.27	1.0	1.7	0.93	0.41	3.16-TR	4.02
FeO	--	--	--	--	0.1	3.1	0.62	0.68	1.24-.06	2.45
MnO	--	--	--	--	0	0.02	0.04	0.01	.14-TR	--
MgO	1.61	1.48	1.50	1.11	1.7	2.8	2.80	0.38	.86-TR	2.44
CaO	0.12	0.04	0.07	0.05	0	0.12	2.09	0.29	1.42-.22	3.11
Na <sub>2</sub> O	0.23	0.47	0.59	0.29	0.2	0.32	0.05	0.49	4.22-.40	1.30
K <sub>2</sub> O	8.26	7.87	8.20	6.97	6.2	4.9	3.72	2.33	12.13-4.50	3.24
P <sub>2</sub> O <sub>5</sub>	--	--	--	--	0.09	0.06	n.d.	0.14	.07-.00	.17
H <sub>2</sub> O	5.58	3.71	4.44	3.30	3.8	3.9	--	--	5.04-.24	5.00
	99.70	99.38	99.66	99.42	99.59	99.14	95.50	99.23	--	99.95

MU-22 - Dark gray sericite schist - Mutuca Mine  
 262 - Dark gray sericite schist - Serra das Gaivotas  
 325 - Dark gray sericite schist - KM 438, Highway BR 040  
 321 - Dark gray sericite schist - Casa de Pedra  
 (MU-22 to 321 done by the author on the MTU-AAS 303), 1976.

RO - Batatal schist. O'Rourke, from the Ganderela Quadrangle (in Herz, 1978)

JH - Quartz sericite phyllite, Moeda Formation? Johnson and Herz, from Cachoeira do Campo (in Herz, 1978)

VV-1 - Pillowed acid lava, Hooggenoeg Formation, Barberton. Viljoen and Viljoen (1969).

VV-2 - Average composition of two siliceous aluminous schists, felsic tuff from the ultramafic unit of Barberton. Viljoen and Viljoen (1969).

JO - Range of 26 rhyolites. Johannsen (1937, v. II, pp. 265).

AC - Average shale (Clarke, 1924) from Pettijohn, 1975.

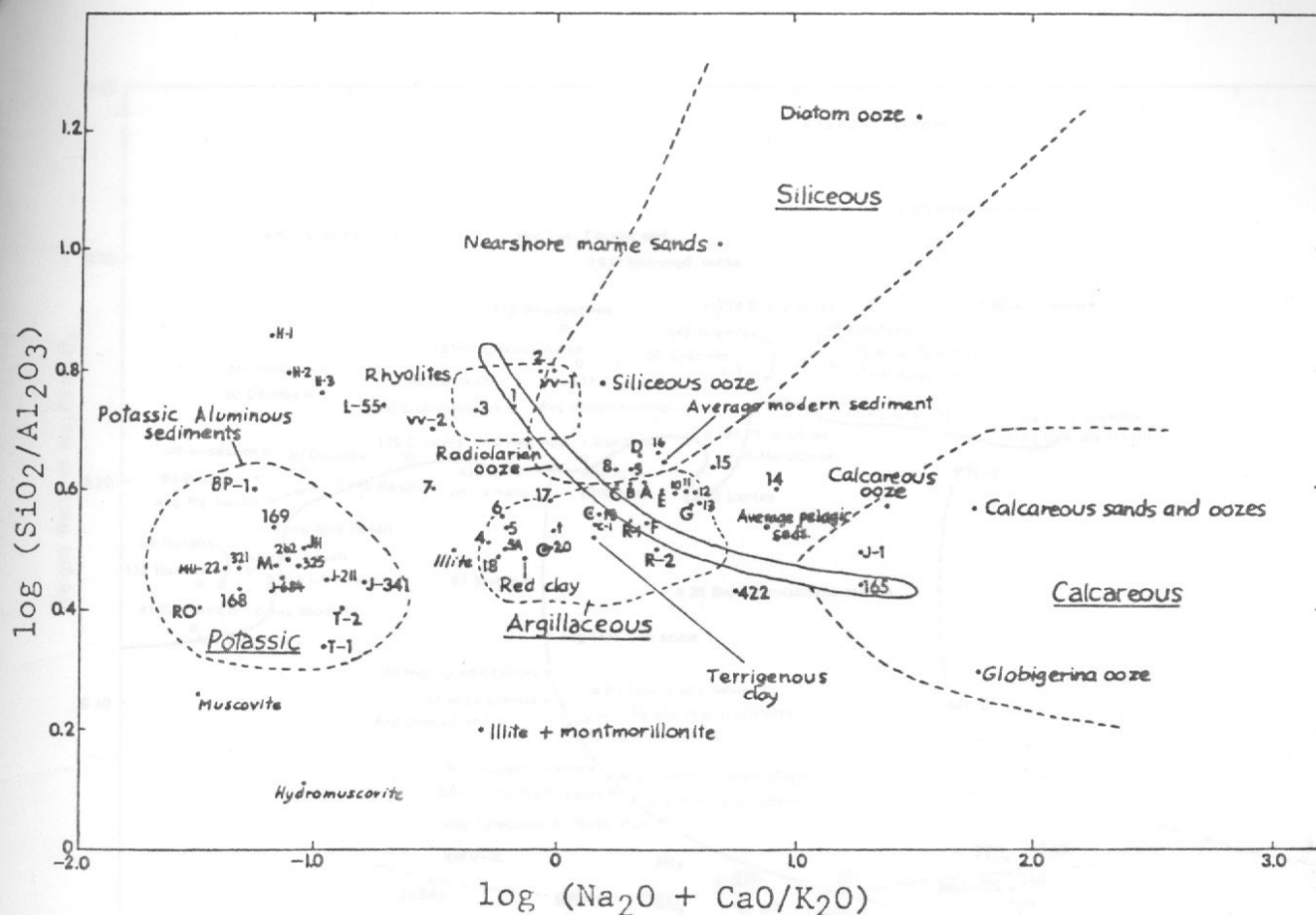


Fig. 17 Chemical compositions of the Batatal and Piracicaba potassic-aluminous schists plotted as a function of  $\log (\text{SiO}_2/\text{Al}_2\text{O}_3)$  and  $\log (\text{Na}_2\text{O} + \text{CaO}/\text{K}_2\text{O})$ . The banana-shaped area denotes the range in composition of igneous rocks with more silicic-, sodium-, and potassium-rich rocks to the left grading into less silicic-, iron- and magnesium-rich rocks to the right. C: Nearshore marine clays; @: Argillaceous pelagic sediments. See next page for legend. Modified from Garrels and Mackenzie, 1971.

J-341: Quartz sericite chloritoid phyllite.  
 gp: Graphitic phyllite.  
 J-211: Quartz sericite phyllite.  
 J-622: Quartz sericite phyllite.  
 168: Silver sericite schist.  
 169: Magnetite sericite chlorite schist.  
 xSA: Staurolite schist (Sabara).  
 Batatal: 321, 325, 262, MU-22: Sericite schists.  
 JH: Sericite schist.  
 RO: Quartz sericite phyllite.





# Explanations to Figures 17 and 18

- 1 - Average calc-alkali rhyolite, 22 analysis (Nockolds, 1954)
- 2 - Average alkali rhyolite, 21 analysis (Nockolds, 1954)
- 3 - Rhyolite (Johnnansan, 1937)
- 4 - Average of 33 Precambrian slates (Nanz, 1953)
- 5 - Average of 36 Paleozoic slates " " "
- 6 - Average of 51 Paleozoic shales " " "
- 7 - Mesozoic and Cenozoic of composite of 27 shales " "
- 8 - Average of the surface of the crystalline shield (Ronov and Yaroshevskiy, 1967)
- 9 - Average of crystalline shield (Holland and Lambert, 1972)
- 10 - Average continental crust " " " "
- 11 - Average continental crust " " " "
- 12 - Average crystalline shield " " " "
- 13 - Average continental crust " " " "
- 14 - Average of the Sconrie assemblage (Lewisian basement) pyroxene granulites " " " "
- 15 - Average of the Lewisian rocks " " " "
- 16 - Average of the Laxford assemblage (Lewisian basement) " "
- 17 - Average of the Moinian rocks (late Precambrian) " "
- 18 - Average of the Dalradian Loven schists (late Precambrian) " "
- 17 & 18 Semipelitic schists
- 19 - Varved argillite, Gowganda Formation, Huronian (Walker & Pettijohn, 1971)
- 20 - Slate of the Minnitaki Lake (Archean, Abram Series " "
- A - Average of the Archean (Holland and Lamberg, 1972)
- B - Average of the surface of the Canadian Shield " "
- C - Average of the Proterozoic " " " "
- D - Average of the Canadian Shield " " " "
- E - Musgrave Range, Australia " " " "
- F - Lofoten-Vesteralen Islands, Norway " " "
- G - Bahia, Brazil (charnockite granulites) " " "
- J-1 - Average of 16 basalts (Johannsen, 1937)
- C-1 - Average shale (Clarke, 1924)
- T - Timiskaming argillite, Ogden Township, Ontario (MacPherson, 1958)
- R-1 - Mudstones of Russian platform (4,030 specimens, 290 analyses, (Ronov and Yaroshevskiy, 1967)
- R-2 - Mudrocks of the Great Caucasus geosyncline (11,151 specimens, 455 analyses) " " "
- BP-1 - Barreiro Formation, graphitic phyllite, Ibirite Quad (Herz, 1978) (Herz, 1978)
- J-211 - Quartz sericite phyllite. Dom Bosco Quad. " " "
- J-341 - Quartz sericite chloritoid phyllite. Dom Bosco Quad. " "
- J-684 - Quartz sericite phyllite. Dom Bosco Quad. " " "
- SA - Sabara Formation. Staurolite schist. Nova Lima Quad " "
- RO - Batatal sericite schist. Gandarela Quad. " " "
- JH - Quartz sericite phyllite (Moeda Form.?) Cachoeira do Campo " "
- M - Mesnard slate (Nanz, 1953)
- T-1 and " " "
- T-2 - Tyler slate " " "
- I - Muscovite, low grade psammitic schist, Inverness-shire (Deer, Howie and Zussman, 1971)

- II - Illite, Pithion, Illinois, USA " " " "
- III - Hydromuscovite, Ogofan, South Water " " " "
- VV-1 - Pillowed lava, Hooggenhoeg Formation, Barberton  
(Viljoen and Viljoen (1969))
- VV-2 - Average of two schistose felsic tuff, Barberton  
" " " " " "
- H-1 - Schistose metarhyolite. Hemlock Formation (Wier, 1967)
- H-2 - Quartz porphyry intrusive (?) in Randville dolomite " " " "
- H-3 - Average of four metarhyolites " " " "
- 168 - Silver sericite schist. Cercadinho Formation. Ibirite Quad.  
(This work, 1976)
- 169 - Dark sericite-chlorite magnetite schist. Cercadinho  
Formation. " " " " " "
- MU-22 - Batatal sericite schist. Mutuca Mine " " " "
- 262 - Batatal sericite schist. Serra das Gaivotas. " " " "
- 325 - Batatal sericite schist. Km 438, Highway BR 040. " " " "
- 321 - Batatal sericite schist. Serra da Moeda, Casa de Pedra. " " " "
- 165 - Talc chlorite schist. Guarita area. " " " "
- 422 - Talc chlorite schist. West part of Mutuca Mine " " " "

Some geochemical association with potash-rich basins

as reported.

On the basis of literature evidence, the  $K_2O$ -enrichment proposed in this study is not as high as in the rocks under discussion. The high  $Al_2O_3$  content may be an indication that the sericite schist was aluminous, or it may reflect nothing more than the high  $K_2O$  content of an original pelite. If the original material had a high  $Al_2O_3$  content, one could propose that the quantity of  $Al_2O_3$  controlled the quantity of  $K_2O$  fixed in the rocks during  $K_2O$  enrichment. In the rocks studied by the author, the enrichment can form up to 2 percent by volume of the rock, representing a  $K_2O$  content for the rock of about 2000 ppm (600 ppm  $H_2O$ ). This value is higher than is commonly regarded as possible by absorption on clays from sea water (Harder, 1961; Reynolds, 1963) and about two orders of magnitude higher than the crustal average (Jurekian and Wedepohl, 1961; Green, 1959).

and felsic tuffs from Barberton (Viljoen and Viljoen, 1969) and of schistose potassic metarhyolites from the Hemlock Formation of Michigan (Wier, 1967). Both of these rocks may have undergone some metasomatism, and may not represent primary compositions.

One may suggest that the high potassium content in these sediments is due to:

- a) Submarine metasomatism, perhaps associated with volcanic processes (Miyashiro et al., 1969).
- b) A process related to the secular evolution of the crust (Holland and Lambert, 1972; Eade and Fahrig, 1971; and Nanz, 1953).
- c) Some geochemical association with potash-rich basins or evaporites.

On the basis of literature evidence, the  $K_2O$ -enrichment proposed in (b) is not nearly as high as in the rocks under discussion. The high  $Al_2O_3$  content may be an indication that the sericite schist was aluminous, or it may reflect nothing more than the high  $K_2O$  content of an original illite. If the original material had a high  $Al_2O_3$  content, one could propose that the quantity of  $Al_2O_3$  controlled the quantity of  $K_2O$  fixed in the rocks during  $K_2O$  metasomatism, to produce illite.

Boron in tourmalines presents yet another problem. In the schists studied by the author tourmaline can form up to 2 percent by volume of the rock, representing a  $B_2O_3$  content for the rock of about 2000 ppm (600 ppm B). This value is higher than is commonly regarded as possible by absorption on clays from sea water (Harder, 1961; Reynolds, 1965) and about three orders of magnitude higher than the crustal average (Turekian and Wedepohl, 1961; Green, 1959).



Dorr and Barbosa (1963, p. 22) postulated that the concentration of tourmaline in parts of the Batatal aluminous potassic schist may well indicate the passage of hydrothermal solutions. By contrast Fleischer and Routhier (1973) have shown that there is a relatively constant boron anomaly (between 127 and 10,000 ppm B) in the Batatal sericite schist over a large region, far beyond the limits of the Passagem stratabound gold deposit. They believe in a consanguineous-syngenetic origin for the boron and gold.<sup>1</sup> Both are thought to have been introduced synchronously with the sedimentation, but not associated with volcanism, the higher concentration of those elements due to a paleogeographic facies differentiation. They believe also that the formation of tourmaline was synmetamorphic and synchronous with the first phase of folding.

Boron, as tourmaline, occurs in large concentrations in a variety of stratabound settings: in the footwall of the Sullivan ore body (Swanson and Gunning, 1945), in the Passagem gold deposit (Fleischer and Routhier, 1973), in black schist in the Adirondacks (Buddington, 1917). The origin of tourmaline in each of these remains obscure.

Boron also forms natural borates, mainly with the Mg-compounds, ascharite:  $\text{MgHBO}_3$ , and boracite:  $(\text{Mg}, \text{Mn}, \text{Fe}) \text{ClB}_7\text{O}_{13}$ , commonly associated with anhydrite, anhydrite-dolomite, or carnalite-sylvite, and in very subordinate amounts with Na-compounds.

---

<sup>1</sup>This suggests that gold, and associated arsenopyrite may be additional anomalous elements in these sedimentary rocks.

However, Braitch (1971) proposed that in most of these instances, the boron accumulated in the  $K_2O$ -rich brines through some unclear secondary redeposition process.

The writer would like to suggest that sedimentation took place within marine, restricted, shallow water basins, near an ancient shoreline. In this environment strong evaporation may have taken place. In some of these basins dolomite formed, together with highly boron-and  $K_2O$ -saturated residual liquors. During the diagenesis of these evaporites and associated clays, illite was formed.

The problem remains as to how the very large quantity of boron became incorporated in these rocks. Several possibilities can be suggested:

- a) From an unknown source in diagenetic or hydrothermal solutions.
- b) From an evaporite or a brine that was rich in both  $K_2O$  and B.
- c) Volcanic emanations.

From these possibilities emerges the suggestion that the high  $K_2O$  and B contents in the schist may be an indication of a common paleogeographic environment, that is, one in which both K and B were introduced into the rocks by seawater evaporation during volcanism.

#### Greenstones

The partly-weathered feldspathic sheared basic rock (Table 6), may be an amphibolite, as suggested by its low  $SiO_2$  and high  $Al_2O_3$  contents. The high Fe and  $Al_2O_3$  contents are the products of weathering. Near the Retiro das Pedras Club, close to the

top of the formation and within the greenschist is a thin layer of quartz muscovite chlorite schist (L-55, Table 6). On the basis of its composition this rock may be a sub-potassic tholeiitic dacite, or perhaps a dacitic tuff.

In the greenstone sequence, the talc chlorite schists (Table 6, Samples 165 and 422) are characterized by very high MgO and relatively low  $\text{SiO}_2$  contents. Some of the silica occurs as scant, microscopic chert lenticles, and the low but consistent  $\text{Al}_2\text{O}_3$  content is related to the chlorite. The rocks resemble tholeiitic picrites on the basis of their  $\text{SiO}_2$ , and MgO contents, but contain a lower quantity of CaO and alkalies. Some of the Batatal greenstones resemble the peridotitic komatiites from South Africa (Viljoen and Viljoen, 1969) in MgO, and the low alkalies, but they have a much lower CaO-content than the komatiites. This low CaO-content might reflect the absence of original calcic pyroxene or plagioclase in these Batatal greenstones.

A partly weathered serpentinite was found in the MBR drill cores at the Tamandua ore deposit.

### Correlations

This work suggests that the greenstone is an excellent marker over a very broad area. For example, in the adjoining area Harder and Chamberlin (1915, p. 357) found a sheet of serpentinitized eruptive rock to rest upon the Batatal schist. This rock occurs at Serra do Caraca, Morro da Mina, and in Boa Vista, near Catas Altas, extending several kilometers northward from there. Maxwell (1972) also recognized in the Alegria District, a suite of rocks which he named the "Greenstone



Table 6

Chemical Analysis of Greenstones of the Batatal Formation  
(Weight Percent)

	(1)	(2)	L-55	165	422	LH	PB	PK	BK
SiO <sub>2</sub>	42.06	45.26	67.68	53.62	48.10	50.3	46.0	44.72	52.73
TiO <sub>2</sub>	--	--	0.69	0.17	0.22	--	0.5	0.52	0.85
Al <sub>2</sub> O <sub>3</sub>	26.72	27.38	12.60	2.91	8.80	16.6	8.8	3.25	9.83
Fe <sub>2</sub> O <sub>3</sub>	19.45	16.87	10.04	9.14	12.08	3.7	6.23	6.02	1.23
FeO	--	--	--	--	--	8.9	4.39	5.52	9.70
Fe	13.6	11.8	--	--	--	--	--	--	--
MnO	0.51	0.17	--	--	--	--	0.21	0.19	0.22
MgO	--	--	2.87	26.68	26.66	6.9	21.29	25.35	10.10
CaO	--	--	0.05	0.30	0.05	10.0	8.85	6.97	9.99
Na <sub>2</sub> O	--	--	0.23	0.04	0.24	2.9	1.78	0.49	2.65
K <sub>2</sub> O	--	--	1.46	0.12	0.11	0.7	.88	0.05	0.46
H <sub>2</sub> O+	--	--	{ 3.35	{ 6.02	{ 3.68	--	.08	5.58	1.93
H <sub>2</sub> O-	--	--					.43	0.21	0.16
P <sub>2</sub> O <sub>5</sub>	0.13	0.13	--	--	--	--	.13	--	0.06
TOTAL	88.87	89.81	98.97	99.00	99.94	100	99.57		

(1) DDH 11/76, depth 60-67 m (with chloritic layers), Tamandua Mine.  
 (2) DDH 11/76, depth 67-78 m, Tamandua Mine.  
 L-55 - Quartz chlorite schist - Retiro das Pedras Club.  
 165 - Talc chlorite schist (with chert laminae), Guarita area.  
 422 - Talc chlorite schist. West part of Mutuca Mine.  
 LH - Average of 50 amphibolites (Lapadu-Hargues, 1953).  
 PB - Porphyritic picrite basalt from New Hebrides. Carmichael, 1974.  
 PK - Peridotitic komatiite from South Africa (Viljoen and Viljoen, 1969).  
 BK - Basaltic komatiite, Barberton type, from South Africa (Viljoen and Viljoen, 1969).

Sequence", above the Batatal schist. These consist of mafic and ultramafic intrusive and extrusive rocks now altered to serpentine, soapstone, talc, and a chlorite schist.

This work also suggests that the sedimentary environment of Proterozoic basins somehow was favorable to the production of shales with anomalous potassium and boron contents.

### Itabira Group

As originally described (Harder and Chamberlin, 1915, pp. 358-362), the Itabira iron formation consists of "a mixture of iron oxide and quartz sand laid down essentially as it occurs today" with some "impure limestone beds in the lower part of the formation at the southeast part of Belo Horizonte." It was redefined and elevated to group status by Dorr and others (1957) because Harder and Chamberlin probably did not include in the formation some dolomitic rocks, previously considered to lie within the Piracicaba Formation. Dorr (1958) subdivided the Itabira Group into two inter-gradational units: the Caue Itabirite, a metamorphosed oxide-facies iron-formation, and the Gandarela Formation, in large part composed of carbonate rocks of various types.

In this section the writer will describe one new type of itabirite, the occurrence of riebeckite in an itabirite, and the variation in itabirite grain size as an indicator of metamorphism.

Caue Itabirite plateaus are impervious blankets of Fe-rich

Distribution, Thickness of the underlying itabirite.

Itabirite (a term common in Brazil and equivalent in current usage to the North American term "iron formation"), which makes up the whole formation, forms prominent ridges and mountain chains in the Quadrilatero Ferrifero. The prominent relief over itabiritic terrain is characterized by either elongate rugged ridges and hogbacks (Fig. 19), or by plateaus of laterite, situated in the upper parts of the mountains, locally known as "chapadas of canga" (e.g. Serra do Rola Moca, Barreiro).

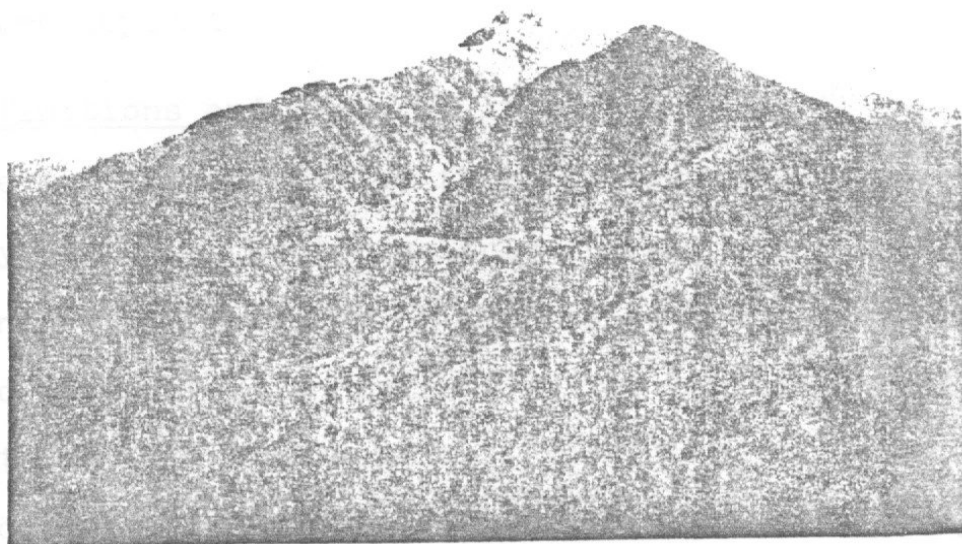


Fig. 19. Typical relief formed by the itabiritic terrain. Serras de Curral and Agua Quente.

Two types of canga are known: 1) canga resulting by weathering and decomposition of itabirite in situ; 2) transported canga, but has been carried through the reconstitution of detrital hematite, ilmenite fragments, and pebbles by yellowish brown and red, hydrated Fe-oxides.



Such canga plateaus<sup>1</sup> are impervious blankets of Fe-rich laterite, formed by weathering of the underlying itabirite. Where located between mountains, canga blankets may form flat bottomed ponds, commonly containing white clay deposits.

Itabirite is widely distributed throughout the study area, and five continuous belts of it, some of which are repetitions due to folding, can be identified geographically (Fig. 20).

The thickness of the itabirite is quite variable and not determinable precisely because of tight folding, the well-recognized ductile character of the rock, and the poorly exposed top and bottom contacts (Pomerene, 1964; Dorr, 1969). The estimated thickness may be 400 to 500 m at Serra da Moeda, about 40 m at Serra de Mutuca, and 200 m in the Capao do Xavier ore deposit.

#### Definitions and Types of Itabirite

The term itabirite was first applied by Eschwege, (1882, in Derby, 1906) to an irregularly coarse, clean iron ore occurring at the Township of Itabira do Campo and subsequently extended in general, in Brazil, to the laminated rock composed of quartz and iron oxide bands. According to the definition of Dorr and Barbosa (1963, p. 18) the rock contains "original chert or jasper bands, recrystallized into granular quartz, and in which the iron is present as hematite, magnetite or martite."

---

<sup>1</sup>Two major types of canga are known: 1) canga resulting by weathering and cementing of itabirite in situ; 2) transported canga that has been derived through the recementation of detrital hematite, itabirite fragments, and pebbles by yellowish brown and red, hydrated Fe-oxides.

This rock is defined as jaspilite in the U.S. (Bailey and James, 1973).

Itabirites show a wide range in composition (Table 7, Fig. 21). Three types of itabirite (or iron formation) are generally recognized in the Serra da Mutuca (Durr, 1969).

All three are characterized by the presence of magnetite.

1. Ferruginous chert, quartz, hematite, and locally magnetite.

2. Magnetite, hematite, and locally magnetite.

3. Magnetite, hematite, and locally magnetite.

4. Magnetite, hematite, and locally magnetite.

5. Magnetite, hematite, and locally magnetite.

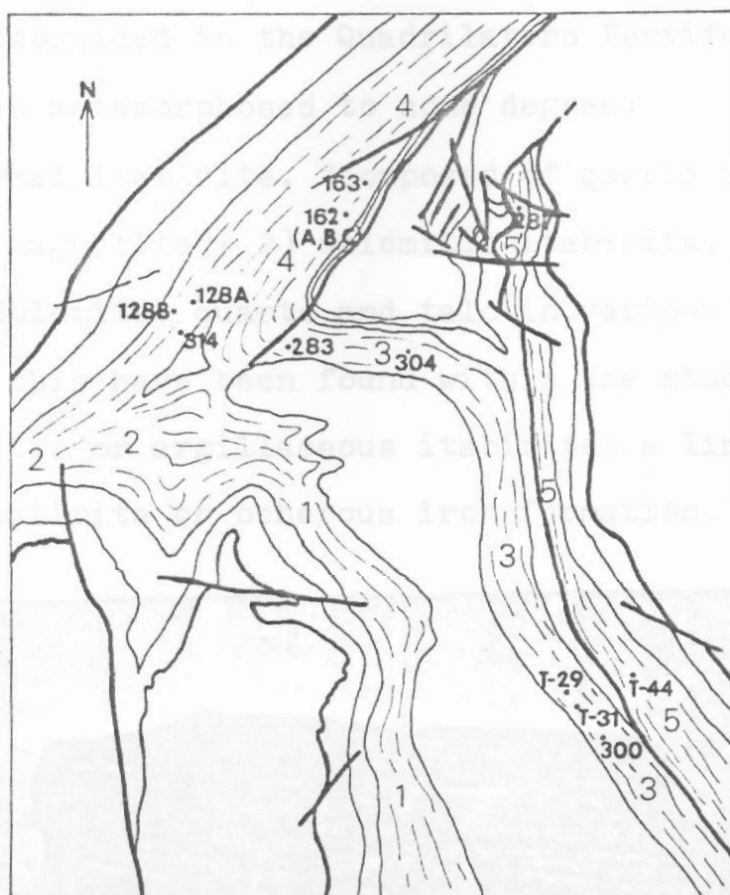


Fig.20 -Distribution of the itabirites in the junction area:

1. Serra da Moeda belt
  2. Serra do Rola Moca-Jangada belt
  3. Capao do Xavier-western Serra do Tamandua belt
  4. Serra do Barreiro-Agua Quante-Curral belt
  5. Serra da Mutuca-eastern Serra do Tamandua belt
- (.T-44-Numbers refer to grain size samples in Fig. 93).

Fig. 21 - Distribution of itabirite. Observe deformation expressed in the siliceous laminae. 2 - 2000 m.

This rock is defined as jaspilite in the U.S. (Bailey and James, 1973).

Itabirites show a wide range in composition (Table 7, Fig. 22). Three types of itabirite (or iron formation) are generally recognized in the Quadrilatero Ferrifero (Dorr, 1969). All have been metamorphosed to some degree:

1) Normal itabirite, "composed of quartz and hematite, and locally magnetite"; 2) dolomitic itabirite, composed of magnetite, dolomite, quartz and talc in various amounts. No outcrops of this have been found within the study area; 3) amphibolitic or argillaceous itabirite; a limonitic, yellowish itabirite or ocherous iron formation.

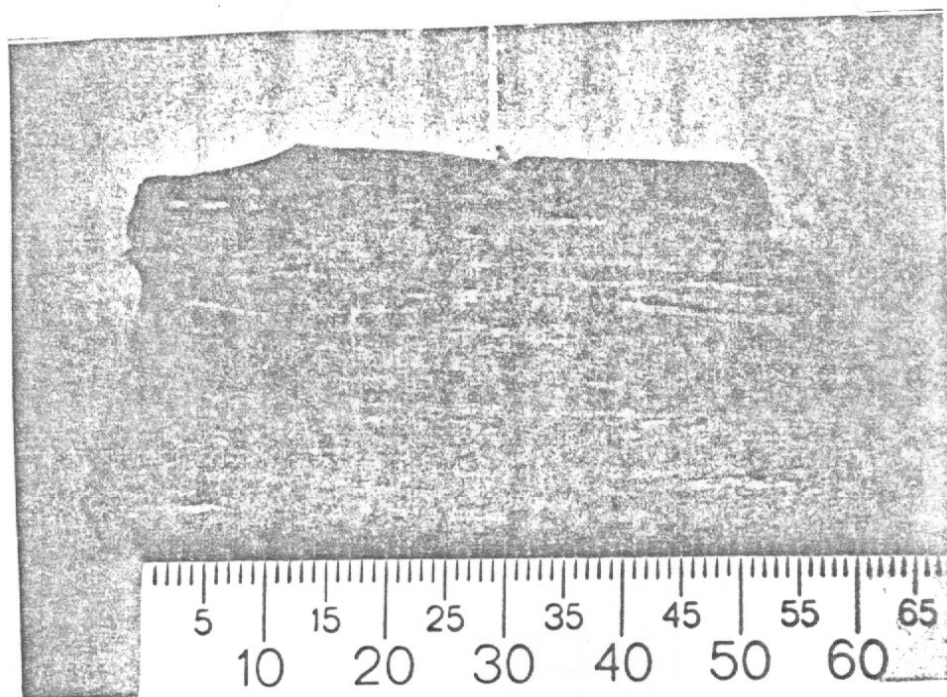


Fig. 21. Laminated itabirite. Observe deformation expressed in the siliceous laminae. Zoroastro Mine.



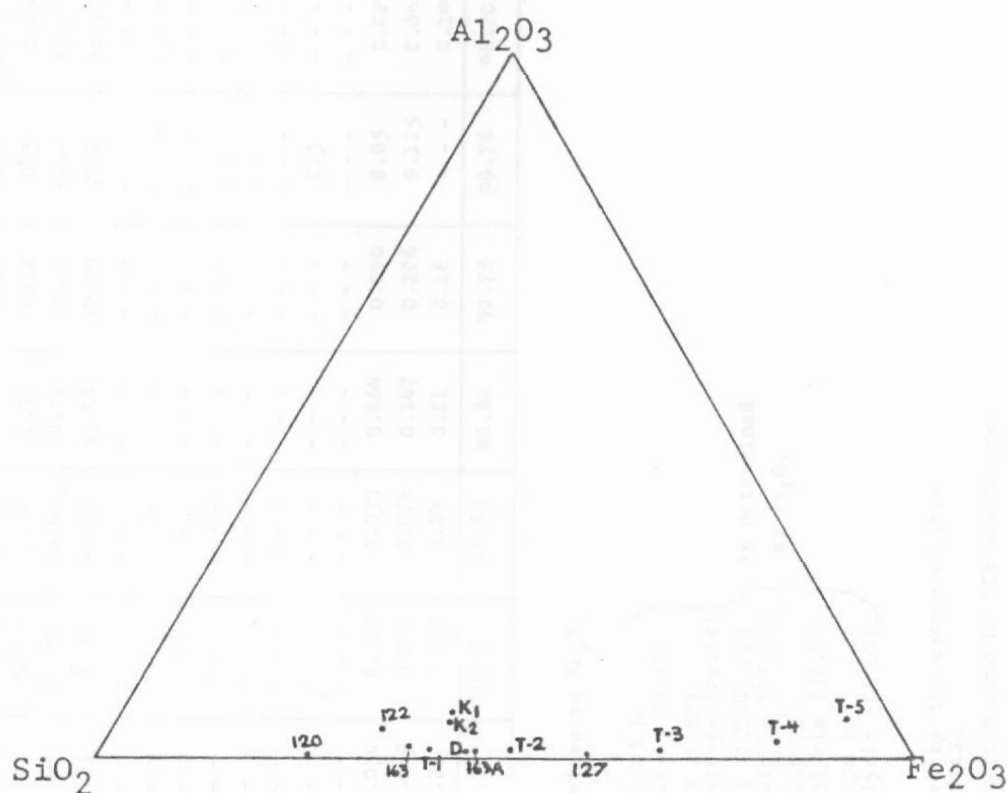


Fig.22 Itabirite compositions.

T<sub>1</sub> to T<sub>5</sub> - Normal itabirite Tamandua ore deposit  
 D - Dorr's average of itabirite composition  
 120 and 122 - Magnetite itabirite  
 K<sub>1</sub> and K<sub>2</sub> - Kaolinitic magnetite iabirite  
 163 and 163-A - Riebeckitic itabirite.  
 127 - Siliceous itabirite.

Table 7  
Chemical Analysis of Itabirites

	163	163A	127	T1	T2	T3	T4	T5	D	TAV
SiO <sub>2</sub>	55.61	53.67	39.37	58.04	49.29	31.99	15.48	6.15	44.7	41.98
Al <sub>2</sub> O <sub>3</sub>	1.10	0.60	0.21	0.91	0.65	1.01	1.30	4.12	0.5	0.86
Fe <sub>2</sub> O <sub>3</sub>	34.81	40.47	58.07	38.40	48.71	64.48	79.70	82.29	54.44	55.07
Fe	24.23	23.18	40.43	27.15	33.91	44.89	55.49	57.29	37.9	36.39
K <sub>2</sub> O	0.13	0.10	0.09	- - -	- - -	- - -	- - -	- - -	- - -	- - -
Na <sub>2</sub> O	0.57	0.52	0.11	- - -	- - -	- - -	- - -	- - -	- - -	- - -
MgO	1.48	1.47	0.01	- - -	- - -	- - -	- - -	- - -	- - -	- - -
CaO	0.10	0.80	0.10	- - -	- - -	- - -	- - -	- - -	- - -	- - -
TiO <sub>2</sub>	0.10	0.12	0.44	- - -	- - -	- - -	- - -	- - -	- - -	- - -
F <sub>2</sub> O	- - -	- - -	- - -	- - -	- - -	- - -	- - -	- - -	- - -	- - -
H <sub>2</sub> O	1.38	2.15	1.10	- - -	- - -	- - -	- - -	- - -	0.3	- - -
CO <sub>2</sub>	- - -	- - -	- - -	- - -	- - -	- - -	- - -	- - -	- - -	- - -
P	- - -	- - -	- - -	0.030	0.018	0.033	0.064	0.090	0.05	0.027
P <sub>2</sub> O <sub>5</sub>	- - -	- - -	- - -	0.069	0.041	0.076	0.147	0.206	0.115	0.082
Mn	- - -	- - -	- - -	0.29	0.117	0.24	0.21	0.16	- - -	0.199
	95.28	99.4	99.4	97.71	98.81	97.80	96.84	92.78	99.76	98.20

163 - Riebeckite itabirite.

163A - Riebeckite itabirite.

127 - Normal Itabirite.

Fe determined as Fe<sub>2</sub>O<sub>3</sub>

T1 - Siliceous itabirite (interval 25.5-28.4% Fe)  
average of 5 analysis (7.4%)

T2 - Iron poor itabirite (interval 30.7-37.2% Fe)  
average of 15 analysis (22.1%)

T3 - Slightly enriched itabirite (interval 41.1-49.2% Fe)  
average of 19 analysis (27.9%)

T4 - Enriched itabirite (interval 50.3-59.9% Fe)  
average of 21 analysis (30.9%)

T5 - Enriched itabirite (interval 5.15-59.3% Fe)  
average of 8 analysis (11.8%)

Fe determined  
as Fe<sub>2</sub>O<sub>3</sub>

D - Dorr's average of itabirite (1963).

The 163, 163A, and 127 samples were analyzed by the author of this report in MTU-303AAS.

T1 to T5 represent averages of chemical analysis done by MDR Laboratory.

TAV - Represents the average of T1, T2, and T3 results.

It is exposed at Mutuca and Zoroastro iron mines, in the central and eastern parts of the Tamandua iron ore deposit, in the southern part of the Capao do Xavier ore deposit, and along the Serras do Curral - Barreiro and Moeda.

In a strict sense, it is not correct to define the third type of itabirite as amphibolitic itabirite because amphibole is a metamorphic rather than a primary mineral. Metamorphic amphibole is not conspicuous everywhere, and amphibole has been found also in the normal itabirite. Where the amphibolitic itabirite is weathered it produces a limonitic itabirite, a yellow, banded, hydrated Fe-oxide rich rock, containing yellowish limonite. Ocherous iron formation (Gair, 1962) represents the weathered and softened limonitic itabirite.

In this report the writer calls attention to one other type of itabirite. This type, characterized by the ubiquitous existence of magnetite, will be identified as magnetite-itabirite. The magnetite-itabirite is a well-banded or laminated rock consisting of extremely fine alternations of yellow, brown and light brown colored laminae, with magnetitic, black laminae. The thickness of the individual laminae varies from submicroscopic (microbands) up to 15 mm (meso and macro-bands, Trendall, 1973). Commonly the lighter bands are thicker than the darker ones. The lighter bands are extremely fine-grained, and composed of chert and small amounts of magnetite in a goethite-stained matrix. Kaolinitic laminae, alternating with lighter, yellowish meso-bands, occur sporadically in the magnetite-poor itabirites.

A particular type of itabirite, frequently referred in the literature as jacutinga (Hussak, 1906), refers to "certain gold



portion of the soft, powdery iron formation, consisting of soft hematite, quartz, talc, kaolin, mica, earthy pyrolusite and tourmaline, in a fine micaceous texture". This material occurs in the Tamandua iron deposit, where some miners recovered gold by panning from the soft jacutinga.

### Textures and Composition

#### Itabirites in General

Itabirite is now a metamorphic rock, so that, except for bedding, all primary features show some modification. The grain size for hematite (Table 8) ranges from 0.01 to 0.15 mm, but in addition, commonly there is an extremely fine-grained dust, between 0.001 and 0.01 mm, as well as dark "clouds" of hematite that parallel the bedding. Quartz is slightly coarser grained, ranging from 0.05 to 0.2 mm, distributed in almost monomineralic laminae, with a granoblastic-polygonal texture. Rarely do the quartz grains show undulant extinction, suggesting that they were recrystallized under conditions of fairly high recrystallization relative to the rates of deformation. The relationship of this grain size variation of quartz to metamorphism and deformation will be discussed further in a later section.

The writer will describe the riebeckite itabirite below. All of the compositional and textural variations of itabirite, except the riebeckite type, have been described previously (Dorr and Barbosa, 1963; Reeves, 1966).

TABLE 8  
TEXTURE AND GRAIN SIZE OF ITABIRITES (Location on Fig. 20)

Type	Texture	Grain Composition	Grain Size (mm)	Grain Shape	Remarks
Itabirite (Hematitic) Capão do Xavier (304)	Granoblastic	Quartz: Hematite:	0.02-0.08 0.04-0.15	polygonal euhedral to irregular	- - - - -
Barreiro (283)	Granoblastic	Quartz: Hematite:	0.01-0.05 0.03-0.08	polygonal sub-euhedral to irregular	- - - - -
Mutuca (287)	Granoblastic to Cataclastic	Quartz: Hematite:	0.04-0.2 0.05-0.15	polygonal euhedral to irregular	Quartz form knots and hematite grew normal to bedding plane
W-Tamandua (T-31)	Granoblastic	Quartz: Hematite:	0.01-0.03 0.02-0.06	polygonal sub-euhedral to irregular	Fluxion in some laminae
E-Tamandua (T-44)	Granoblastic	Quartz Hematite Talc	0.03-0.13 0.02-0.05 0.04-0.12	polygonal euhedral, elongated elongated and tabular flakes	Quartz non undulant Hematite blood red color Talc pale green color
Mylonitic Riebeckitic Itabirite (163) Barreiro - Agua Quente	Granoblastic, with stringers 0.1 to 0.2 mm-thick	Quartz matrix: ribs: Magnetite: Riebeckite: Grunerite: Carbonate Apatite	0.05-0.1 0.05-0.2 0.02-0.15 0.03-0.15 0.05-0.10 0.04-0.12 0.2	polygonal polygonal octahedral, rounded slender slender irregular, euhedral hexagons	Magnetite presents hematite; coronas and along its octahedral planes Riebeckite: pleochroism: $\alpha$ deep blue $\beta$ colorless $\gamma$ brownish length fast Interf. colors: yellow brown to yellow Grunerite: optic sign: (-)? pleochroism: colorless to pale brown
Gruneritic Itabirite. Barreiro-Agua Quente (162A)	Cataclastic Zones	Quartz: Magnetite: Grunerite:	0.01-0.08 0.04-0.15 0.01-0.13	incipient polygonal irregular slender	Quartz grains strained Magnetite grains broken
(162B)	Granoblastic Matrix	Quartz: Magnetite: Grunerite:	0.01-0.04 0.02-0.04 0.01-0.04	polygonal octahedral slender	Homogeneous grain size No straining in quartz
(162C)	Granoblastic (micro-fold)	Quartz: Magnetite:	0.08-0.2 0.03-0.05	polygonal octahedral	Large predominance of quartz over magnetite
Magnetite Itabirite Barreiro (128A)	Massive (Fine-grained matrix)	Quartz: Magnetite:	0.001 0.01-0.06	irregular octahedral	Fibrous quartz between some lamina
Barreiro (128B)	Massive (Fine-grained matrix)	Quartz: Magnetite:	0.02-0.05 0.01-0.05	irregular octahedral	- - - - -
Barreiro (314)	Massive to micro-laminated	Quartz: Magnetite:	0.01 0.02-0.1	irregular octahedral	Very fine-grained kaolinitic laminae. Magnetite: scant.
Morro do Chapéu (300)	Granular	Quartz: Magnetite:	0.01-0.07 0.01-0.05	polygonal octahedral	- - - - -
W-Tamandua (T-29)	Massive (Fine-grained matrix)	Quartz: Magnetite:	0.01-0.04 0.01-0.06	irregular octahedral	"Dusty" quartz.

## Riebeckite Itabirite

A variety of itabirite containing riebeckite, and metamorphosed under conditions of intense penetrative deformation is a very widespread type in the northern part of the area, along Serra do Curral, between the Morros do Barreiro and Agua Quente. It is a massive, hard, dark almost black, dense, rock exhibiting a contorted lamination, and a strong penetrative foliation accentuated by whitish, minute, lenticular quartz rods on the outcrop.

Under the microscope the rock shows a planar structure formed of discontinuous, thin, wavy, films of magnetite and amphiboles (riebeckite and grunerite) that form the foliation, set in a quartzose matrix. This matrix consists of rods of coarser grained quartz, with the long axes up to 8 mm long and short axes between 1 and 3 mm. These rods show an internal foliation that is perpendicular to the foliation in the matrix. For this reason the rods are considered to have been formed by shear and extensive recrystallization of the finer-grained matrix quartz. In the quartz rods the foliation is formed of elongated aggregates of magnetite octahedra, up to 1 mm long.

Grunerite, in slender, brownish, in some cases acicular grains was apparently formed through a reaction involving magnetite and the quartz-rich matrix material which surrounds the magnetite grains. Chakraborty and Taron (1968) described a similar reaction from a banded iron formation in India.

The overall composition of the rock is estimated to be: quartz, 47%; magnetite, 40%; amphiboles, 10%, carbonates, 2.5%; apatite, 0.5%.



Riebeckite in prismatic, slender crystals was identified by XRD (Tables 9 and 10), Electron microprobe and optic methods. It shows an indigo-blue to colorless pleochroism, and a large 2V. Although the Mg-content is low (Table 12), some grains show a distinct negative elongation and a smaller 2V which are considered characteristic of magnesioriebeckite (Ernst, 1960).

Both riebeckite and grunerite can form under a wide variety of metamorphic conditions. Riebeckite is a wide-spread mineral in iron formations, having been reported from most iron formation areas of the world: Ruckmick (1963) found magnesioriebeckite-crossite in the iron formation from Cerro Bolivar, Venezuela. In the Brockmann iron formation from W-Australia, La Berge (1966a) mentioned riebeckite, stilpnomelane and dolomite occurring locally in a cherty magnetite-siderite-minnesotaite rock. La Berge (1966b) studied crocidolite-rich bands associated with stilpnomelane-rich units of probable pyroclast origin, within the Kuruman iron formation of South Africa, and believed that much of the sodium was supplied by volcanic sources. Beukes (1973) studied riebeckite in the Griqualand iron formation from South Africa, interbedded with jasper, below oolitic jasper and an intraformational breccia, and suggested that the enrichment in sodium was favored by shallow-water conditions. Klein (1974) pointed out that riebeckitic crocidolite in the Sokoman iron formation in the Shefferville area of the Labrador Trough occurs in highly deformed, crenulated rock with magnetite, stilpnomelane and quartz, as very low-grade metamorphic products of Na-rich bulk compositions. Immega and Klein (1976) found riebeckite in the older iron formation from Montana in more-highly metamorphosed

Table 9

Comparative X-ray Diffraction Pattern for Riebeckite  
and Grunerite from S. do Barreiro, Minas Gerais,  
Brazil in relation to ASTM standards\*

Riebeckite-ASTM		Brazil		Grunerite-ASTM		Brazil	
Syntectic	Rumania	MG		Labrador		MG	
(d <sub>A</sub> ) I/I <sub>1</sub>	(d <sub>A</sub> ) I/I <sub>1</sub>	(d <sub>A</sub> ) I/I <sub>1</sub>		(d <sub>A</sub> ) I/I <sub>1</sub>		(d <sub>A</sub> ) I/I <sub>1</sub>	
9.03 - 4	9.32 - 4			9.21 - 50			
8.40 - 100	8.40 - 100	8.42 - 100		8.33 - 100		8.34 - 100	
4.88 - 8	4.89 - 10	4.81 - 5		5.20 - 5			
4.51 - 20	4.51 - 16	4.52 - 5		4.84 - 30		4.84 - 35	
3.88 - 8	3.88 - 10			4.68 - 30		4.62 - 15	
3.65 - 6	3.66 - 10	3.64 - 10		4.58 - 35		4.56 - 40	
3.42 - 16	3.42 - 12	3.42 - 15		4.16 - 40		4.18 - 70	
3.27 - 6	3.27 - 14	3.26 - 5		3.88 - 50		3.86 - 30	
3.108 - 55	3.12 - 55	3.11 - 90		3.59 - 5		3.46 - 30	
2.98 - 20	2.98 - 10			3.47 - 55		3.46 - 30	
2.80 - 8	2.80 - 18			3.28 - 50		3.27 - 45	
2.73 - 50	2.73 - 40	2.73 - 80		3.07 - 80		3.06 - 70	
2.61 - 12	2.60 - 14	2.71 - 15		2.99 - 40		3.00 - 5	
2.53 - 45	2.54 - 12	2.52 - 25		2.77 - 90		2.76 - 60	
2.32 - 16	2.32 - 12	2.32 - 15		2.639 - 70		2.69 - 60	
2.296 - 4	2.30 - 4	2.29 - 10		2.50 - 60		2.50 - 40	
2.28 - 4	2.27 - 10			2.41 - 20		2.41 - 15	
2.259 - 10	2.19 - 4	2.24 - 70		2.30 - 40		2.29 - 20	
2.18 - 10	2.13 - 16	2.17 - 5		2.225 - 40		2.23 - 40	
2.08 - 4	2.03 - 6	2.04 - 5		2.02 - 50		2.01 - 5	
	2.00 - 6	1.99 - 10		1.66 - 30		1.66 - 40	
	1.66 - 10	1.66 - 15					

Table 10

Chemical Compositions of Riebeckites  
From the Riebeckite Itabirite

(weight %; done by the author in the MTU-EPMA, 1976)

	(1)	(2)	(3)	(4)	(5)	(6)	(7)	MgT	FeT
SiO <sub>2</sub>	68.81	67.92	62.28	63.05	62.53	60.19	66.48	56.07	50.50
Al <sub>2</sub> O <sub>3</sub>	.15	.08	.19	.13	.21	.21	.23	- - -	- - -
FeO	23.00	23.89	20.98	21.27	23.76	23.46	22.19	- - -	22.64
Fe <sub>2</sub> O <sub>3</sub>	- -	- - -	- - -	- - -	- - -	- - -	- - -	18.83	16.78
Na <sub>2</sub> O	3.12	2.49	5.39	5.85	4.47	6.41	7.29	9.10	8.19
MgO	4.39	5.84	5.10	4.64	7.11	6.13	7.63	14.11	- - -
CaO	.18	.20	.14	.08	.10	.06	.18	- - -	- - -
K <sub>2</sub> O	.13	.16	.14	.13	.11	.12	.12	- - -	- - -
H <sub>2</sub> O	- - -	- - -	- - -	- - -	- - -	- - -	- - -	2.10	1.89
	97.98	100.56	94.22	95.16	98.12	96.58	100.12	100.00	100.00

MgT - Theoretical composition of the Magnesioriebeckite

FeT - Theoretical composition of iron-rich riebeckite



mineral assemblages. Clearly riebeckite indicates metamorphism of rocks that were formed in a soda-rich environment, perhaps where sodium remained in the pore fluid in interstratal solutions, (French, 1973). In the study area the riebeckite-itabirite shows a broad lateral distribution, suggesting the coincidence of a particular stratigraphic unit with Na-rich conditions, and suggesting shallow-waters high in sodium.

#### Gandarela Formation

##### Definition, Regional Distribution, and Thickness

In this paper the name Gandarela Formation is assigned to the sequence of rocks that overlies the thick, laminated, yellowish magnetite itabirite (slaty iron formation), commonly termed amphibolitic itabirite by Dorr (1969) in the upper part of the Caue Itabirite Formation, and underlies the typical lithologies (ferruginous quartzite, white quartzite, and "silver" sericite schist) at the base of the Cercadinho Formation. In the present area the formation contains three main lithologies: a magnetite chlorite schist, a feldspathic mafic rock, and dolomite.

At its type locality at Fazenda do Gandarela, in the Gandarela Quadrangle (Dorr, 1958b), the Gandarela Formation consists essentially of dolomitic strata, dolomitic phyllite, dolomitic itabirite, and phyllite, and is about 750 m thick. In the Santa Barbara and Cocais Quadrangles (Simmons, 1968), about 55 km NE of the present area the formation is 40 m thick, and in the Gongo Soco Quadrangle (Moore, 1969), some 40 km NE of the study area, it is 900 m thick. When Dorr (1958) elevated the Piracicaba Formation (Harder and Chamberlin, 1915, p. 362)

to group status, the dolomites in the lowest part of the unit were named Gandarela Formation and included in the Itabira Group.

The redefinition of the Gandarela Formation is not without its problems. Distinct lithologic types are lacking from the base and top of the Gandarela, and some phyllites within it are indistinguishable from those in the overlying Cercadinho Formation as defined by Dorr (1958). This similarity among phyllites was noted by Harder and Chamberlin (1915) and by Johnson (1962). Adding to the problem are the deep residual soils and the complex structures. Thus, one must resort to such field criteria as the occurrence in the saprolite of greenish chlorite flakes, magnetite octahedra, or a yellowish pigmentation as indication of Gandarela Formation.

#### Magnetite Chlorite Schist (Greenstone) and Amphibolite

##### Distribution

The main lithology is a fine-grained deep-green magnetite-chlorite schist, a greenschist, probably derived from a mafic volcanic rock. This rock is widespread along the eastern flank of the Moeda range, crops out at several places in the Ribeirao do Mata Porcos, in the western flank of Serra do Itabirito and Serra do Saboeiro, and in the core of the Moeda Syncline. The greenschist crops out commonly in the cores of anticlines, being overlain on the flanks by quartzite of the Cercadinho Formation.

Excellent outcrops of the Gandarela greenschist occur along the Belo Horizonte-Rio de Janeiro (BR 040) Highway at km 386-387, 394-396, and 410, in creeks between Corrego do Lopes and Corrego do Eixo, near Ribeirao Mata Porcos (Marinho da Serra and

Itabirito Quadrangle). At Buraco do Engenho Grande and Bocaina quarries, the greenschist encloses mineable lenses of stromatolitic dolomite. There are also good outcrops in road cuts along the road linking Morro do Chapéu Golf Club and BR 040 (km 425), near the dolomite at Capitão do Mato, and in the Feixos - Ouro Podre water supply area.

#### Field Description

In general the rock is well foliated and chloritic. In this chloritic matrix are perfect octahedra, or clusters of grains of magnetite, from submicroscopic to about 1/4 mm in diameter. Some of the magnetite is random in occurrence, and some form 1/2 to 2-mm, magnetite-rich layers in a generally chloritic matrix. Locally, as for example, at km 394-396 (BR 040), magnetite octahedra occur in 2 to 5 mm grains, as disseminations.

In the creek between Corrego do Eixo and Corrego do Lopes there are white layers, several mm thick, in the greenschist, formed of quartz and kaolinite (after feldspar?). There are also very thin, bright green, talc-rich layers in the greenschist.

The greenschist weathers to a varicolored clayey saprolite, with preserved schistosity. In partly weathered material the common colors are white, red, brown, yellow, and greyish.

To the west of the outcrop of greenschist on the Morro do Chapéu road there is an outcrop of weathered, yellowish-brown microbrecciated amphibolite. Angular breccia fragments, less than 15 mm in diameter are distributed irregularly within the matrix. Within a few meters, the material loses its brecciated character, increases in feldspar content, and grades into a rock



with a porphyritic texture to form an amphibolite. This amphibolite which crops out in an extension of at least 400 m along the Morro do Chapéu road is slightly banded. This banding is accentuated by the preferred orientation of feldspars and altered mafic minerals (Fig. 23). The feldspars, which range in size from 1 to 5 mm, are now kaolinite, and mafic minerals are hydrated, brownish clay minerals with iron oxide pigmentation. No quartz has been recovered by panning. The rock is designated as "anf" in the Geologic Map.

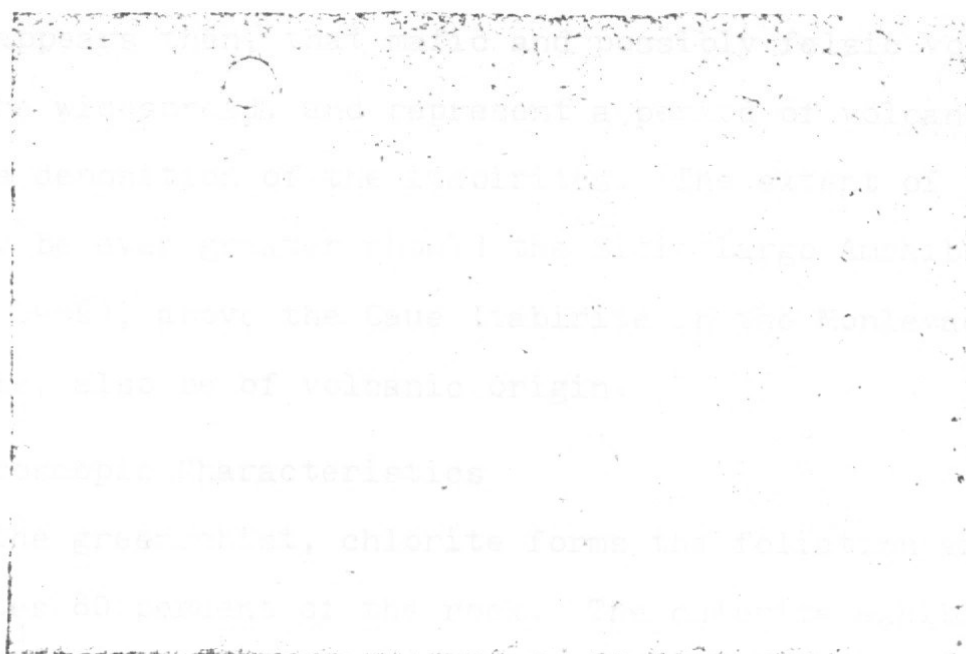


Fig. 23. Weathered amphibolite of the Gandarela Formation. White spots were feldspars transformed into kaolinite. Morro do Chapéu road. Coin is 2.5 cm in diameter.

This amphibolite is similar in texture to the Sitio Largo amphibolite of the Gandarela Formation (Reeves, 1966). The amphibolite is overlain by a partly weathered, yellowish, fine-grained well-foliated greenschist which is exposed for 300 m along the Morro do Chapéu road. This greenschist crops out

also in the hill behind the Skol Brewery. Locally it grades into a fine-grained amphibolite. It occurs also at the top of Serra do Barreiro, on the Vargem da Caveira area.

A magnetite-bearing chlorite schist also is described in the Gandarela Formation by Johnson (1962) from north of Ribeirao da Colonia (Dom Bosco Quadrangle). He interprets it to be possibly a lava. Guild (1957) found a coarse-grained magnetite amphibole schist near S. Juliao, and a probable felsic flow or tuff above the Caue Itabirite, just south of the village of Esmeril (Congonhas Quadrangle).

It appears then, that mafic and possibly felsic volcanic rocks were widespread, and represent a period of volcanism after the deposition of the itabirites. The extent of these rocks may be even greater should the Sitio Largo Amphibolite (Reeves, 1966), above the Caue Itabirite in the Monlevade Quadrangle, also be of volcanic origin.

#### Microscopic Characteristics

In the greenschist, chlorite forms the foliation and constitutes 80 percent of the rock. The chlorite exhibits a deep green (parallel to foliation) to greyish (perpendicular to foliation) pleochroism, and occurs in flakes generally less than 0.05 mm in length. Sporadic lenticles composed of flakes perpendicular to foliation measure 0.35 mm, with individual flakes within the lenticle about 0.08 mm. Octahedral magnetite porphyroclasts, scattered throughout the matrix or forming magnetite-rich bands, form about 8 percent of the rock. There is also microscopic, comminuted magnetite that occurs in flattened lenticles, along shear planes, surrounded by a

whitish network composed mainly of feldspar and dusty nebulae of iron oxides and leucoxene. Some magnetite also occurs in helicitic structure along foliation and is surrounded by eye-shaped pressure shadows. Interstitial magnetite with inclusions of rutile and silicates are common.

Rutile occurs as rounded and elongated grains within magnetite as well as in grain clusters and in composite grains with magnetite. In some grains rutile follows (111) planes within magnetite or irregular fractures coated by silicates.

Talc occurs commonly in larger flakes than chlorite, in pressure shadow zones, in places intergrown with chlorite or stilpnomelane. Stilpnomelane (ferri-stilpnomelane?), in yellowish brown flakes, is associated commonly with talc in these shadow zones, suggesting a reaction (Fig. 24):

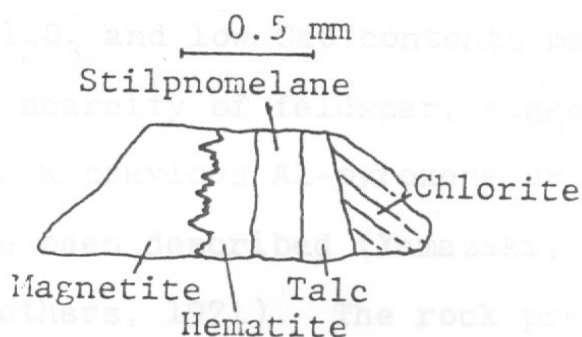


Fig. 24. Possible reaction between a partly oxidized magnetite grain and chlorite.



There is also some fractured 0.10 to 0.35 mm long apatite and euhedral sphene grains along the foliation.

### Petrology

The Gandarela greenschist is a hard, fresh-looking rock as it crops out between km 410 and 413 of Highway BR 040. It is characteristically a MgO-rich rock, with very low amounts of CaO, Na<sub>2</sub>O, and K<sub>2</sub>O, and about 10% Al<sub>2</sub>O<sub>3</sub>, and remarkably high amounts of titania (2.7% TiO<sub>2</sub>; Table 11). MgO and Al<sub>2</sub>O<sub>3</sub> are concentrated mainly in the chlorite. The rock also contains high amounts of Fe<sub>2</sub>O<sub>3</sub> (29.8%) which is in the magnetite and chlorite. As this rock is near the contact with itabirite, and the amount of magnetite decreases with the distance from the itabirite, it is assumed that some of the iron has become incorporated to the greenschist.

The original composition of the rock is a puzzle, and perhaps a superposition of events or contaminations must account for its ultimate composition (W.I. Rose, Jr., personal communication, 1977). The high Al<sub>2</sub>O<sub>3</sub> and low CaO contents may indicate some disequilibrium and scarcity of feldspar, suggesting the existence of either a previous Al-pyroxene or hornblende inclusions, as have been described (Yamazaki, 1966, in Ernst, 1968 and Deer and others, 1971). The rock presents some similarities to peridotitic komatiites from South Africa (Anhaeusser, 1976; Viljoen and Viljoen, 1969), but its Al<sub>2</sub>O<sub>3</sub> and Fe<sub>2</sub>O<sub>3</sub> contents are higher, and MgO is relatively lower.

The composition of the Sitio Largo amphibolite, which overlies the itabirite in the Monlevade District, and the average of tholeiitic basalts (Nockolds, 1954) are quite similar.

Table 11

Chemical Composition of Greenstone  
and Amphibolite of the Gandarela Formation  
(in weight percent)

	P-22	Rod	PKO	SL	TB
SiO <sub>2</sub>	35.10	35.69	42.67	48.4	50.83
TiO <sub>2</sub>	2.70	0.07	0.30	1.4	2.03
Al <sub>2</sub> O <sub>3</sub>	10.30	2.77	3.33	15.7	14.07
Fe <sub>2</sub> O <sub>3</sub>	29.80	10.52	6.28	3.3	2.88
FeO	---	0.80	4.74	9.9	9.00
MnO	---	0.12	0.19	0.2	0.18
MgO	19.10	34.39	29.03	6.1	6.34
CaO	0.37	2.45	4.49	9.5	10.42
Na <sub>2</sub> O	0.19	0.06	0.28	1.7	2.23
K <sub>2</sub> O	0.10	0.05	0.05	.34	0.82
H <sub>2</sub> O	2.30	10.49	7.28	2.6	0.91
P <sub>2</sub> O <sub>5</sub>	---	0.02	---	1.3	0.23
	99.91	99.81	99.76	99.27	- - -

P-22 Greenschist (Magnetite talc chlorite schist, Km 410, Highway BR 040)  
done by the author in the MTU 303 AAS

ROD -Serpentinized ultramafic rocks (Roodekrans Complex, Anhaeusser, 1976)

PKO -Peridotitic Komatiites from Barberton (Viljoen and Viljoen, 1969)

SL -Sitio Largo Amphibolite, Gandarela Formation, (Reeves, 1966)

TB -Average tholeiitic basalt (Nockolds, 1954, 137 analysis)

## Dolomite

### Stratigraphic Position

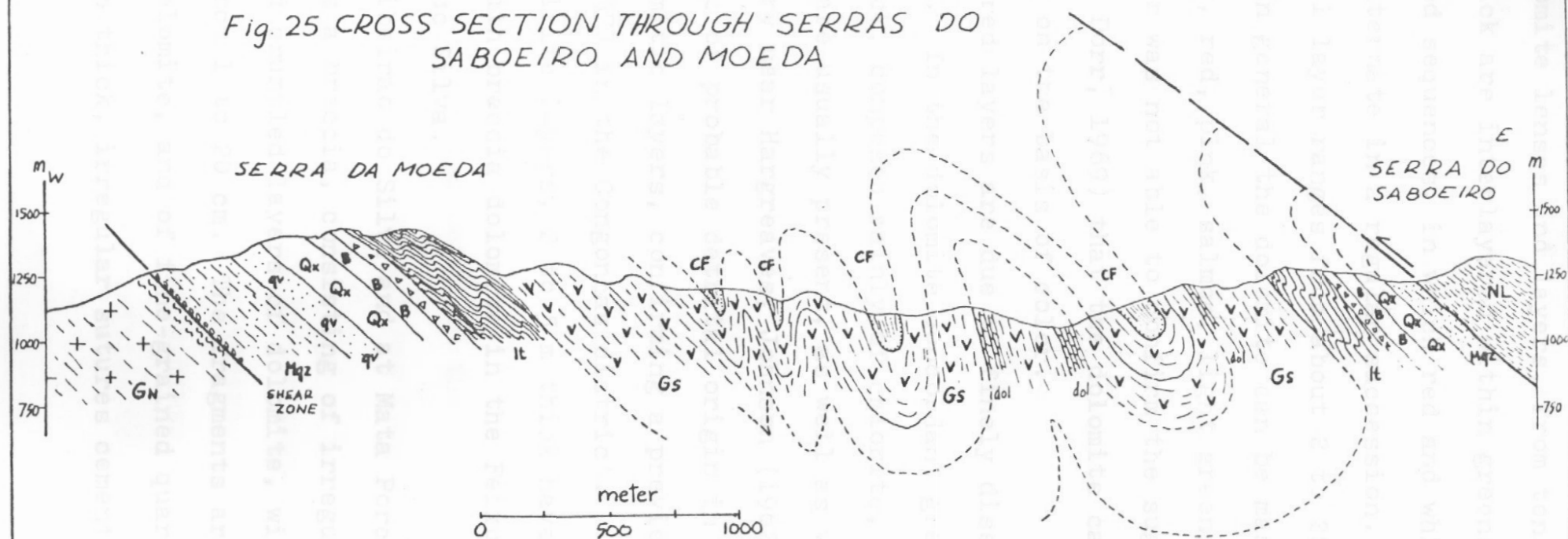
In the Moeda and Dom Bosco synclines there are several dolomite lenses and layers, rarely stromatolitic. Wallace (1965) considered only those dolomites outcropping at the Capita do Mato and north of Serra do Saboeiro as occurring in the Gandarela Formation, and placed the dolomite lenses at Ribeirao do Mata Porcos into the Fecho do Funil Formation. All of the dolomitic lenses considered here are in contact with greenschists or thin itabiritic units, or are covered by graphitic phyllite. No dolomite layers or lenses have been found above the ferruginous quartzite or the "silver sericite schist" of the Cercadinho Formation.


Cross sections through Ribeirao do Mata Porco Valley (Fig. 25) show the general structure and the stratigraphic position of the dolomite within the Gandarela greenschists.

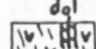
Another reason for placing the dolomites within the Moeda Syncline in a single formation is the ubiquitous presence of an intra-formational dolomitic breccia in the typical Gandarela dolomite (Guild, 1957; Dorr, 1969). Dolomites studied by Wallace (1965) at the Ribeirao do Mata Porco also contain an intraformational breccia, and for this reason the writer considers these dolomites to belong to the Gandarela Formation.



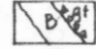
Fig. 25 CROSS SECTION THROUGH SERRAS DO SABOEIRO AND MOEDA

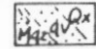


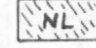
 CF- Cercadinha Formation:  
black, white quartzite, sericite schist

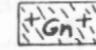
 Gandarela Formation:  
Gs- greenstone; dol- dolomite

 Itabirito Cavê:  
Itabirite: It.

 Batatal Formation  
gt- greenstone; B- sericite schist

 Moeda Formation  
Qx- quartz schist  
qv- greenschist and  
green quartzite  
Mqz- quartzite, conglomerate

 Nova Lima Group  
Greenschist

 Bonfim Gneiss

### Field Description

Dolomite lenses and layers, from tens of centimeters up to 200 m-thick are interlayered within greenschists. The dolomites are banded sequences, in which red and white, or gray and white layers alternate in a regular succession. Thickness of each individual layer ranges from about 2 to 20 mm, with some up to 50 cm. In general the dolomite can be massive or, white, gray, dark gray, red, pink, salmon, light green, or cream in color. The writer was not able to confirm the suggestion of O'Rourke (1954, in Dorr, 1969) that the dolomite can be subdivided into 3 members on the basis of color.

The red layers are due to finely disseminated martitized magnetite. In the dolomite concordant greenish layers, 10 to 20 mm-thick, composed mainly of chlorite, talc, tremolite, and dolomite are usually present, as well as very thin chert layers. In a quarry near Hargreaves, Johnson (1962) noticed magnetite and quartz of probable detrital origin in thin bands concordant with dolomitic layers, confirming a previous observation of Guild (1957) in the Congonhas district.

Itabirite layers, 2 to 5 m thick have been encountered in contact with breccia dolomite in the Feixos area as well as in Ribeirao do Silva.

At Ribeirao do Silva and at Mata Porcos the dolomite is present as a breccia, consisting of irregularly distributed, broken and crumpled layers of dolomite, with fragments varying in size from 1 to 20 cm. The fragments are of banded and massive dolomite, and of fine-grained quartzite, arranged along 5 to 10 mm thick, irregular sutures cemented by a matrix of

calcite, dolomite, and silica.

At the Ribeirao do Silva quarries, there have been found several zones of brecciated dolomite, apparently not connected at the surface. Some of the brecciated zones consist of a matrix of abundant, impure, siliceous, magnetitic, dolomite in which smaller angular fragments of fine-grained quartzitic material and slightly rounded pieces of dolomite (Guild, 1957) are present. Guild described the rock as being "evidently an infraformational breccia conglomerate, formed by the breaking up of thin siliceous beds, no doubt cherts and carbonate beds soon after deposition". There is the possibility that the breccias were formed along an erosion surface. Dolomite breccia has also been mapped by Pomerene (1964) at Acaba Mundo quarry (Belo Horizonte Quadrangle) and by Guild (1957) 2.2 km south of Usina (S. Juliao Quadrangle).

Because the dolomite breccias are so widespread in occurrence, the possibility arises that they were formed at a unique period of time, and denote unique conditions of formation. The brecciated zones might represent a sea level oscillation, or a slight uplift of the area, near the end of deposition of the Gandarela Formation. Dorr (1969) appears to have assumed that the breccia is situated in the upper part of the formation, but unfortunately, the writer has found no evidence in support of this attractive idea.

Stromatolites occur at Borges quarry, located approximately 2 km from Retiro das Almas Belvedere, (Fig. 26) and near an abandoned manganese mine (Barra Mansa Mining Co.) at Ribeirao do Silva. They suggest affinities to the Collenia group



but display a different morphology from those described by Dardenne and Rocha Campos (1975). In that stromatolites denote a shallow carbonate environment, there could be many mechanisms operating to produce dolomite breccia. Thus, these may be more diagnostic of the environment than of a particular stratigraphic position.

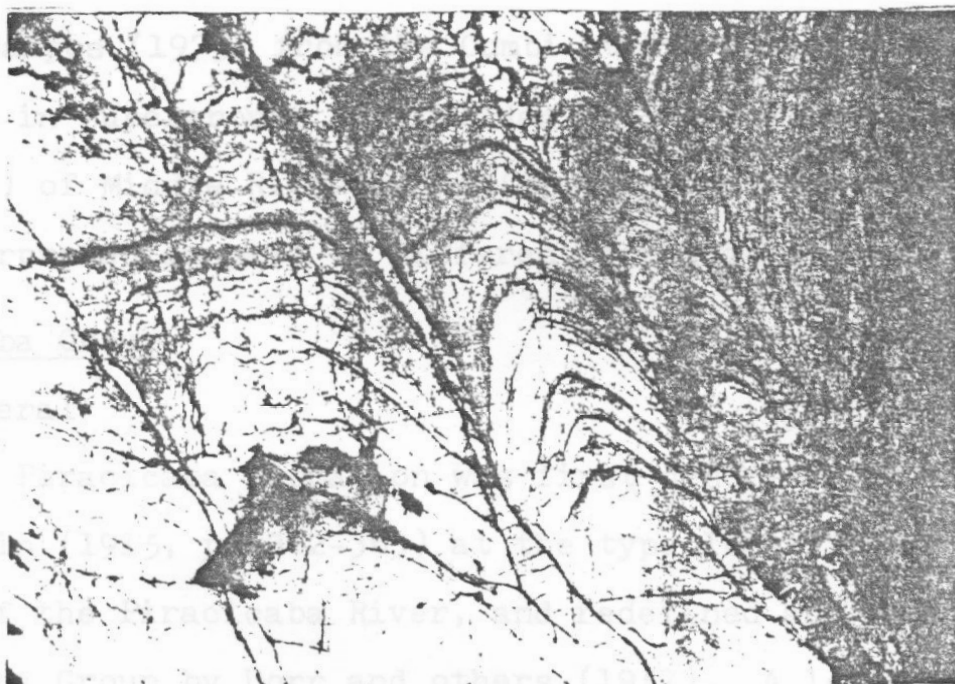


Fig. 26. Stromatolites of the Collenia type, in the Gandarela dolomite. Borges quarry, near Retiro das Almas (Belvedere).

Stromatolites associated with mafic volcanic rocks of the Wolkberg Group of South Africa have been described by Button (1972), who suggested that the algal colonies evolved prior to about 2.0 billion years ago in small volcanic lakes, different to the shelf-carbonate deposition. The Gandarela stromatolites present a similar depositional setting, that is, they form lenticular bodies within mafic volcanic rocks, suggesting similar environment to that found in recent atoll or barrier reef formations,

The morphology of stromatolites from Borges quarry are quite different from those found at Cumbi quarry (S. Nordeng, personal communication, 1978). Stromatolites at Borges quarry may be classified in the Collenia Group, similar to those found by Almeida (1944, 1958) in dolomites of the Sao Roque and Corumba Series, both of which are correlated with rocks of the Minas Series. The columnar stromatolites described by Dardenne and R. Campos (1975) from the Cumbi quarry consist of two types, included in supergroups Kussielides and Tungussides (group Baicalic) of Middle Riphean age (950-1350 m.y.). Thus, they are interpreted as part of different formations.

### Piracicaba Group

#### General

The Piracicaba Formation was first described by Harder and Chamberlin (1915, p. 362-363) at the type-locality on the upper course of the Piracicaba River, and redefined and renamed the Piracicaba Group by Dorr and others (1957). A local erosional disconformity between the Piracicaba Group and the Gandarela Formation is mentioned by Dorr (1969, pp. 48) only on the west side of the Quadrilatero Ferrifero. Near Ouro Preto the Piracicaba rocks are overlain by the Itacolomi Series (Guimaraes, 1931, pp. 8). Although the Piracicaba Group has been subdivided into five formations, from the base to top: Cercadinho (Pomerene, 1958), Fecho do Funil (Simmons, 1958), Taboões quartzite, Barreiro (both Pomerene, 1958), and Sabara Formation (Gair, 1958), these do not occur everywhere in the map area. Ferruginous and white quartzite, silver sericite schists, chlorite schists, graphite schists and impure dolomite are the typical lithologies in this group.

### Distribution and Thickness

The Piracicaba Group is present both in the northwest and the southeast parts of the study area, near Miguelao dam. In the northwest part all formations are present, and crop out along sub-parallel strips trending northeast-southwest. In the southeast part of the area, only the Cercadinho and Fecho do Funil formations are present in a small hill, which marks the nose of the Moeda structure. In the Moeda plateau the Sabara Formation is missing.

In general, the Cercadinho Formation is the most persistent and easily recognizable, and the graphitic phyllites of the Barreiro Formation, although absent in some places is a readily-recognized unit of the Piracicaba Group.

In the present area of study, the thickness of the Piracicaba Group could not be determined due to tectonic complexity and weathering.

Harder and Chamberlin (1915) believed that their Piracicaba Formation was more than 300 m thick, and Dorr (1969) thought the minimum remaining thickness of the Piracicaba Group to be 4,800 m. Gair (1958) suggests that the thickness of the Sabara Formation ranges between 3,000 and 3,500 m. Consequently the total thickness of the remaining formations is 972 m.

### Lithology and Stratigraphy

According to Pomerene (1958), the bulk of the Cercadinho Formation consists of a) a basal white quartzite; b) ferruginous quartzite; c) silver sericite schist or phyllite within dark gray chlorite-sericite schist; and d) minor magnetite-chlorite



schist. The schists are deeply weathered and indistinguishable from the schist of the Fecho do Funil and Gandarela Formations.

Pomerene (1964) described a polymict basal conglomerate of the Cercadinho Formation, from one locality in the Macacos Quadrangle.

The quartzites form 0.5 to 1.5 m thick beds which are interbedded with thin layers of silver sericite schist (Fig. 27).

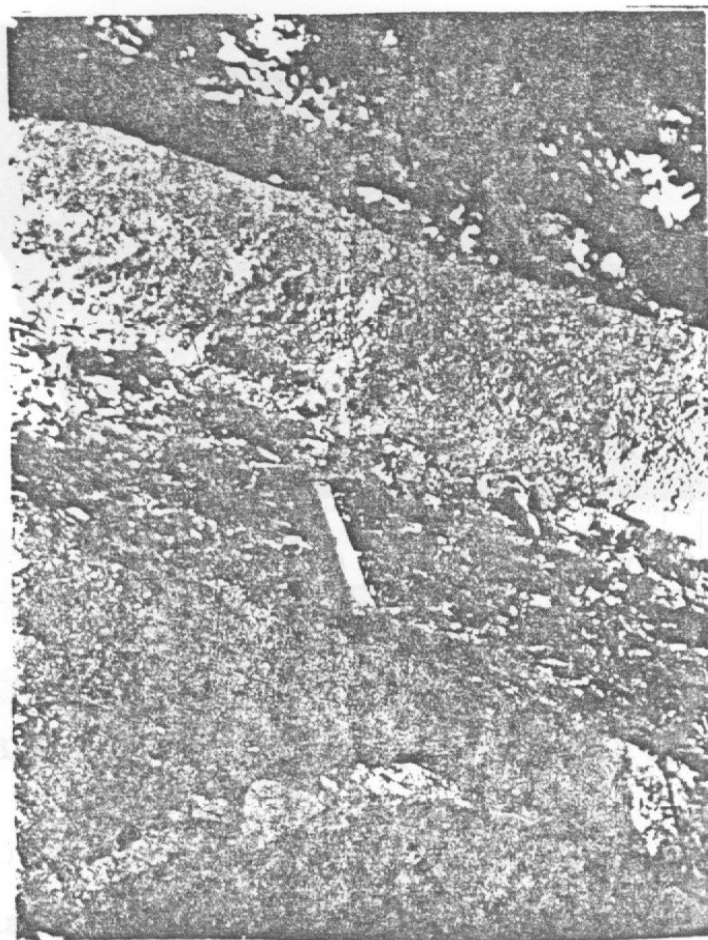


Fig. 27. White quartzite with thin layers of silver sericite schist. Cercadinho Formation. Barreiro Road.

Commonly the white quartzite is almost pure, fine- to medium-grained, but does contain sporadic pyrite, chlorite and sericite flakes. It weathers easily to a sand on the outcrop.

recognizable by its typical silvery sheen, strong anisotropy,

The ferruginous quartzite is composed of well-rounded, coarse- to medium-grained quartz grains which form 70 weight percent of the rock, irregularly distributed in a dark brown to black matrix consisting mainly of limonite and hematite (30 weight percent; Fig. 28). Black tourmaline and zircon occur in subordinate amounts. The rock is usually massive, but Pomerene

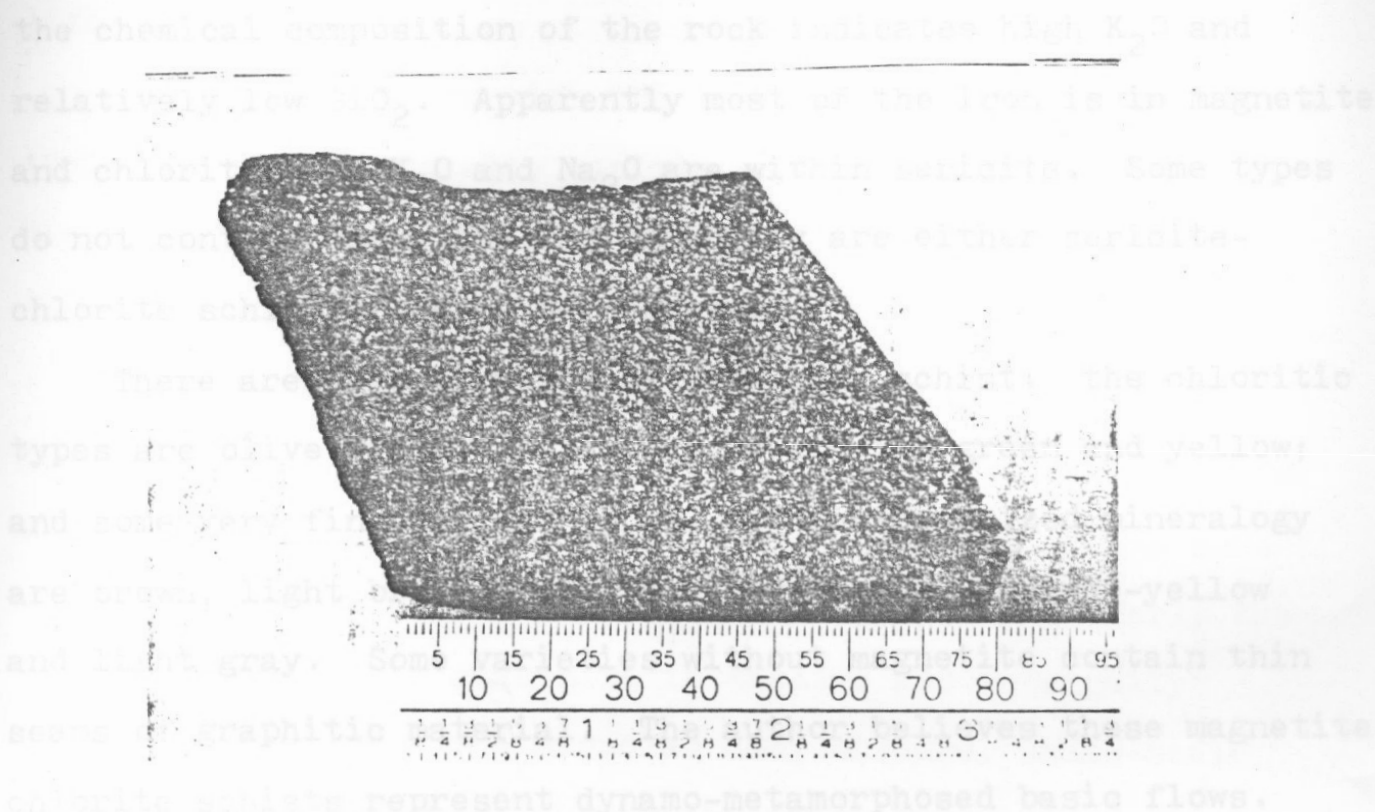


Fig. 28. Black, ferruginous quartzite. Cercadinho and Barreiro Road.

(1964) observed hematite flakes arranged along the cross-bedding. The white and black quartzites and the silver sericite schist form definite, long lenticular bodies within the main, dark gray schist.

The silver sericite schist is exposed both in intercalations, 30 to 40 cm thick, although in some places only 1 or 2 cm thick, within the quartzites, and also in individual lenses, 1 to 2 m thick within the main schist. This silver schist is easily recognizable by its typical silvery sheen, strong anisotropy,

stratigraphic position and lithological association. Its chemical composition shows a very high  $K_2O$  and low-Fe contents (Table 12).

The chlorite-sericite-magnetite schist contains these minerals in varying proportions, locally with anomalously high magnetite content. The amount of quartz is usually low, and the chemical composition of the rock indicates high  $K_2O$  and relatively low  $SiO_2$ . Apparently most of the iron is in magnetite and chlorite, and  $K_2O$  and  $Na_2O$  are within sericite. Some types do not contain magnetite and generally are either sericite-chlorite schist or sericite schists.

There are several types of dark gray schist: the chloritic types are olive green, olive gray, yellowish green and yellow; and some very fine-grained types, with unrecognized mineralogy are brown, light brown, pale tan, purple gray, orange-yellow and light gray. Some varieties without magnetite contain thin seams of graphitic material. The author believes these magnetite-chlorite schists represent dynamo-metamorphosed basic flows.

In addition the lithologies discussed above, chert and graphitic phyllites are present. Stratigraphically higher, enclosed in greenschists and graphitic schists, the author has found a few layers, 10 to 30 cm thick of black, fine-grained, slightly recrystallized chert, with thin, 1 to 2 cm-thick bands of white chert. These rocks are probably in the upper part of the Piracicaba Group, rather than within the Sabara Formation. The cherts are so unaltered that one can see in them sub-microscopic to microscopic spheroidal, greyish micro-granules



that could constitute primitive micro-organisms. These are distributed irregularly in clusters within a darker part of the chert. At the contacts between the white and dark chert layers are thin, black, 1 to 3 mm-thick chert lenses.

The graphitic phyllites form lenses within the now weathered greenschists and phyllites, represented by purplish, reddish and light-orange schists.

The author agrees with the view of Pomerene (1964) that a graphite-bearing, locally pyritic rock unit represents the Barreiro Formation.

### Primary Structures

Bedding is very conspicuous within the Piracicaba Group. The sequence of white and black quartzite and silver sericite schist, and the graphitic lenses constitute some of the more conspicuous beds. Their sharp contacts establish clearly the bedding planes. The quartzite is massive and internally structureless. Near the Miguelao dam, obscure, small-scale cross-bedding is visible within the white and black quartzites. Pomerene (1964) found some littoral type cross-bedding and oscillation ripple marks within the ferruginous quartzite near Lagoa Seca in a roadcut of the Highway BR 040, in the Belo Horizonte Quadrangle.

### Environment of Deposition

The writer believes that the Piracicaba Group was deposited in restricted, shallow basins and lagoons, in apparent continuity with the atoll and barrier reef formation which characterizes

the Gandarela Formation. This interpretation differs only slightly from that of Dorr (1969) who postulated a stable shelf environment for all the Piracicaba Group except for the Sabara Formation. This represents sedimentation after a period of erosion that removed parts of the underlying Gandarela Formation. Dorr suggested that the Cercadinho Formation is "typical of near-shore or deltaic sediments deposited on a rather flat surface," and the Fecho do Funil Formation indicates a "gradual encroachment and deepening of the sea." Dardenne and Rocha Campos (1975) described stromatolites within the Fecho do Funil dolomites, and suggested a sedimentation in shallow and quiet waters.

The writer interprets the lenticular character, purity and cleanliness of the basal quartzites, and cross-bedding and oscillation ripple marks to indicate that the deposition within the lagoons was controlled by sea level fluctuations and tides, which dictated the capacity of the waves and surf to override the reef and reach the lagoon. Winds probably added some sand into the lagoon from adjoining areas of sand dunes. Sparse, thin, lenticular conglomerates are local, and denote deposition in areas of slightly higher relief around the lagoons. The reduced thickness of the individual banks of quartzite indicates sedimentation in shallow waters, in a short span of time.

The silver sericite schists (Table 12) present a very high  $K_2O$  content seldom found in common sedimentary pelitic material.

The magnetite-chlorite schists which occur in thin layers, in alteration with pelitic schists and phyllites tend to increase slightly in frequency upwards. They may represent mafic flows or sills.

Piracicaba } Cercadinho  
Fecho do Funil  
Tabas  
Bonero  
Sabara

Table 12

Chemical Compositions of Schists of the Piracicaba Group  
(% Weight)

	168	169	J-211	J-341	J-682b	BP-1	A-4953	C-1	J-1	JO
SiO <sub>2</sub>	61.52	46.07	57.3	58.6	61.9	68.8	60.0	58.10	50.31	77.82-68.10
Al <sub>2</sub> O <sub>3</sub>	22.40	13.48	20.4	22.1	19.7	17.0	18.7	15.40	15.54	16.74-11.27
Fe <sub>2</sub> O <sub>3</sub>	0.44	28.47	10.1	2.7	1.7	3.9	4.1	4.02	3.09	3.16-TR
FeO	--	--	1.2	5.8	2.4	.34	4.7	2.45	7.72	1.24-.06
K <sub>2</sub> O	9.70	7.61	5.7	3.2	5.4	3.6	3.0	3.24	.68	12.13-4.50
Na <sub>2</sub> O	0.44	0.32	.40	.26	.20	.18	1.1	1.30	2.94	4.22-.40
MgO	0.80	1.42	.66	2.2	3.9	.49	2.4	2.44	6.67	.86-TR
CaO	0.04	0.19	.18	.13	.03	.01	.73	3.11	9.50	1.42-.22
TiO <sub>2</sub>	1.06	0.34	.70	.75	.24	.63	.75	.65	2.25	.47-TR
H <sub>2</sub> O+	{ 3.18	{ 2.08	{ 2.8	{ 4.1	{ 4.4	{ 3.6	{ 3.2	{ 5.00	--	5.04-.24
H <sub>2</sub> O-										
CO <sub>2</sub>	--	--	<.05	<.05	<.05	<.05	<.05	2.63	--	.21-.00
P <sub>2</sub> O <sub>5</sub>	--	--	.16	.09	.05	.05	.14	.17	.24	.07-.00
MnO	--	--	.02	.16	.02	.02	.14	--	.21	.14-TR
	99.58	99.98	99.6	100.1	99.9	100.1	99.00	--	--	--

- 168 - Silver sericite schist. Cercadinho Formation. Barreiro Road  
 169 - Dark sericite-chlorite-magnetite schist. Cercadinho Formation. Barreiro Road  
 J-211 - Quartz sericite phyllite. Dom Bosco Quad.  
 J-341 - Quartz sericite chloritoid phyllite. Dom Bosco Quad.  
 J-6828 - Quartz sericite phyllite. Dom Bosco Quad.  
 BP-1 - Barreiro Formation - graphitic phyllite. Ibirite Quad.  
 A-4953 - Sabara Formation - Staurolite schist. Nova Lima Quad.
- 168 } Done by the author in the MTU 303AAS.  
 169 }
- C-1 - Average shale, Clark (1924).  
 J-1 - Average of 16 basalts, Johannsen (1937).  
 JO - Johannsen (1937, p. 265, v. 11). Range of 26 rhyolites.

From Herz, 1978



The black and white cherts, and thin lenses and beds of locally pyritiferous graphitic phyllites and schists may indicate sporadic, euxinic conditions landward, in deeper waters (S. Sabara Nordeng, 1978, personal communication). Alternatively, such black sediments can only be interpreted to denote conditions, below wave base, during which organic input was greater than its destruction in Precambrian times when bottom feeders were absent. These carbonaceous phyllites of the Barreiro Formation were analyzed by Breger (in Simmons, 1968) who found insoluble and soluble organic compounds to form up to 1.5% of the rock.

Sabara Formation

North of the Curral thrust fault the correct stratigraphic designation of the sedimentary strata remains problematic. These strata have been mapped as Sabara by Gair, and included in the Minas Series (Gair, 1958). By contrast, Guimaraes (1964) proposed that the Sabara in general might be much younger, and should be placed in the Itacolomi Series. The present writer is of the opinion that in the map area the so-called Sabara strata could be as old as Nova Lima.

In the type area the Sabara Formation (Gair, 1958) shows many of the characteristics of a eugeosynclinal sedimentary sequence (Dorr, 1969), and on this basis, it contrasts markedly with the other nearshore or more shallow-water lithologies of the Piracicaba Group. In the present map area, north of the Curral thrust fault, the Sabara differs from all other occurrences of Sabara and Minas rocks in being intruded and metamorphosed by granite. The two features: the eugeosynclinal nature of the

Sabara sediments and their intrusions by granite (although dated at 595 m.y. and 800-895 m.y., both K/Ar by Herz, 1970), suggest to the writer that the so-called Sabara strata may not be Sabara at all, but might be even Nova Lima.

In the map area the Sabara are deeply weathered. According to previous work, it may overlies either the Cercadinho (Gair, 1962), the Barreiro (Pomerene, 1964), or either the Barreiro or the Taboões quartzite (Simmons, 1968) on the north flank of Serra do Curral. The writer has discovered in a roadcut of the highway to Cidade Industrial, between S. Domingos and the Highway BR 040 a fault breccia with large blocks of weathered schist and phyllite, in the contact zone between the Sabara Formation and rocks of the Piracicaba Group. The existence of the fault explains the obscure character of the contact, and the hypothetical erosional surface proposed to occur below the Sabara Formation by Simmons (1968) and Pomerene (1964). Thus the stratigraphic position of the Sabara to the Piracicaba Group is unclear.

A critical geological feature is the remarkable similarity between the Sabara and Nova Lima lithologies and thicknesses, and the fact that both rock units are cut and metamorphosed by granitic intrusions. None of the Piracicaba units are so intruded.

#### COMPARISONS BETWEEN THE GEOLOGY OF THE QUADRILATERO FERRIFERO AND UPPER MICHIGAN

The geology of the Quadrilatero Ferrifero and the Marquette area, Michigan is remarkably similar. This points to similarities in the broadest tectonic framework which in turn produced similar types of sedimentary and igneous rocks, although not in the

precisely same sequence.

1. The Archaean geology of both areas are remarkably similar (Table 13). Both areas have reworked basement gneisses and migmatites, the ages of the Michigan rocks being slightly older than those in the Quadrilatero Ferrifero. Metamorphism is also similar: amphibolite to granulitic. This similarity proceeds in the younger sequences of extensive submarine volcanics in an orogenic environment, development of serpentinites, and deposition of graywackes and graphitic schists. All of these were metamorphosed to the greenschist facies and intruded by synkinematic granodiorite plutons (Table 13).

2. The Maquine Group which does not occur everywhere on the Nova Lima, or Barbacena Group, seems to correspond to the Huronian Formations of Ontario, but is absent in Michigan.

3. In the Middle Precambrian (Table 14), comparisons are also consistent in terms of lithology, deformation and the sequence of events. The basal Moeda Formation of Quadrilatero Ferrifero with its quartzites and conglomerates, could be correlated with either the Enchantment Lake Formation or the Mesnard Quartzite of Michigan. The correlative unit for the Batatal sericite schist would be, either the slate of the upper part of the Mesnard Quartzite, or perhaps the Siamo Slate (Fig. 18). Both the Batatal sericite schist and the Mesnard slate are potassium rich.

4. Both areas contain stromatolites: in Michigan in the Kona dolomite, and in Brazil in the Gandarela Formation. However, they occupy different positions relative to the main iron formations.



Table 13

LOWER PRECAMBRIAN CORRELATIONS

## QUAD. FERRIF. - MICHIGAN (MARQUETTE AREA)

(Sims, 1976; Van Schmus, 1976; Gair and Thaden, 1968)-Michigan  
(Modified from Herz, 1971; Pires, 1977) - Quad. Ferrifero

QUAD. FERRIFERO		MICHIGAN	
UNCONFORMITY			
Maquine Group: Quartzite, conglomerate, dolomite, quartz sericite schist.		Huronian rocks are absent in Michigan; a strong similarity between the rocks of the Maquine Group and those of the Huronian terrains in Ontario, Canada is suggested.	
—2700 m.y.—UNCONFORMITY—		—2650 m.y.—UNCONFORMITY—	
Nova Lima Group: (=Barbacena Group)	Metamorphism	Greenstones	Metamorphism:
Metavolcanics, metabasalt, amphibolite, talc schist, serpeninite, chert, gray- wacke, graphitic schist, iron formation, Mn- formation	Greenschist facies to amphi- bolite at con- tact with the plutons. Syn- kinematic plu- tonic grano- diorites	Metabasalt, meta- volcanics, gray- wackes, iron forma- tion, chert, euxinic shales, rare sili- ceous marbles.	Greenschist, amphi- bolite facies, intrusive synkinematic plutonic granites
—3000 m.y.(?)—		—3200-3800 m.y.—relationship uncertain—	
Reworked basement: Migmatite, gneiss, amphibolite, tonalites, charnockites (Mantiqueira Group)	Metamorphism:  Amphibolite to granulite	Reworked basement gneiss, amphibolite migmatites, granites, pelitic gneiss, hybrid rocks.	Metamorphism:  Amphibolite to granulite

<p>Table 14  MIDDLE PRECAMBRIAN CORRELATION  (Lithofacies)  (Quad. Ferrifero - Michigan)  (Acc. to Sims, 1976; Van Schmus, 1976; Gair and Thaden, 1968) - Michigan  (Modified from Herz, 1971; Dorr, 1969; Guimaraes, 1964)  Quad. Ferrifero</p>	
QUAD. FERRIFERO	MICHIGAN
ITACOLOMI SERIES (8?) Intraformational conglomerates, quartzites, sericite quartzite	
UNCONFORMITY	
MINAS SERIES	Marquette Supergroup
Piracicaba Group	Baraga Group
Graphitic schists	Michigamme Formation
dolomite with stromatolites (Tungussides type)	Upper Slate (includes dolomite,
metabasalt flows	Bijiki IF graphitic phyllite, quartzite, graywacke, dolomite, slate, iron-formation
sericite schist	Lower Slate
quartzite	
ferruginous quartzite	
	(7)
Itabira Group	Clarksburg Volcanics (6)
Gandarela Formation	Greenwood iron formation (5)
Greenstones	
metagabbros	Goodrich Quartzite (8?)
dolomite with stromatolites (Collenia type) (3)	UNCONFORMITY
itabirite: (thin beds) (5)	Menominee Group
Itabirite Caue (4)	Negaunee Iron-Formation (4)
Caraca Group	Siamo Slate slate
Batatal Formation	sericite-chlorite slate Felch (2?)
Greenstone, meta-gabbro, serpentinite, chert, dolomite	metachert, graywacke
sericite schist (2)	Ajibik Quartzite (lithology similar to Mesnard)
	UNCONFORMITY
Moeda Formation	Chocolay Group
Congl., quartzite, grit, quartz schist (1)	Wewe slate (Chlorite, sericite qrtzite.)
	Kona Dolomite with stromatolite (Collenia) and silicified breccia zones. (3)
	Mesnard Slate (2)
	"Quartzite": Quartzite, Conglomerate (1)
	Enchantment Lake Conglomerate, arkose, graywacke, sericite slate (1)

Numbers in parentheses correlate units in the table above.

5. The Itabirite Caue and the Negaunee iron formation are similar in sedimentological facies (Dorr, 1969; James, 1954), but the Negaunee iron formation contains a more varied mineralogy and, perhaps, some preserved primary microscopic features which have not been recognized in the Quadrilatero Ferrifero.

6. In both areas there are mafic volcanic rocks. Those in the Quadrilatero Ferrifero overlie and underlie the iron formation; whereas, in Michigan where there are more volcanic horizons, some iron formations are both overlain and underlain by flows. The greenstones of the Gandarela Formation are lithologically comparable to those of the Clarksburg volcanics member or of the Hemlock Formation, south of Marquette area.

7. The lithologies in the Piracicaba Group and in the upper part of the Michigamme Formation (lower slate, Bijiki iron formation and upper slate) are similar, suggesting similar depositional environments. Graphitic phyllites, dolomites, dolomitic phyllites, quartzites, thin layers of iron formation, sericite schists, and thin mafic flows are present in both units. The chemical composition of the Tyler Slate (Nanz, 1953), which is correlated to the Michigamme Formation shows a high  $K_2O$  content, similar to the sericite schists of the Piracicaba Group (Fig. 18).

8. In both areas there are intraformational conglomerates suggesting periods of erosion. Both the Itacolomi conglomerate and the Goodrich Quartzite contain pebbles of iron formation (Guimaraes, 1931; Van Schmus, 1976).



9. Michigan structure is dominated by the vertical movement of basement blocks according to Cannon and Simmons (1973); whereas, in the Quadrilatero Ferrifero, the dominant movement had a more pronounced horizontal component.

10. The Michigamme Formation, a thick sequence of slates with minor graywacke, graphitic schist and iron formation is the uppermost unit of the Marquette Range Supergroup. It represents a more geosynclinal-type of sedimentation, succeeding a more shelf type period. The Sabara is also geosynclinal, possibly succeeding sediments deposited under shallow water conditions (Dorr, 1969).

In conclusion, these similarities in sedimentary rocks, metamorphism, and deformation suggest strongly that both formations were formed in similar environments, and were affected by similar events, but in geographically remote areas (Table 15).

## STRUCTURAL GEOLOGY

The supracrustal rocks in the area have undergone a complex polyphase deformation. Such structural style is indicated by

Table 15 A Tentative of General Correlation of Events and Ages (From Sims, 1976; and modified from Herz, 1971)				
ERAS	OROGENIC CYCLES		QUAD. FERRIFERO	MICHIGAN
	Q3	MICH		
Paleozoic	Brazilian		Faulting	
			Extensive pegmatitization	
Upper Precambrian			Recrystallization in granites	
			Deformation (D <sub>4</sub> )	
			Thermal event (loss of argon in granites)	
	Urucacian		Granite-gneiss formed at the periphery of the granodiorites	Continental rifting. Deposition of Jacobsville ss. Keweenaw volcanics
	Espinheco		Thermal event affected the granodiorites	
			Post-metamorphic granites	
			Deformation D <sub>2</sub> -D <sub>3</sub> Metamorphism	Rapakivi-type batholith
			Itacolomi deposition	Diabase, gabbro dikes
			Minas deposition	Mild thermal metamorphism and folding
Middle Precambrian	Transamazonian		Emplacement of granites and granodiorites	Deposition of the Marquette Supergroup
				Diabase, gabbro dikes
	Penokean		Cratonization	Cratonization Long erosional interval (Huronian deposition in some areas between 2150-2400 m.y.)
	Guriense-Jaquie		Extensive migmatization of the Nova Lima (Barbacena) rocks, generation of leucogranites and granodiorites	
	Algonian		Deformation (D <sub>1</sub> ) and synchronous metamorphism of the Rio das Velhas, and emplacement of syntectonic granodiorites	Faulting
				Post-tectonic syenodioritic plutons
				Diapiric rise of granite plutons with intense deformation and thermal metamorphism
				Formation of the greenstones; submarine volcanism, dacitic pyroclastics, sedimentation
				Regional deformation, metamorphism and minor anatexis
Lower Precambrian			Marine Sedimentation	Development of gneisses
			Formation of the Nova Lima (=Barbacena) greenstone belt; submarine volcanism, sedimentation	
			Gneiss, migmatite generation	
			(Reworked basement)	

## STRUCTURAL GEOLOGY

The supracrustal rocks in the area have undergone a complex polyphase deformation. Such structural style is indicated by the major features in the area: the anomalous junction of a northeasterly trending anticline with a north-south syncline (Fig. 28b). Dorr commented (1969, pp. 87 and 88) that the nature of this junction of the Moeda syncline with the Serra do Curral is enigmatic and not clearly understood. The present structural investigation consists of a series of detailed studies of the various structural elements and fabrics, the establishment of their mutual interrelationships, and the integration of these structural patterns into the larger framework. The analysis of structures visible in hand specimens and outcrops established both the dimensions of mesoscopic structures and their geometry. For the latter, the Schmidt equal-area stereonet was used and the point density was contoured according to the Kalsbeek contouring net method (Ragan, 1968). Microscopic structures were studied in thin sections of oriented samples. Macroscopic structures were studied from map informations, air photographs and the occasional large features visible on hill sides.

The study of structures on these scales provided a basic understanding of the geometry of the major structures as a whole, the recognition of the different tectonic episodes which had affected the strata, and the identification of domains and subdomains that possess similar structural characteristics.

<ul style="list-style-type: none"> <li>→ Cause Itabirite</li> <li>→ Natural Formation</li> <li>→ Moeda Formation</li> <li>→ Nova Lima Group</li> <li>(Sabara on northwest?)</li> </ul>	<ul style="list-style-type: none"> <li>→ Domain limit</li> <li>→ Attitude of bedding</li> <li>→ Z/S symmetry of folds</li> <li>→ Lamination</li> </ul>	<ul style="list-style-type: none"> <li>→ Thrust fault</li> <li>→ Fault: normal, tear</li> <li>→ Breccia zone</li> </ul>
--	--	---



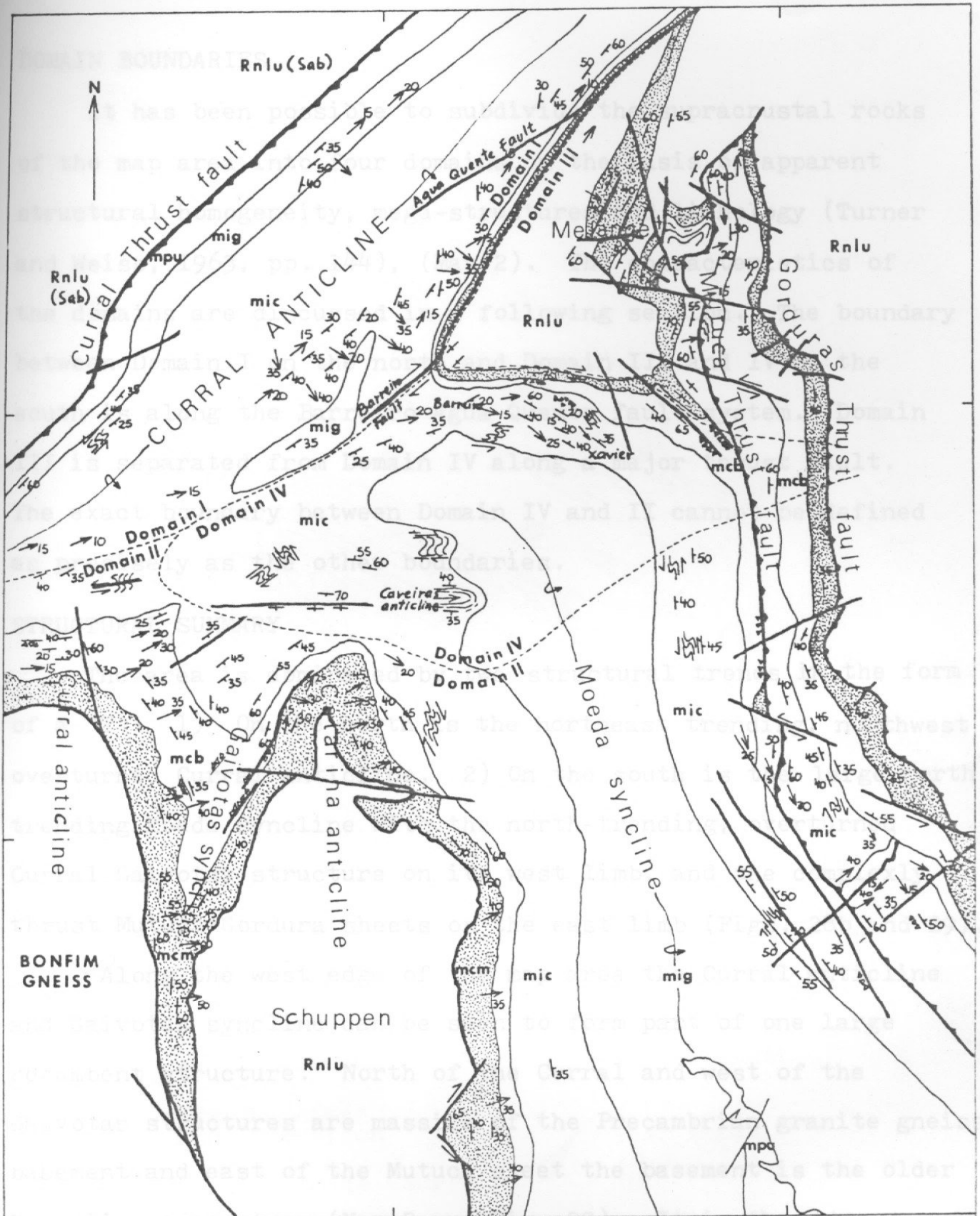


Fig. 28b. STRUCTURAL MAP OF THE JUNCTION AREA

mpu	Piracicaba Group
mig	Gandarela Formation
mic	Caue Itabirite
mcb	Batatal Formation
mcm	Moeda Formation
Rnlu	Nova Lima Group (Sabara on northwest?)

0 1 2  
Km  
--- Domain limit  
- Attitude of bedding  
Z/S symmetry of folds  
→ Lineation

Thrust fault  
Fault: normal, tear  
Breccia zone

## DOMAIN BOUNDARIES

It has been possible to subdivide the supracrustal rocks of the map area into four domains on the basis of apparent structural homogeneity, mega-structures and lithology (Turner and Weiss, 1963, pp. 144), (Map 2). The characteristics of the domains are discussed in a following section. The boundary between Domain I on the north and Domain III and IV on the south is along the Barreiro-Agua Quente fault system. Domain III is separated from Domain IV along a major thrust fault. The exact boundary between Domain IV and II cannot be defined as precisely as the other boundaries.

## STRUCTURAL SUMMARY

The area is dominated by two structural trends in the form of a "T": 1) On the north is the northeast trending, northwest overturned Curral anticline. 2) On the south is the large north trending Moeda syncline with the north-trending, overturned Curral-Gaivotas structure on its west limb, and the complexly thrust Mutuca-Gordura sheets on the east limb (Figs. 28b and 29).

Along the west edge of the map area the Curral anticline and Gaivotas syncline can be seen to form part of one large recumbent structure. North of the Curral and west of the Gaivotas structures are massifs of the Precambrian granite gneiss basement and east of the Mutuca sheet the basement is the older Nova Lima greenstone (Map 2 and Fig. 29). It is the writer's interpretation that the Curral-Gaivotas and Mutuca structures were produced by south to north movement, and that the Moeda syncline and Mutuca-Gorduras sheets were compressed from east to west. In the field there is much good evidence for these two

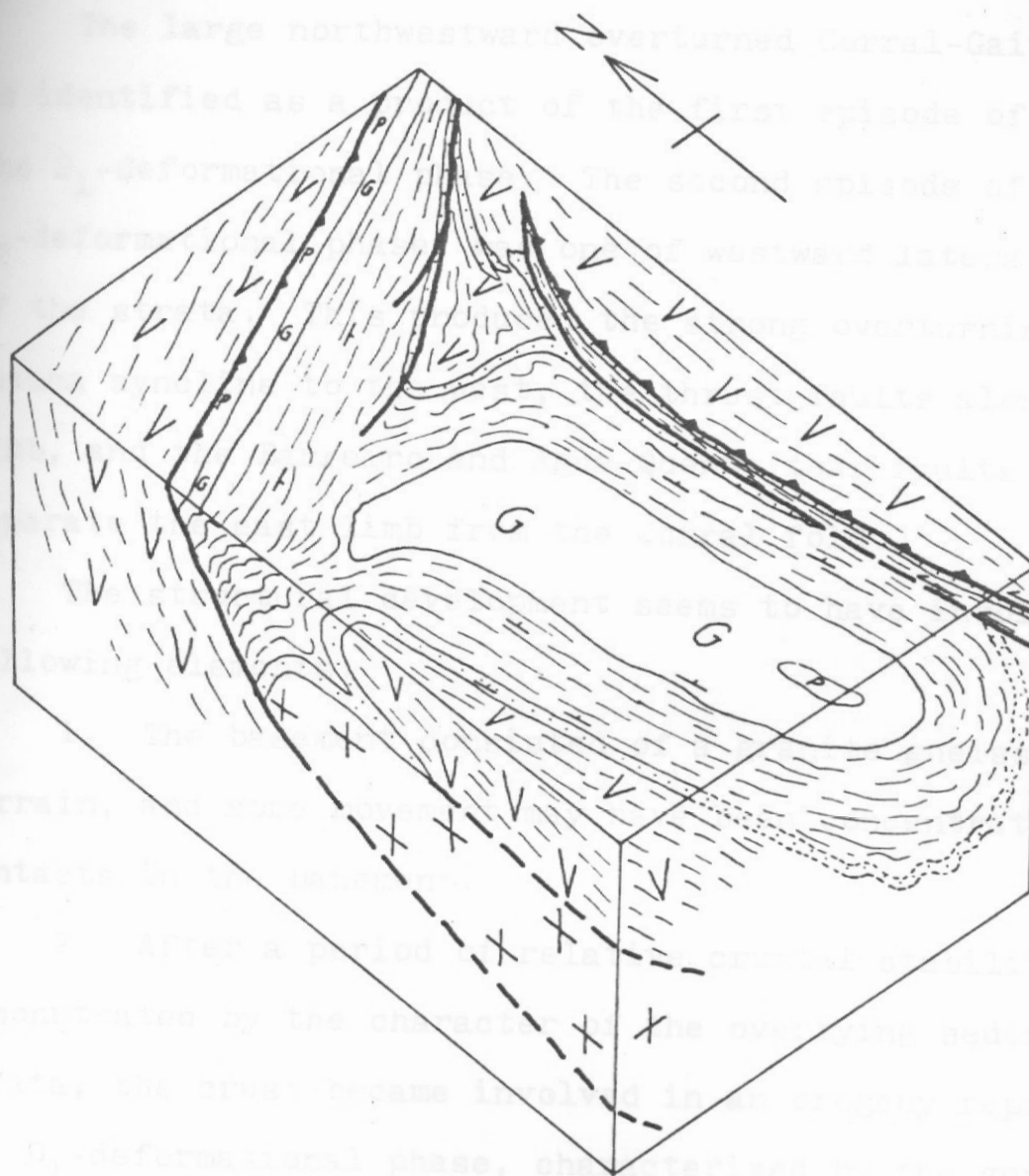


Fig.29 Block-diagram showing the structure of the study area in diagrammatic form.

- |   |                     |  |                      |
|---|---------------------|--|----------------------|
| <span style="border: 1px solid black; padding: 2px;">P</span> | Piracicaba Group    |  | Thrust Fault         |
| <span style="border: 1px solid black; padding: 2px;">G</span> | Gandarela Formation |  | Tear Fault           |
| <span style="border: 1px solid black; padding: 2px;"></span>  | Itabirite Caue      |  | Attitude of layering |
| <span style="border: 1px solid black; padding: 2px;"></span>  | Caraca Group        |  |                      |
| <span style="border: 1px solid black; padding: 2px;"></span>  | Nova Lima Group     |  |                      |
| <span style="border: 1px solid black; padding: 2px;"></span>  | Bonfim Gneiss       |  |                      |



directions of strain on the mesoscopic scale.

The large northwestward overturned Curral-Gaivotas fold is identified as a product of the first episode of folding, the  $D_1$ -deformational phase. The second episode of folding, the  $D_2$ -deformational phase, was one of westward lateral compression of the strata. This produced the strong overturning of the Mutuca syncline to the west, the thrust faults along its east limb, and the Barreiro and Agua Quente tear faults that separate the east limb from the Curral fold.

The structural development seems to have involved the following elements:

1. The basement consisted of a granite gneiss/greenstone terrain, and some movement may have been concentrated along contacts in the basement.
2. After a period of relative crustal stability as demonstrated by the character of the overlying sedimentary strata, the crust became involved in an orogeny representing the  $D_1$ -deformational phase, characterized by the general northward and northwestward horizontal displacement of a rock mass that extended far beyond the limits of the present map area. During this stage the basement was quite active. In the western part of the area the gneissic basement carried the sedimentary cover northward. It pushed the Minas rocks against the gneissic massif on the north, to produce the overturned Curral anticline. Because the Curral anticline extends far to the northeast, it seems probable that east of the present Moeda syncline the Nova Lima greenschist basement also moved northwesterly to squeeze the Minas rocks against the gneissic massif on the north.

Quite possibly some of the Gorduras-Mutuca thrust faults may date from this time period.

On the western flank this northerly-directed tectonic movement caused a slice of Nova Lima greenschist to deform along the anisotropic contact between the granitic gneiss basement and the Minas rocks, and to produce a schuppen structure. This greenstone slice may have promoted the formation of the east-plunging Catarina anticline.

During this north-south deformation a strong penetrative foliation was developed subparallel to the bedding, and folds were also developed in which the fold B-axes trend from east-west to northeast-southwest, presumably perpendicular to the direction of transport.

The bulge of Nova Lima greenschist northeast of Morro do Barreiro, on the northeast side of the Moeda syncline, was formed in a complex structural zone between the Curral anticline and the Mutuca thrust sheet. In this area of Nova Lima greenschist are discontinuous slices and shreds of Moeda quartzites and conglomerates, forming a melange.

The age of this bulge is uncertain: it may have formed during the  $D_1$ -stage, synchronously with the formation of the Catarina anticline, or during  $D_2$ , during the growth of the Barreiro and Agua Quente tear faults, as the east limb of the Moeda syncline was overturning.

3. A second distinct tectonic phase, ( $D_2$ ) expressed by a westward transport of strata, resulted in the formation of the overturned Moeda syncline and in the coincident and

subsequent thrusting along the east limb in particular. This westward transport also generated the Barreiro and Agua Quente tear faults, that grew westward as the east limb became progressively more overturned, and extensive kinking of beds along the eastern flank of the Moeda syncline.

## DOMAIN I

### General

Domain I is situated in the northwest part of the study area and represents a 13 km-long segment of an overturned anticline (Fig. 30) that extends along a northeast-southwest trend for at least 150 km. Along its extent the north limb is overturned, and the beds are in thrust contact with eugeosynclinal-type metasedimentary basement rocks placed by this writer into the Nova Lima Group of Archaean age. This long range has been given a variety of local geographic names along its extent: the study area is situated in the central, Barreiro-Rola Moca, portion.

Simmons (1968) considered the homocline as representing an elongated overturned syncline. In the present map area Pomerene (1964) and Dorr (1969) interpreted the structure as a large syncline, with the north limb completely destroyed by an invading granite. As noted above, this writer believes the contact to be a thrust against "Sabara", which is here interpreted as Nova Lima greenschist, intruded by granite. Thus, all of the rocks to the north of the thrust are older than the Minas Series.



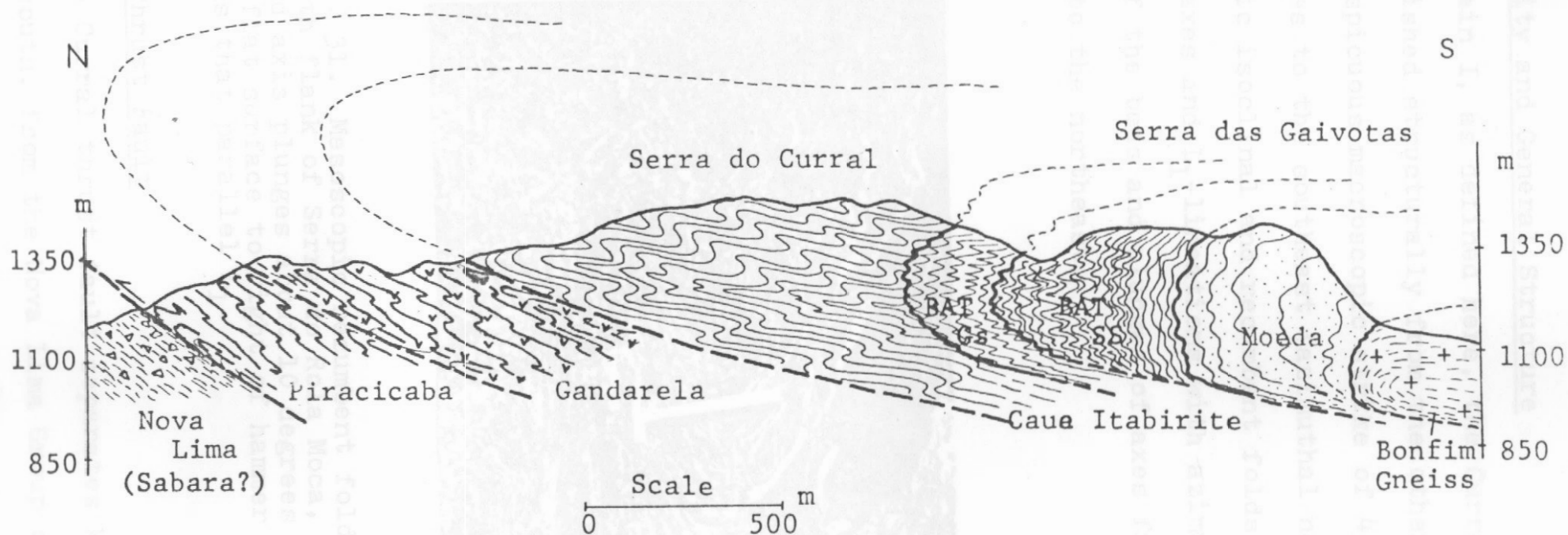


Fig. 30 GEOLOGIC CROSS-SECTION THROUGH SERRAS DAS GAIVOTAS AND CURRAL,  
SHOWING THE DEVELOPMENT OF THE CURRAL-GAIVOTAS RECUMBENT FOLD.

BAT Gs: Batatal greenstones  
BAT SS: Batatal sericite schist

## Homogeneity and General Structure

Domain I, as defined here, the Curral anticline is distinguished structurally from the other domains principally by a conspicuous macroscopic strike of 45 and a dip of 10 to 60 degrees to the southeast (azimuthal notation is used). Mesoscopic isoclinal and recumbent folds (Fig. 31) exhibit  $B_1$ -fold axes and  $L_1$ -lineations with azimuths parallel to the strike of the beds and plunges of axes from horizontal to 50 degrees to the northeast.

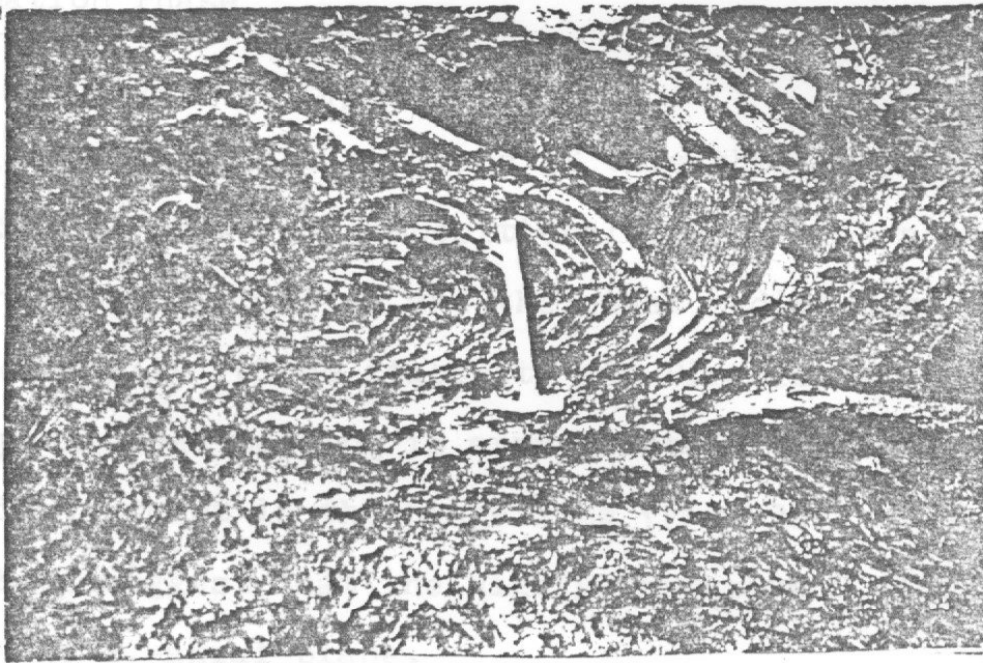


Fig. 31. Mesoscopic recumbent fold within itabirite. North flank of Serra do Rola Moca, near the summit. Fold axis plunges about 10 degrees away from observer. On flat surface to right of hammer are faint quartz rods that parallel  $L_1$ .

## Curral Thrust Fault

The Curral thrust fault separates Minas rocks of Domain I on the south, from the Nova Lima Group on the north. The fault surface is poorly exposed due to weathering, but it can be

identified near the Barreiro road as a strong shear zone which runs between graphite and chlorite schists of the Piracicaba Group on the south and partly weathered greenschists of the Nova Lima Group on the north. Near the fault the Piracicaba rocks were deformed into mesoscopic, recumbent folds, exhibiting quasi-horizontal, close spaced axial planes. The fault is visible in a roadcut along the new road which connects Cidade Industrial to Highway BR 040, near Sao Domingos, wherein large blocks of phyllite and schist lie within a partly weathered, strongly deformed matrix.

### D<sub>1</sub>-Deformation Phase

#### Mesoscopic Analysis of S<sub>0</sub>-Surfaces

As noted in earlier sections of this thesis, primary bedding (S<sub>0</sub>) as shown by compositional layering is a characteristic feature of itabirites and the other sedimentary rocks. In the isoclinally folded itabirite and Piracicaba sequences the well pronounced bedding is approximately parallel to the S<sub>1</sub>-foliation, except in the hinge zone (Fig. 32). Field relationships suggest that the highly pervasive S<sub>1</sub>-foliation parallels the S<sub>1</sub>-axial plane.



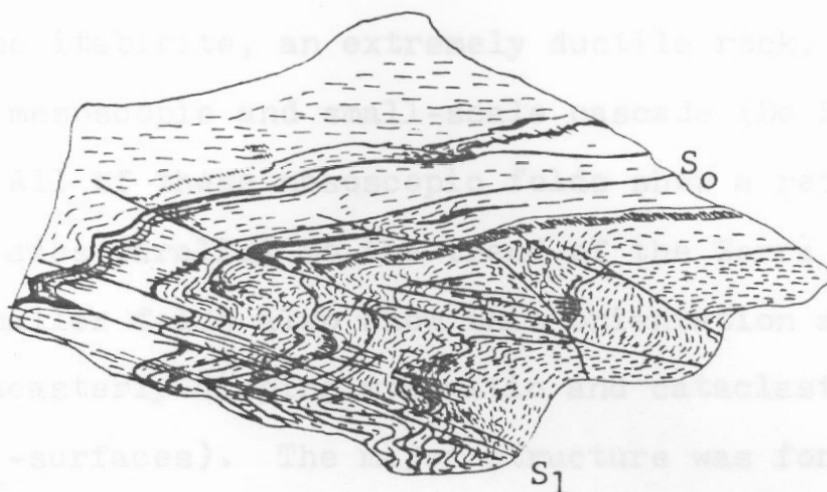


Fig. 32. Slippage along the  $S_1$ -surfaces in the hinge zone of a mesoscopic fold in itabirite. Observe crumpling. Serra da Barreiro. Natural scale.

In the core zone of some mesoscopic folds the rock laminae are crumpled and wrinkled along the numerous  $S_1$ -surfaces, suggesting the rock was deformed also under a quasi-brittle regime in later phases of the  $D_1$ -episode (Fig. 32).

In detail, Domain I occupies the overturned remaining lower limb, and perhaps the hinge, of the frontal lobe of a north-westerly transported anticlinal thrust. The gross geometry is depicted clearly in the stratigraphy and in the relationships of younger sedimentary rocks to the older basement. The upper limb of the anticline is represented in the central part of the area (Vargem da Caveira) by partly weathered and brecciated, yellowish greenschist of the Gandarela Formation. In the field

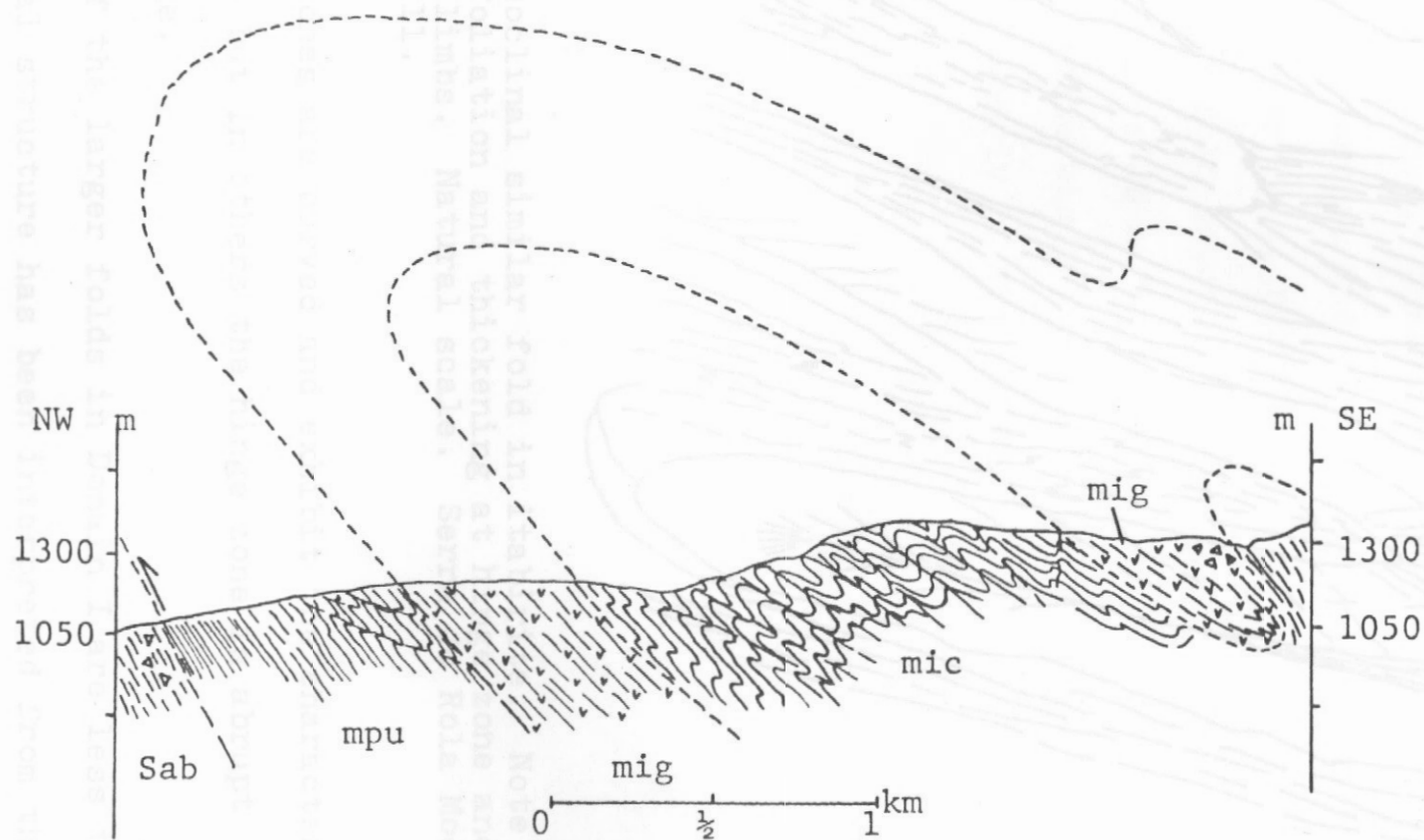
this large recumbent fold is depicted by a mesoscopic fabric of major and minor isoclinal folds and strongly compressed intrafolial folds.

Within the itabirite, an extremely ductile rock, there are generally mesoscopic and small-scale cascade (De Sitter, 1964) folds. All of these mesoscopic folds show a recumbent geometry with axes parallel to the trend of the Serra do Curral. The axes of smaller folds also show this orientation as do the numerous southeasterly-dipping mylonitic and cataclastic foliations ( $S_1$ -surfaces). The major structure was formed during the  $D_1$ -phase of folding, the earliest recognizable penetrative phase of the deformation in the area, and was modified by later movements. A major key to this interpretation was the recognition of a large scale, macroscopic cascade fold, located at the north tip of the Serra das Gaivotas, and also the recognition of the kinematically active character of the cataclastic foliation.

A cross section through the Domain I shows the development of the recumbent Curral anticline, and the subhorizontal  $S_1$ -surfaces transecting bedding. In the upper limb of the anticline in Vargem da Caveira, brecciated Gandarela greenschist and fine-grained amphibolite form a small, macroscopic overturned syncline. Probably the breccia was formed during the differential movements between the itabirite and greenstone in a more brittle regime, in the last stage of folding.

Fig. 32b CROSS-SECTION THROUGH SERRA DO BARREIRO-CURRAL, SHOWING  
THE CURRAL ANTICLINE

Sab - Sabara Formation (=Nova Lima?)  
mpu - Piracicaba schist and quartzite  
mig - Gandarela greenstone  
mic - Caue itabirite





indicated by measurements (Fold 4, Class 2 of Ramsay classification, 1967, p. 365).

Mesosopic cascades of folds in itabirite, showing sub-horizontal axial planes and steeply dipping axial planes. Apparent vertical shortening is significant. Thickening in the larger folds is observed. In some of these cases, the folds have been compressed into a series of smaller folds (1962) (Fig. 34). The folds are of the "similar" type, of isoclinal type.

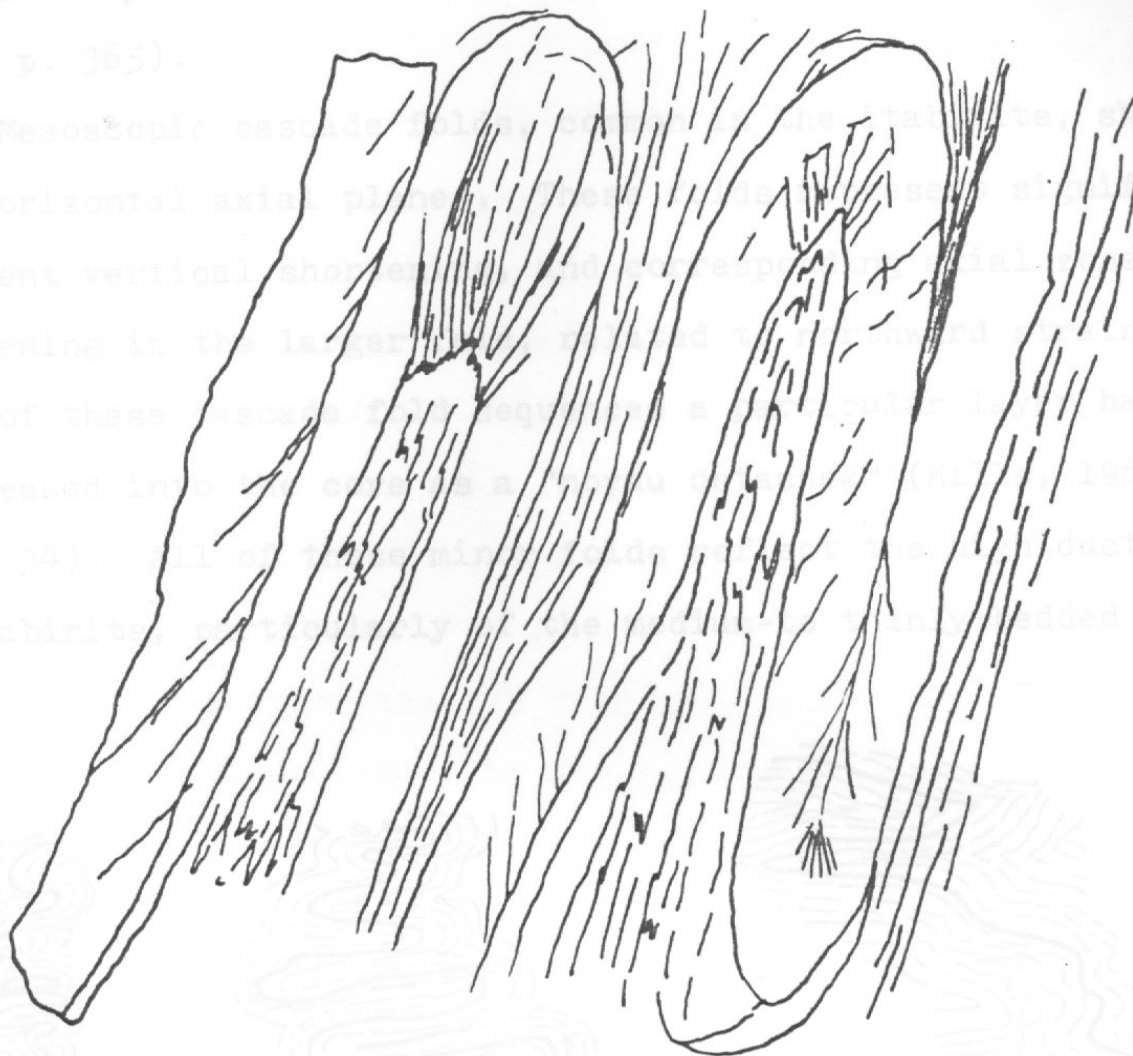


Fig. 33. Isoclinal similar fold in itabirite. Note fanning of foliation and thickening at hinge zone and thinning on limbs. Natural scale. Serra do Rola Moca, north foothill.

Some hinge zones are curved and exhibit the characteristic cleavage fanning, but in others the hinge zone is abrupt similar to a hinge.

Amplitudes of the larger folds in Domain I are less than 5m, and the general structure has been interpreted from the Z/S symmetry of the parasitic folds. The  $B_1$ -axes of the lesser folds are subparallel to the axes of the larger ones. These minor folds are isoclinal, show thickening of layers at the fold hinge (Fig. 33), and are of the "similar" type, as

indicated by measurements (Fold 4, Class 2 of Ramsay classification, 1967, p. 365).

Mesoscopic cascade folds, common in the itabirite, show sub-horizontal axial planes. These folds represent significant apparent vertical shortening, and corresponding axial zone thickening in the larger fold, related to northward strain. In some of these cascade fold sequences a particular layer has been compressed into the core as a "noyau detachee" (Hills, 1962) (Fig. 34). All of these minor folds reflect the high ductility of itabirite, particularly of the medium-to thinly-bedded types.

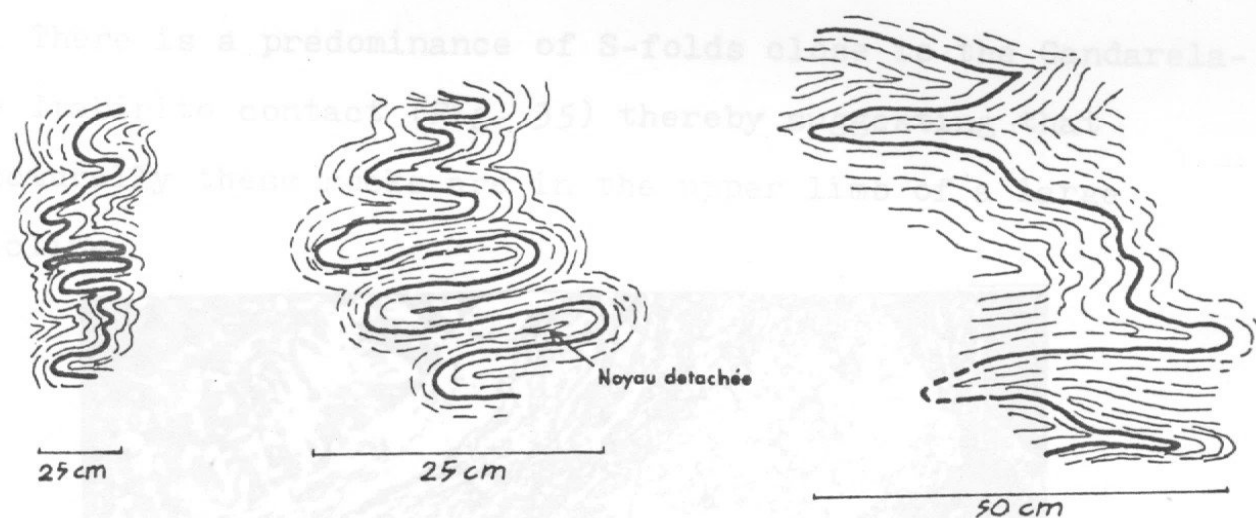


Fig. 34. Mesoscopic cascade folds within itabirite, some showing a "noyau detachee", and others an acute hinge zone. Serra do Rola Moca foothill, north flank. Vertical plane.

Subsidiary minor folds within the mesoscopic parasitic folds in hinge zones demonstrate that the ductile itabirite beds migrated away from the limbs, while the more siliceous parts behaved more competently and acquired more curvilinear shapes (Fig. 35). Ramsay (1967) referring to similar examples,

explains that the different physical behavior of each particular layer may reflect differential viscosities between two adjacent compositional layers, during deformation.

#### Pattern of Z/Symmetry in Folds

The geometry of the minor folds can be used to decipher the geometry of the still larger structures (Whitten, 1966; Hobbs and others, 1976). The systematic variation in asymmetrical folds or the direction of overturning, or sense of movement of folds (Cloos, 1936 in Fleuty, 1964) has been referred as "vergence" from the German "Vergenz"). In this work, the term Vergence expresses the Z/S fold symmetry.

There is a predominance of S-folds close to the Gandarela-Caue Itabirite contact (Fig. 35) thereby suggesting that structurally these rocks are in the upper limb of a large anticline.

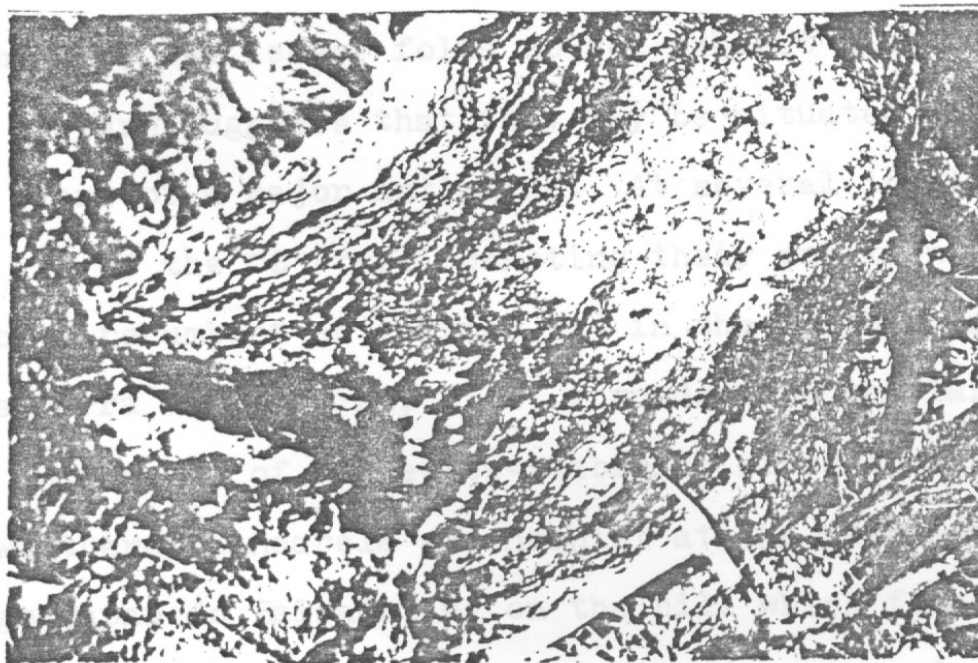


Fig. 35. Tightly folded itabirite showing S-folds on the upper limb, and fluxion in the hinge zone; summit of Serra do Barreiro.



The intrafolial folds at the summit of Serra do Barreiro also display the S-fold symmetry, suggesting that they are situated on the upper limb of the overturned anticline (Fig. 36). S-folds also occur near Vargem da Caveira, at the summit of the Serra do Barreiro.

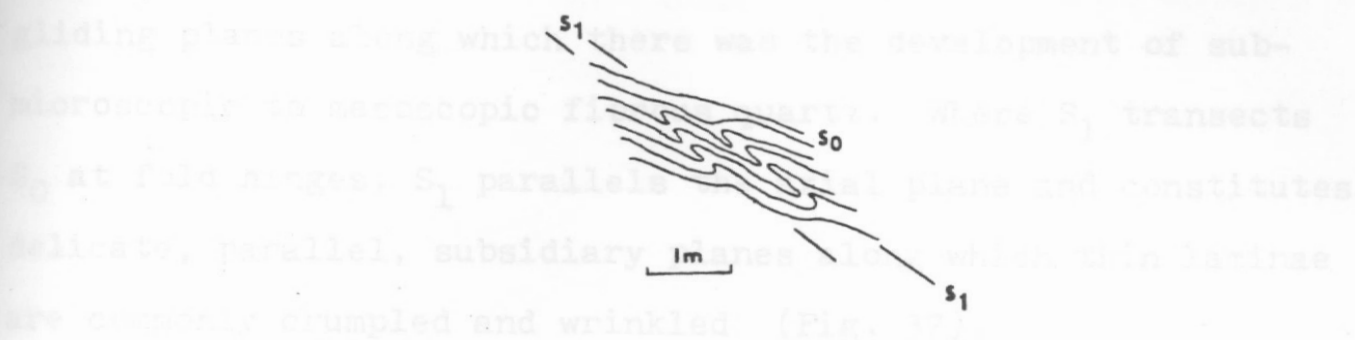


Fig. 36. Symmetry of S-folds in intrafolial parasitic folds. Summit of the Serra do Barreiro.

In roadcuts along the Casa Branca road, in the west part of Domain I, the lesser folds do not exhibit clear asymmetry, which in turn suggests that they may be situated along the axial plane of a major anticline. At several localities the folds are of the "Z"-type, denoting their position on the lower limb of a recumbent anticline: 1) in the northern foothills of the Serra do Barreiro; 2) at a roadcut on the Barreiro road; 3) in an outcrop of magnetite-itabirite close to the contact with weathered Gandarela greenschist at the headwaters of the Corrego Capao do Balsamo; 4) on the hill which forms the headwaters of the Corrego do Barreiro, near Agua Quente; 5) near the south entrance of the COMAG adit that connects Corrego da Catarina with Capao do Balsamo; and 6) in the zone

Fig. 37. Crenulation foliation within itabirite. Observe  $S_1$  and  $S_2$  surfaces and a folded cherty lamina (black). Agua Quente area. Natural scale.

between Domains I and IV. In these areas there are more "Z"-folds than "S"-folds, and further, from fold geometry it seems that the lower limb is more sheared than the upper.

#### Mesoscopic Analysis of $S_1$ -Surfaces

$S_1$ -surfaces are represented by parallel, pervasive planes which parallel the bedding in most places, and represent active gliding planes along which there was the development of sub-microscopic to mesoscopic fibrous quartz. Where  $S_1$  transects  $S_0$  at fold hinges,  $S_1$  parallels the axial plane and constitutes delicate, parallel, subsidiary planes along which thin laminae are commonly crumpled and wrinkled (Fig. 37).

There are also shear folds (Hills, 1963, pp. 233) both within thinly laminated magnetite-itabirite, and in the Piracicaba schists. These shear folds were formed through discrete displacements along parallel  $S_1$ -surfaces, defining horizontal transport. In some cases a well pronounced mesoscopic crenulation foliation (Whitten, 1966, pp. 232), or crenulation cleavage (Hobbs and others, 1976) forming  $S_1$ -surfaces, cut across the itabirite along the hinge zones.

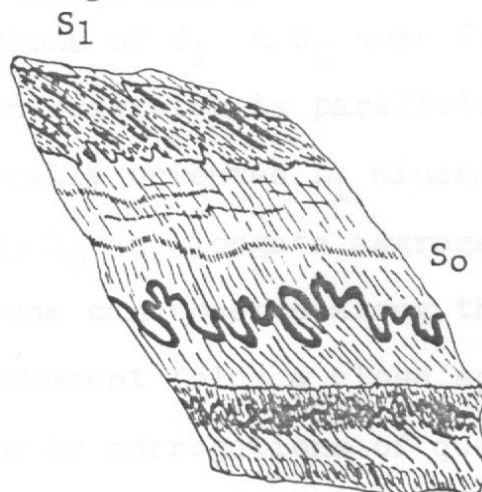


Fig. 37. Crenulation foliation within itabirite. Observe  $S_1$  and  $S_0$  surfaces and a folded cherty lamina (in black). Agua Quente area. Natural scale.

$S_1$ -surfaces constitute potential thrust planes, as for example in the upper limb of the structure, within itabirites near Gandarela greenschist exposures. There the  $S_1$ -surfaces lie approximately subhorizontal and intersect the bedding in cascade folds, and crosscut  $S_0$  at regular intervals of about 1 m (Fig. 38). Each  $S_1$  surface is a minor but active thrust plane. Along some of these sub-parallel  $S_1$ -surfaces alternate sense of motion can be observed.

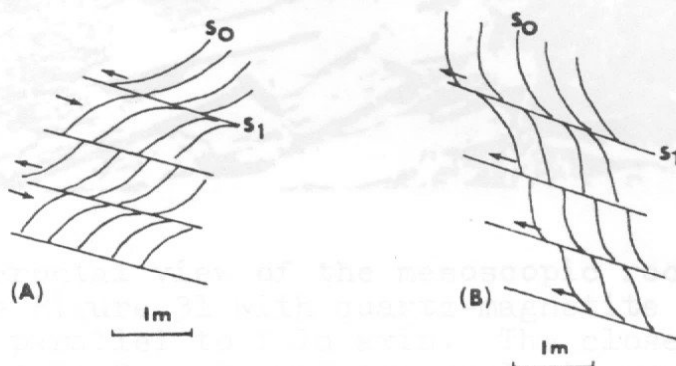


Fig. 38. Small scale thrusts along the  $S_1$ -surfaces, showing in (A) alternate sense of motion. Serra do Barreiro.

#### Mesoscopic Analysis of $L_1$ -Lineations

In itabirite and Piracicaba schists there are numerous parallel intersections of  $S_1$  on  $S_0$  near fold hinges. This cleavage/bedding intersection is paralleled also by a well-developed, tectonically oriented  $L_1$  mineral lineation that can be identified along  $S_0$  as elongate aggregates of quartz and magnetite. Thus, one can observe along the  $S_0$  surfaces in some mesoscopic recumbent folds a close spaced  $L_1$ -lineations represented by ribs or corrugations of quartz and iron oxides parallel to the  $B_1$ -fold axis (Fig. 39).



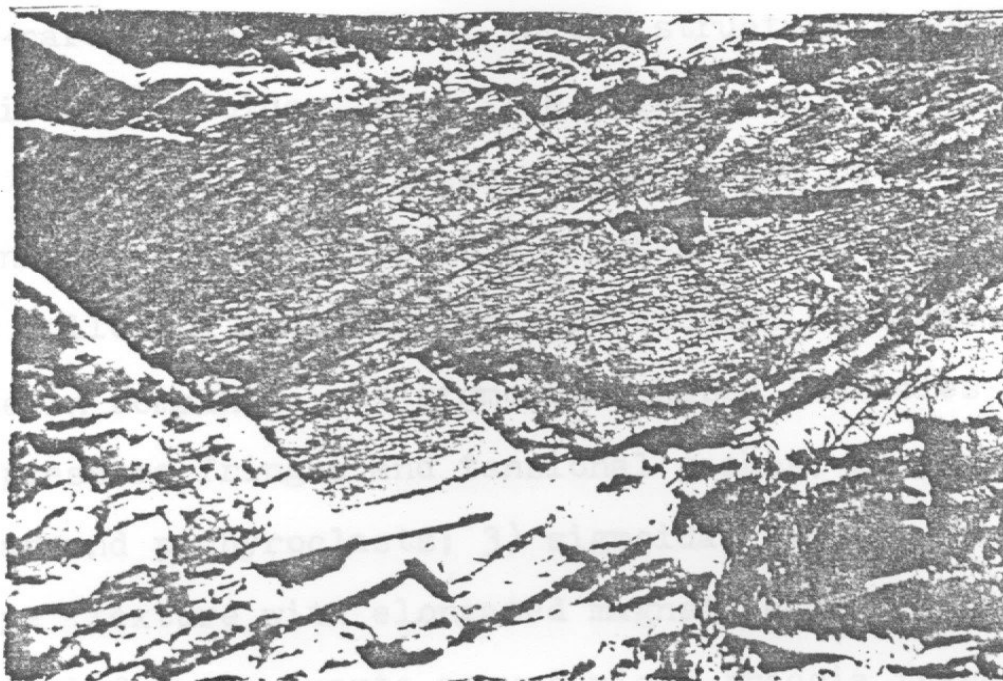


Fig. 39. Frontal view of the mesoscopic recumbent fold seen in the Figure 31 with quartz-magnetite corrugations forming  $L_1$  parallel to fold axis. The close-spaced fracture may be  $S_2$ . Pencil for scale is approximately parallel to fold axis. Serra Rola Moca, north flank.

The  $L_1$ -lineation are plotted in Fig. 50 showing a strong maximum at 55 and gentle plunges to the northeast.

#### Microscopic Analysis of Rock Fabric

It is possible to determine by microscopic observations how the rock was strained during  $D_1$ -deformation.

Under the microscope some  $S_1$ -surfaces can be seen to be strained zones, consisting of rectangular quartz grains, sliced hematite layers, and grains of magnetite elongated along  $S_1$ . Such granulated quartz and finely comminuted magnetite suggest a dynamic rather than a dynamothermal origin for  $S_1$ .

In the iron oxide-rich lamina the tiny hematite and magnetite grains are arranged parallel to  $S_1$  in a manner similar to a "deck-of-cards", and identical to the structure found in some mesoscopic shear folds. Also, the relative motion along the several, successive  $S_1$ -surfaces resembles the pattern exhibited by the unidirectional slide of a "deck-of-cards".

The following microfabrics were studied in magnetite itabirite in Domain I: 1) sigmoidal shaped lenticles displaying pressure fringes and tensional gashes; 2) pressure shadows around porphyroclasts; 3) sigmoidal fibrous quartz in "tiger-eye" texture with elongated magnetite agglomerates; 4) sigmoidal fibrous quartz around micro-breccia fragments. All of these discussed individually in the following sections, are interpreted to have been developed in conditions in which quartz recrystallized and magnetite barely fractured. The asymmetry of these fabrics helps to identify the relative sense of motion within the rock as generally one of rotation, along  $S_1$ -surfaces, or along gliding planes coincident with the  $S_0$ -surface. Fig. 40 shows the general relationships of the textures studied.

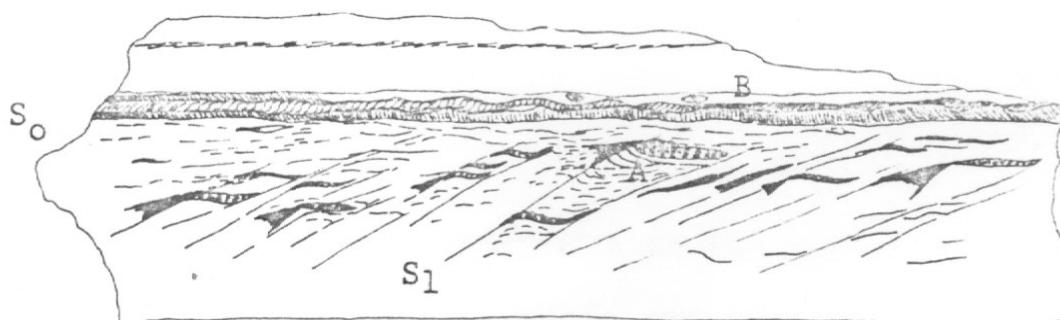


Fig. 40. Magnetite itabirite containing lenticles (A), and sandwiched laminae of fibrous quartz-magnetite (B) Serra do Barreiro. Natural scale.

### Sigmoidal-Shaped Lenticles

Under the microscope one can identify an important type of indicator of relative movement in magnetite itabirites. These are sigmoidal shaped lenticles (Fig. 41) that display "Triangular fringe" and "tension gash" textures, which can be used to identify the sense of rotation, and to define  $L_1$  (Spry, 1976, pp. 240; Hobbs, et al., 1976, pp. 274). Lenticles, 3 to 10 mm-long, consist of magnetite porphyroclasts, in aggregates or isolated octahedra, within a yellowish, fine-grained matrix or with quartz. The sigmoidal shape of the lenticles can be used to determine the relative sense of rotation along the pervasive  $S_1$ -foliation (Fig. 41). This relative rotational movement has produced the "triangular fringes" on the other side of the  $S_1$ -plane, and the "tensional gashes" below and above the opposite ends of the lenticle. Quartz recrystallized with a fibrous habit within these lenticles. For a similar situation Sander (1970, pp. 115) suggested that deformation took place in a viscous, ductile state.



# Pressure Shadows Development

Isolated magnetite porphyroclasts in the magnetite

itabirite exhibit pressure shadows of fibrous quartz produced

by the rotation of porphyroclasts. The  $S_0$  is perpendicular

to the direction of rotation. The fibrous quartz

shows a tension gash. The fibrous quartz is parallel to

$S_1$ , and the fibrous magnetite porphyroclasts

coincide with the direction of rotation of the quartz is itabirite.

showing that both are the product of the same movement, (Fig.

42). This structure proves that the itabirite is rigid during

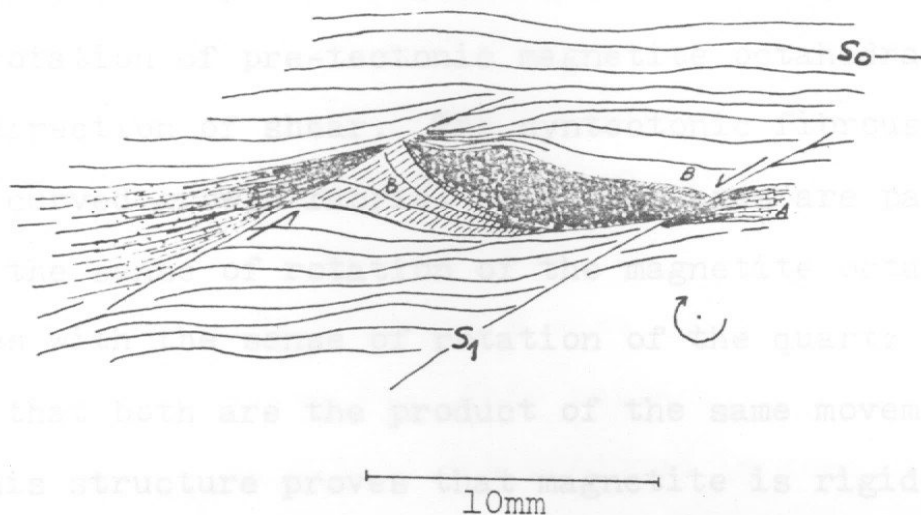


Fig. 41. Rotation along  $S_1$ -planes of a rigid lenticle composed of magnetite aggregates within a ductile matrix. (A) "Triangular fringe" was derived by local compression and dissolution of quartz against the  $S_1$ -surface during rotation of the lenticle. Tiny magnetite grains are more concentrated in this zone by residual accumulation. (B) "Tension gash" originated in a tensional zone formed by the addition of quartz to produce the apparent rotated shape of the lenticle. Quartz recrystallized in fibrous habit parallel to  $S_1$ , and is represented by the small, straight segments. Arrows denote sense of motion. Serra do Barreiro.

In the triangular fringe zone (Fig. 41) magnetite grains are comminuted and distributed along linear zones toward a vertex in the lenticle tip. The tensional gash zone contains no magnetite, confirming that the fibrous quartz which post-dates  $S_0$ , was formed during the rotation of the lenticle, in the available space. (Ramsay, 1967, p. 182; Turner and

Pressure solution may contribute to the generation of such textures. Thus, while magnetite was being compressed and comminuted in region A, quartz redeposition proceeded with strain in the region B. to dissipative forces and a boundary layer about the rigid particle (Elliott, 1972).

### Pressure Shadows Development

Isolated magnetite porphyroclasts in the magnetite itabirite exhibit pressure shadows of fibrous quartz produced by the rotation of pre-tectonic magnetite octahedra perpendicular to the direction of shear. The syntectonic fibrous quartz shows a curved growth fabric. Rotation axes are parallel to  $L_1$ , and the sense of rotation of the magnetite octahedra coincides with the sense of rotation of the quartz lenticles, showing that both are the product of the same movement, (Fig. 42). This structure proves that magnetite is rigid during deformation, and supports the fabric to permit the growth of fibrous quartz.

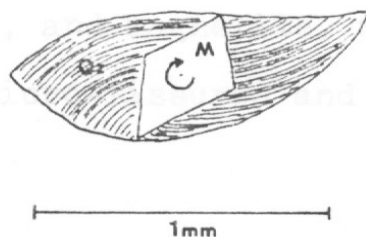


Fig. 42. Pressure shadow filled up by quartz (Qz) recrystallized during rotation of magnetite (M). Arrow denotes sense of rotation. Serra do Barreiro.

The pressure shadows are elongated in the direction of maximum finite extension (Ramsay, 1967, p. 182; Turner and Weiss, 1963, p. 211). The rotation of the pre-tectonic magnetite grains has occurred without affecting the internal cohesion of the rock itself, although introducing inhomogeneity into the flow pattern, and give rise to dissipative forces and a boundary layer about the rigid particle (Elliott, 1972).

### Sigmoidal, Recrystallized Fibrous Quartz Along $S_1$ -Surface

Laminated itabirite surfaces ( $S_0$ ) are accompanied by another pattern of quartz growth (Fig. 43): a "tiger-eye" structure sandwiched between magnetite-rich laminae. The fibrous quartz-rich laminae are 1 to 2 mm thick and parallel to the  $S_1$ -surface. In the adjoining magnetite-rich laminae the elongate magnetite aggregates show internal fracture surfaces inclined across  $S_1$ . This pattern is interpreted to indicate that fibrous quartz was produced in tensional regions during compression and rotation of a rock in which the fabric was supported by the rigid magnetite laminae (Fig. 43). Hence, quartz which is a tectonically active mineral becomes elongated (Nicolas and Poirier, 1976), and fibrous during dissolution and recrystallization, and magnetite, which is a tectonically passive mineral, is micro-fissured and rotated normal to the strain.



Fig. 43. Fibrous quartz recrystallized between the rotated micro-breccia fragments. fQz - Fibrous Quartz; M - Magnetite-rich layer. Natural scale. Serra do Barreiro.



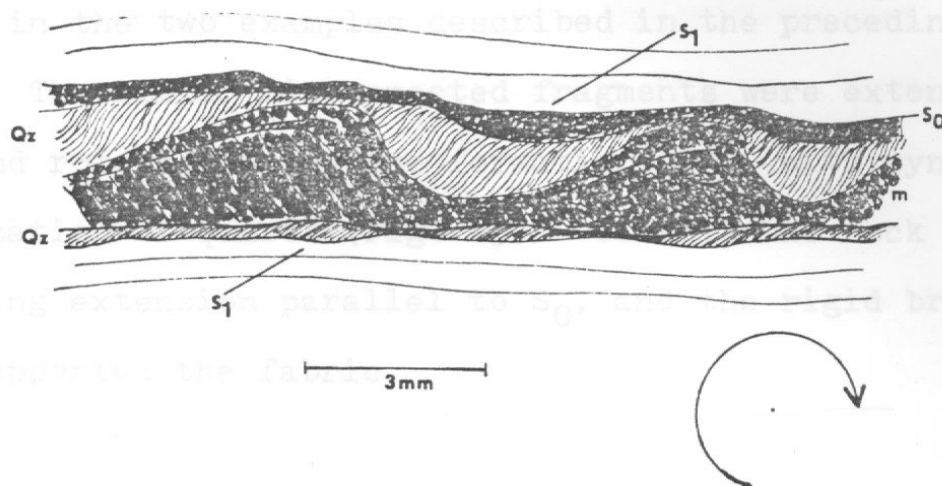


Fig. 43. Synkinematic recrystallization of quartz in tensional regions coincided with rotation of the magnetite aggregates in the compressional regions. Layers of fibrous (Qz) quartz parallel to  $S_1$ , alternating with wavy layers of magnetite (m), in which fractures are at an angle to  $S_1$ . Arrow denotes sense of rotation. Serra do Barreiro.

#### Sigmoidal Fibrous Quartz Formed Around Rotated Breccia Fragments

In a micro-brecciated magnetite-itabirite, quartz recrystallized in a sigmoidal fibrous habit, between the small fragments of breccia (Fig. 44).

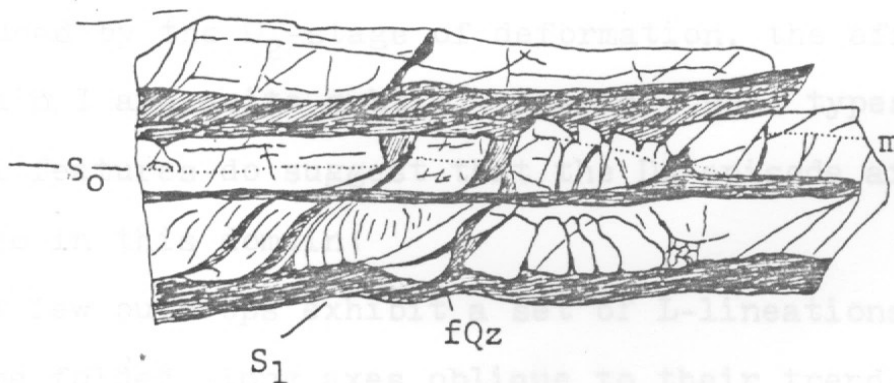


Fig. 44. Fibrous quartz recrystallized between the rotated micro-breccia fragments. fQz - Fibrous Quartz; m - Magnetite-rich layer. Natural scale. Serra do Barreiro.

The orientation, inclination and rotation of the fibers is the same as in the two examples described in the preceding paragraphs. The small, disconnected fragments were extended along  $S_0$ , and rotated during the formation of  $S_1$  with synchronous recrystallization of quartz (Fig. 45). Clearly the rock fabric was undergoing extension parallel to  $S_0$ , and the rigid breccia fragments supported the fabric.

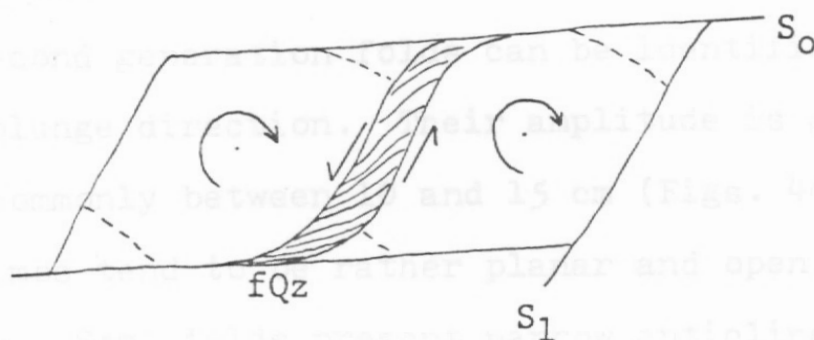


Fig. 45. Formation of fibrous quartz (fQz) during the rotation of the breccia fragments. Growth orientation of the fibres was controlled by the rotation of the fragments.

## D<sub>2</sub> - Deformation Phase

### General

Whereas to the south in Domain II the major structures were produced by the  $D_2$ -stage of deformation, the effects of  $D_2$  in Domain I are quite subtle. However, some types of structural features do suggest that the  $D_2$ -episode affect the strata also in this domain:

- 1) A few outcrops exhibit a set of L-lineations that have become folded along axes oblique to their trend. These younger fold axes are thought to be  $B_2$ .

2) There are rare minor folds in which the axes trend almost perpendicular to the trend of the major recumbent structure and the corresponding mesoscopic fabric. These folds are thought to be  $B_2$ .

3) A few outcrops show minor thrust planes which transect the earlier structures, and which exhibit a definite westward imbrication.

### Folding and Lineations

The second generation folds can be identified by their different plunge direction. Their amplitude is generally less than 1 m, commonly between 10 and 15 cm (Figs. 46 and 47). The fold limbs tend to be rather planar and open, with small undulations. Some folds present narrow anticlines separated by wide, tabular zones resembling cusped structure (Hills, 1963, pp. 215), with rupture along the hinge. Where deformation has been stronger, these ruptures can form an imbricate structure (Fig. 48). The  $L_1$ -lineation is refolded by the younger  $B_2$ -structures (Fig. 47). The  $B_2$ -fold axes plunge southeast and south, and the axial planes dip vertically, northeast, or east. A well-developed cleavage is pronounced in the hinge zones.

Fig. 48. Imbricate structure along the east-west direction. Thrust to west. Serra do Barreiro.

The  $L_1$ -lineations are plotted on Fig. 50. They occur as minute, aligned corrugations and ribs on  $S_0$ -surfaces, and as well-defined, close-spaced fracture-intersections on the earlier, mesoscopic planar structures as seen in Fig. 47.



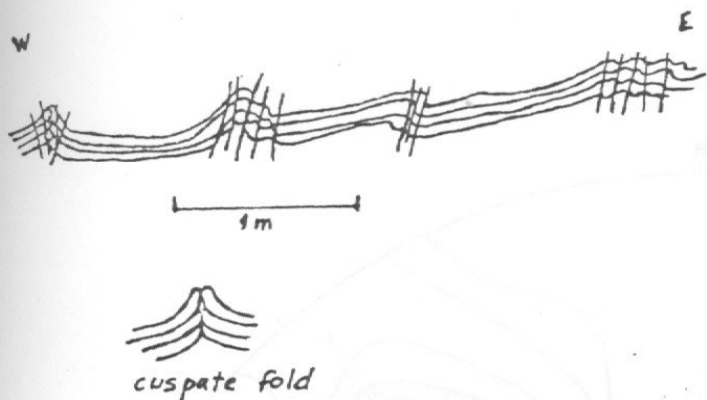


Fig. 46. Cuspate and asymmetric folds separated by flat areas. Serra do Barreiro.

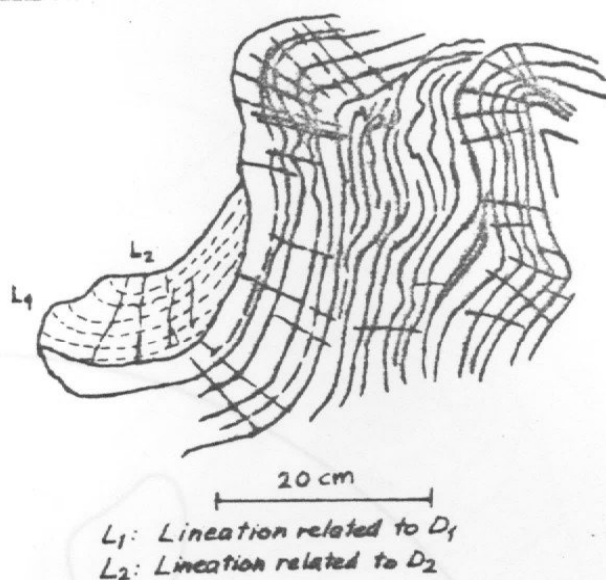


Fig. 47. Detail of fold, showing cleavage fanning and  $L_1$ -lineation deformed by  $L_2$ -lineation. Drawing from a photograph taken by the author. Serra do Barreiro.

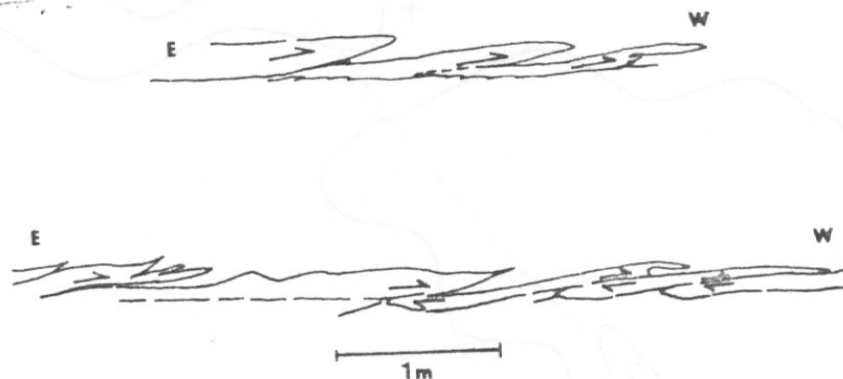


Fig. 48. Imbricate structure along the east-west direction. Thrust to west. Serra do Barreiro.

The  $L_2$ -lineations are plotted on Fig. 50. They occur as minute, aligned corrugations and ribs on  $S_0$ -surfaces, and as well-defined, close-spaced fracture-intersections on the earlier, mesoscopic planar structures as seen in Fig. 47.

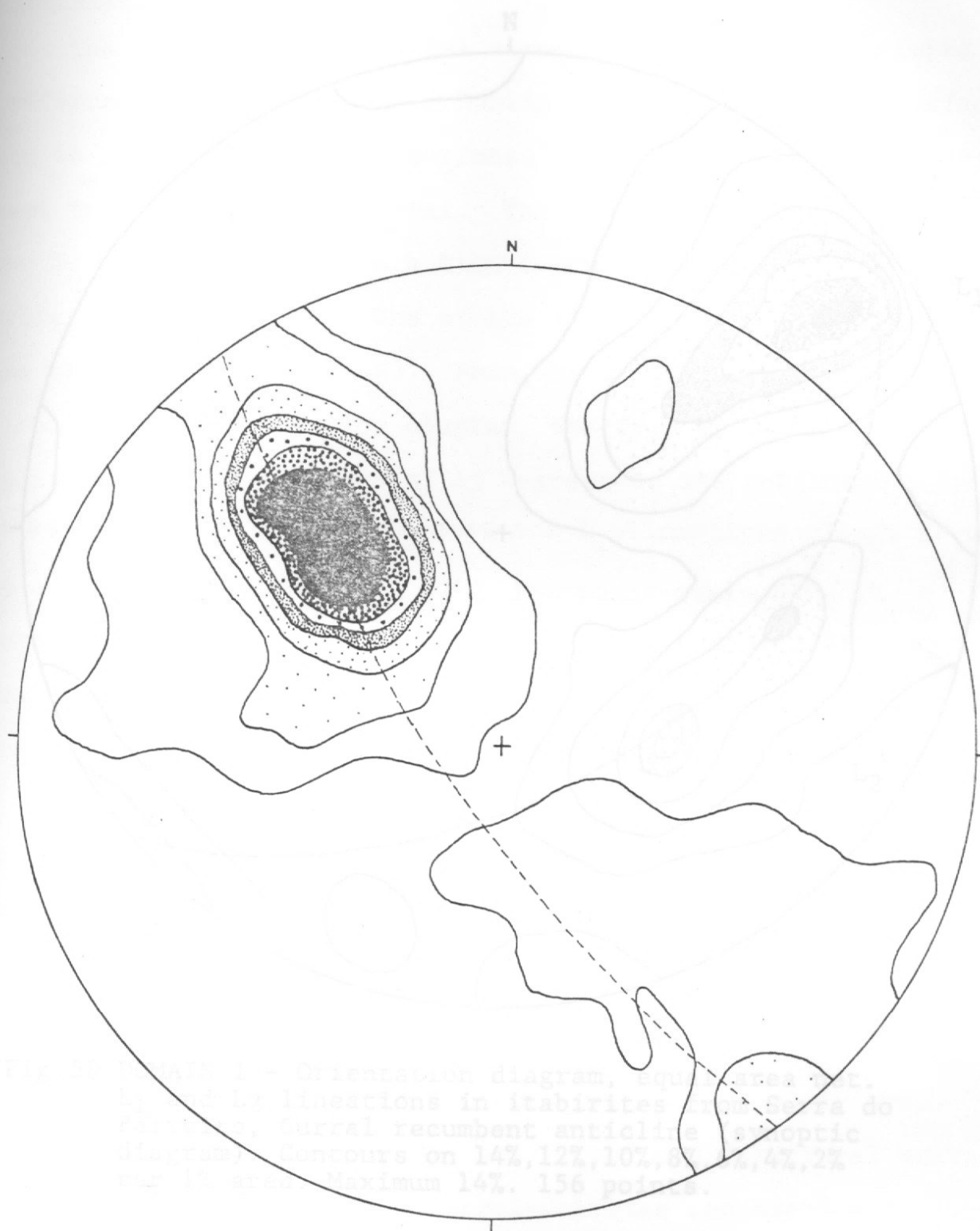


Fig.49 DOMAIN I - Orientation diagram, equal area net.  
S-pole to bedding in magnetite itabirite from Serra do  
Barreiro. Contours 14%, 12%, 10%, 8%, 6%, 4%, 2% per 1% area.  
Maximum 16%. 184 points.

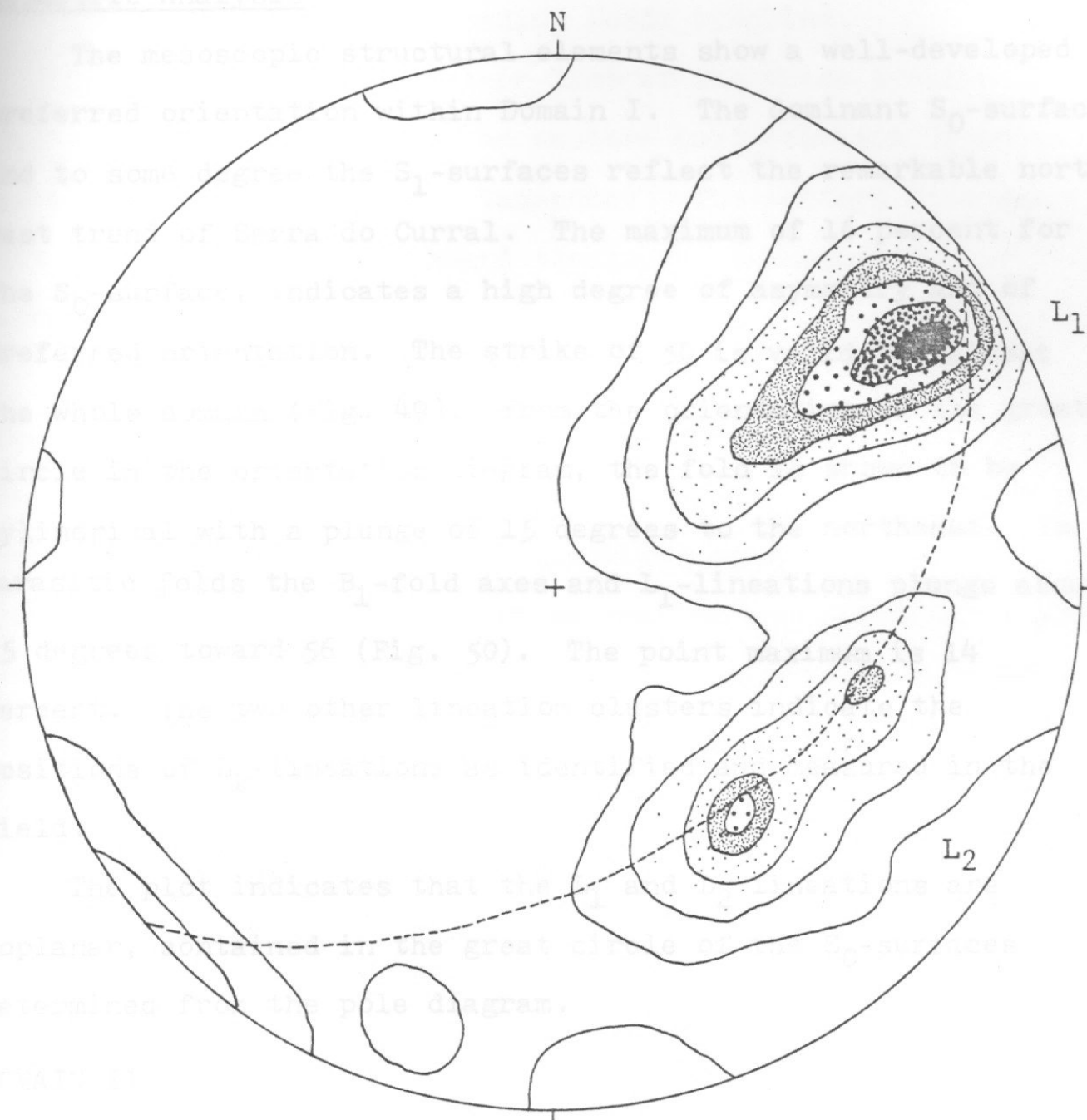


Fig. 50 DOMAIN I - Orientation diagram, equal area net.

L<sub>1</sub> and L<sub>2</sub> lineations in itabirites from Serra do Barreiro, Curral recumbent anticline (synoptic diagram). Contours on 14%, 12%, 10%, 8%, 6%, 4%, 2% per 1% area. Maximum 14%. 156 points.



### Geometric Analysis

The mesoscopic structural elements show a well-developed preferred orientation within Domain I. The dominant  $S_0$ -surfaces and to some degree the  $S_1$ -surfaces reflect the remarkable north-east trend of Serra do Curral. The maximum of 16 percent for the  $S_0$ -surface, indicates a high degree of asymmetry and of preferred orientation. The strike of 50 is valid for almost the whole domain (Fig. 49). From the orientation of the great circle in the orientation diagram, the fold is shown to be cylindrical with a plunge of 15 degrees to the northeast. In the parasitic folds the  $B_1$ -fold axes and  $L_1$ -lineations plunge about 15 degrees toward 56 (Fig. 50). The point maximum is 14 percent. The two other lineation clusters indicate the positions of  $L_2$ -lineations as identified and measured in the field.

The plot indicates that the  $L_1$  and  $L_2$  lineations are coplanar, contained in the great circle of the  $S_0$ -surfaces determined from the pole diagram.

### DOMAIN II

#### General

Domain II occupies the southern part of the study area. This domain can be subdivided into three main structural units:

- 1) In the west is the Curral-Gaivotas recumbent anticline with a core of Bonfim gneiss overlain by the Catarina recumbent anticline with a Nova Lima greenschist core, separated by the tight Gaivotas syncline. The folds plunge east, and were

produced by tectonic transport from the south.

2) The north-south trending Moeda syncline.

3) The overturned eastern limb of the Moeda syncline, duplicated by faulting into an eastern belt (eastern Tamandua) and a western belt (western Tamandua). The eastern Tamandua belt was formed by a northward transport, subsequently affected by westward thrusting.

In this domain bedding has been obliterated by intense shearing commonly to a greater degree than in Domain I. In Domain I the rocks show much internal folding, but in the western part of the Domain II the geologic units show deformation mainly along anisotropic surfaces such as bedding and lithologic contacts. However, the foliation of the Bonfim Gneiss also is subparallel to the contact with rocks of the Moeda Formation, and for this reason the gneisses are cataclastic and mylonitic along the western flank of Serra das Gaivotas. The rocks of the eastern flank are much more sheared, especially those of eastern Tamandua, which exhibit strong internal deformation.

#### Curral-Gaivotas Recumbent Fold

##### Macroscopic Structures

Along the western part of the area the recumbent Curral anticline, the main structure in Domain I, continues southward to merge with a series of recumbent structures. These consist, from bottom to top, the Curral anticline, the Gaivotas syncline, and the Catarina anticline. All of these folds show similar geometry, so that the assignment of the more southerly with

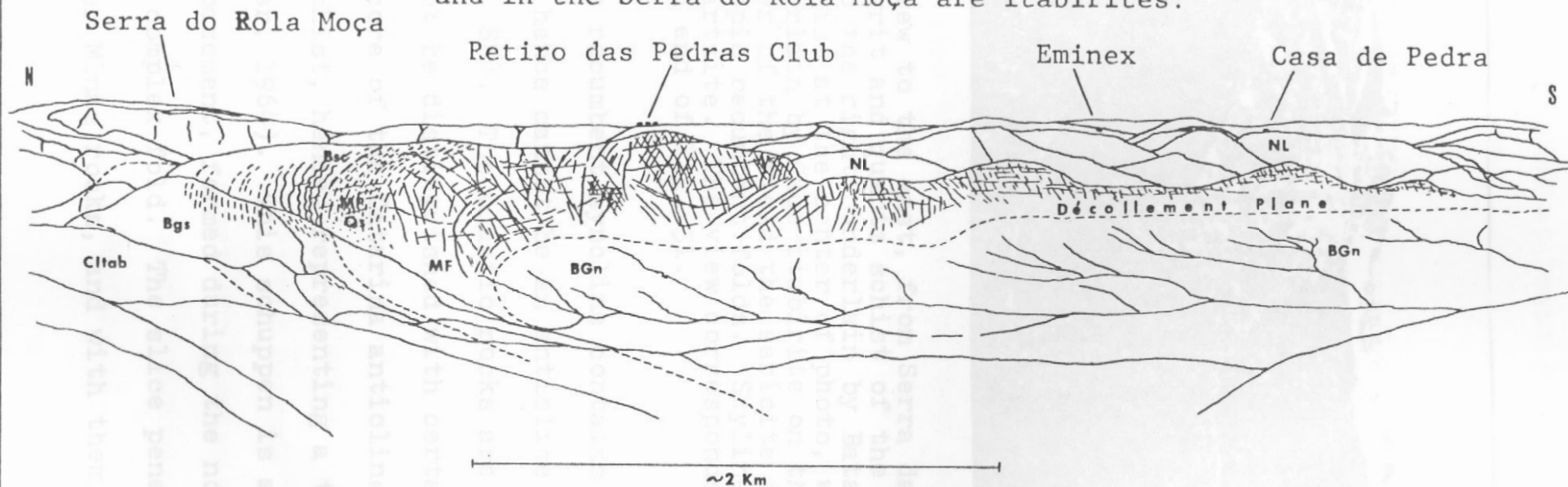
Domain II, rather than Domain I is merely to facilitate description.

The general structure of the western part of Domain II is a sequence of large northward-transported recumbent fold sheets, tilted between 30 and 45 degrees to the east by later deformation (Figs. 29 and 51). The lowest structure is the Curral recumbent anticline, cored by the Bonfim Gneiss and bounded at the top by an east-dipping fault plane. The Catarina anticline, at the top, also plunges east, but these fold axes must reverse their plunges to the west somewhere within the north-trending Moeda syncline.

The contact plane between the lowest limb of the Gaivotas syncline and the Bonfim Gneiss forms a north-south-oriented, east-plunging, 6 km-long, thrust plane, which extends northward for at least  $1\frac{1}{2}$  km into Caraca rocks before it disappears. A macroscopic recumbent, cascade fold occurs north of the gneissic core, in the upper part of the Moeda and lower part of the Batatal Formation (Fig. 52).



Fig.51 PANORAMIC VIEW OF THE CURRAL OVERTHRUST AT  
SERRA DAS GAIVOTAS, FROM SERRA DA JANGADA,  
LOOKING TO EAST.  
Scarps in the foreground are Moeda Formation,  
and in the Serra do Rola Moça are itabirites.



Explanation:

- Citab - Caue Itabirite
- Bgs - Batatal greenstones
- Bsc - Batatal sericite schist
- MF - Moeda clastic rocks
- Qs - Moeda quartz schist
- NL - Nova Lima greenschist
- BGn - Bonfim Gneiss



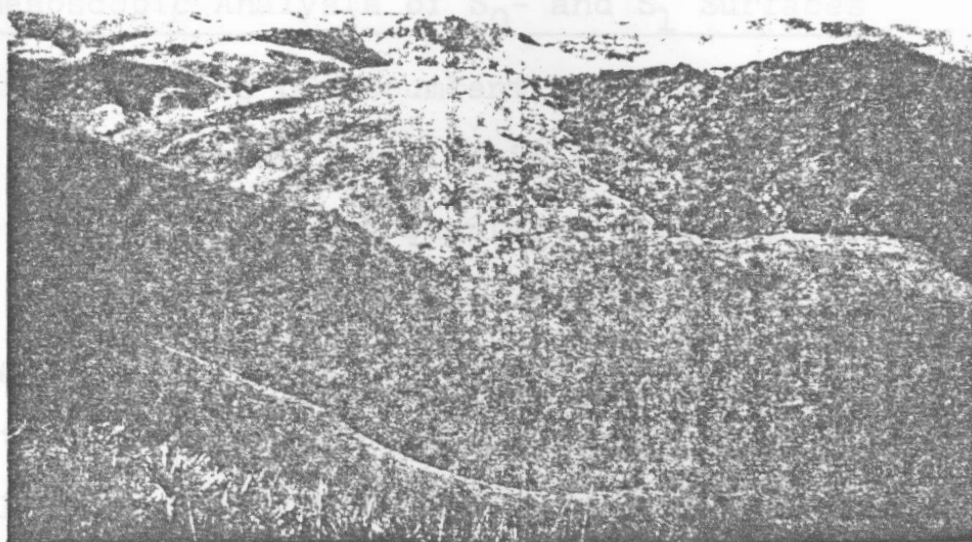


Fig. 52. View to the east, from Serra da Jangada. Quartzite, grit and quartz schist of the Moeda Formation to the right; underlain by Batatal sericite schist at the center of photo, which in turn is underlain by Caue itabirite on the left. In the center of the field the sericite schists show mesoscopic recumbent folds. Skyline consists of Moeda quartzite. The view corresponds structurally to the north end of Fig. 51.

The Gaivotas recumbent syncline contains younger rocks in the core, and hence cannot be an anticline as suggested by Dorr (1969, p. 88). The clastic rocks are strongly deformed, and bedding cannot be distinguished with certainty from foliation. The core of the Catarina anticline is occupied by Nova Lima greenschist, hence, representing a typical schuppen structure (Gansser, 1964). This schuppen is a dislodged slice of the Archaean basement, formed during the northward movement of the recumbent complex fold. The slice penetrated into the enveloping younger Minas rocks, and with them, was brought

northward for a distance of at least 5 km (Fig. 53).

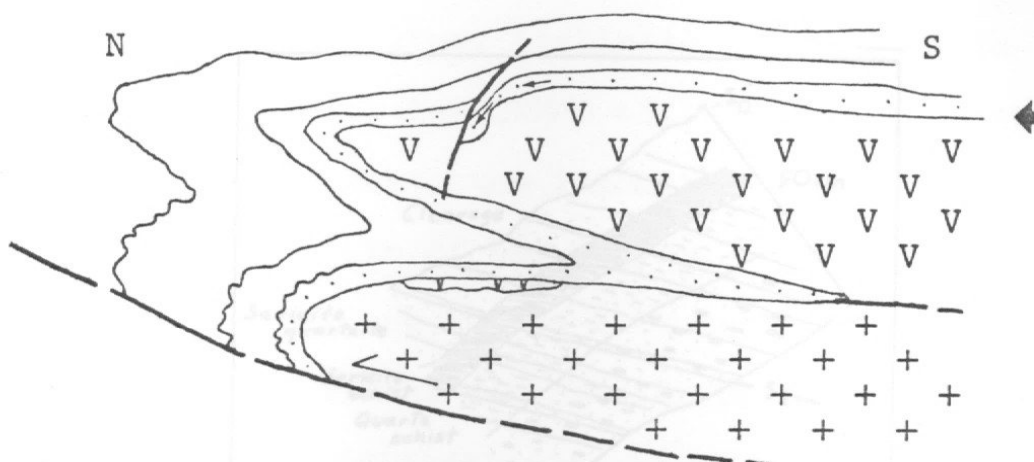
## Mesosopic Structures

### Mesosopic Analysis of $S_0$ - and $S_1$ Surfaces

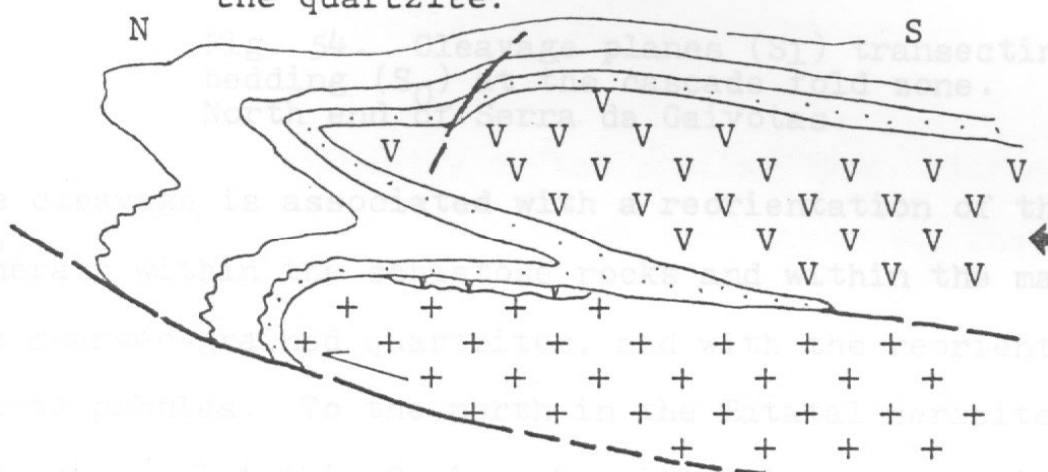
In the series of recumbent folds,  $S_0$ -surfaces are defined by: 1) compositional banding in the quartz schist; 2) thin layers of coarse-grained quartzite within the Batatal sericite schist; 3) discrete separation planes within the Moeda quartzite; 4) conglomerate lenses within the quartzite; 5) compositional lamination in itabirite; and 6) contact between Moeda and Batatal Formations. However, in the strata surrounding the Gaivotas and Catarina anticline, the rocks have been more deformed, and the bedding is more obscure. This suggests an increase in strain higher in the structure.

The nature of strain is controlled by lithology. For example, at Serra das Gaivotas conglomerate lenses are highly deformed, with a strong penetrative foliation parallel to the bedding. All clasts are flattened in the plane of the foliation and elongated to form a penetrative east-plunging lineation. Quartzite and chert clasts are now ribbons, but vein quartz pebbles are egg-shaped, an indication of the fact that fine-grained mineral aggregates deform more readily.

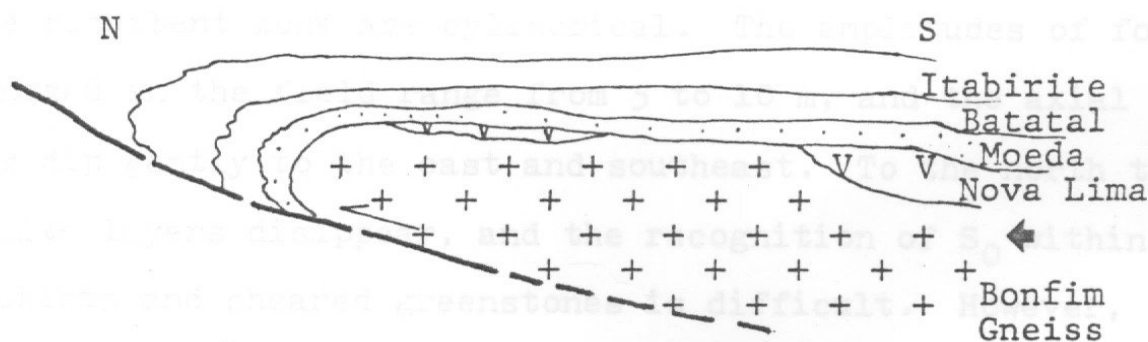
At the nose of the Curral recumbent anticline, a vertical sequence of mesoscopic recumbent and cascade folds at the contact between Moeda and Batatal Formations display well-pronounced cleavage planes. The close-spaced, sub-horizontal, cleavage planes, parallel to the axial surface, intersect a sequence



3. Formation of the Quartzitic Tip by differential response to stresses in the greenschist and in the quartzite.



2. Development of the Catarina Structure, with the formation of a schuppen structure.



1. Development of the Curral-Gaivotas Recumbent Fold.

Fig. 53

of thin clastic beds (Fig. 54).

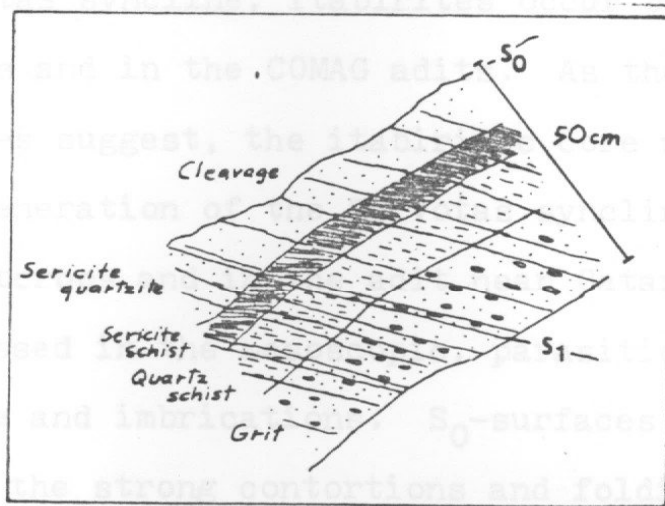


Fig. 54. Cleavage planes ( $S_1$ ) transecting bedding ( $S_0$ ) at the cascade fold zone. North end of Serra da Gaivotas.

The cleavage is associated with a reorientation of the micaceous minerals within the schistose rocks and within the matrix of the coarser-grained quartzites, and with the reoriented small quartz pebbles. To the north in the Batatal sericite schist and greenschist this  $S_1$  is subhorizontal and approximately at right angles to the contact between those rocks, as it should be.

Close to the contact with greenschists the itabirite displays numerous mesoscopic parasitic folds. In general, folds in the recumbent zone are cylindrical. The amplitudes of folds recognized in the field range from 5 to 10 m, and the axial planes dip gently to the east and southeast. To the north the quartzite layers disappear, and the recognition of  $S_0$  within the schists and sheared greenstones is difficult. However, there a strong penetrative foliation pervades those rocks forming shear folds.



On the southern flank of the Serra do Rola Moca, in the core of the Gaivotas syncline, itabirites occur both in excellent outcrops and in the COMAG adits. As the major regional structures suggest, the itabiritic core moved northward during the generation of the Gaivotas syncline. In the field, both on outcrops and in the adit near Catarina this movement is expressed in the mesoscopic, parasitic folds showing northward vergence and imbrications.  $S_0$ -surfaces are well-preserved despite the strong contortions and folding, and  $S_1$ -surfaces commonly parallel to  $S_0$  can be recognized only in fold hinges.

Folds are dominantly of the similar type, although intra-folial and disharmonic styles are also present. The fold in Figure 55 is thought to reflect on the mesoscopic scale the fold pattern of the large Gaivotas recumbent syncline. In some mesoscopic folds the cores show reversed folds, suggesting that the folding was tight (Turner and Weiss, 1963). Transposition begins with tight folding, which continues until discrete repetition takes place along subparallel  $S_1$ -foliation.



Fig. 55. Mesoscopic recumbent similar fold in itabirite, showing reversed fold in the core. Coin is 2 cm. COMAG Tunnel, Catarina area.

In the adit the writer noted a spectacular example of the transpositions of bedding in the itabirite (Fig. 56). This structure is produced when the mechanical properties of layers are strongly contrasting (Turner and Weiss, 1963; Kerrich and Allison, 1978). Transposition begins with tight folding, which continues until discrete rupturing takes place along subparallel  $S_1$ -foliation.

in the minor folds, which also represents  $L_1$ , plunge 25 to 30 degrees toward 40 to 60, at the north end of the Serra das Gravatás (Fig. 57). As expected, these orientations closely subparallel the directions of  $L_1$  and the  $B_1$ -fold axes in the itabirites within Domain 1; hence, these fabric elements

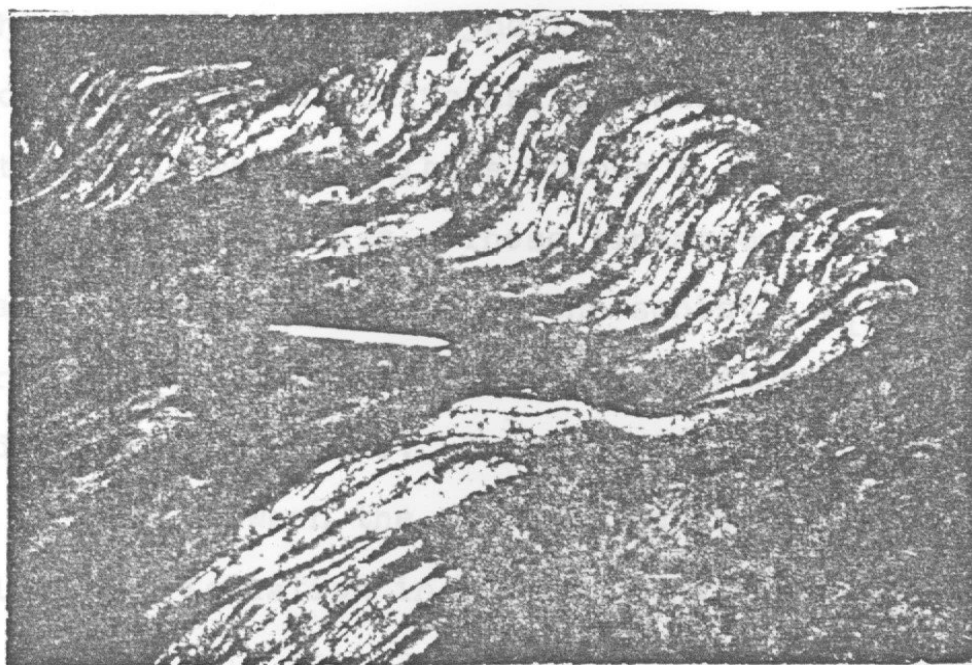


Fig. 56. Contorted slices of competent cherty layers within itabirite formed by transposition of bedding. COMAG Tunnel. Catarina area. Pencil for scale.

Rotation of the axial surfaces along  $B_1$ -axes, subsequent to the slicing produces the ultimate sinusoidal-shaped shreds (Fig. 56).

#### Mesoscopic Analysis of $L_1$ -lineation

$L_1$  is defined by corrugations and quartz ribs within the itabirite, and by wrinkles within the sericite schist. In the clastic rocks, it is defined by the elongation of quartz pebbles, kinking in micaceous layers, and by quartz rods.  $B_1$ -fold axes in the minor folds, which also represents  $L_1$ , plunge 25 to 30 degrees toward 40 to 60, at the north end of the Serra das Gaivotas (Fig. 57). As expected, these orientations closely subparallel the directions of  $L_1$  and the  $B_1$ -fold axes in the itabirites within Domain I; hence, these fabric elements

correspond to the  $D_1$ -episode. Their eastward tilt and deformation is considered to represent the  $D_2$ -phase of tectonism.

The lower limb of the syncline, which is on the eastern slope of the Serra das Gaivotas, contains sheared Batatal sericite schist which exhibits strong  $L_1$ -lineations plunging to the east and northeast. These lineations are formed by penetrative corrugations within the schist.  $L_1$  was derived by the northward tectonic transport and folding of the cover rocks, related to the  $D_1$ -episode. Discontinuous breccia zones occur at the contact between the sericite schist and quartzites, and also along the foliation in the coarse-grained quartzite lenses within the sericite schist.

#### Quartz Rods

Quartz rods are concentrated in the quartzose zones within the quartzite, and in some segregations of milky quartz. They consist of parallel "pencils" and striations plunging 25-30 degrees toward azimuths between 40 and 60 (Fig. 57). The quartz rods are crosscut by orthogonal extension fractures.

#### Elongation of Quartz Pebbles

At the upper part of the Moeda Formation there are sporadic conglomerate lenses, which contain quartz pebbles with long axes plunging 15-25 degrees toward the directions between 20 and 50, at the north part of Serra das Gaivotas (Fig. 57).

#### Deformation Along Lithologic Contacts

Strain along a lithologic contact can produce folds, shearing parallel to the contact, or a breccia, dependent on



lithology and, perhaps, the rate of strain.

### Decollement Zone

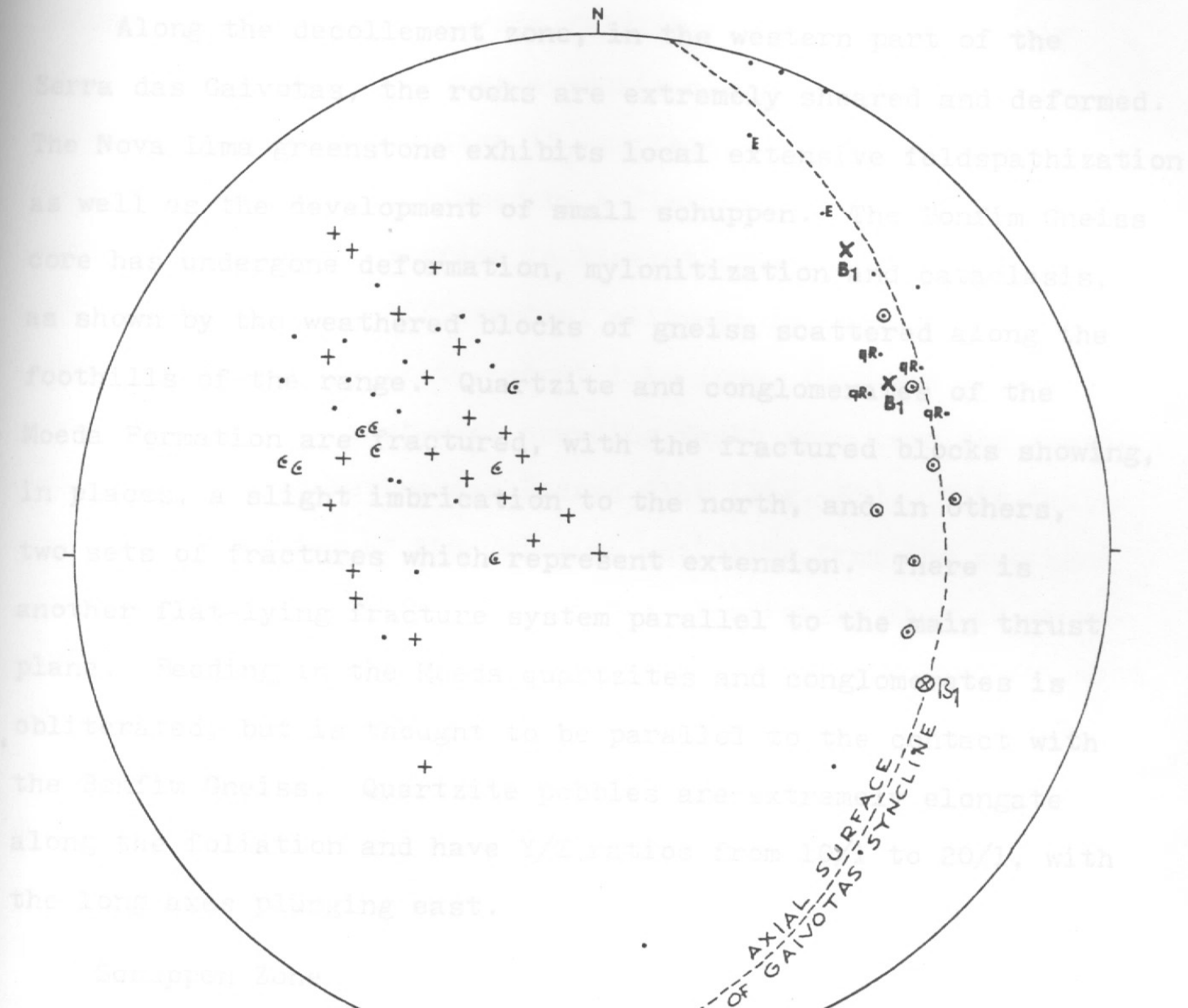


Fig.57 DOMAIN II - Orientation diagram, equal area net.

- 28 S-poles to bedding, +22 S-poles to foliation,
- 8 poles to cleavage, •7 L<sub>1</sub>-lineation,
- qR-quartz rods, XB<sub>1</sub>-fold axis, •E-elongation of long axis of quartz pebbles in clastic rocks of the Moeda Formation. Nose of the Curral anticline, north part of Serra das Gaivotas.

The structures at the upper part of the schuppen (east

lithology and, perhaps, the rate of strain.

### Decollement Zone

Along the decollement zone, in the western part of the Serra das Gaivotas, the rocks are extremely sheared and deformed. The Nova Lima greenstone exhibits local extensive feldspathization as well as the development of small schuppen. The Bonfim Gneiss core has undergone deformation, mylonitization and cataclasis, as shown by the weathered blocks of gneiss scattered along the foothills of the range. Quartzite and conglomerates of the Moeda Formation are fractured, with the fractured blocks showing, in places, a slight imbrication to the north, and in others, two sets of fractures which represent extension. There is another flat-lying fracture system parallel to the main thrust plane. Bedding in the Moeda quartzites and conglomerates is obliterated, but is thought to be parallel to the contact with the Bonfim Gneiss. Quartzite pebbles are extremely elongate along the foliation and have Y/Z ratios from 10/1 to 20/1, with the long axes plunging east.

### Schuppen Zone

The contorted character of the unconformity surface and the sinuous shape of the Moeda Formation at the western flank of the Moeda structure reflect the effects of differential slippage of the clastic rocks over the greenschist due to differences in the ductilities and the relative intensities of transport.

The structures at the upper part of the schuppen (east

side) reflect the behavior of the two mechanically different rock types: 1) in the greenschist, the  $S_1$ -surfaces are kinematically passive wherein folding was developed by slip or flow along discrete displacements along the surfaces parallel to the axial plane ( $S_1$ -surface); and 2) in the clastic rocks, folding was developed by a flexural-slip mechanism, in which the  $S_0$ - or  $S_1$ -surface is kinematically active. One of the effects of this differential slippage is represented by a wedge or tip of quartzite, about 1 km long, that was inserted downward along an east-west trending fault zone into the greenschist, north of Retiro das Pedras Club (Fig. 53). This fault separates the nose of the Catarina anticline from the southern part of the schuppen block. A wedge of strongly sheared greenschist was inserted along the fault during the downward movement of the quartzitic tip. The structure was tilted later about 30 to 40 degrees to the east, along a north-south rotation axis during the  $D_2$ -deformational phase.

Near the basal part of the structure, at margins of the Ribeirao do Morro Velho, small wedges of tuffaceous greenschist and talc-rich zones of the Nova Lima Formation were tectonically inserted into the brecciated conglomerate, thus indicating transposition of bedding along the extremely deformed contact between Moeda and Nova Lima Formations.

#### Moeda-Batatal Contact Zone

On a more limited scale, spectacular recumbent cascade folds (Figs. 51 and 52) occur near the core of the Curral anticline along the contact between Moeda and Batatal Formations.

This contact is marked by abrupt interlayers of quartz schist and sericite schist within sericite quartzite and grit. The sericite schists were made more competent by the presence of the sericite quartzite interbeds, so that they became folded instead of sheared.

The contact between the Batatal schists and the Moeda quartzites along the eastern flank of the structure, in the Corrego da Catarina, is marked by sheared and brecciated zones trending nearly parallel to the contact zone. These breccia zones are composed mainly of fragments of quartz schist and quartzite, cemented by a mixture of siliceous, schistose and ferruginous material. Some breccia zones are as much as 10 m thick.

The breccia is interpreted to represent shear under brittle conditions, perhaps subsequent to the fold generation.

In the northern part of the Serra das Gaivotas are several, east-west oriented breccia zones within the greenschists and near the contact with the itabirite. These breccias are restricted to the Batatal Formation and consist of angular fragments of white chert in a brownish, fine-grained groundmass. The breccia indicates a brittle regime probably during  $D_1$ -deformation, but some fluxion zones (Higgins, 1971) within the breccia suggest that a viscous cataclastic flow also took place (Fig. 58).



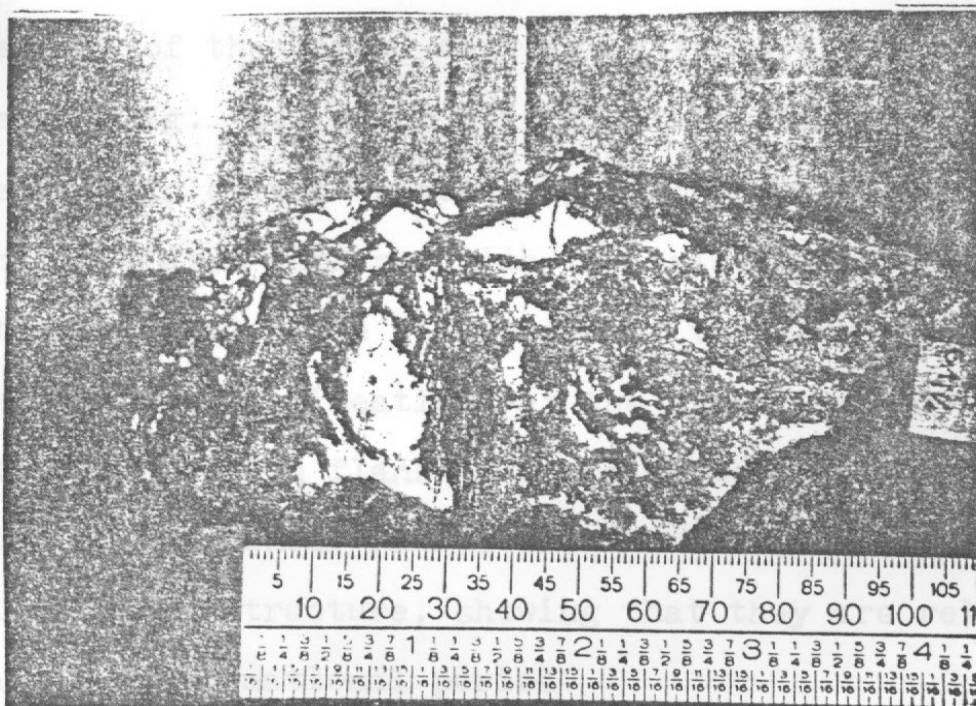


Fig. 58. Breccia showing white chert fragments within a fine-grained matrix. Observe fluxion zones. South flank of the Serra do Curral.

#### Geometric Analysis of the Curral-Gaivotas Structure

The strong pervasive  $S_1$ -surfaces represented by foliation and cleavage in the nose of the Curral-Gaivotas recumbent anticline (Fig. 57), and bedding ( $S_0$ ) are oriented north-south to northeast with dips to east and southeast. The orientation of some of these surfaces parallel the northeast trend of  $S_0$ -surfaces in the Domain I, but on the other hand, some are parallel to the preferred orientation of  $S_0$ -surfaces in the Gaivotas syncline and Catarina anticline. The parallelisms of the S-surfaces found at Domains I and II, and those encountered at the Gaivotas and Catarina structures indicate they belong to the same  $D_1$ -deformational phase.

The linear trend of the  $L_1$ -lineation,  $B_1$ -axis of small folds, quartz rods and elongation of quartz pebble long axis, at the nose of the Curral-Gaivotas structure, plunge east and northeast (Fig. 57), which coincides with the plunge orientation of the  $\beta_1$ -axis of the Gaivotas syncline. Those linear fabric elements are also coplanar with the axial surface of the Gaivotas syncline. The elongation of the long axes of quartz pebbles and the  $L_1$ -lineations at the upper limb of the Catarina anticline or western flank of Serra da Moeda (Fig. 60), are parallel to the linear fabric elements of the nose of the Curral-Gaivotas structure, showing that they are related to the same  $D_1$ -deformational period.

The lower and upper limbs of the Gaivotas recumbent syncline are oriented with a strike of  $344$  dipping  $40$  degrees to east and  $25$  with dip of  $32$  degrees to east, defining a  $\beta_1$ -axis plunging  $33$  degrees toward  $110$  determined by the intersection of the two surfaces (Fig. 59). The plot for  $S_0$ -surfaces of the upper limb of the Catarina anticline, on the western flank of the Serra da Moeda, displays a strong preferred orientation of  $16$  percent maximum for a strike of  $4$  dipping  $35$  degrees to east (Fig. 60).

Fig. 59 DOMAIN II - Orientation diagram, equal area net. S-pole to bedding in elastic rocks of the Moeda Formation in the Gaivotas syncline at Serra das Gaivotas. A: lower limb; B: upper limb. Contours: 14%, 12%, 10%, 8%, 6%, 4%, 2% per 1% area. Maximum 13%. 83 points.

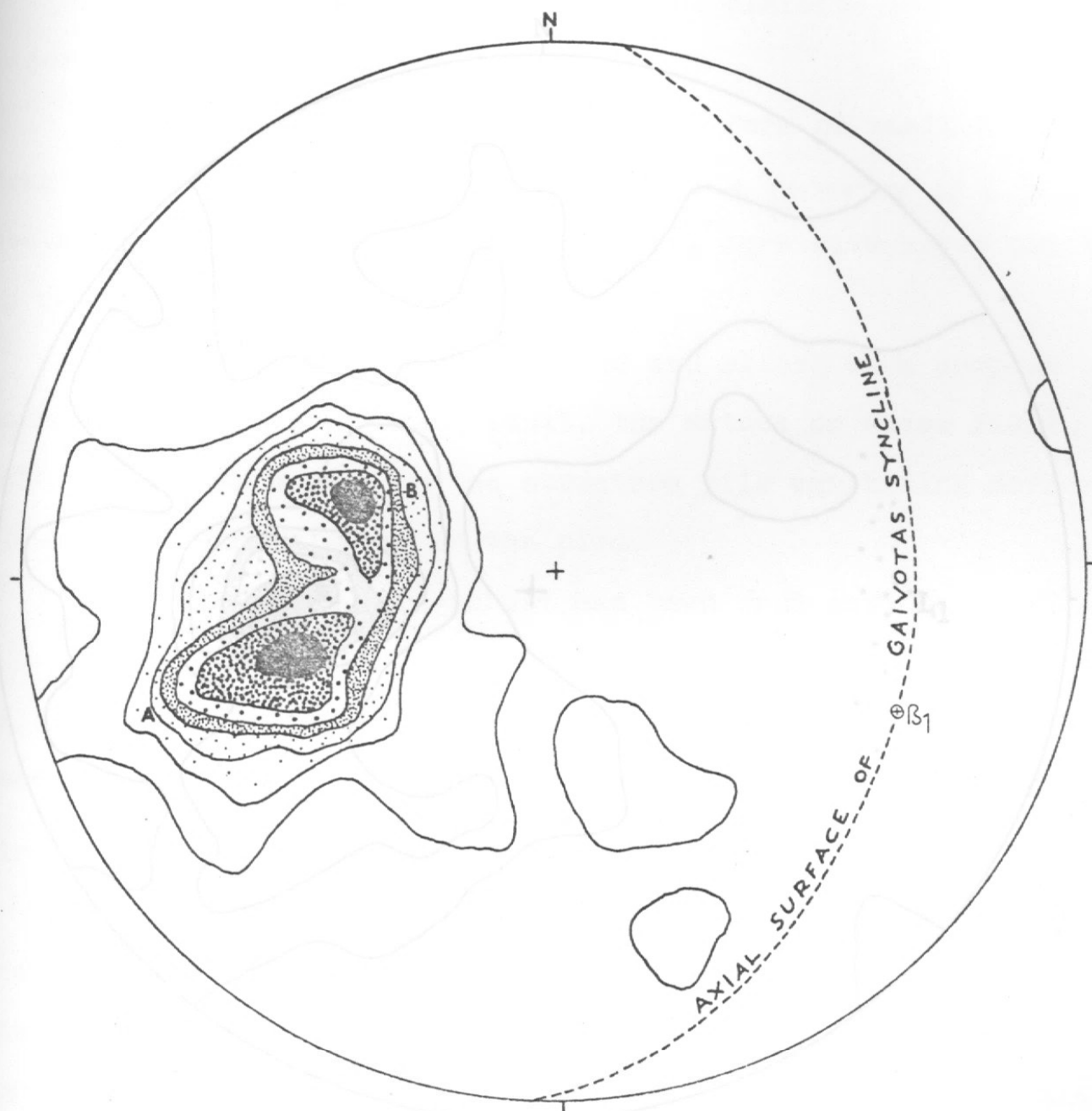


Fig.59 DOMAIN II - Orientation diagram, equal area net. S-pole to bedding in clastic rocks of the Moeda Formation in the Gaivotas syncline at Serra das Gaivotas. A: lower limb; B: upper limb. Contours 14%, 12%, 10%, 8%, 6%, 4%, 2% per 1% area. Maximum 15%. 88 points.

# Tanandua Area

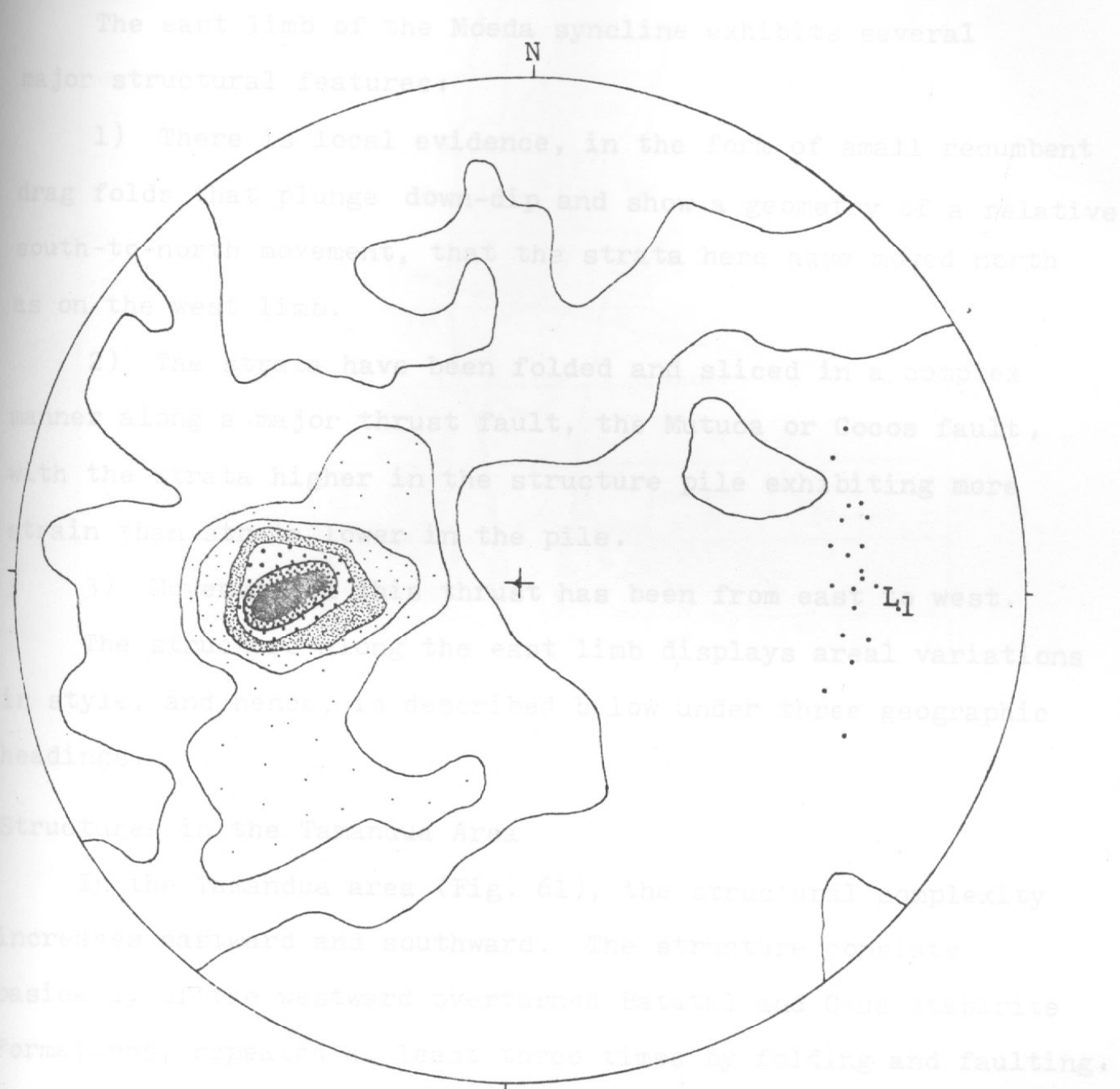


Fig.60 DOMAIN II - Orientation diagram, equal area net. S-poles to bedding=foliation in clastic rocks of the Moeda Formation and sericite schist of the Batatal Formation, in the upper limb of the Catarina anticline. Contours on 14%,12%,10%,8%,6%,4%, 2% per 1% area. Maximum 16%. 107 points. L1=long axis elongation of quartz pebbles. Western flank of Serra da Moeda.



## Tamandua Area

The east limb of the Moeda syncline exhibits several major structural features:

1) There is local evidence, in the form of small recumbent drag folds that plunge down-dip and show a geometry of a relative south-to-north movement, that the strata here have moved north as on the west limb.

2) The strata have been folded and sliced in a complex manner along a major thrust fault, the Mutuca or Cocos fault, with the strata higher in the structure pile exhibiting more strain than strata lower in the pile.

3) Movement on this thrust has been from east to west.

The structure along the east limb displays areal variations in style, and hence, is described below under three geographic headings.

### Structures in the Tamandua Area

In the Tamandua area (Fig. 61), the structural complexity increases eastward and southward. The structure consists basically of the westward overturned Batatal and Caue Itabirite Formations, repeated at least three times by folding and faulting. The great width of the Caue itabirite, about 1500 m, was attributed by Pomerene (1964) to tight isoclinal folding which he thought repeated the formation five times. Field evidence indicates at least three repetitions; however, within the itabirite there could be even more than five repetitions.



In the Tamandua area, the lithologic units are separated by the Mutuca thrust fault into a western belt (Western Tamandua) composed of amphibolite and greenschist of the Gandarela Formation, the Caue Itabirite and the Batatal Formation, and into an eastern belt (eastern Tamandua) formed by the Caue Itabirite, Batatal and Moeda Formations (Fig. 62, and Map 2). It should be noted that in the Tamandua area the Mutuca fault is known as the Cocos fault. The eastern and western belts exhibit different types and intensities of deformation and structural evolution, and hence they can be discussed separately.

#### Western Tamandua Belt

##### Fabric Elements

In the Western Tamandua Belt, bedding is conspicuous and defined in the itabirite by compositional layering of magnetite and of brown and yellowish fine-grained matrix material which is paralleled by the foliation in the Gandarela greenschists. Bedding features and internal structures indicate that this belt did not undergo as much deformation as the eastern belt. Large-scale westward displacements are not observed. Thus, the rocks can be considered to have been rotated during  $D_2$ , almost in situ, and to be parautochthonous or autochthonous in relation to the eastern belt.

The S-pole diagram (Fig. 63) for the layering within the itabirite at Morro do Tamandua shows a strong preferred orientation, valid for the eastern belt, displaying 16 percent maximum for a direction with strike 330 and a dip of 45 degrees to northeast.

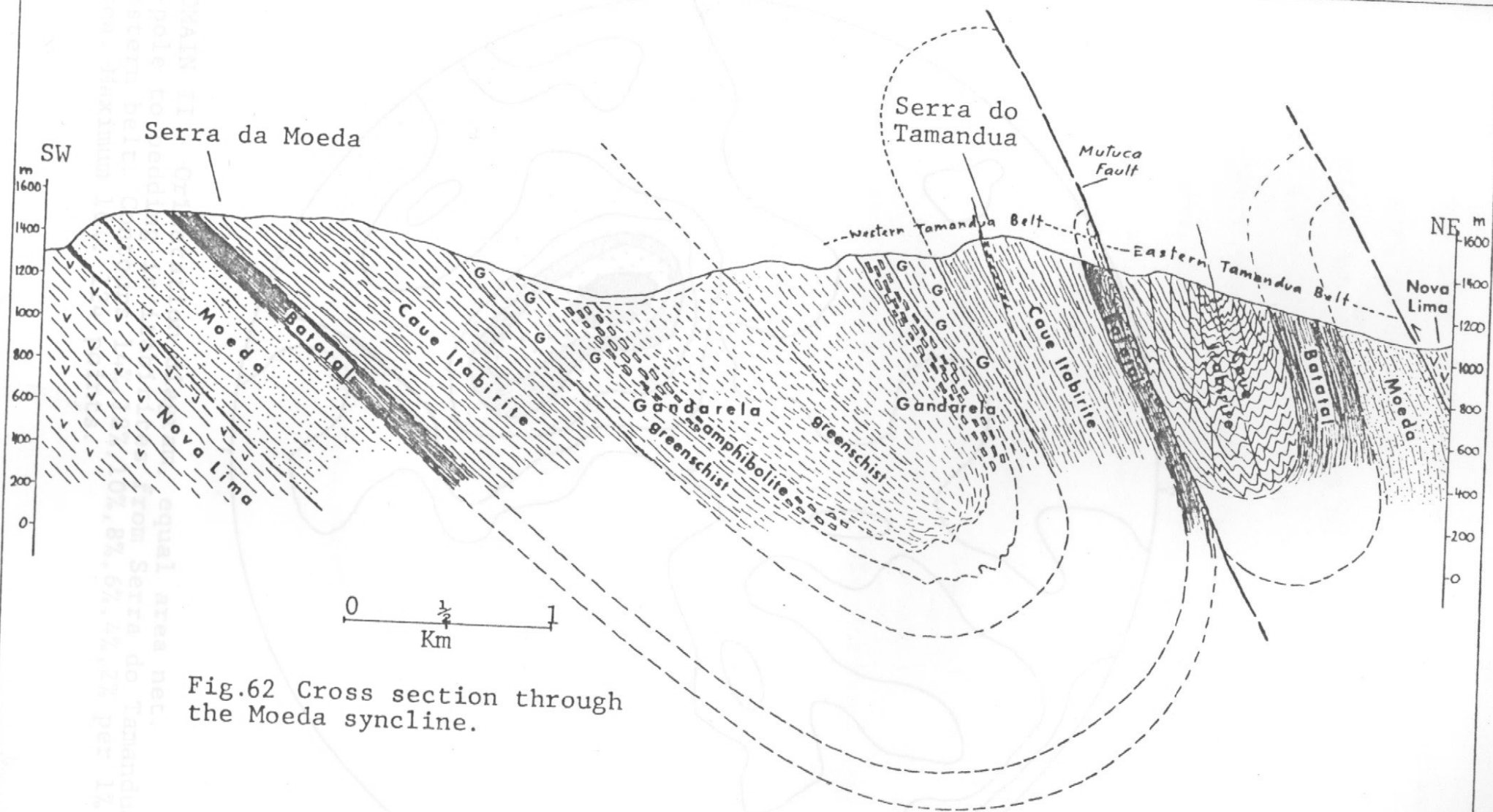


Fig.62 Cross section through the Moeda syncline.



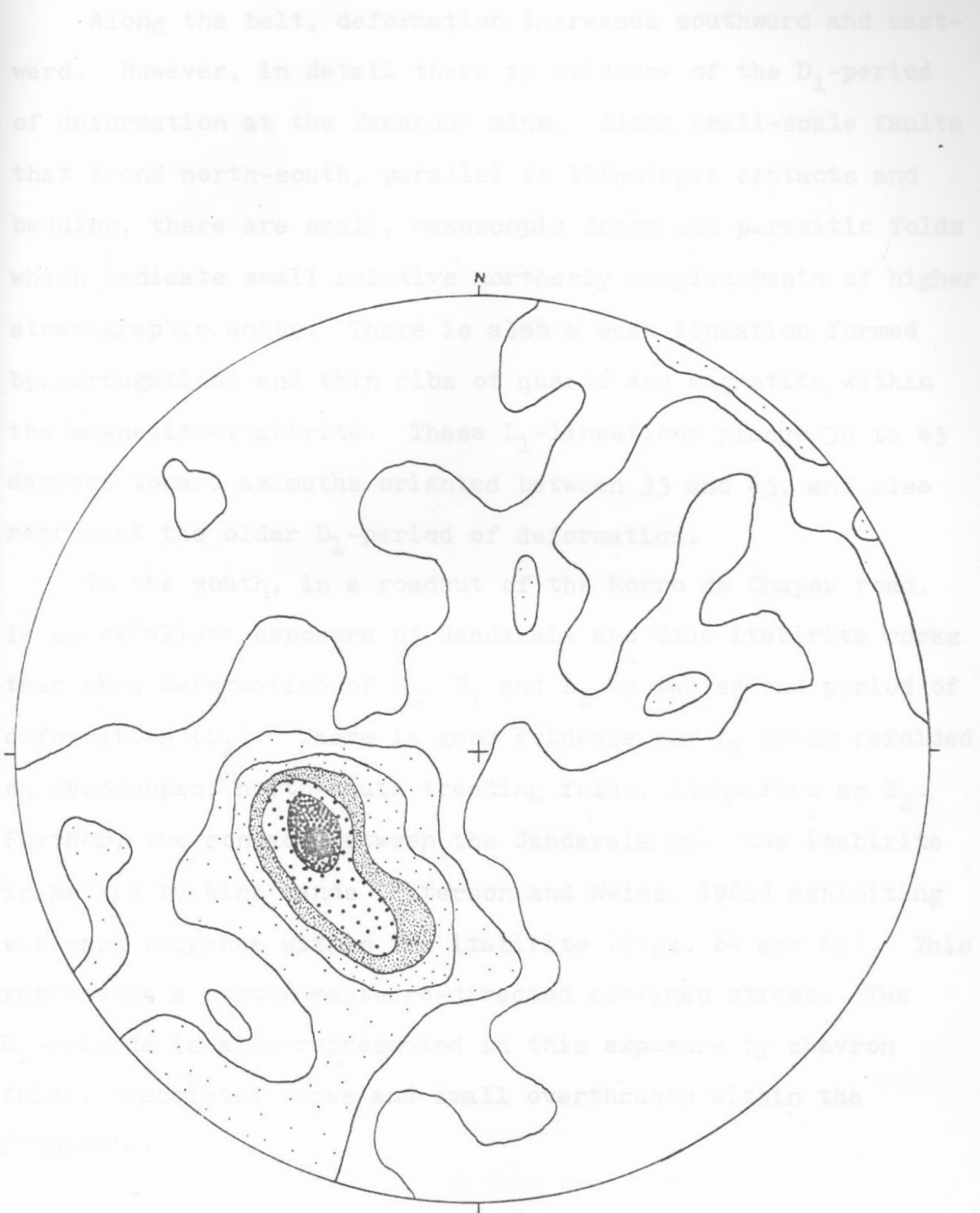


Fig. 63 DOMAIN II - Orientation diagram, equal area net.  
S-pole to bedding in itabirites from Serra do Tamandua,  
western belt. Contours 14%, 12%, 10%, 8%, 6%, 4%, 2% per 1%  
area. Maximum 16%. 124 points.

Along the belt, deformation increases southward and eastward. However, in detail there is evidence of the  $D_1$ -period of deformation at the Tamandua mine. Along small-scale faults that trend north-south, parallel to lithologic contacts and bedding, there are small, mesoscopic drags and parasitic folds which indicate small relative northerly displacements of higher stratigraphic units. There is also a weak lineation formed by corrugations and thin ribs of quartz and magnetite within the magnetite-itabirite. These  $L_1$ -lineations plunge 30 to 45 degrees toward azimuths oriented between 35 and 65, and also represent the older  $D_1$ -period of deformation.

To the south, in a roadcut of the Morro do Chapéu road, is an excellent exposure of Gandarela and Caue itabirite rocks that show deformation of  $S_0$ ,  $S_1$  and  $L_1$  by the second period of deformation ( $D_2$ ). There is good evidence for  $L_1$  being refolded on mesoscopic, north-south trending folds, identified as  $B_2$ . Further, the contact between the Gandarela and Caue itabirite is marked by kink bands (Paterson and Weiss, 1961) exhibiting westward vergence within the itabirite (Figs. 64 and 65). This represents a strong eastward-directed confined stress. The  $D_2$ -episode is also represented in this exposure by chevron folds, brecciated zones and small overthrusts within the itabirite.

In the present area, it would seem that the limbs of the anticline had become elongated to such an extent that the eastern limb was covered and became the Mutuca fault. To the east of Peixos area (Fig. 28b), a slice of Moeda quartzite remains along the fault.

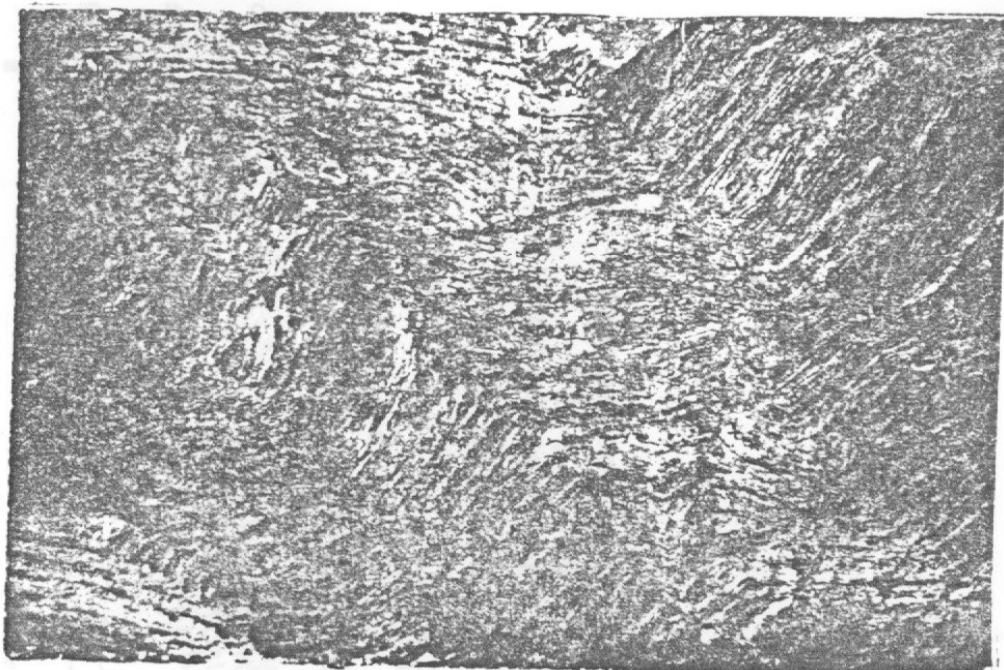


Fig. 64. Kink bands in itabirites. Stress was from east to west. Field of horizontal view is about 5 m. Morro do Chapéu road.

#### Mutuca Thrust Fault

The boundary between the two Tamandua belts is the large Mutuca, or Cocos thrust fault (Fig. 66). The Cocos and Tamandua faults are separated by a slice of Batatal amphibolites and greenstones, about 200 m thick, which disappears south of Section 9000. The Batatal rocks are extremely sheared and occupy the same structural position as the anticline of Moeda conglomerate and Nova Lima greenschists in Domain III. In the present area, it would seem that the limbs of the anticline had become elongated to such an extent that the eastern limb was severed and became the Mutuca fault. To the east of Feixos area (Fig. 28b), a slice of Moeda quartzite remains along the fault.

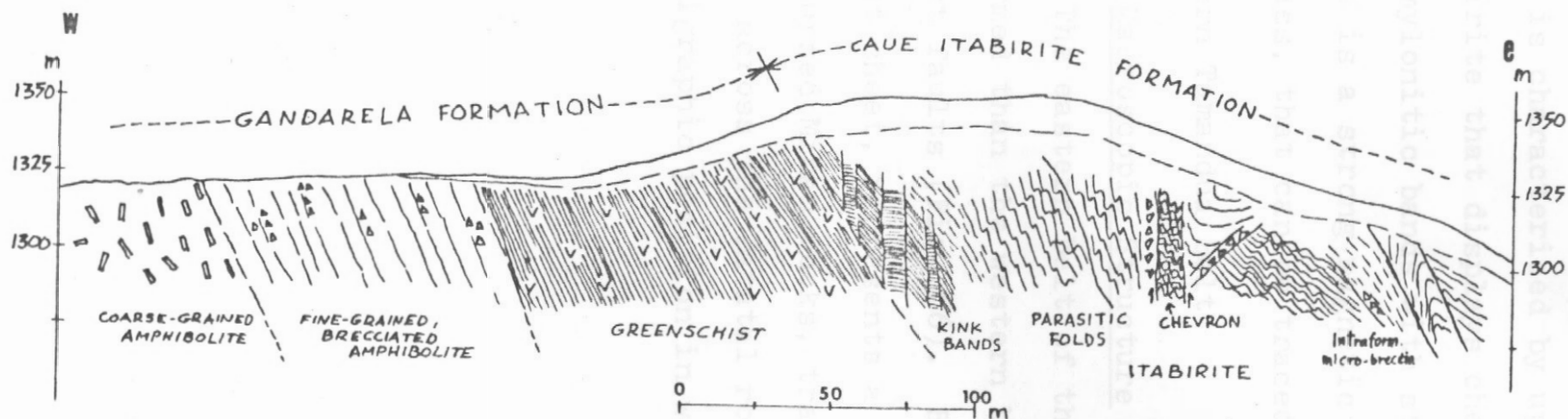


Fig.65 Section of Gandarela-Itabirite Caue Formations, Morro do Chapéu road, within Tamandua belt. Note orientation of kink bands, and occurrence of breccia zones.



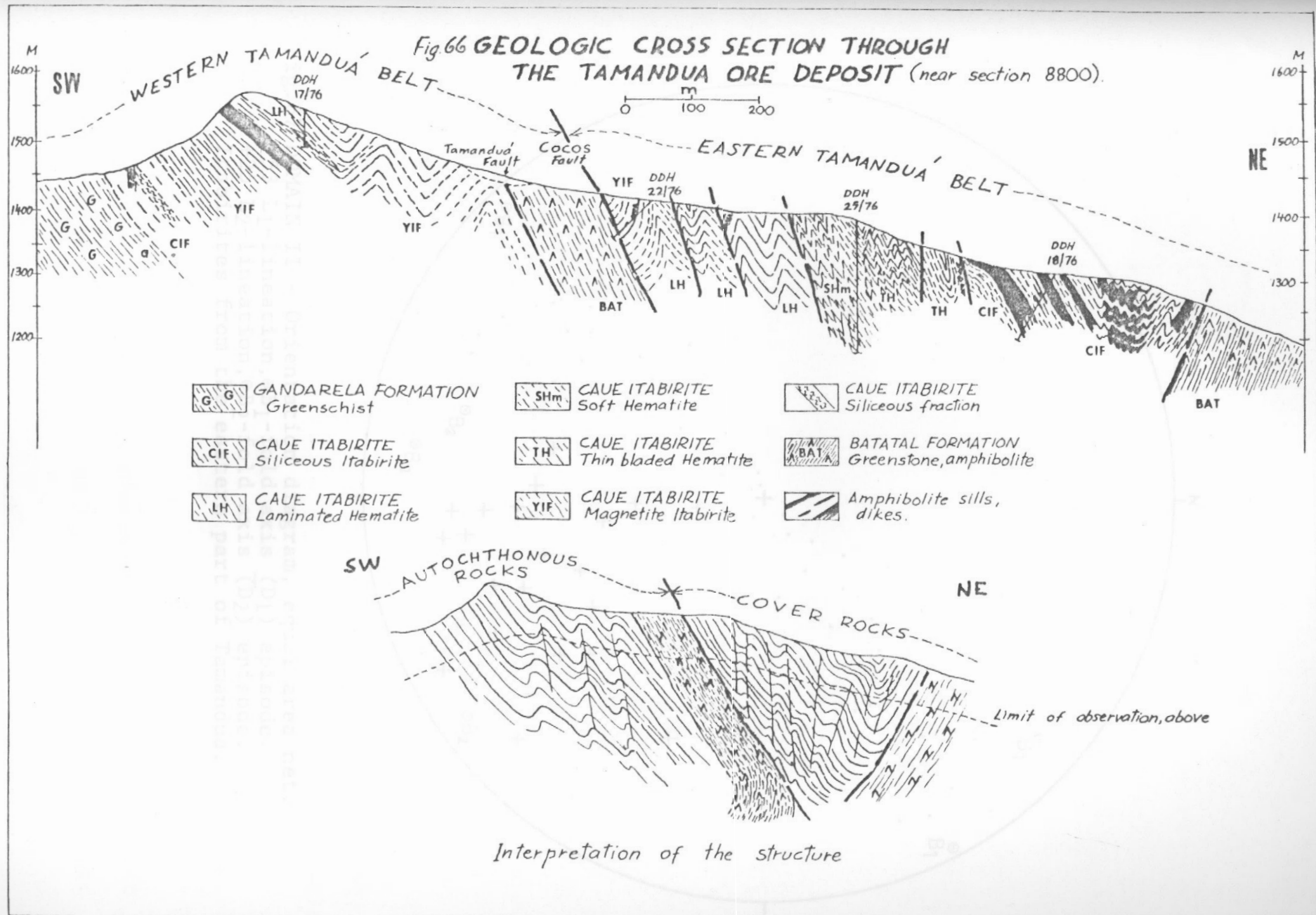
zone, suggesting a residual from a northward transport.

To the south of Section 9000 (Fig. 61) the Cocos fault zone is characterized by up to 5 m of strongly deformed itabirite that displays chevron and tight folds, and of laminated and mylonitic bands with steep dips. Along this fault segment, there is a strong magnetic anomaly, detectable by a pocket compass, that can be traced for at least 500 m.

### Eastern Tamandua Belt

#### Macroscopic Structure

The eastern belt of the Tamandua structure is much more deformed than the western belt, showing many more subsidiary thrust faults (Fig. 66). Basically this belt, the Tamandua thrust sheet, represents a translated sheet of stratigraphically overturned Minas rocks, transported along the Mutuca thrust fault across the Batatal rocks that occupy the lowermost stratigraphic position in western Tamandua belt.



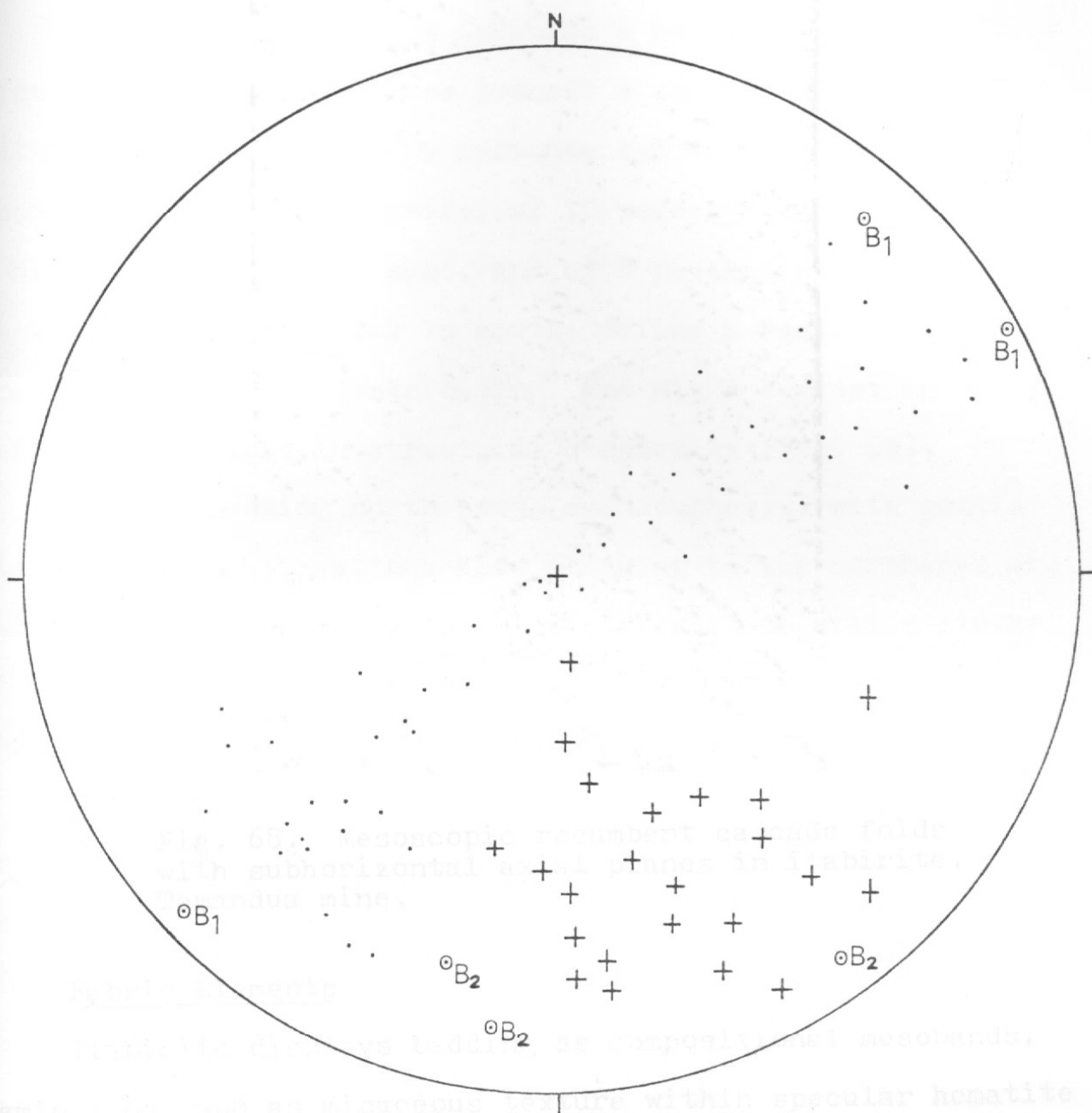


Fig.67 DOMAIN II - Orientation diagram, equal area net.

•53 L<sub>1</sub>-lineation, ⊙B<sub>1</sub>-fold axis (D<sub>1</sub>) episode.  
 +25 L<sub>2</sub>-lineation, ⊙B<sub>2</sub>-fold axis (D<sub>2</sub>) episode.

Itabirites from the eastern part of Tamandua.

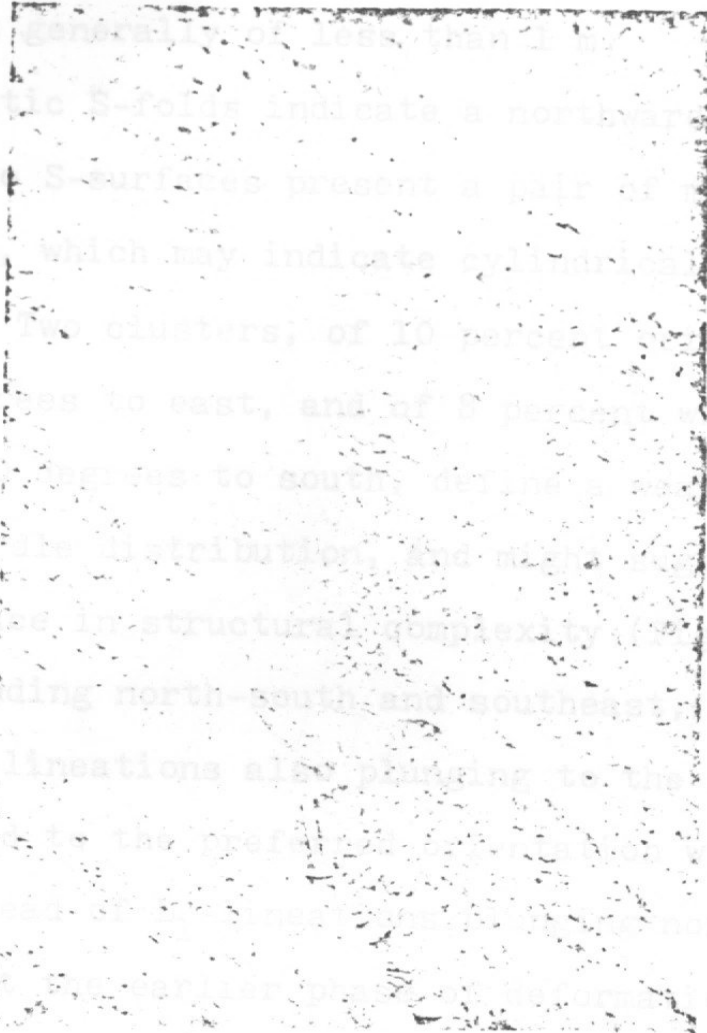


Fig. 68. Mesoscopic recumbent cascade folds with subhorizontal axial planes in itabirite, Tamandua mine.

### Fabric Elements

Itabirite displays bedding as compositional mesobands, lamination, and as micaceous texture within specular hematite units. There is also a strong  $S_1$ -penetrative foliation parallel to bedding. These surfaces are folded to varying degrees on northeast-trending  $B_1$ -fold axes, some of which plunge to the east and some to the west (Fig. 67). The earlier folds are considered to be  $D_1$ , and the reversal in plunge is thought to denote younger folds, related to  $D_2$ . Furthermore, mesoscopic



folds are of parasitic, asymmetric, and cascade types (Fig. 68) with amplitudes generally of less than 1 m.

The parasitic S-folds indicate a northward transport. A plot of poles to S-surfaces present a pair of maxima of 335 with steep dips, which may indicate cylindrical folds or sheeting normal to 335. Two clusters, of 10 percent oriented at 343 and a dip of 30 degrees to east, and of 8 percent with strike of 74 and dip of 30 degrees to south, define a weakly developed great circle girdle distribution, and might suggest an earlier deformed S-surface in structural complexity (Fig. 69).

B-axes trending north-south and southeast, with gentle plunges, and  $L_2$ -lineations also plunging to the northeast are seemingly related to the preferred orientation with a strike of 335. The spread of  $L_1$ -lineations plunging northeast and southwest reflect the earlier phase of deformation.

The details of the structural pattern remain unclear. From a regional point of view, it would seem reasonable to presume that the strata became transported northerly during the formation of the extensive northeast-trending Curral anticline, during  $D_1$ . A study of maps suggests that there may be evidence for such extensive movement in structures in this limb farther to the south, outside of the present study area. However, in the present area the evidence for  $D_1$  is not as clear and unequivocal as that for  $D_2$ .

## Distribution of Hematite Ore

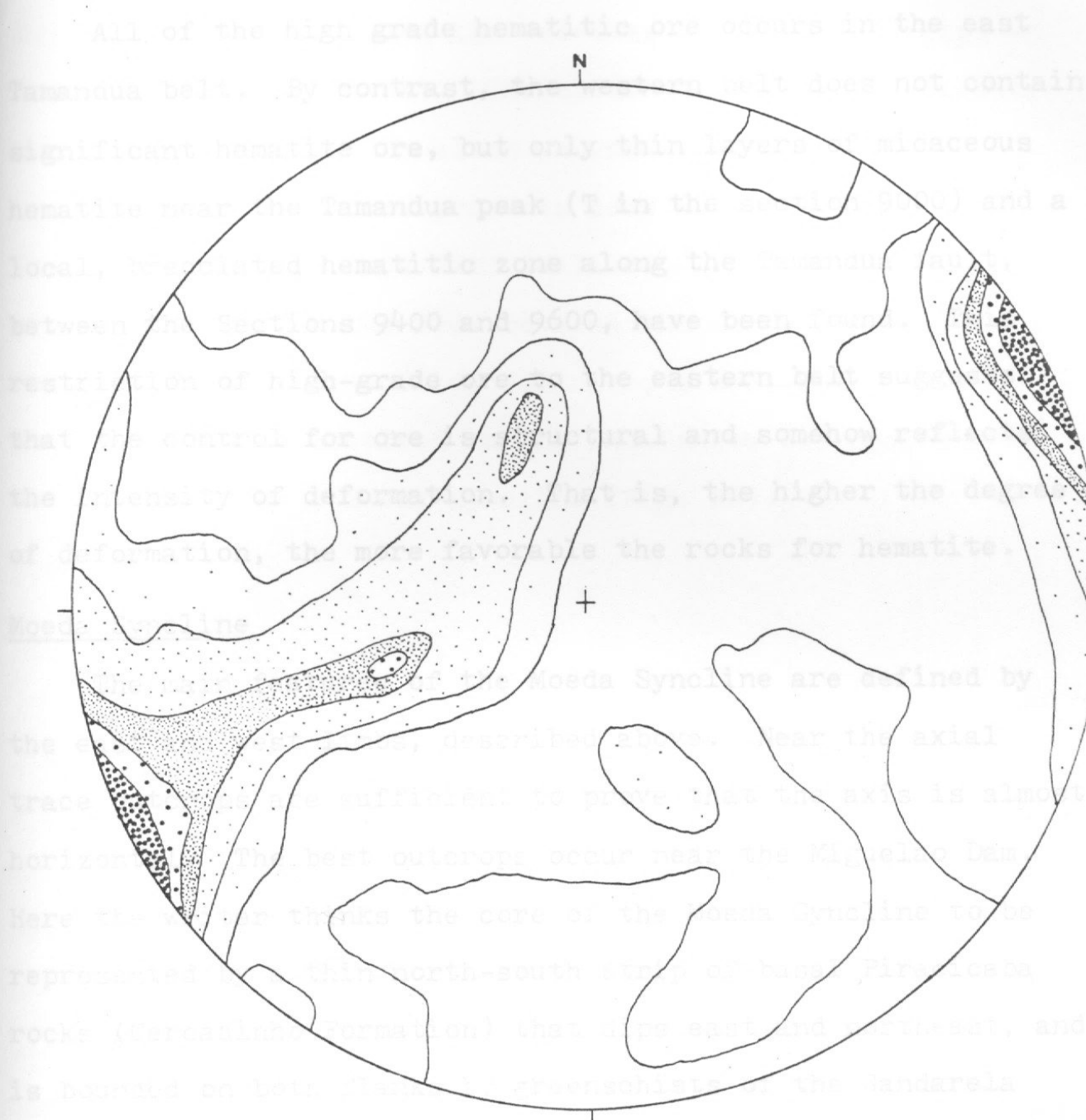


Fig. 69 DOMAIN II - Orientation diagram, equal area net.  
 S-pole to foliation=bedding in itabirite from the  
 Tamandua ore deposit, eastern belt.  
 Contours 12%, 10%, 8%, 6%, 4%, 2% per 1% area  
 Maximum 12%. 246 points.

in this locality. The only structures are the gently undulating surface dipping to the east. At the north end of the outcrop, the Caradocian rocks are cut out by a small thrust fault that dips to the east (Fig. 63).

## Distribution of Hematite Ore (Fig. 70) shows a point maximum

All of the high grade hematitic ore occurs in the east Tamandua belt. By contrast, the western belt does not contain significant hematite ore, but only thin layers of micaceous hematite near the Tamandua peak (T in the section 9000) and a local, brecciated hematitic zone along the Tamandua fault, between the Sections 9400 and 9600, have been found. This restriction of high-grade ore to the eastern belt suggests that the control for ore is structural and somehow reflects the intensity of deformation. That is, the higher the degree of deformation, the more favorable the rocks for hematite.

### Moeda Syncline

The main features of the Moeda Syncline are defined by the east and west limbs, described above. Near the axial trace outcrops are sufficient to prove that the axis is almost horizontal. The best outcrops occur near the Miguelao Dam. Here the writer thinks the core of the Moeda Syncline to be represented by a thin north-south strip of basal Piracicaba rocks (Cercadinho Formation) that dips east and northeast, and is bounded on both flanks by greenschists of the Gandarela Formation. Bedding is defined by composite layering within quartzite and silver sericite schist, nearly parallel to the foliation in the greenschists. No folds could be identified in this locality. The only structures are the gently undulating surfaces dipping to the east. At the north end of the outcrop, the Cercadinho rocks are cut out by a small thrust fault that dips to the east (Fig. 62).

The plot of  $S_0$ -surfaces (Fig. 70) shows a point maximum of 14 percent on bedding that strikes about 330 and dips 45 degrees to the northeast. The spread of the poles suggests some slight deformation along an east-west axis.

The Moeda syncline presents dome structures between the Codornas and Agua Limpa dams (Wallace, 1965) where the folds are more open. In the area between the Serras da Moeda and Saboeiro, where tight folds dominate, a succession of anticlines and synclines is observed making indefinite the position of the axial plane of the Moeda syncline (Fig. 26).

### DOMAIN III

#### General

Domain III consists of the northern portion of the east limb of the Moeda Syncline and includes the most complex structures in the map area. The reason for this complexity arises from the fact that the strata are considered first to have been folded on east-west axes when the rocks were thrust northerly during the formation of the overturned Curral anticline, and then refolded, thrust faulted, and rotated westerly during the formation of the overturned Moeda syncline. It is proposed that the westward rotation was facilitated by the movement on the Agua Quente and Barreiro tear faults, along the southeast flank of the Curral anticline.

The nature of the geometric and temporal relationships between the northeast-trending Curral anticline and the south-trending Moeda syncline is the key to understanding the structure in this small complex domain. Pomerene (1964)



proposed that the main structural relationship is that of a sinuous, thrust surface where the Moeda syncline abuts the Curral homocline. He proposed that the connection between the Mutuca Fault and a supposed Galvotas Fault was made through a contorted plane. Borr (1969, p. 107) proposed the structure at this junction to be a single thrust fault consisting of parts of the supposed Galvotas and Barreiros faults.

The writer's main objective in this section is to clarify the nature of the relationship between Domain I and III on the basis of new structural data. He has not found it possible to separate satisfactorily the various fabric elements into earlier ( $D_1$ ) and late ( $D_2$ ) phases.

As an indication of the structural complexity and the intensity of deformation, the units (see Geologic Map). For purposes of this study, Domain III can be subdivided further into three subdomains on the basis of relative structural homogeneity (see Fig. 71).

1. The "Wedge-shaped subdomain" contains the complex cataclastic interdigitations and represents the structurally and geographically basal rocks. The interdigitated zone can be called a "tectonic melange" (Greenly, 1919, in Rocks and others, 1976).

Fig. 70 DOMAIN II - Orientation diagram, equal area net. S-pole to bedding in quartzite and silver sericite schist of the Piracicaba Formation from Miguelao dam. Contours, 14%, 12%, 10%, 8%, 6%, 4%, 2% per 1% area. Maximum 15%. 126 points.

structurally low melange and the structurally uppermost

proposed that the main structural relationship is that of a sinuous, thrust surface where the Moeda syncline abuts the Curral homocline. He proposed that the connection between the Mutuca Fault and a supposed Gaivotas Fault was made through a contorted plane. Dorr (1969, p. 89) proposed the structure at this junction to be a single thrust fault consisting of parts of the supposed Gaivotas and Barreiro faults.

The writer's main objective in this section is to clarify the nature of the relationship between Domains I and III on the basis of new structural data. He has not found it possible to separate satisfactorily the various fabric elements into earlier ( $D_1$ ) and late ( $D_2$ ) phases.

As an indication of the structural complexity and the intensity of deformation, the Nova Lima greenschists and the Moeda clastic rocks, mainly conglomerates, now occur as tectonically interdigitated units (see Geologic Map). For purposes of description, Domain III can be subdivided further into three subdomains on the basis of relative structural homogeneities, and structural complexity (Fig. 71):

1. The W-subdomain (West subdomain), contains the conglomerate-greenschist interdigitations and represents the structurally and stratigraphically basal rocks. The interdigitated zone can be named a "tectonic melange" (Greenly, 1919, in Hobbs and others, 1976).

2. The M-subdomain (Middle subdomain) represents the severely sheared axial or intermediate zone between the structurally low melange and the structurally uppermost

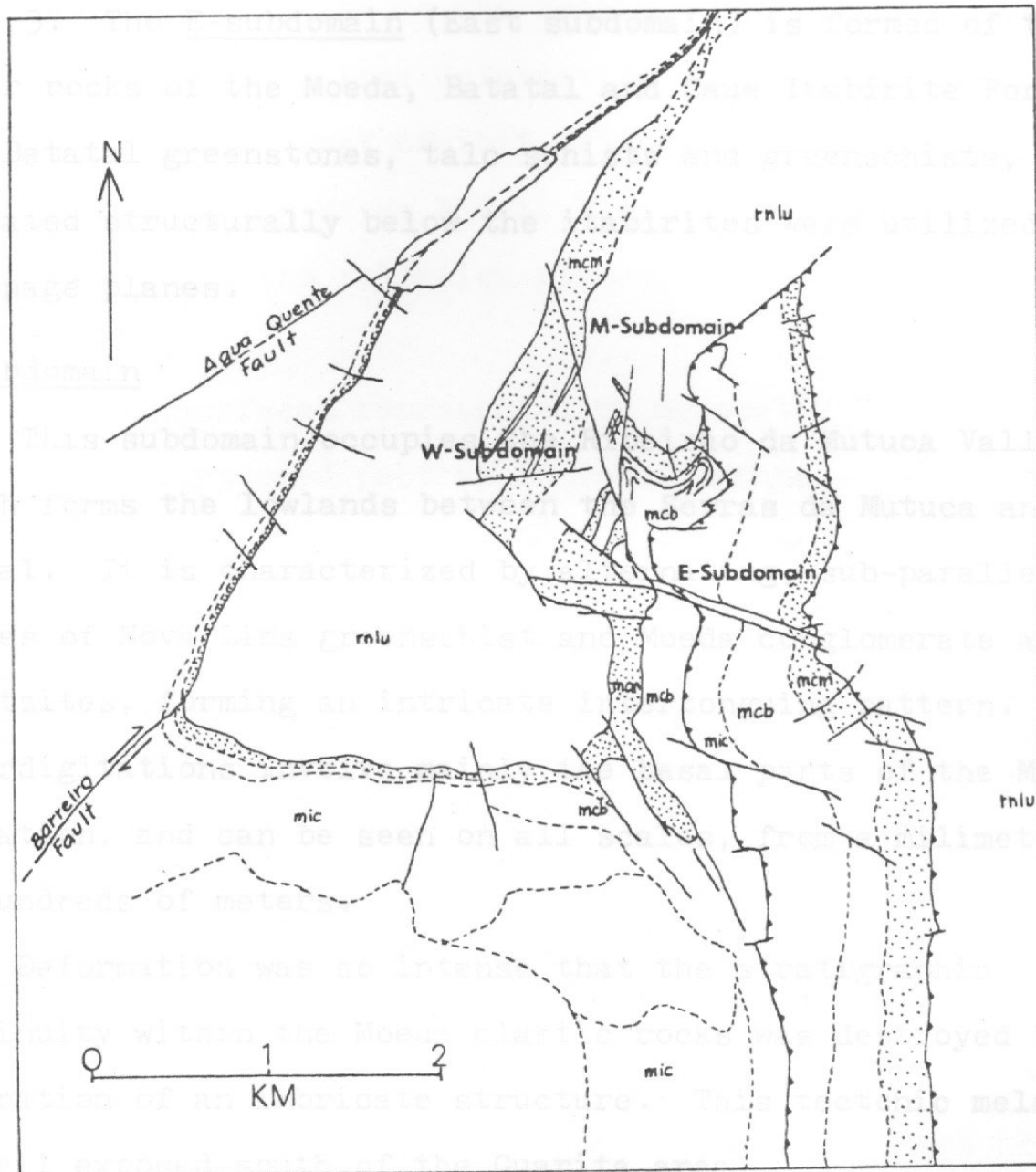


Fig.71 Map showing subdivision of the Domain III (Mutuca area) into structural subdomains, as discussed in the text.  
 mic=Itabirite Caue; mcb=Batatal Formation;  
 mcm=Moeda Formation; rnlu=Nova Lima Group.

E-subdomain. It consists of Batatal greenstones and sericite schist, and of some quartzites and quartz schist presumably of the upper part of the Moeda Formation, at the front of this intermediate zone. The strata exhibit excellent recumbent folds.

3. The E-subdomain (East subdomain) is formed of the cover rocks of the Moeda, Batatal and Caue Itabirite Formations. The Batatal greenstones, talc schists and greenschists, situated structurally below the itabirites were utilized as slippage planes.

#### W-Subdomain

This subdomain occupies the Ribeirao da Mutuca Valley, which forms the lowlands between the Serras da Mutuca and Curral. It is characterized by alternating, sub-parallel slices of Nova Lima greenschist and Moeda conglomerate and quartzites, forming an intricate intertonguing pattern. These interdigitations involve mainly the basal parts of the Moeda Formation, and can be seen on all scales, from a millimeter up to hundreds of meters.

Deformation was so intense that the stratigraphic continuity within the Moeda clastic rocks was destroyed by the generation of an imbricate structure. This tectonic melange is well exposed south of the Guarita area.

#### Mesoscopic Analysis

In the tectonic melange more competent conglomerate and quartzite form phacoids in an incompetent greenschist matrix. These narrow wedges and slices of greenschists are elongated in a north-south direction. This orientation indicates transport



approximately normal to the compression.

The exotic blocks and slices of Moeda conglomerate were forced against and interpenetrated into the greenschist along a dense network of shear planes and conjugate joints that are oriented at low-angles to the bedding and foliation. In the Moeda conglomerate, this deformation is reflected in quartz and chert pebbles that exhibit Y/Z ratios (Ramsay, 1967, p. 210) of 10/1 or 10/2, near km 439 of Highway BR 040. Pebbles are flattened along the foliation planes, and their long-axes dip to the east.

The  $S_1$ -surfaces represented by mylonitic flow zones curve around the flattened pebbles in conglomerates. All evidence of  $S_0$  is gone. Conglomerate bodies, deformed tectonically into lenses, crop out between KM 439 and 441 of Highway BR 040. These small phacoids of talc-schist and greenschist alternate with the conglomerate in a distance of a few meters. Locally a talc-rich matrix surrounds completely the pebbles and cobbles.

Near Guarita, outcrops show an intricate tectonic inter-fingering between 5 to 10m-thick slices of Nova Lima greenschist, Batatal dark sericite schist and coarse-grained quartzite, and narrow lenses of quartz schist and grit of the Moeda Formation (Fig. 72). This relationship suggests that at least locally the melange may involve not only the whole Moeda Formation but also the very basal parts of the Batatal Formation. It should be remembered that in the Mutuca area the Moeda Formation is usually less than 100 m thick, rather than the normal 400 m, and that the thinning is probably due to tectonics.

In the melange, the narrow wedges and phacoids of green-schist show a pronounced north-south elongation at the surface. This orientation suggests transport parallel to the shear, either north-south, or in the plane of the dip.

It is difficult to understand the origin of the melange in detail. Structurally it occupies a position originally between the Curral anticline on the north and northward moving strata on the south. Later, this structural situation was between tear faults on the north and major, overriding thrusts on the east.



Fig. 72. Moeda quartzite (dark, on left) with a slice of Nova Lima greenschist (light). Main contact with Nova Lima is in the rubbly zone, center of photo. Nova Lima schist on right. Note hammer, right center, for scale. Near Guarita.

## Microscopic Analysis

Under the microscope, the thinly interpenetrated quartzite-conglomerate/greenschist melange exhibits the effects of strong deformation: larger quartz grains commonly show pressure solution, stretching and bridging; grains are serrated along the foliation, and between the grains, in a more progressive deformation, the elongated and sliced quartz grains exhibit interfingering and "brick pile" texture with recrystallized muscovite. Most of the grains are strained. The matrix is completely recrystallized, and several stages of polygonization from sparse, armoured relicts to completely recrystallized grains are observed. Schist slices and fragments are flattened and smeared along the foliation. Schists invariably present a cataclastic to mylonitic texture.

## Geometric Analysis

Measurements of  $S_1$  in the Nova Lima greenschists and the Moeda clastic rocks reveal two maxima: 10 percent for an orientation of 12 and dip of 35 degrees to east and 8 percent at 340 dipping 40 degrees to west (Fig. 73). The large, irregular spread of foliation below the 2 percent contour line reflects the structural complexity. The late-stage westward rotation is probably reflected in the north-south orientation.

The lack of preferred orientation, in comparison to all other stereonet is indicative of the special structural conditions in this subdomain. Contour, 10%, 8%, 6%, 4%, 2% per 1% area. Maximum 102. 286 points.

# Barreiro-Agua Quente Faults

The key to understanding the larger scale structure was in the recognition of the Barreiro and Agua Quente faults in the field, and their interpretation as two faults along which the east limb of the Moeda syncline became detached from the Curral anticline.

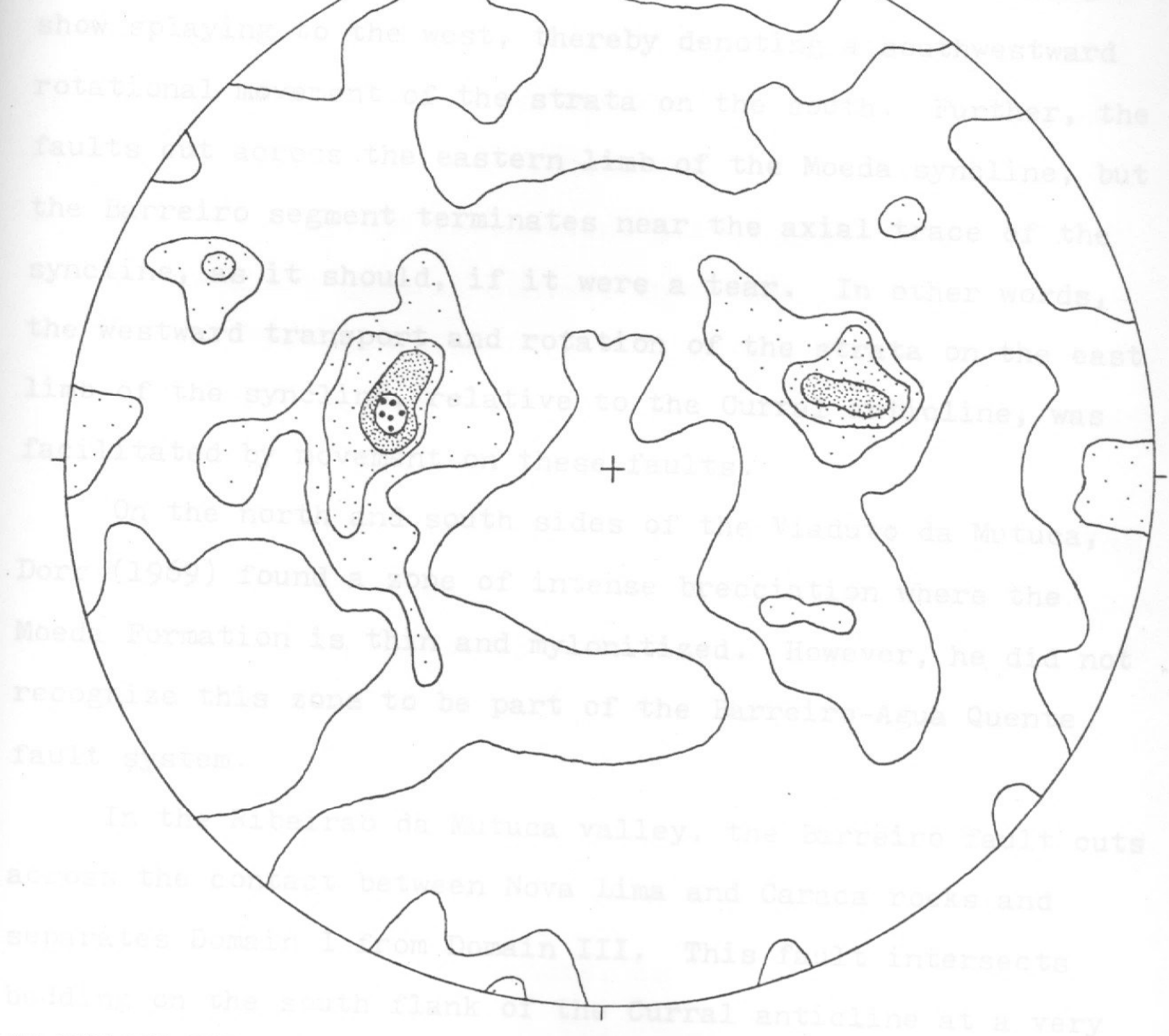


Fig.73 DOMAIN III - Orientation diagram, equal area net. S-pole to foliation (=bedding ?) of the clastic rocks of the Moeda Formation and greenschists of the Nova Lima Group from W-sub domain (Melange area). Contour, 10%,8%,6%,4%,2% per 1% area. Maximum 10%. 288 points.

The rocks are extremely sheared. The Agua Quente is a 30-degree splay off the Barreiro fault.



## Barreiro-Agua Quente Faults

The key to understanding the larger scale structure was in the recognition of the Barreiro and Agua Quente faults in the field, and their interpretation as tear faults along which the east limb of the Moeda syncline became detached from the Curral anticline. It is important to note that the faults show splaying to the west, thereby denoting a southwestward rotational movement of the strata on the south. Further, the faults cut across the eastern limb of the Moeda syncline, but the Barreiro segment terminates near the axial trace of the syncline, as it should, if it were a tear. In other words, the westward transport and rotation of the strata on the east limb of the syncline, relative to the Curral anticline, was facilitated by movement on these faults.

On the north and south sides of the Viaduto da Mutuca, Dorr (1969) found a zone of intense brecciation where the Moeda Formation is thin and mylonitized. However, he did not recognize this zone to be part of the Barreiro-Agua Quente fault system.

In the Ribeirao da Mutuca valley, the Barreiro fault cuts across the contact between Nova Lima and Caraca rocks and separates Domain I from Domain III. This fault intersects bedding on the south flank of the Curral anticline at a very slight angle, and exhibits comminuted rock, breccia, and chevron zones. Where Nova Lima greenschist is displaced southwestward, the rocks along the fault zone are extremely sheared. The Agua Quente is a 30-degree splay off the Barreiro fault.

### M-Subdomain

The M-subdomain comprises the elongate area covered by the Mutuca thrust fault and fold zone and lies between W-subdomain (Ribeirao da Mutuca area) and the E-subdomain (Serra da Mutuca and Mutuca mine). The Mutuca fault was recognized by Pomerene (1964) along the Serra da Mutuca and Feixos area along a distance of about 7.5 km. The fault has been traced for another 4 km to south to Tamandua by the present writer. The position of the Mutuca thrust fault (Figs. 74 and Map 2) was controlled by the incompetent lithologies in the Batatal schists, and the general contact in anisotropy between these schists and the itabirite (Roberts, 1972).

The complexity of the structure is indicated by duplication of the Batatal Formation into parallel belts trending north-south on both sides of the Mutuca mine (Figs. 71 and 74), the overturning of the stratigraphy to the east of Serra da Mutuca, and the duplication at Serra do Tamandua of the Batatal and Caue Itabirite Formations (Fig. 62, structural map).

#### Structural Complexity Below the Mutuca Thrust Fault

In the western part of the Mutuca thrust fault, near Guarita, the recumbent fold (Fig. 75) located in the northern or frontal part of the structure, is structurally situated underneath the Mutuca fault. The upper limb of the fold, in Moeda quartzite, is shown in Fig. 75. In the field one can note that its fold axis is oriented almost east-west, indicating northward transport. The axial plane of the recumbent fold, which is almost horizontal increases in dip to the east as it

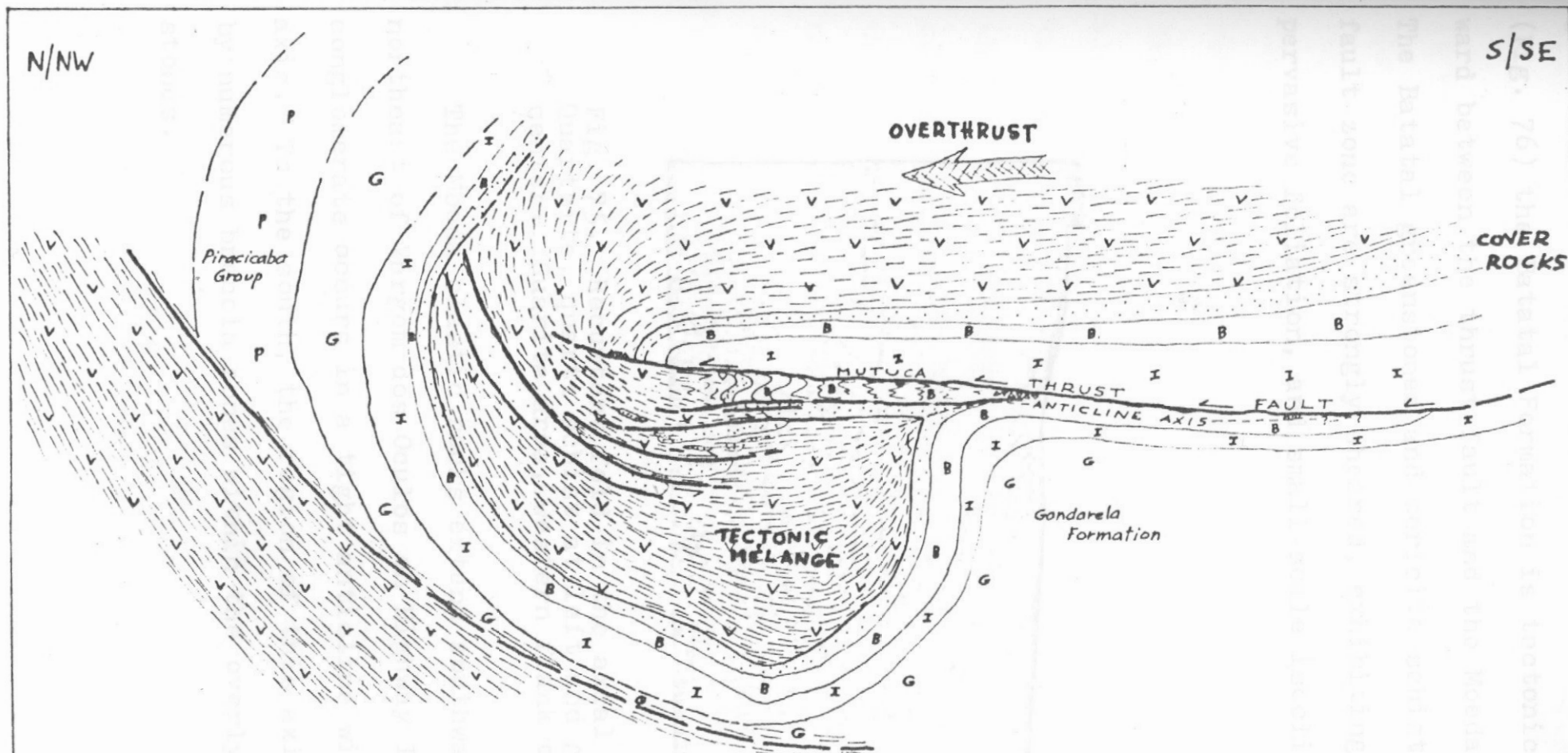
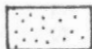
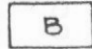
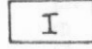
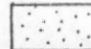

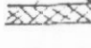
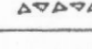


Fig. 74. DOMAIN III - Deformational Picture of the Mutuca overthrust view down plunge.

COVER ROCKS

- |   |                              |   |                   |
|---|------------------------------|---|-------------------|
|  | QUARTZITE, GRIT CONGLOMERATE | — | MOEDA FORMATION   |
|  | GREENSTONES, SERICITE SCHIST | — | BATATAL FORMATION |
|  | ITABIRITE, HEMATITE ORE      | — | CAVE ITABIRITE    |

MÉLANGE

- |   |                               |   |                                 |
|---|-------------------------------|---|---------------------------------|
|  | QUARTZITE, GRIT, CONGLOMERATE | — | MOEDA FORMATION (EXOTIC SLICES) |
|  | GREENSCHISTS                  | — | NOVA LIMA GROUP                 |
|  | TRANSPORT DIRECTION           |   |                                 |
|  | BRECCIA                       |   |                                 |

gets closer to the thrust fault zone. Near the Mutuca mine (Fig. 76) the Batatal Formation is tectonically thinned northward between the thrust fault and the Moeda clastic rocks. The Batatal greenstones and sericite schist along the thrust fault zone are strongly sheared, exhibiting a characteristic pervasive foliation, and small-scale isoclinal folds.



Fig. 75. Recumbent fold in the axial zone, M-subdomain. Quartzite, quartz schist at left and greenschist at center. Guarita area, western flank of Serra da Mutuca.

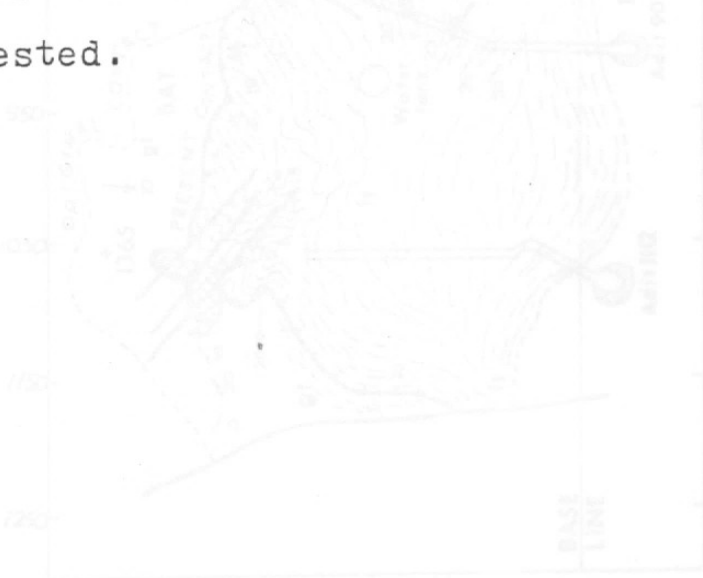
The Moeda clastic rocks extend southward to about 2 km northeast of Vargem dos Oculos on Highway BR 040. Here, the conglomerate occurs in a tight anticline with a vertical plunging axis. To the south, the region of this axial plane is occupied by numerous breccia zones within the overlying Batatal greenstones.



## Structural Situation Along the Mutuca Thrust Fault

In the Mutuca mine the surface of the Mutuca thrust fault is very irregular and contorted on the mesoscopic scale. In the north, between sections +150 and -50 at Mutuca mine (Fig. 76), it is steep. Along the fault zone, totally exposed at Mutuca mine, mesoscopic recumbent, disharmonic and cascade folds with east-west trending axial planes present fold axes dipping westward and eastward, indicating further deformation along north-south axis. It was possible to determine that the thrust plane dips more steeply at the mine than to the east, where the plane was exposed by mining activities at the base of hematite-rich itabirite lying subhorizontally at the summit of the Mutuca mine, at topographic elevations of 1365 and 1372 m, near sections 100 and 1050 (Figs. 76, 81 and 82). This surface can be traced near section 1050, by the occurrence of Batatal talc schist now exposed in the footwall rocks.

Along the Mutuca thrust fault mesoscopic recumbent folds and subsidiary faults are common (Fig. 77). These structures exhibit east-west trending fold axes, plunging between 20 and 40 degrees to the east. In a few a northward transport is suggested.



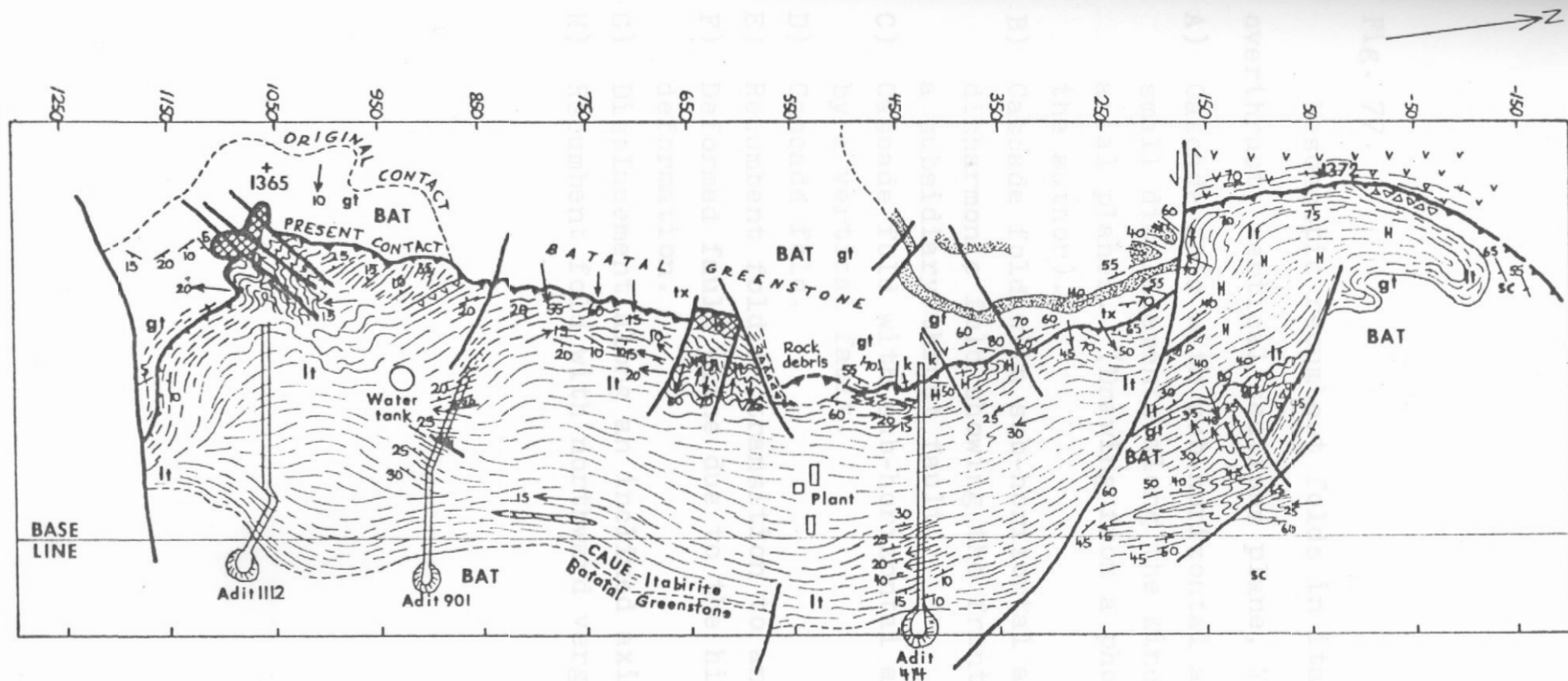




Fig. 76 GEOLOGIC MAP OF THE MUTUCA MINE

0 100 200  
m

- |   |
|---|
| <span style="border: 1px solid black; padding: 2px;">II</span> CAUE ITABIRITE                                 |
| <span style="border: 1px solid black; padding: 2px;">BAT</span> BATATAL FORMATION                             |
| gt=Greenstone   |
| tx=talc schist  |
| sc=sericite schist  |
|  =dolomite lenses at depth |

- |   |
|---|
|  MOEDA FORMATION |
| <span style="border: 1px solid black; padding: 2px;">v v v</span> NOVA LIMA GROUP                   |

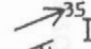
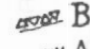

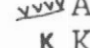
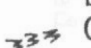

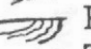



- |   |  |
|---|--|
|  Lineation           |  Breccia zone     |
|  Attitude of bedding |  Amphibolite      |
|  Chevron fold        |  Kaolinite        |
|  Parasitic fold      |  Compact hematite |
|  Thrust fault        |  |
|  Normal, tear fault  |  |

Fig. 77.

Mesosopic recumbent folds in itabirite along the Mutuca overthrust, vertical sections plane, Mutuca mine.

- A) Cascade fold with sub-horizontal axial planes. Note small displacements along the kinematically active axial planes. (Drawing from a photograph taken by the author).
- B) Cascade fold with sub-horizontal axial planes and a disharmonic fold showing the front lobe truncated by a subsidiary thrust fault.
- C) Cascade fold with sub-horizontal axial planes truncated by a vertical fault.
- D) Cascade fold.
- E) Recumbent fold in transition to an imbricate fault.
- F) Deformed fault plane due to the high ductility during deformation.
- G) Displacement along an inclined axial plane.
- H) Recumbent fold with northward vergence.

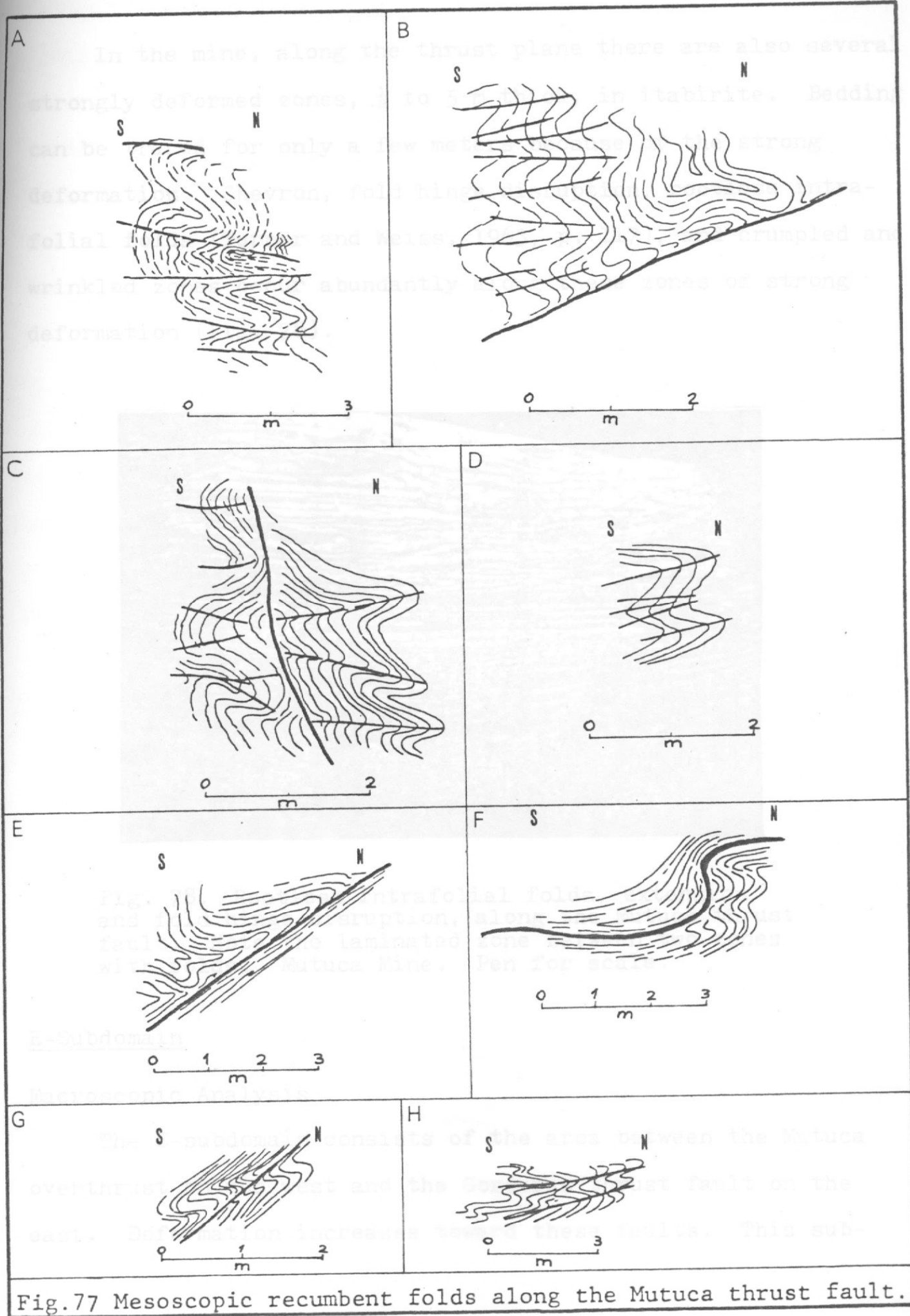


Fig.77 Mesoscopic recumbent folds along the Mutuca thrust fault.



In the mine, along the thrust plane there are also several strongly deformed zones,  $\frac{1}{2}$  to 5 m thick, in itabirite. Bedding can be traced for only a few meters because of the strong deformation. Chevron, fold hinge disruption, rootless intrafolial folds (Turner and Weiss, 1963, p. 117), and crumpled and wrinkled zones occur abundantly along these zones of strong deformation (Fig. 78).

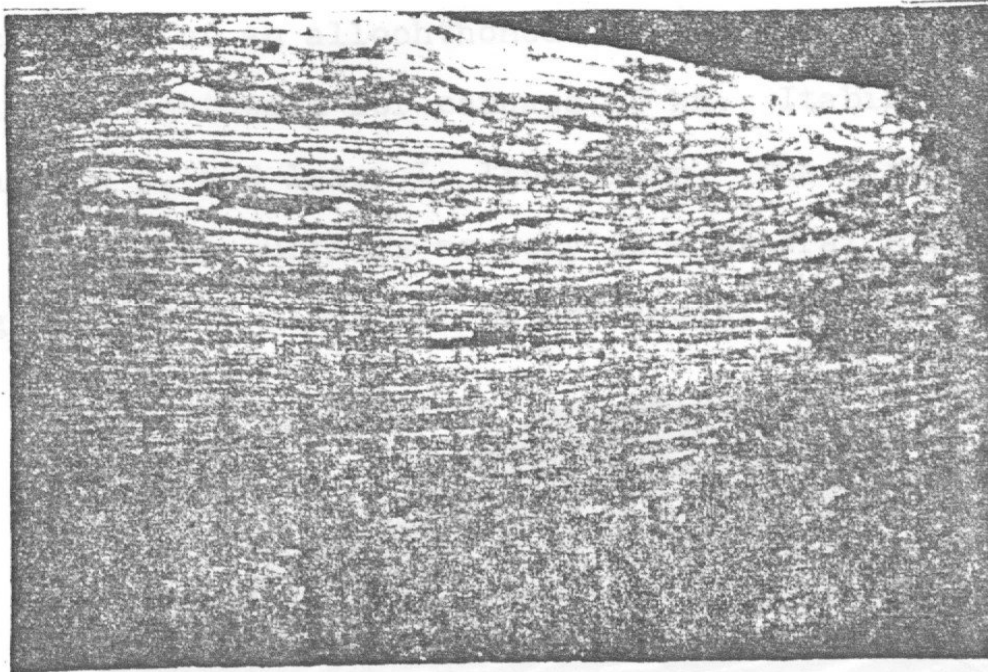


Fig. 78. Rootless intrafolial folds, extension and fold hinge disruption, along the Mutuca thrust fault. Note the laminated zone between two zones with folds. Mutuca Mine. Pen for scale.

### E-Subdomain

#### Macroscopic Analysis

The E-subdomain consists of the area between the Mutuca overthrust on the west and the Gorduras thrust fault on the east. Deformation increases toward these faults. This sub-

domain contains the cover rocks consisting of an overturned sequence, 400 m thick, of Caue Itabirite, Batatal and Moeda Formations, and with the Nova Lima greenschist structurally above the Moeda Formation (Fig. 71). Bedding is present in the itabirite and also within certain Batatal greenstones and Moeda quartzites. The Minas rocks terminate to the north due to structural complexity.

The strata in this subdomain constitutes an overthrust sheet composed of an allochthonous rock segment, transported tectonically northward for perhaps 10 km. Itabirites exhibit both earlier  $L_1$  and later  $L_2$  lineations. The earlier lineation occurs on bedding surfaces as very fine mineral striation or ribbing (Fig. 79), along the Mutuca fault. The structure could

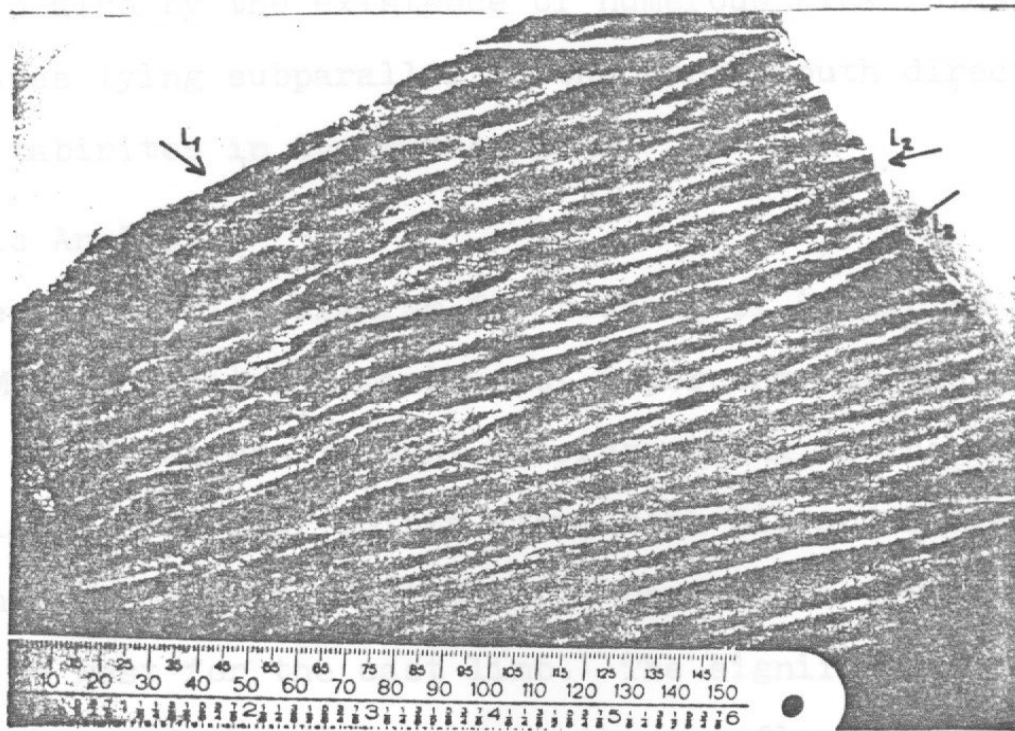


Fig. 79. Sets of  $L_2$ -corrugations deform  $L_1$ -lineation on  $S_0$ -surface of itabirite. Mutuca Mine.

100  
be named more appropriately a parautochthonous nappe because its root or origin can be approximately traced (Hills, 1963, p. 251). Evidence will be presented of both a northward  $D_1$  and a westward  $D_2$  deformation phase.

Refolding relationships can be observed also in a roadcut of the Macacos road, wherein the Batatal dark sericite schist exhibits  $L_1$ -lineation folded by mesoscopic folds with  $B_2$ -axis trending north-south. The plunges of  $L_1$  vary from westerly to easterly, indicative of rotation on a north-south axis (Fig. 80). The younger lineation is a crumple lineation, also on itabirite bedding. This  $L_2$ -lineation plunges up to 50 degrees toward azimuths between 155 and 210, fairly close to that of  $B_2$ . East-west strain, subparallel to the  $B_2$ -fold axes, is indicated also by the existence of numerous kink folds, with kink planes lying subparallel to the north-south direction, in the itabirites in the Mutuca Mine.

#### Geometric Analysis

The orientation diagram for bedding of itabirite in the Mutuca Mine indicates a maximum of 6 percent for the strike 13 and dip of 60 degrees to east, corresponding to the west limb with a large spread of points along both dip and strike (Fig. 81). There is another maximum of 6 percent at 320 dipping 35 degrees to west for the east limb. The significant variations in the values of the dips between the two flanks indicates an asymmetric character for the structure. These surfaces define a  $\beta_2$ -fold axis plunging 25 degrees toward 176 which plot in the

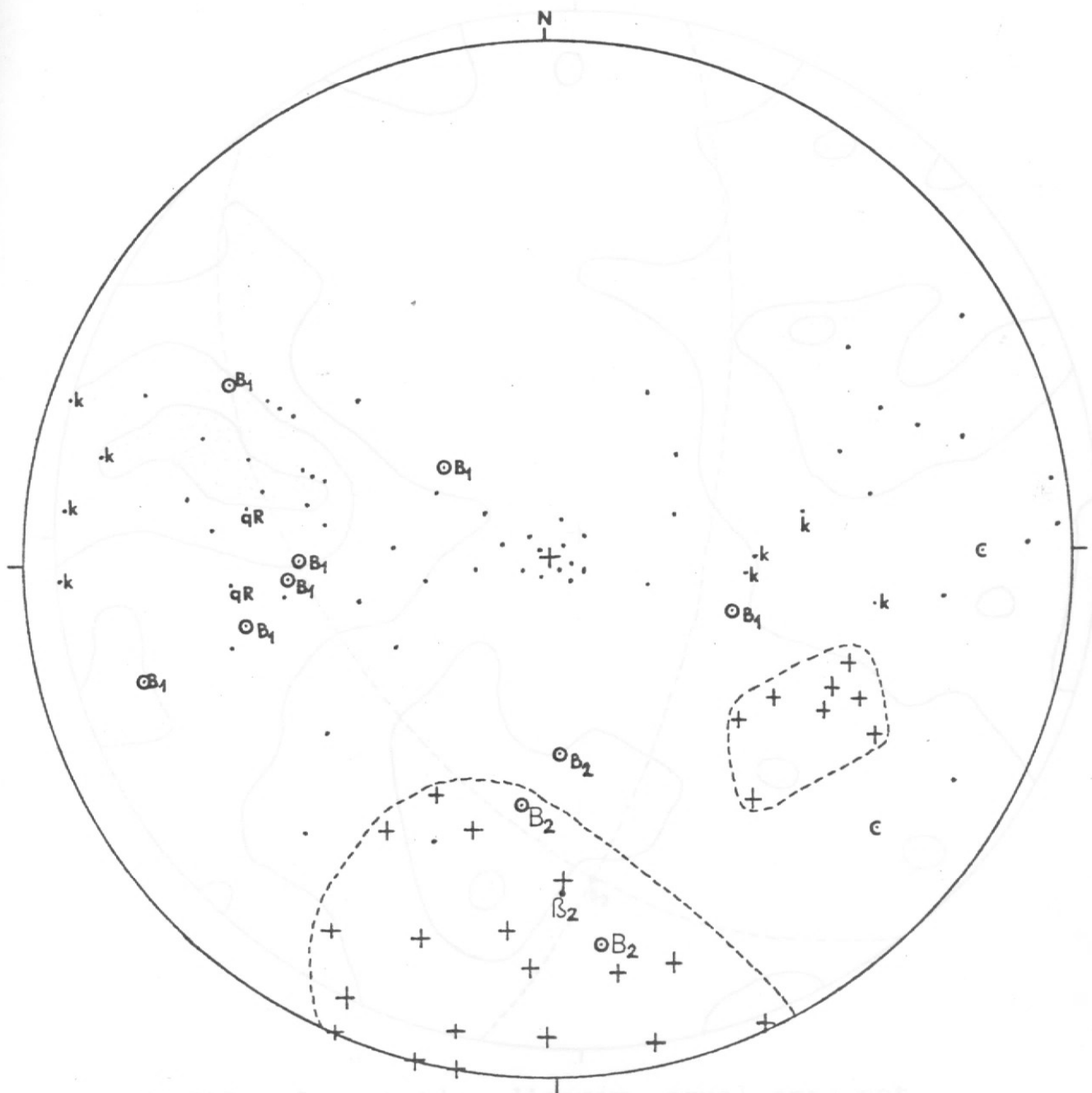


Fig. 81 DOMAIN III - Orientation diagram, equal area net.

Fig. 80 DOMAIN III - Orientation diagram, equal area net.

• 56 L<sub>1</sub>-lineation, • B<sub>1</sub>-fold axis, • qR-quartz rods,  
 • k 8 poles to kink planes, • 2 poles to cleavage,  
 + 17 L<sub>2</sub>-lineation, • B<sub>2</sub>-fold axis, β<sub>2</sub>-Beta axis from  
 Fig. 81. Itabirites from Mutuca mine, E-subdomain.





Fig. 81 DOMAIN III - Orientation diagram, equal area net.  
 S-pole to foliation=bedding in itabirites from the  
 Mutuca mine. E-sub domain. Contours 6%, 4%, 2% per 1%.  
 Maximum 6%. 281 points.

field of younger lineations, presumably  $L_2$  (Fig. 81). A younger set of lineations, plunging between 35 and 45 degrees toward 140, intersects the east-west trending lineation and could also be related to the  $L_2$ -set (Fig. 80).

Cross-sections through Sections 100 and 1050 at Mutuca mine show how gentle and undulating the  $S_0$ -surfaces in the east flank of the structure are, and how steep in the west limb (Figs. 82 and 83).

#### Deformation Along the Gorduras Thrust Fault

The Gorduras thrust fault, probably active during both  $D_1$  and  $D_2$  deformational phases, has strongly deformed the quartzite and conglomerates of the Moeda Formation below the thrust, and has brought up the Nova Lima greenschist. Along the fault, the Nova Lima greenschist is crumpled, wrinkled and injected with quartz veins. In the basal conglomerate, pebbles have long axes that plunge down the dip of the beds, the quartzite and quartz schists were deformed along close-spaced, subparallel shear planes dipping to the east. Along these shear planes quartz has recrystallized in a sugary and coarse-grained texture (Fig. 84), forming veins and pockets. Quartz schists exhibit signs of recrystallization in 3 to 4 mm long, elongated quartz knots and ribs, and also in the muscovite that recrystallized in flakes up to 3 mm in diameter.

Fig.82 CROSS SECTION THROUGH SERRA DA MUTUCA  
(near section 1050, Mutuca mine).

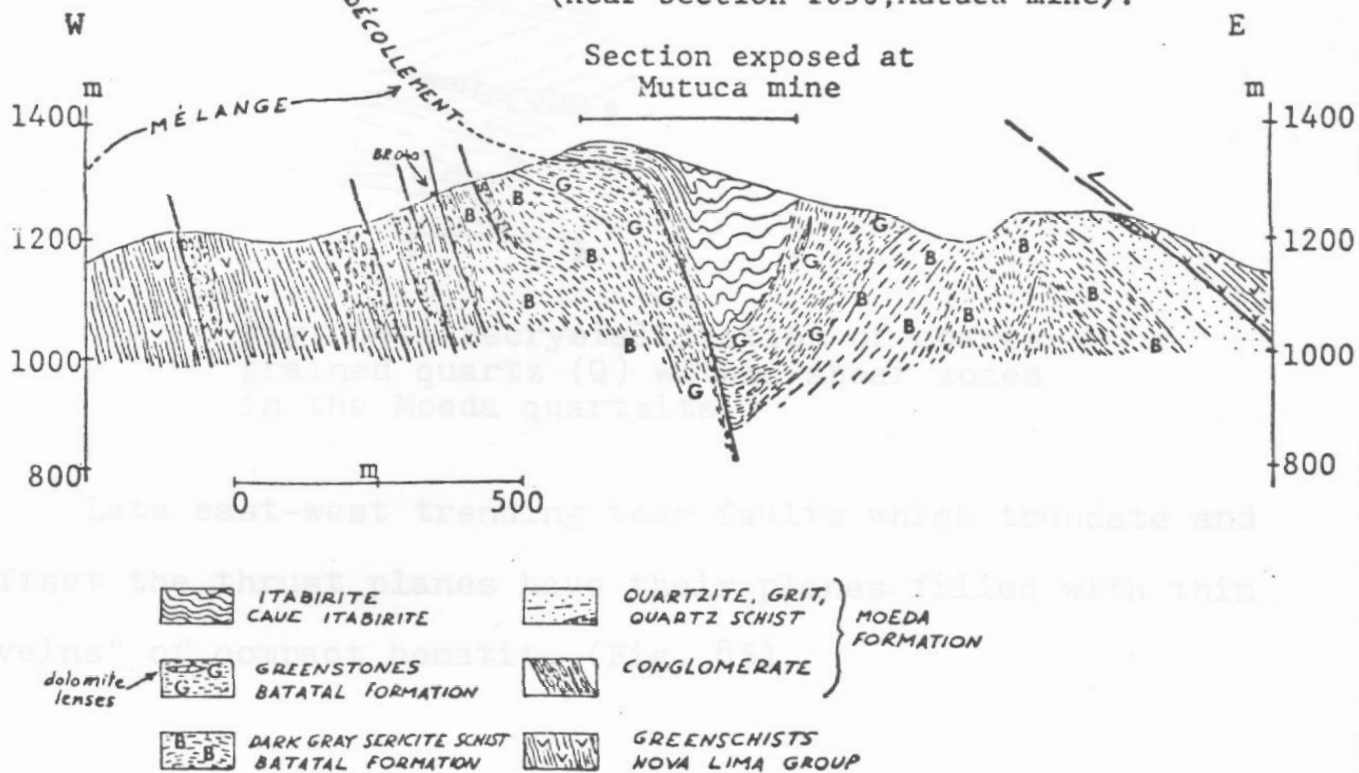
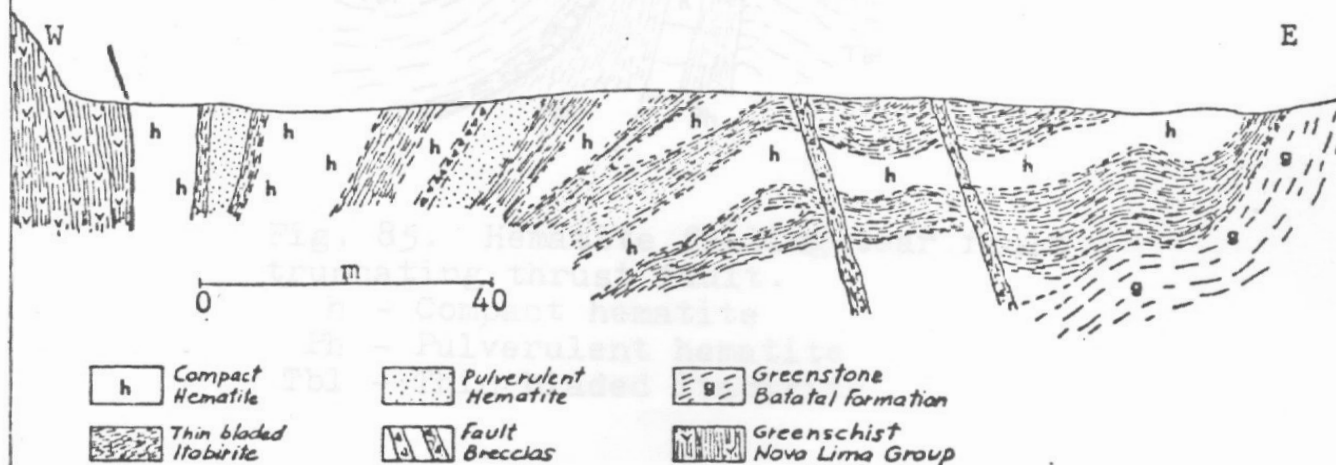


Fig.83 CROSS SECTION THROUGH SECTION 100 - MUTUCA MINE



## DOMAIN IV

### General

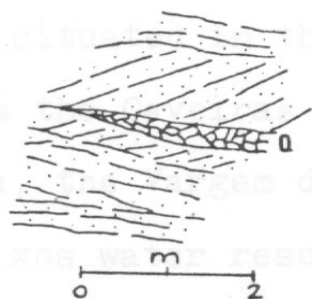


Fig. 84. Recrystallization of coarse-grained quartz (Q) within shear zones in the Moeda quartzite.

Late east-west trending tear faults which truncate and offset the thrust planes have their planes filled with thin "veins" of compact hematite (Fig. 85).

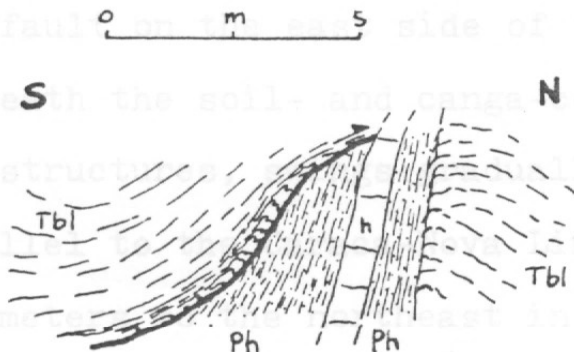


Fig. 85. Hematite filling tear fault truncating thrust fault.

In the west Caveira area a

- h - Compact hematite
- Ph - Pulverulent hematite
- Tbl - Thin bladed itabirite

where the laterite cover is thin and outcrops are better, there are numerous macroscopic and mesoscopic sequences of asymmetric and symmetric folds situated near the core of the overturned Moeda syncline.



## DOMAIN IV

### General

Domain IV is situated in the central part of the study area, and includes the Caveiras area, the northern part of the Serra da Moeda, the Vargem dos Oculos plateau, and the terrain of the Feixos water resource area. It includes the Vargem da Caveira, Morro do Barreiro, and the Capao do Xavier ore deposit zone. Structurally the area lies between the curving north end of the Moeda syncline and the Curral overturned anticline. In this area, Pomerene (1964) supposed the transition from the syncline to the anticline to be made by means of a major thrust fault extending from the eastern flank of the Gaivotas syncline to the western flank of the Mutuca structure. Dorr (1969) proposed an alternative explanation, that the thrust fault on the east side of the Serra das Gaivotas continues underneath the soil- and canga-covered area at the junction of the structures, swings gradually to the northeast, runs nearly parallel to the Caraca-Nova Lima contact, and dies out several kilometers to the northeast in the older rocks. The present writer did not find any evidence for these faults, neither in the field nor during his subsequent map studies.

In the western and eastern parts of Domain IV, on the Caveira area and Vargem dos Oculos plateau, where the laterite cover is thin and outcrops are better, there are numerous macroscopic and mesoscopic sequences of asymmetric and symmetric folds situated near the core of the overturned Moeda syncline.

175  
As noted by Pomerene (1964), some of these folds have their B-axes approximately perpendicular to the Moeda syncline.

### Caveiras Anticline

The Caveiras anticline, in itabirites, is folded on an easterly axis, more nearly parallel to the Curral anticline than to the Moeda syncline. For this reason it is considered to be related to the  $D_1$ -episode. The writer considers it to represent a subsidiary fold related to a northerly-directed stress. The north limb of the Caveiras anticline shows two maxima of 12 percent, defining strikes of 20 and dip of 50 degrees to west, and 68 dipping 35 degrees to northwest; there is another cluster of 10 percent at 277 dipping 50 degrees to north. The south limb has one maximum of 12 percent at 70 dipping 35 degrees to south, and another cluster of 10 percent at 45 and dip of 50 degrees to southeast. The two limbs define a  $\beta$ -axis plunging 10 degrees toward 68 (Fig. 86). The two pairs of maxima with dips of about 35 degrees and 45 degrees, and a slight change in strike suggest some rotation from the fold axis, perhaps during the  $D_2$ -event, or due to differential intensity of relative movement along the Caue itabirite-Gandarela contact.

### Barreiro Structure

The Barreiro area occurs very close to the Barreiro fault, and the complexity of the structure may be a reflection of its tectonic position. The structure involves itabirites at the surface. A geometrical analysis of  $S_0$ -surfaces of these

*S-pole to bedding in itabirites from the Caveiras anticline.  
212 points. The two limbs are clearly depicted.*

itabirites (Fig. 87) indicates several maxima: 12 percent at 330 dipping 70 degrees to west, 8 percent at 85 dipping 50 degrees to south, 8 percent at 20 dipping 45 degrees to south-east, and 8 percent at 337 and dip of 70 degrees to east.

The three maxima of 8 percent probably reflect the gentle curvature of itabirites on the southeast flanks of the Curral anticline. The 12 percent maximum represents the westward dip of the overturned strata on the east side of the Munda syncline. This data is interesting in that it proves that this small subdominant fold is related to both the D<sub>1</sub> and D<sub>2</sub> phases of deformation. A section of the three S-surfaces of 8 percent dipping 45 degrees toward 320 and another dipping 50 degrees toward 330 is parallel to the trend of the Curral anticline.

#### Xavier Structure

The structure in the Xavier area is a complex of numerous hematite folds. The folds are mostly of "lamellar" and "compact" hematite. The numerous hematite grades into brecciated hematite at the limits of the ore deposit. To the north, the zone of brecciated hematitic material is related to the formation of the complex

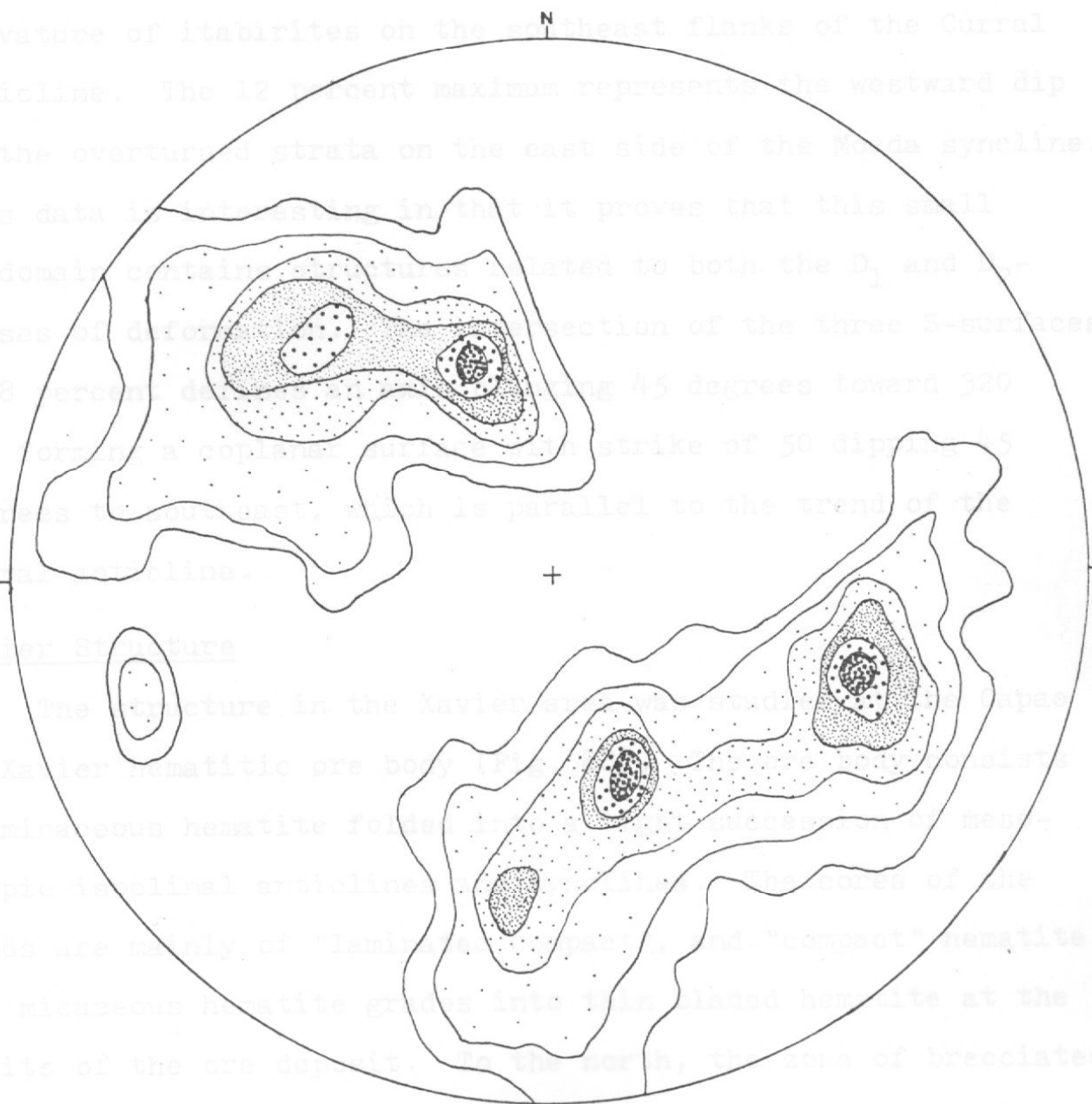


Fig. 86 DOMAIN IV - Orientation diagram, equal area net. S-pole to bedding in itabirites from the Caveiras anticline. Contours 12%, 10%, 8%, 6%, 4%, 2% per 1% area. Maximum 12%. 212 points. The two limbs are clearly depicted.

itabirites (Fig. 87) indicates several maxima: 12 percent at 330 dipping 70 degrees to west, 8 percent at 85 dipping 50 degrees to south, 8 percent at 20 dipping 45 degrees to southeast, and 8 percent at 337 and dip of 70 degrees to east.

The three maxima of 8 percent probably reflect the gentle curvature of itabirites on the southeast flanks of the Curral anticline. The 12 percent maximum represents the westward dip of the overturned strata on the east side of the Moeda syncline. This data is interesting in that it proves that this small subdomain contains structures related to both the  $D_1$  and  $D_2$ -phases of deformation. The intersection of the three S-surfaces of 8 percent defines an axis plunging 45 degrees toward 320 and forming a coplanar surface with strike of 50 dipping 45 degrees to southeast, which is parallel to the trend of the Curral anticline.

#### Xavier Structure

The structure in the Xavier area was studied at the Capao do Xavier hematitic ore body (Fig. 88). The ore body consists of micaceous hematite folded into a tight succession of mesoscopic isoclinal anticlines and synclines. The cores of the folds are mainly of "laminated compact", and "compact" hematite. The micaceous hematite grades into thin bladed hematite at the limits of the ore deposit. To the north, the zone of brecciated hematitic material is related to the formation of the complex overturned structure in Domain III, which developed around a core of Nova Lima rocks.



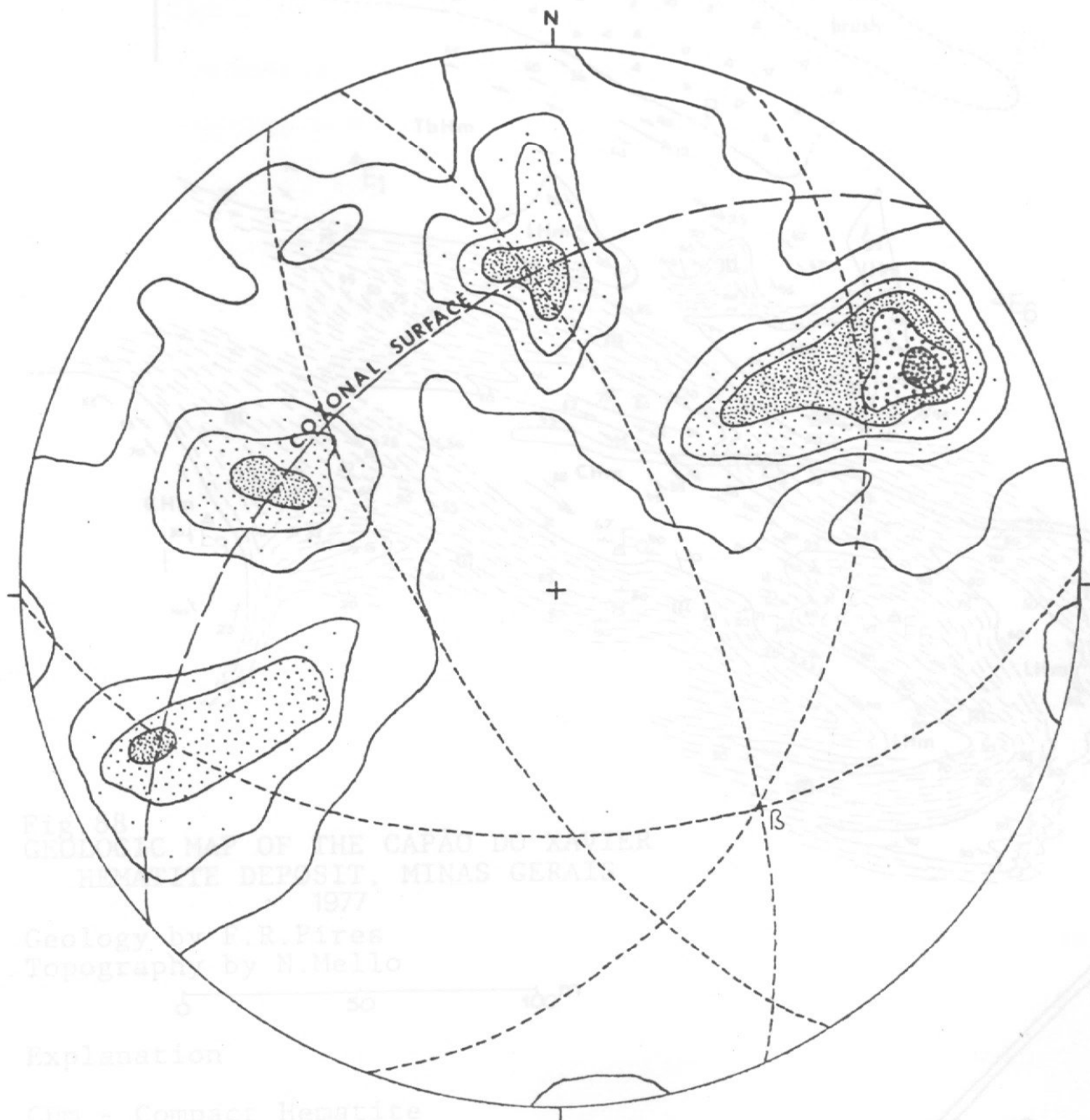


Fig.87 DOMAIN IV - Orientation diagram, equal area net.  
 S-pole to bedding in itabirites at Morro do Barreiro.  
 Contours on 12%, 10%, 8%, 6%, 4%, 2% per 1% area. Maximum  
 12%. 381 points.

- Explanation
- Ch - Compact hematite
  - Lch - Laminated compact hematite
  - - Attitude of vertical beds
  - - Parasitic folds
  - - Plunging fold axis
  - - Chevron fold
  - - Survey station
  - - Bench



Structurally the ore body shows a strong northwest-southeast orientation, expressed by a strong foliation in the micaceous hematite and in the orientation of fold axes. From megascopic field considerations, the major structure of the ore body is probably not that of a folded lens of compact and laminated hematite enclosed in micaceous hematite. Instead these hematites may represent an earlier infolding of compact and laminated hematite with micaceous hematite on an approximate east-west axis, followed by a cross folding of the sequence on an almost parallel axis. Thus the curved southeast end of the compact-laminated hematite zone may be such a refolded fold.

From a geometric analysis, a point maximum of 12 percent for a strike with preferred orientation 302 dipping 32 degrees to southwest on the north flank of the structure, and a cluster oriented 320 and dip of 45 degrees to northeast, with 8 percent appears to represent the two limbs of a major syncline (Fig. 89). These clusters define a  $\beta$ -axis oriented 312 with an almost horizontal plunge. The girdle around the  $\beta$ -axis reflects considerable variations in dips.

Most fold lineations and mesoscopic fold axes are oriented 305. Some fold lineations oriented with azimuths from 10 to 30 have very steep plunges. The 310-oriented folds have been affected clearly by a younger set of fold lineations oriented 330 to 10 (Fig. 90).

Fig. 89 DOMAIN IV - Orientation diagram, equal area net.  
S-pole to foliation in micaceous and laminated hematite from  
Capac do Xavier iron ore deposit. Contour, 12%, 10%, 8%, 6%, 4%,  
2% per 1% area. Maximum 12%. 299 points.



Fig.89 DOMAIN IV - Orientation diagram, equal area net.  
S-pole to foliation in micaceous and laminated hematite from  
Capao do Xavier iron ore deposit. Contour, 12%,10%,8%,6%,4%,  
2% per 1% area. Maximum 12%. 299 points.



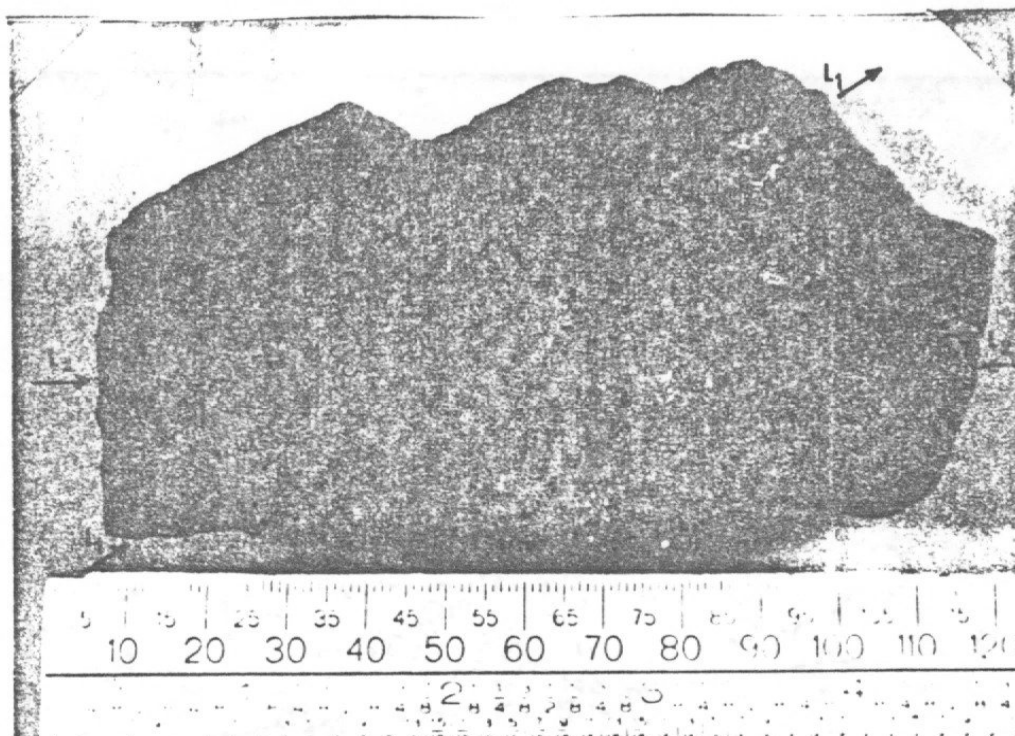


Fig. 90. Fold in itabirite, with the axis oriented horizontal ( $L_2$ ). The hinge zone of the fold is crossed diagonally by earlier fold corrugations ( $L_1$ ), producing a spiral pattern. Xavier ore deposit.

#### Limit Zone Between Domain III and Domain IV

This limit zone is marked by the strongly deformed contact zone between the Nova Lima greenschists and the Minas rocks. Deformation along the lithologic contacts produced different effects in the rocks, according to the competence of the rocks, and the relative sense and intensities of movements. The Moeda quartzite and conglomerate were so severely deformed that quartz pebbles are black due to internal strain, and quartzite formed a strong penetrative foliation which constitutes small plates in the more siliceous beds. Along the contact, the Nova Lima greenschist moved relatively to the east, transporting the stratigraphically lower beds of Moeda quartzite in the process, as shown in the quartz-filled tension gashes (Fig. 91).



Fig. 91. Quartz-filled tension gashes exhibit relative sense of movements. Contact zone Moeda quartzite - Nova Lima greenschist. North of Xavier. Pencil for scale.

At the contact between the Moeda and Batatal Formations the upper, quartz schist moved eastward also, as shown in the mesoscopic parasitic folds. It should be noted that westward thinning of the Moeda Formation in that region could be attributed, in part, to these internal relative movements.

The Batatal greenstones at the contact with the Caue itabirite is strongly brecciated (Fig. 92); these breccias are exposed for 250 m along the contact, being about 10 m thick, and composed of small fragments of a weathered basic rock.

In this domain the different mesoscopic and microscopic mechanical behavior between the two flanks of the Moeda structure

is noteworthy. On the eastern limb, extension has occurred as a result of the differential internal movement of the lithological units, producing a general thinning. On the western flank, there has been shortening and thickening by folding, as demonstrated by the deformed contact between the itabirite and Gardarela formations, and by the existence of numerous mesoscopic anticlines, e.g., the Caveiras anticline.

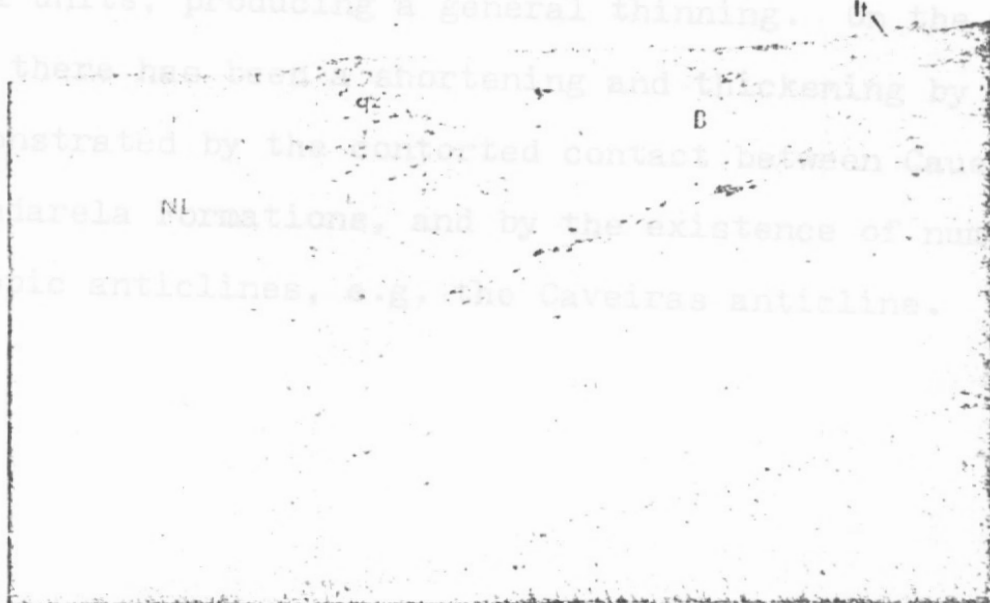


Fig. 92. Contact zone between the Nova Lima (NL) greenschist and Moeda quartzite (qz). The breccia zone in the Batatal greenstone is also shown at the right of the letter (B). It = itabirite. North of Xavier ore deposit.

The itabirites northeast of Xavier moved relatively to the west along the contact with the Batatal greenstones, which have moved eastward, north of the Xavier ore deposit. This fact might explain the thickening of the Batatal Formation to the east of the Xavier area. The hematitic itabirite at the contact with the Batatal Formation is strongly brecciated. Part of this breccia zone is shown in the geologic map of the Xavier ore deposit (Fig. 88).

#### Concluding Remarks

In this Domain the different mesoscopic and microscopic mechanical behavior between the two flanks of the Moeda structure

is noteworthy. On the eastern limb, extension has occurred as a result of the differential internal movement of the lithological units, producing a general thinning. On the western flank, there has been a shortening and thickening by folding, as demonstrated by the contorted contact between Caue itabirite and Gandarela Formations, and by the existence of numerous mesoscopic anticlines, e.g. the Caveiras anticline.

indicated by the predominance of sericite and chlorite schists. These rocks exhibit the following metamorphic features most characteristic of a strong dynamic component during metamorphism:

1. Development of a strong foliation through the growth of tabular or lamellar minerals, such as micaceous minerals and talc.

2. Increase in the grain size of quartz in itabirites, in response to greater strain, as well as the formation of micaceous hematite, talc and amphiboles.

An extensive growth of quartz and muscovite in the sediments and of chlorite in the mafic and ultramafic greenstones seems to have occurred during the  $D_1$ -deformational phase of tectonism. By contrast, the second deformational phase ( $D_2$ ) was one of lateral compression of the recumbent folds against the Bonfim dome. The western basal contact of the Moeda clastic rocks against the basement is marked by mylonite and kyanite (Guild, 1957), the latter indicative of high pressures during tectonism. For example, the Rio do Peixe and Saboeiro thrust faults are also  $D_2$  and are associated with kyanite wherever they cut across Piracicaba aluminous schists. In the São Juliao Quadrangle,



## METAMORPHISM

Although the older rocks around the Quadrilatero Ferrifero have undergone five major thermal events related to metamorphism, deformation and granite generation (Guimaraes, 1958; Amaral and others, 1966; Herz, 1970, 1978), in the study area the Minas rocks have undergone only regional low-grade metamorphism as indicated by the predominance of sericite and chlorite schists. These rocks exhibit the following metamorphic features most characteristic of a strong dynamic component during metamorphism:

1. Development of a strong foliation through the growth of tabular or lamellae minerals, such as micaceous minerals and talc.

2. Increase in the grain size of quartz in itabirites, in response to greater strain, as well as the formation of micaceous hematite, talc and amphiboles.

An extensive growth of quartz and muscovite in the sediments and of chlorite in the mafic and ultramafic greenstones seems to have occurred during the  $D_1$ -deformational phase of tectonism. By contrast, the second deformational phase ( $D_2$ ) was one of lateral compression of the recumbent folds against the Bonfim dome. The western basal contact of the Moeda clastic rocks against the basement is marked by mylonite and kyanite (Guild, 1957), the latter indicative of high pressures during tectonism. For example, the Rio do Peixe and Saboeiro thrust faults are also  $D_2$  and are associated with kyanite wherever they cut across Piracicaba aluminous schists. In the Sao Juliao Quadrangle,

where this late westward tectonic transport was the predominant tectonic feature (Guild, 1957), kyanite is common along the fault zones, again strongly relating kyanite development to the late thrusting.

In the following pages the writer will confine his comments on metamorphic effects to: 1) itabirites; 2) per-aluminous potassic schists of the Batatal Formation and Piracicaba Group; and 3) greenstones of the Batatal and Gandarela Formations.

#### ITABIRITES

James (1955) suggested that one can use the variation in grain size of recrystallized cherts of iron formations as an index of metamorphic grade. Whereas the relationships may be direct in thermally metamorphosed cherts they are far from simple in the more complexly metamorphic rocks in the present area. Nevertheless, the data in Fig. 93 leads to the following observations:

1. In some localities quartz shows either a large range in grain size, or a bimodal distribution between matrix and recrystallized grains. This fact leads the writer to propose that much of the increase in grain size must be an indicator of the dynamic and kinematic conditions (Spry, 1976) which prevailed in that particular area. Spry (1976) pointed out that slight heating or even faulting is apparently sufficient to provide the required activation energy for recrystallization of cherts. Therefore, the grain size variations suggest that the temperatures may have been rather constant during metamorphism throughout the area, but that strain rates varied.

Fig. 93 METAMORPHIC GRADE OF ITABIRITES BY QUARTZ GRAIN-SIZE,  
AS USED IN CLASSIFICATION OF MICHIGAN IRON-FORMATION

Michigan iron-formation metamorphic facies (James, 1955)				Low Grade		Medium Grade		High Grade
				Chlorite zone	Biotite zone	Garnet zone	Staurolite zone	Sillimanite zone
Quartz grain-size(mm)				0	0.05	0.1	0.15	0.2
Cave itabirite								
Type	No.	Rock location and mineralogy		Grain Sizes (mm)				
				0	0.1	0.2	0.3	
Hematitic Itabirite	304	Capão do Xavier	Q H	—	—	—		
	283	Barreiro	Q H	—	—			
	287	Mutuca mine	Q H	—	—	—		
	T-31	W-Tamandua'	Q H	—	—			
	T-44	E-Tamandua'	Q H T	—	—	—		
Riebeckitic Itabirite	163	Barreiro— Agua Quente	Qm Qr M R G C A	—	—	—		
	162A	Barreiro— Agua Quente	Q M G	—	—	—		
	162B	Barreiro— Agua Quente	Q M G	—	—	—		
	162C	Barreiro— Agua Quente	Q M	—	—	—		
	128A	Barreiro	Q M	—	—	—		
	128B	Barreiro	Q M	—	—	—		
Magnetite Itabirite	314	Barreiro	Q M	—	—	—		
	300	Morro do Chapéu	Q M	—	—	—		
	T-29	W-Tamandua'	Q M	—	—	—		

See Fig. 20 for sample location

Q=quartz; H=hematite; Qm=quartz matrix; Qr=quartz rods  
C=carbonate; M=magnetite; R=riebeckite; G=grunerite;  
T=taalc; A=apatite.

2. The occurrence of riebeckite and grunerite, and the relative coarser grain size of quartz in the severely sheared Barreiro-Agua Quente area point to a medium-grade of metamorphism. Riebeckite can occur under a wide range of metamorphic conditions, but always above the greenschist grade (Ernst, 1960, 1968), and grunerite is relatively common in medium-grade rocks (Miyashiro, 1973). The presence of those minerals suggest that the grade of metamorphism must be above the greenschist grade in this subdomain explaining the coarser grain size of quartz.

3. The Mutuca overthrust sheet, where strong deformation occurred, is marked by coarse grain size of both quartz and hematite. Quartz-specularite veins, with large hematite crystals, appear to have accompanied the development of this large overthrust.

4. In the western part of the Tamandua ore deposit, the rocks are less deformed and the grain size of quartz is finer (Fig. 71, samples T-29, T-31 and 300) than the eastern part (Fig. 71, T-144). There the itabirite contains talc, and hence may have been more ductile. If so, this might explain this difference in grain size.

5. At the north flank of the Serra do Curral-Barreiro, the grain size of the magnetite itabirite is very fine, commonly less than 0.05 mm, characteristic of the chlorite zone (Winkler, 1976). This conforms to the finding of Herz (1978) that the chlorite isograd may encircle this area. Also, the fine grain size of quartz would suggest a lack of strain.

6. This study demonstrates that grain size measurements may be used as a general indicator of strain.



# PERALUMINOUS POTASSIC SCHISTS

The low metamorphic grade of these peraluminous potassic schists is denoted by the ubiquitous presence of muscovite and quartz with minor phases such as altered albitic feldspar with a graphitic dust, and subordinate tourmaline, zircon, apatite and hematite. The absence of the K-feldspar-sillimanite pair in these rocks denotes temperatures below  $680^{\circ}\text{C}$  (Winkler, 1976).

In the thin lenses of quartzite within the Batatal schist, muscovite has recrystallized extensively among the serrated and embayed quartz grains that have become shattered and stretched along the  $S_0/S_1$  surface. Muscovite recrystallized in bridging zones, apparently as the result of pressure solution from the fine-grained sericite (Spry, 1976).

Compositionally, these aluminous schists cluster mainly around the muscovite area in the AKF-diagram, some being more potassic, four falling within the muscovite-chloritoid-chlorite field, and some being more aluminous.

The absence of paragonite on the basis of XRD runs suggests a low abundance of  $\text{Na}_2\text{O}$  in relation to  $\text{Al}_2\text{O}_3$  and  $\text{K}_2\text{O}$ ;  $\text{Na}_2\text{O}$  possibly may occur within muscovite structure or in the cloudy feldspars. Muscovite grew in the more dynamic environment under higher  $P_{\text{H}_2\text{O}}$  conditions in preference to microcline. Further the absence of microcline in the more potassic types (Fig. 94, samples 325, 262, 168 and MU-22) may be due to the existence of finely disseminated graphite which may have inhibited recrystallization. No chloritoid can be expected in sericite schist (sample 321) within the muscovite-chloritoid-chlorite field for the same reason.

Chloritoid has been found in rocks with moderately higher

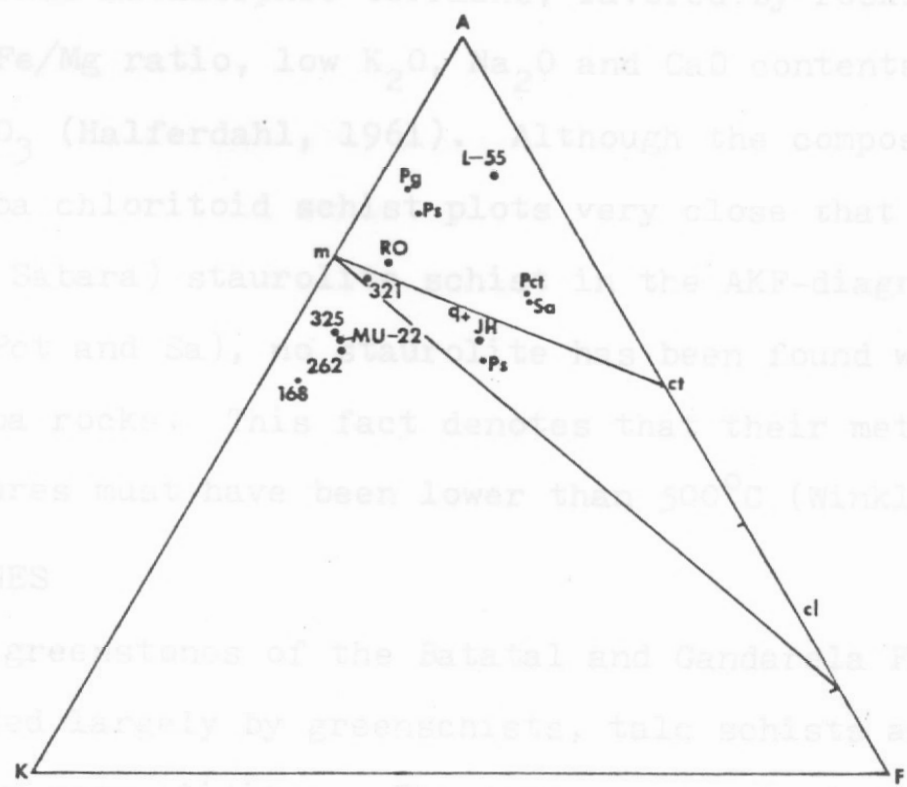


Fig.94 -Low-grade AKF-diagram of rocks of the Batatal Formation and Piracicaba Group.

- Batatal sericite schists: samples 262,321,325 and MU-22 (this work), and RO and JH (from Herz,1978). Sericite chlorite schist: L-55 (this work).
  - Piracicaba rocks: sericite schists: 168 (this work), Ps, Pg(Graphitic phyllite), Pct (chloritoid sericite schist) from Herz, 1978.
  - +Moeda Formation: quartz schist (q);
  - Sabara Formation: staurolite schist (Sa).
- m=muscovite, cl=chlorite, ct=chloritoid.

One type of Gandarela greenstone has a relatively high abundance of MgO, Fe and Al<sub>2</sub>O<sub>3</sub>, and low abundances of alkalis and CaO, giving rise to the formation of Mg-chlorites. Such chlorites are stable under low to high grades of metamorphism. These Mg-rich rocks are interpreted by the writer to represent

iron content and lower  $K_2O$ , in the Moeda plateau near Codornas dam. Although the precise P-T conditions for the formation of chloritoid are unknown (Winkler, 1976), the mineral is common in low-grade metamorphic terrains, favored by rocks exhibiting a large Fe/Mg ratio, low  $K_2O$ ,  $Na_2O$  and  $CaO$  contents, and relatively high  $Al_2O_3$  (Halferdahl, 1961). Although the composition of the Piracicaba chloritoid schist plots very close that of the Nova Lima (or Sabara) staurolite schist in the AKF-diagram (Fig. 94, Samples Pct and Sa), no staurolite has been found within the Piracicaba rocks. This fact denotes that their metamorphic temperatures must have been lower than  $500^{\circ}C$  (Winkler, 1976).

#### GREENSTONES

The greenstones of the Batatal and Gandarela Formations are represented largely by greenschists, talc schists and amphibolites, with minor serpentinites. The common characteristic of the greenstone is the ubiquitous presence of chlorite, magnetite and talc, and in the amphibolites of altered feldspars and mafic minerals. Greenstones, when fresh are light to dark green and strongly foliated, and the amphibolites, despite being weathered exhibit preserved texture with kaolinized plagioclases set in a strongly oriented matrix composed of altered mafic minerals. Some of the Batatal serpentinites were converted to a foliated talc schist, but others, as the ones at Tamandua exhibit a massive texture.

One type of Gandarela greenstone has a relatively high abundance of  $MgO$ , Fe and  $Al_2O_3$ , and low abundances of alkalis and  $CaO$ , giving rise to the formation of Mg-chlorites. Such chlorites are stable under low to high grades of metamorphism. These Mg-rich rocks are interpreted by the writer to represent

serpentinized peridotitic komatiites with aluminous hornblende inclusions, metamorphosed under higher  $P_{H_2O}$  and strong dynamic conditions. The pre-existing peridotite is thought to have been serpentinized and then converted to a silica-deficient talc-chlorite-magnetite assemblage.

These greenstones are thought to be the result of serpentinization and steatitization of an original ultramafic rock, which involved extensive migration of elements. A higher  $fCO_2$  during serpentinization favor outward migration of CaO from the ultramafic. Moderate amounts of  $CO_2$  would convert the ultramafic rock to a talc-magnesite rock (Winkler, 1976); in low  $fCO_2$  condition the reaction between serpentinite and quartz will result in the generation of talc with liberation of water. The original existence of  $Al_2O_3$  implies the formation of chlorite, that together with talc is stable under a wide range of metamorphism. Magnetite remained as one of the initial products of the serpentinization by the breakdown of olivine and perhaps pyroxenes and behaved as rigid porphyroclast during chloritization and formation of stilpnomelane and talc in pressure shadow zones.

This mineral pair was derived from the reaction between oxidized magnetite and chlorite, and some altered plagioclase, perhaps induced by the lower pressure around the rigid, pre-tectonic magnetite octahedra set in the chloritic matrix (Spry, 1976). In the ACF-diagram (Fig. 95) the rocks P-22, 165 and 422 fall within the chlorite-talc-epidote field of low-grade metamorphism, very close to the composition of ideal chlorite, and close to the talc corner. This strongly suggests an ultramafic affiliation for this rock.



## REFERENCES CITED

- Allen, J.R., 1965, A Review of the Origin and Characteristics of Recent Alluvial Sediments: *Sedimentology*, 5, p. 89-191.
- Almeida, P.F.M., 1944, *Colônia Itapevenses sp.m. - Um Fossil Precambriano no Estado de S. Paulo*: Univ. S. Paulo, Faculdade Fil. Ciênc. e Letras. Geol., n.1, p. 89-104.
- \_\_\_\_\_, 1958, *Geografia de Colônia em Dolomitos da Serra Corumbá, M.T.*: *Rev. Geol. e Miner. Mt. Prel. e Est.* No. 106, 11 p. Rio de Janeiro.
- Amaral, G., Cordani, U.G., Kawashita, K., and Reynolds, J.H., 1966, Potassium-argon Dates on Basaltic Rocks from Southern Brazil: *Geochim. et Cosmochim. Acta*, v. 30, p. 159-169.
- Anhaeusser, C.R., 1972, Geological and Geochemical Investigations of the Apuleian Ultramafic Complex and Surrounding Archaean Volcanic Rocks; Krugerdom District: *Inf. Circ. no. 103*. Econ. Geol. Res. Unit, Univ. Witwatersrand. 16 p.
- Bailey, R.W., and Jamieson, H.L., 1973, Proterozoic Iron-Formations of the United States: *Econ. Geol.*, 68, p. 934-959.
- Barbosa, A.L., 1968, *Roteiro de excursão aos arredores de Ouro Preto, Brasil: 22º J. Bras. Geol.*, 1968, Belo Horizonte, Roteiro das Excursões, p. 15-16.
- Barbosa, A.L., 1969, Contribuição à geologia do Estado de Minas Gerais: *Mineração e Metalurgia*, 14, no. 1, p. 3-19.
- \_\_\_\_\_, 1974, Evolution du geosynclinal Espinhaco: *Intern. Geol. Cong., 19th, Algiers 1972, Comptes rendus*, sec. 13, pt. 2, fasc. 14, p. 17-36.
- Baukes, A., 1960-1964, *Geology of Southern Africa*. 4 vols.
- Braiter, R., 1966, *Geology of the Transvaal*. 2 vols.
- Buddington, C.I., 1956, *Metamorphism and Petrology*. New York: McGraw-Hill.
- Burton, A., 1972, Algal Stromatolites of the Early Proterozoic Wolkberg Group, Transvaal Sequence: *Inf. Circ. no. 69*. Econ. Geol. Res. Unit, Univ. Witwatersrand, 9 p.

Fig.95 -Low-grade ACF-diagram of rocks of the Gandarela and Batatal Formations.  
Gandarela rocks: P-22 and SL.  
Batatal rocks: 165 and 422.

P-22: Talc magnetite chlorite schist (minor: albite, stilpnomelane, sphene, apatite and rutile).  
SL: Sitio Largo amphibolite, from Reeves, 1966.  
165 and 422: Talc chlorite schist.  
E=epidote, Cl=chlorite, T=talc, Ac=actinolite.  
Mean value of tholeiites indicated.

# REFERENCES CITED

- Allen, J.R., 1965, A Review of the Origin and Characteristics of Recent Alluvial Sediments: *Sedimentology*, 5, p. 89-191.
- Almeida, F.F.M., 1944, *Collenia itapevensis* sp.m - Um Fossil Precambriano no Estado de S. Paulo: Univ. S. Paulo. Faculdade Fil. Cienc. e Letras. Geol. n.1, p. 89-104.
- \_\_\_\_\_, 1958, Ocorrência de *Collenia* em Dolomitos da Serie Corumba, M.T.: Div. Geol. e Miner. Nt. Prel. e Est. No. 106, 11 p. Rio de Janeiro.
- Amaral, G., Cordani, U.G., Kawashita, K., and Reynolds, J.H., 1966, Potassium-argon Dates of Basaltic Rocks from Southern Brasil: *Geochim. et Cosmochim. Acta*, v. 30, p. 159-189.
- Anhaeusser, C.R., 1976, Geological and Geochemical Investigations of the Roodekrans Ultramafic Complex and Surrounding Archaean Volcanic Rocks; Krugersdorp District: Inf. Circ. no. 103. Econ. Geol. Res. Unit. Univ. Witwatersrand. 16 p.
- Bailey, R.W., and James, H.L., 1973, Precambrian Iron-Formations of the United States: *Econ. Geol.*; v. 68, p. 934-959.
- Barbosa, A.L.M., 1968, Roteiro de excursao nos arredores de Ouro Preto, Brasil: 22nd. Bras. Geol. Cong., Belo Horizonte, Roteiro das Excursoes, p. 15-20.
- Barbosa, O., 1949, Contribuicao a geologia do centro de Minas Gerais: *Mineracao e Metalurgia*, v. 14, no. 79, p. 3-19.
- \_\_\_\_\_, 1954, Evolution du geosyclinal Espinhaco: Intern. Geol. Cong., 19th, Algiers 1952, Comptes rendus, sec. 13, pt. 2, fasc. 14, p. 17-36.
- Beukes, N.J., 1973, Precambrian Iron-Formations of Southern Africa: *Econ. Geol.*, v. 68, p. 960-1004.
- Braitsch, O., 1971, Salt Deposits and Their Origin and Composition: Springer-Verlag, N.Y., (1971), p. 297.
- Buddington, A.F., 1917, Report on the Pyrite and Pyrrhotite Veins in Jefferson and St. Lawrence Counties, N.Y.: New York Defense Council Bull., no. 1, p. 40.
- Button, A., 1972, Algal Stromatolites of the Early Proterozoic Wolkberg Group, Transvaal Sequence: Inf. Circ. no. 69. Econ. Geol. Res. Unit Univ. Witwatersrand, 9 p.

Cannon, W.F. and Simmons, G.C., 1973, Geology of Part of the Southern Complex, Marquette District Michigan: Jour. Research USGS. v. 1, no. 2, p. 165-172.

Carmichael, I.S.E., Turner, F.J., and Verhoogen, J., 1974, Igneous Petrology: McGraw-Hill Book Co.

Chkraborty, K.L., and Taaron, P.B., 1968, Thermal Metamorphism of the Banded Iron-Formation of Orissa, India: Geol. Soc. Am. Bull., v. 79, p. 365-374.

Clarke, F.W., 1924, The Data of Geochemistry: U.S. Geol. Surv., Bull 770.

Dardenne, M.A. and Rocha Campos, M.C., 1975, Estromatolitos colunares na Serie Minas (MG): Rev. Bras. de Geociencia: v.5, no. 2, p. 99-105.

Deer, W.A., Howie, R.A., and Zussman, J., 1971, An Introduction to the Rock-Forming Minerals: J. Wiley & Sons Inc., N.Y., 528 p.

Derby, O.A., 1906, The Serra do Espinhaco: Jour. Geology, v. 14, no. 5, p. 374-401.

de Sitter, L.U., 1964, Structural Geology, 2nd ed., McGraw-Hill, New York, 551 p.

Dorr, J.V.N., 2d., 1958a., The Caue Itabirite: Soc. Bras. Geologia, Bol., v. 7, no. 2, p. 61-62.

\_\_\_\_\_, 1958b., The Gandarela Formation: Soc. Bras. Geologia, Vol., v. 7, no. 2, p. 63-64.

\_\_\_\_\_, 1969, Physiographic stratigraphic and structural development of the Quadrilatero Ferrifero, Minas Gerais, Brasil: U.S. Geol. Survey Prof. Paper 641-A, 110 p.

Dorr, J.V.N., 2d., and Barbosa, A.L.M., 1963, Geology and Ore Deposits of the Itabira District, Minas Gerais, Brazil: U.S. Geol. Survey Prof. Paper 341-C, 110 p.

\* Dorr, J.V.N., 2d., Gair, J.E., Pomerene, J.B., and Rynearson, G.A., 1957, Revisao da estratigrafia Precambriana do Quadrilatero Ferrifero: Brasil, Dept. Nac. Producao Mineral, Div. Fomento Prod. Min., Avulso 81, 31 p.

\* Dorr, J.V.N., 2d., Herz, N., Barbosa, A.L.M., and Simmons, G.C., 1960 - Esboço Geologico do Quadrilatero Ferrifero de Minas Gerais, Brasil (The geology of the Quadrilatero Ferrifero, Minas Gerais, Brasil): Brasil Dept. Nac. Producao Mineral, Pub. Especial 1, 120 p.

- Eade, K.E., and Fahrig, W.F., 1971, Geochemical Evolutionary Trends of Continental Plates - A Preliminary Study of the Canadian Shield: Geol. Survey Can. Bull. 179.
- Ebert, H., 1963, The Manganese-Bearing Lafaiete-Formation As a Guide-Horizon in the Pre-Cambrian of Minas Gerais: Acad. Bras. Cienc. Anais, v. 35, no. 4, p. 545-559.
- Elliot, D., 1972, Deformation Paths in Structural Geology: Geol. Soc. Am. Bull., v. 83, p. 2621-2638.
- Ernst, V.G., 1960, Stability Relations of Magnesioriebeckite: Geochim. et Cosmochim. Acta., 19, p. 10-40.
- \_\_\_\_\_, 1968, Amphiboles, Crystal Chemistry: Phase Relations and Occurrence-Springer-Verlag, N.Y. Inc., 125 p.
- Fleischer, R., and Routhier, P., 1973, The "Consanguineous" Origin of a Tourmaline-Bearing Gold Deposit: Passagem de Mariana (Brasil). Econ. Geol., v. 68, p. 11-22.
- Fleuty, M.J., 1964, The Description of Folds: Geol. Assoc. Proc., 75, Pt. 4, p. 461-489.
- French, B.M., 1973, Mineral Assemblages in Diagenetic and Low-Grade Metamorphic Iron-Formation: Econ. Geol., v. 68, p. 1063-1074.
- Gair, J.E., 1958, The Sabara Formation: Soc. Bras. Geol. Bol., v. 7, no. 2, p. 68-69.
- \_\_\_\_\_, 1962, Geology and Ore Deposits of the Nova Lima and Rio Acima Quadrangles, Minas Gerais, Brasil: U.S. Geol. Survey, Prof. Paper 341-A, 67 p.
- Gair, J.E., and Thaden, R.E., 1968, Geology of the Marquette and Sands Quadrangles, Marquette Country, Michigan: U.S. Geol. Survey, Prof. Paper 397, 770 p.
- Gansser, A., 1964, Geology of the Himalayas: Wiley-Interscience, N.Y., 289 p.
- Garrels, R.M., and Mackenzie, F.T., 1971, Evolution of Sedimentary Rocks: W.W. Norton & Co., N.Y., 397 p.
- Green, J., 1959, Geochemical Table of the Elements for 1959: Geol. Soc. America Bull., v. 70, p. 1127-1183.
- Guild, P.W., 1957, Geology and Mineral Resources of the Congonhas District, Minas Gerais, Brasil: U.S. Geol. Survey, Prof. Paper 290, 90 p.



Guimaraes, D., 1931, Contribuicao a Geologia do Estado de Minas Gerais, Brasil: Sv. Geologia Mineral., Bol. 55, 36 p.

\_\_\_\_\_, 1935, Contribuicao ao estudo da origem dos depositos de ferro e manganês do centro de Minas Gerais: Brasil, Div. Fomento Producao Mineral, Bol. 8, 70 p.

\_\_\_\_\_, 1958, Geologia estratigrafica e economica do Brasil: B. Horizonte, Estab. Graficos Sta. Maria S.A., 450 p.

\_\_\_\_\_, 1964, Geologia do Brasil: Mem. no. 1 - DNPM - DFPM - MME - p. 674.

Halferdahl, L.B., 1961, Chloritoid - its Composition, X-ray and Optical Properties, Stability, and Occurrence: Jour. Petrology, v. 2, p. 49-135.

Harder, E.C., and Chamberlin, R.T., 1915 - The Geology of Central Minas Gerais, Brasil: Jour. Geology, v. 23, no. 4, p. 341-378; no. 5, p. 385-424.

Harder, H., 1961, Einbau von Bor in detritische Tonminerale. Geochim. Cosmochim. Acta. 21, p. 284-294.

\* Herz, N., 1970, Gneissic and Igneous Rocks of the Quadrilatero Ferrifero, Minas Gerais, Brasil: U.S. Geol. Survey, Prof. Paper 641-B, 58 p.

\_\_\_\_\_, 1978, Metamorphic Rocks of the Quadrilatero Ferrifero, Minas Gerais, Brasil: U.S. Geol. Survey, Prof. Paper 641-C.

Higgins, M.W., 1971, Cataclastic Rocks: U.S. Geol. Survey, Prof. Paper, 687, 97 p.

Hills, E.S., 1962, Outlines of Structural Geology: Methuen & Co. Ltd., 182 p.

\_\_\_\_\_, 1963, Elements of Structural Geology: Methuen and Co., London, 483 p.

Hobbs, B.E., Means, W.D., and Williams, P.F., 1976, An Outline of Structural Geology - John Wiley & Sons, Inc., New York, 571 p.

Holland, J.G. and Lambert, R. St. J., 1972, Major Element Chemical Composition of Shields and the Continental Crust: Geochim. et Cosmochim. Acta., v. 36, p. 673-683.

217

Hussak, E., 1906, O Palladio e a Platina no Brasil. An. Escola de Minas de Ouro Preto, no. 8, 96 p.

Immega, I.P., and Klein, Jr. C., 1976, Mineralogy and Petrology of Some Metamorphic Precambrian Iron-Formation in South-western Montana: Am. Mineralogist, v. 61, p. 1117-1144.

James, H.L., 1954, Sedimentary Facies of Iron-Formation: Econ. Geology, v. 49, p. 235-293.

\_\_\_\_\_, 1955, Zones of Regional Metamorphism in the Precambrian of Northern Michigan. Geol. Soc. Am. Bull., v. 66, no. 12, p. 1455-1488.

Johannsen, A., 1937, A Descriptive Petrography of the Igneous Rocks, v.3, The Intermediate Rocks: Chicago. Chicago Univ. Pres, 360 p.

Johnson, R.F., 1962, Geology and Ore Deposits Cachoeira do Camp, Dom Bosco, and Ouro Branco quadrangles, Minas Gerais, Brasil: U.S. Geol. Survey, Prof. Paper 341-B, 39 p.

Kerrich, R., and Allison, I., 1978, Flow Mechanisms in Rocks: Microscopic and Mesoscopic Structures, and Their Relation to Physical Conditions of Deformation in the Crust: Geoscience Canada, v. 5, p. 109-118.

Klein, Jr. C., 1974, Grenalite, Stilpnomelane, Minnesotaitite, Crocidolite and Carbonates in a Very Low-Grade Metamorphic Precambrian Iron-Formation: Can. Mineral., v. 12, p. 475-498.

LaBerge, G.L., 1966a, Altered Pyroclastic Rocks in Iron-Formation in the Hamersley Range, Western, Australia: Econ. Geol., v. 61, p. 147-161.

\_\_\_\_\_, 1966b, Altered Pyroclastic Rocks in South Africa Iron-Formation: Econ. Geol., v. 61, p. 572-581.

Lapadu-Hargues, P., 1953, Sur la composition chimique moyenne des amphibolites: Soc. Geol. France, Bull, 6th. ser., v. 3, p. 153-173.

MacPherson, H.G., 1958, A Chemical and Petrographic Study of Precambrian Sediments: Geochim. Cosmochim., Acta., v. 14, p. 73-92.

\* Maxwell, C.H., 1958, The Batatal Formation: Soc. Bras. Geologia, Bol., v. 7, no. 2, p. 60-61.

- Maxwell, C.H., 1972, Geology and Ore Deposits of the Alegria District, Minas Gerais, Brasil: U.S. Geol. Survey, Prof. Paper 341-J, 72 p.
- McKee, E.D., and Weir, G.W., 1953, Terminology For Stratification and Cross-Stratification in Sedimentary Rocks: Bull. G. S.A., v. 64, p. 381-390.
- Miyashiro, A., 1973, Metamorphism and Metamorphic Belts: William Clowes and Sons. Ltd., London, 492 p.
- Miyashiro, A., Shido, F., and Ewing, M., 1969, Diversity and Origin of Abyssal Tholeiite From the Mid-Atlantic Ridge Near 24° and 30° North Latitude: Contrib. Mineral. Petrol., v. 23, p. 38-52.
- Moore, S.L., 1969, Geology and Ore Deposits of the Antonio dos Santos Gongo Soco and Conceicao do Rio Acima quadrangles, Minas Gerais, Brasil: U.S. Geol. Survey Prof. Paper 341-I, 50 p.
- Nanz, Jr. R.H., 1953, Chemical composition of Precambrian Slates With Notes on the Geochemical Evolution of Lutites: Jour. Geol., v. 61, p. 51-64.
- Nicolas, A. and Poirier, J.P., 1976, Crystalline Plasticity and Solid State Flow in Metamorphic Rocks: John Wiley & Sons, N.Y., 444 p.
- Nockolds, S.R., 1954, Average Chemical Compositions of Some Igneous Rocks. Bull., Geol. Soc. Am., v. 65, p. 1007-1032.
- Paterson, M.S. and Weiss, L.E., 1961, Symmetry Concepts in the Structural Analysis of Deformed Rocks: Bull., Geol. Soc. Am., 72, p. 841-882.
- Pettijohn, F.J., 1975, Sedimentary Rocks: Harper & Son Publishers, N.Y., 628 p.
- Pires, F.R., 1977, Geologia do Distrito Manganesifero de Conselheiro Lafaiete: Instituto de Geociencias - UFRJ. Tese de Mestrado.
- \* Pomerene, J.B., 1958(a), The Cercadinho Formation: Soc. Bras. Geol., Bol., v. 7, no. 2, p. 64-65.
- \_\_\_\_\_, 1958(b), The Tabooes Quartzite: Soc. Bras. Geol., Bol., v. 7, no. 2, p. 66-67.
- \_\_\_\_\_, 1958(c), The Barreiro Formation: Soc. Bras. Geol., Bol., v. 7, no. 2, p. 67-68.

Spry, A., 1976 - Metamorphic Textures: Pergamon Press, Ltd., London, 350 p.



- Pomerene, J.B., 1964, Geology and Ore Deposits of the Belo Horizonte, Ibirite and Maçacos Quadrangles, Minas Gerais, Brasil: U.S. Geol. Survey Prof. Paper 341-D, 84 p.
- Ragan, D.M., 1968, Structural Geology. An Introduction to Geometrical Techniques: John Wiley & Sons, N.Y., 208 p.
- Ramsay, J.G., 1967, Folding and Fracturing of Rocks. McGraw-Hill, N.Y., 568 p.
- Read, H.H., 1951, Mylonitization and Cataclasis in Acidic Dykes in the Inch (Aberdeenshire) Gabbro and its aureole: Proc. Geol. Ass., Lond., 62, no. 4, 237 p.
- Reeves, R.G., 1966, Geology and Mineral Resources of the Monlevade and Rio Piracicaba Quadrangles, Minas Gerais, Brasil: U.S. Geol. Survey Prof. Paper 341-E, 58 p.
- Reynolds, R.C. Jr., 1965, The Concentration of Boron in Precambrian Seas: Geochim. Cosmochim., Acta, 29, p. 1-16.
- Roberts, J.L., 1972, The Mechanics of Overthrust Faulting: A Critical Review: 24th Int. Geol. Cong. Sec. 3, p. 593-595.
- Ronov, A.B., and Yaroshevskiy, A.A., 1967, Chemical Structure of the Earth's Crust: Geochemistry International, Pt. II, p. 1041-1066.
- Ruckmick, J.C., 1963, The Iron Ores of Cerro Bolivar, Venezuela: Econ. Geol., v. 58, p. 218-236.
- \* Rynearson, G.A., Pomerene, J.B., and Dorr, J.V.M., 2d., 1954, Contacto basal da Serie de Minas na parte ocidental do Quadrilatero Ferrifero, Minas Gerais, Brasil: Brasil Dept. Nac. Prod. Min., Div. Geol. e Mineralogia, Avulso 34, 18 p.
- Sander, B., 1970, An Introduction to the Study of Fabric of Geological Bodies: Pergamon Press. 639 p.
- \* Simmons, G.C., 1958 - The Fecho do Funil Formation: Soc. Brasileira de Geologia, Bol. 7, no. 2, p. 65-66.
- \_\_\_\_\_, 1968, Geology and Iron Deposits of the Western Serra do Curral, Minas Gerais, Brasil: U.S. Geol. Survey Prof. Paper 341-G, 57 p.
- Sims, P.K., 1976, Precambrian Tectonics and Mineral Deposits, Lake Superior Region: Econ. Geol., v. 71, no. 6, Presidential Address, p. 1092-1118.
- Spry, A., 1976 - Metamorphic Textures: Pergamon Press, Ltd., London, 350 p.



- Swanson, C.O., and Gunning, H.C., 1945, Geology of the Sullivan Mine: Canadian Inst. Min. Met., Trans., v. 48, p. 645-667.
- Trendall, A.F., 1973, Precambrian Iron Formations of Australia: Econ. Geol., v. 68, p. 1023-1034.
- Turekian, K.K., and Wedepohl, K.H., 1961, Distribution of the Elements in Some Major Units of the Earth's Crust: Geol. Soc. Am. Bull. 72, p. 175-192.
- Turner, F.J., and Weiss, L.E., 1963, Structural Analysis of Metamorphic Tectonites: McGraw-Hill Book Company, Inc., London, 545 p.
- Van Schmus, W.R., 1976, Early and Middle Proterozoic History of the Great Lakes Area, North America, in Global Tectonics in Proterozoic Times: Royal Soc. (London) Philos. Trans., A.V. 280, p. 605-628.
- Viljoen, M.J., and Viljoen, R.P., 1969, The Geological and Geochemical Significance of the Upper Formations of the Overwacht Group: Geol. Soc. South Africa. Spec. Pub. 2, p. 113-151.
- Walker, R.G., and Pettijohn, F.J., 1971, Archaean Sedimentation: Analysis of the Minnitaki Basin, Northwestern Ontario, Canada. Geol. Soc. Am., v. 82, p. 2099-2130.
- Wallace, R.M., 1958, The Moeda Formation: Soc. Bras. Geologia, Bol., v. 7, no. 2, p. 59-60.
- \_\_\_\_\_, 1965, Geology and Mineral Resources of the Pico de Itabirito district, Minas Gerais, Brasil: U.S. Geol. Surv. Prof. Paper 341-F, 68 p.
- Whitten, E.H.T., 1966, Structural Geology of Folded Rocks: Chicago, Rance McNally and Co., 661 p.
- Wier, K.L., 1967, Geology of the Kelso Junction Quadrangle-Iron County, Michigan: Bull. 1226, U.S. Geol. Survey, Wash., 47 p.
- Winkler, H.G.F., 1976, Petrogenesis of Metamorphic Rocks: Springer-Verlag, N.Y., 4th ed., 334 p.